

Journal Information

Maejo International Journal of Science and Technology (ISSN 1905-7873 © 2015), the international journal for preliminary communications in Science and Technology is the first peer-refereed scientific journal of Maejo University (www.mju.ac.th). Intended as a medium for communication, discussion, and rapid dissemination of important issues in Science and Technology, articles are published online in an open access format, which thereby gives authors the chance to communicate with a wide range of readers in an international community.

Publication Information

Three issues of MIJST are published per year (Jan.–April, May–Aug., Sept.–Dec.). Articles are available online and can be accessed free of charge at <http://www.mijst.mju.ac.th>. Printed and bound copies of each volume are produced and distributed to selected groups or individuals. This journal and the individual contributions contained in it are protected under the copyright by Maejo University.

Abstracting/Indexing Information

MIJST is covered and cited by Science Citation Index Expanded, SCOPUS, Journal Citation Reports/Science Edition, Zoological Record, Directory of Open Access Journals (DOAJ), CAB Abstracts, ProQuest, Google Scholar, EBSCO and ACI.

Contact Information

Editorial office: Maejo International Journal of Science and Technology (MIJST), 1st floor, Orchid Building, Maejo University, San Sai, Chiang Mai 50290, Thailand

Tel: +66-53-87-5532

E-mail: duang@mju.ac.th



MAEJO INTERNATIONAL JOURNAL OF SCIENCE AND TECHNOLOGY

Editor

Duang Buddhasukh, Maejo University, Thailand.

Associate Editors

Jatuphong Varith, Maejo University, Thailand.

Wasin Chareerntanakul, Maejo University, Thailand.

Niwooti Whangchai, Maejo University, Thailand.

Morakot Sukchotiratana, Chiang Mai University, Thailand.

Nakorn Tippayawong, Chiang Mai University, Thailand.

Editorial Assistants

Jirawan Banditpuritat, Maejo University, Thailand.

Editorial Board

- | | |
|---|--|
| Prof. Dr. Praveen Agarwal | Anand International College of Engineering, India. |
| Assoc. Prof. Dr. Mohammad R. Alizadeh | Rice Research Institute of Iran, Guilan, Iran. |
| Asst. Prof. Dr. V. Ananthaswamy | The Madura College, Tamil Nadu, India. |
| Dr. Serkan Araci | Hasan Kalyoncu University, Turkey. |
| Assoc. Prof. Dr. Abdon Atangana | University of the Free State, South Africa. |
| Emeritus Prof. Dr. Huseyin Bor | P.O. Box 121, TR-06502 Bahcelievler, Ankara, Turkey. |
| Emeritus Prof. John Bremner | University of Wollongong, NSW, Australia. |
| Dr. Pei-Yi Chu, M.D. | Changhua Christian Hospital, Taiwan, R.O.C. |
| Asst. Prof. Ekachai Chukeatirote | Mae Fah Luang University, Thailand. |
| Assoc. Prof. Amar Debbouche | Guelma University, Algeria. |
| Dr. Deepmala | Indian Statistical Institute, India. |
| Prof. Richard L. Deming | California State University Fullerton, Fullerton CA. |
| Prof. Cynthia C. Divina | Central Luzon State University, Philippines. |
| Prof. Dr. Rakesh Dube | Dr A P J Abdul Kalam Technical University, India. |
| Asst. Prof. Dr. Mostafa Eslami | University of Mazandaran, Babolsar, Iran. |
| Prof. Mary Garson | The University of Queensland, Brisbane, Australia. |
| Assoc. Prof. Dr. A. Nirmala Grace | VIT University, India. |
| Prof. Kate Grudpan | Chiang Mai University, Thailand. |
| Dr. Soon Min Ho | INTI International University, Malaysia. |
| Assoc. Prof. Dr. Duangrat Inthorn | Mahidol University, Thailand. |
| Prof. Minoru Isobe | Nagoya University, Japan. |
| Prof. Dr. Sriman N. Iyengar | VIT University, India. |
| Asst. Prof. Dr. Dariusz Jakobczak | Technical University of Koszalin, Poland. |
| Prof. Dr. Prakash Naraiyan Kalla | University, Bikaner, Campus Jaipur, India. |
| Dr. Nakul Karkare | York Hospital, PA, USA. |
| Prof. Kunimitsu Kaya | Tohoku University, Japan. |
| Prof. Dr. Margaret E. Kerr | Worcester State College, Worcester, MA. |
| Prof. Tanongkiat Kiatsiriroat | Chiang Mai University, Thailand. |
| Asst. Prof. Dr. Ignacy Kitowski | State School of Higher Education in Chelm, Poland. |
| Asst. Prof. Dr. Andrzej Komosa | University of Maria-Curie Sklodowska, Poland. |
| Prof. Dr. Monai Krairiksh | King Mongkut's Institute of Technology Ladkrabang, Thailand. |
| Asst. Prof. Dr. Pradeep Kumar | Jaypee University of Information Technology, India. |
| Asst. Prof. Dr. Sunil Kumar | National Institute of Technology, India. |
| Mr. Shyam Nandan Kumar | Lakshmi Narain College of Technology, India. |
| Prof. Dr. T. Randall Lee | University of Houston, USA. |
| Asst. Prof. Ma. Dr. Elizabeth C. Leoveras | Central Luzon State University, Philippines. |
| Prof. Dr. Subrata Mallick | Siksha O Anusandhan University, India. |
| Asst. Prof. Dr. Vishnu Narayan Mishra | Sardar Vallabhbhai National Institute of Technology, India. |
| Prof. Amarendra N. Misra | Central University of Jharkhand, India. |
| Dr. Robert Molloy | Chiang Mai University, Thailand. |
| Prof. Mohammad A. Mottaleb | Northwest Missouri State University, USA. |
| Asst. Prof. Anand Nayyar | KCL Institute of Management and Technology, India. |
| Engr. Obeta Nwachkwu | Enugu State University of Science and Technology, Nigeria. |
| Assoc. Prof. Dr. Kaew Nualchawee | Geoinformatics and Space Technology Development of Agency, Thailand. |
| Prof. Dr. Yoko Oki | Okayama University, Japan. |
| Prof. R. Ponalagusamy | National Institute of Technology, India. |
| Assoc. Prof. Dr. Sunil Dutt Purohit | Rajasthan Technical University, India. |
| Prof. Stephen G. Pyne | University of Wollongong, Australia. |
| Dr. Khaled Nabih Rashed | National Research Centre, Giza, Egypt. |
| Prof. Dr. Mohammad Mehdi Rashidi | Tongji University, Shanghai, China. |

Prof. Renato G. Reyes	Central Luzon State University, Philippines.
Prof. Dr. Hidehiro Sakurai	Institute for Molecular Science, Myodaiji, Japan.
Prof. Muhammad Qaiser Shahbaz	King Abdul Aziz University, Jeddah, Saudi Arabia.
Prof. Dr. Sung le Shim	University of Seoul, Korea.
Asst. Prof. Dr. Satish K. Singh	Indian Institute of Information Technology, Allahabad, India.
Prof. Paisarn Sithigorngul	Srinakharinwirot University, Thailand.
Prof. S. Smys	Karpagam College of Engineering, Coimbatore, India.
Prof. Anupam Srivastav	IFTM University, Moradabad, India.
Prof. Hari M. Srivastava	University of Victoria, Canada.
Prof. Maitree Suttajit	Naresuan University (Payao Campus), Thailand.
Prof. Dr. Asif Tanveer	University of Agriculture Faisalabad, Pakistan.
Asst. Prof. Thanaphong Thanasaksiri	Chiang Mai University, Thailand.
Asst. Prof. Dr. Narin Tongwittaya	Maejo University, Thailand.
Dr. Mohammad Valipour	Islamic Azad University, Kermashah, Iran.
Prof. Keshav D. Verma	S.V. (P.G.) College, Aligarh, India.
Assoc. Prof. Malinee Wongnawa	Prince of Songkla University, Thailand.
Dr. Guo-Cheng Wu	Neijiang Normal University, Sichuan, China.
Prof. Xiao-Jun Yang	China University of Mining and Technology, Jiangsu, China.
Prof. Yudong Zhang	Nanjing Normal University, China.
Prof. Zhihua Zhang	Beijing Normal University, China.
Asst. Prof. Dr. Rushan Ziatdinov	Keimyung University, Daegu, South Korea.
Dr. Mahdi Zowghi	Department of Business Management, PWCS, Tehran, Isan.

Consultants

Asst. Prof. Chamnian Yosraj, Ph.D., President of Maejo University
 Assoc. Prof. Thep Phongpanich, Ed. D., Former President of Maejo University
 Assoc. Prof. Chalermchai Panyadee, Ph.D., Vice-President in Research of Maejo University

**MAEJO INTERNATIONAL JOURNAL
OF SCIENCE AND TECHNOLOGY**

*The International Journal for the Publication of Preliminary
Communications in Science and Technology*





CONTENTS

Page

<i>Fazilah Abd Manan*</i> , <i>Tsun-Thai Chai</i> and <i>Azman Abd Samad</i>	288-300
Environmental pollution in Malaysia: Are medicinal plants potential phytoremediation agents?	
<i>Ömür Deveci*</i> and <i>Metin Avci</i>	301-311
Fibonacci p -sequences in groups	
<i>Navid Feroze*</i> , <i>Tabassum Naz Sindhu</i> , <i>Muhammad Aslam</i> and <i>Wasif Yaseen</i>	312-327
Doubly censored mixture of two Rayleigh distributions: Properties and applications	
<i>Sangdo An</i> , <i>Hyeyun Ku*</i> and <i>Pierre Y. Julien</i>	328-343
Numerical modelling of local scour caused by submerged jets	
<i>Theerapong Theppakorn*</i>	344-354
Chemical constituents of Oolong tea produced in Thailand and their correlation with infusion colour	
<i>Yaw-Huei Chen</i> and <i>Patcharanut Daowadung*</i>	355-369
Assessing readability of Thai text using support vector machines	
<i>Ratchana Boonmee</i> and <i>Sirirat Rengpipat*</i>	370-381
Effects of <i>Musa</i> (ABB group) prebiotic and <i>Bacillus subtilis</i> S11 probiotic on growth and disease resistance of cultivated Pacific white shrimp (<i>Litopenaeus vannamei</i>)	
<i>Wanticha Savedboworn</i> and <i>Penkhae Wanchaitanawong*</i>	382-393
Viability and probiotic properties of <i>Lactobacillus plantarum</i> TISTR 2075 in spray-dried fermented cereal extracts	
<i>Ying Wu</i> , <i>Feng Qi*</i> and <i>Da-Wei Niu</i>	394-402
Integral inequalities of Hermite-Hadamard type for the product of strongly logarithmically convex and other convex functions	
<i>Piyanun Ruangurai</i> , <i>Mongkol Ekpanyapong*</i> , <i>Chatchai Pruetong</i> and <i>Thaisiri Watewai</i>	403-412
Automated three-wheel rice seeding robot operating in dry paddy fields	

**MAEJO INTERNATIONAL JOURNAL
OF SCIENCE AND TECHNOLOGY**

Volume 9, Issue 3 (September – December 2015)

Author Index

Author	Page	Author	Page
An S.	328	Niu D.-W.	394
Aslam M.	312	Pruetong C.	403
Avcı M.	301	Qi F.	394
Boonmee R.	370	Rengpipat S.	370
Chai T.-T.	288	Ruangurai P.	403
Chen Y.-H.	355	Samad A. A.	288
Daowadung P.	355	Savedboworn W.	382
Deveci Ö.	301	Sindhu T. N.	312
Ekpanyapong M.	403	Theppakorn T.	344
Feroze N.	312	Wanchaitanawong P.	382
Julien P. Y.	328	Watewai T.	403
Ku H.	328	Wu Y.	394
Manan F. A.	288	Yaseen W.	312

Instructions for Authors

A proper introductory e-mail page containing the title of the submitted article and certifying its originality should be sent to the editor (Duang Buddhasukh, e-mail: duang@mju.ac.th). The manuscript proper together with a list of suggested referees should be attached in separate files. The list should contain at least 5 referees with appropriate expertise. Three referees should be non-native from 3 different countries. Each referee's academic/professional position, scientific expertise, affiliation and e-mail address must be given. The referees should not be affiliated to the same university/institution as any of the authors, nor should any two referees come from the same university/institution. The editorial team, however, retain the sole right to decide whether or not the suggested referees are approached.

Failure to conform to the above instructions will result in non-consideration of the submission.

Please also ensure that English and style is properly edited before submission. UK style of spelling should be used. Authors who would like to consult a professional service can visit www.editage.com/?ref=referral, www.bioedit.co.uk (bioscience and medical papers), www.scribendi.com, www.letpub.com, www.papersconsulting.com, www.sticklerediting.com, Cambridge Proofreading (<http://proofreading.org/>), www.ProofreadingServices.com, www.horizonproofreading.org, Help.Plagtracker, www.ninjaessays.com/editing/, <http://bid4papers.com/editing-services.html>, www.enago.com, www.medsciediting.com, www.manuscriptedit.com, <http://www.proofreadmyfile.com>, ProofreadMyDocument, www.24x7editing.com, www.tulyasys.com, www.regentediting.co.uk, www.editnpublish.com, www.sciencedocs.com or www.geediting.com.

Important : Manuscript with substandard English and style will not be considered.

Warning : Plagiarism (including self-plagiarism) may be checked for at *the last* stage of processing and, if detected, will result in a rejection and blacklisting.

Manuscript Preparation

Manuscripts must be prepared in English using a word processor. MS Word for Macintosh or Windows, and .doc or .rtf files are preferred. Manuscripts may be prepared with other software provided that the full document (with figures, schemes and tables inserted into the text) is exported to a MS Word format for submission. Times or Times New Roman font is preferred. The font size should be 12 pt and the line spacing 'at least 17 pt'. A4 paper size is used and margins must be 1.5 cm on top, 2.0 cm at the bottom and 2.0 cm on both left and right sides of the paper. Although our final output is in .pdf format, authors are asked NOT to send manuscripts in this format as editing them is much more complicated. Under the above settings, a manuscript submitted should not be longer than **15 pages** for a full paper or **20 pages** for a review paper.

A template file may be downloaded from the *Maejo Int. J. Sci. Technol.* homepage. ([DOWNLOAD HERE](#))

Authors' full mailing addresses, homepage addresses, phone and fax numbers, and e-mail addresses homepages can be included in the title page and these will be published in the manuscripts and the Table of Contents. The corresponding author should be clearly identified. It is the corresponding author's responsibility to ensure that all co-authors are aware of and approve of the contents of a submitted manuscript.

A brief (200 word maximum) Abstract should be provided. The use in the Abstract of numbers to identify compounds should be avoided unless these compounds are also identified by names.

A list of three to five keywords must be given and placed after the Abstract. Keywords may be single words or very short phrases.

Although variations in accord with contents of a manuscript are permissible, in general all papers should have the following sections: Introduction, Materials and Methods, Results and Discussion, Conclusions, Acknowledgments (if applicable) and References.

Authors are encouraged to prepare Figures and Schemes in colour. Full colour graphics will be published free of charge.

Tables and Figures should be inserted into the main text, and numbers and titles supplied for all Tables and Figures. All table columns should have an explanatory heading. To facilitate layout of large tables, smaller fonts may be used, but in no case should these be less than 10 pt in size. Authors should use the Table option of MS Word to create tables, rather than tabs, as tab-delimited columns are often difficult to format in .pdf for final output.

Figures, tables and schemes should also be placed in numerical order in the appropriate place within the main text. Numbers, titles and legends should be provided for all tables, schemes and figures. Chemical structures and reaction schemes should be drawn using an appropriate software package designed for this purpose. As a guideline, these should be drawn to a scale such that all the details and text are clearly legible when placed in the manuscript (i.e. text should be no smaller than 8-9 pt).

For bibliographic citations, the reference numbers should be placed in square brackets, i.e. [], and placed before the punctuation, for example [4] or [1-3], and all the references should be listed separately and as the last section at the end of the manuscript.

Format for References

Journal :

1. D. Buddhasukh, J. R. Cannon, B. W. Metcalf and A. J. Power, "Synthesis of 5-n-alkylresorcinol dimethyl ethers and related compounds *via* substituted thiophens", *Aust. J. Chem.*, **1971**, *24*, 2655-2664.

Text :

2. A. I. Vogel, "A Textbook of Practical Organic Chemistry", 3rd Edn., Longmans, London, **1956**, pp. 130-132.

Chapter in an edited text :

3. W. Leistritz, "Methods of bacterial reduction in spices", in "Spices: Flavor Chemistry and Antioxidant Properties" (Ed. S. J. Risch and C-T. Ito), American Chemical Society, Washington, DC, **1997**, Ch.2.

Thesis / Dissertation :

4. W. phutdhawong, "Isolation of glycosides by electrolytic decolourisation and synthesis of pentinomycin", *PhD Thesis*, **2002**, Chiang Mai University, Thailand.

Patent :

5. K. Miwa, S. Maeda and Y. Murata, "Purification of stevioside by electrolysis", *Jpn. Kokai Tokkyo Koho 79 89,066* (**1979**).

Proceedings :

6. P. M. Sears, J. Peele, M. Lassauzet and P. Blackburn, "Use of antimicrobial proteins in the treatment of bovine mastitis", Proceedings of the 3rd International Mastitis Seminars, **1995**, Tel-Aviv, Israel, pp.17-18.

Websites :

7. S. Simon, "What is an odds ratio?", **2008**, <http://www.childrensmarcy.org/stats/definitions/or.htm> (Accessed: October 2011).

Manuscript Revision Time

Authors who are instructed to revise their manuscript should do so within **45** days. Otherwise the revised manuscript will be regarded as a new submission.

Manuscript Processing Time

As a result of a large number of submissions, there may be a long delay in the evaluation or publication of a paper. A duration of at least 6-8 months between submission and acceptance (or rejection) can normally be expected.

Report

Environmental pollution in Malaysia: Are medicinal plants potential phytoremediation agents?

Fazilah Abd Manan^{1,*}, Tsun-Thai Chai^{2,4} and Azman Abd Samad³

¹ Department of Biosciences and Health Sciences, Faculty of Biosciences and Medical Engineering, Universiti Teknologi Malaysia, 81310 UTM Johor Bahru, Johor, Malaysia

² Department of Chemical Science, Faculty of Science, Universiti Tunku Abdul Rahman, 31900 Kampar, Malaysia

³ Department of Biotechnology and Medical Engineering, Faculty of Biosciences and Medical Engineering, Universiti Teknologi Malaysia, 81310 UTM Johor Bahru, Johor, Malaysia

⁴ Centre for Biodiversity Research, Universiti Tunku Abdul Rahman, 31900 Kampar, Malaysia

* Corresponding author, e-mail: fazilah@fbb.utm.my

Received: 22 June 2014 / Accepted: 21 September 2015 / Published: 28 September 2015

Abstract: Phytoremediation is a plant-based approach to controlling pollution, an alternative to the conventional physical and chemical remediation techniques. In Malaysia many small-scale studies on phytoremediation have been conducted. However, the establishment of phytoremediation strategy at larger field sites is rather lacking. Depending on plant species and existing environmental factors, bioactive compounds from medicinal plants have the potential for remediating specific pollutants. The wealth of plant resources in Malaysia presents an opportunity for the phytoremediation technique to be applied as part of the environmental management programmes in future. Nevertheless, the ability of medicinal plants to accumulate pollutants has led to safety concerns when the plants are used as therapeutic agents or medicine. This paper reports the current status of environmental pollution in Malaysia and the potential uses of medicinal plants to treat pollutants in the environment.

Keywords: pollution, medicinal plants, phytoremediation, Malaysia

INTRODUCTION

Phytoremediation is a natural, non-invasive pollutant clean-up technique by means of plants and their associated microbes [1]. Many plant species have their own adaptation mechanisms that allow them to survive under a highly polluted environment. Indeed, some plants known as hyperaccumulators are able to survive or thrive on heavy-metal-polluted soils despite high levels of metals in their tissues [2, 3].

Plants also exhibit valuable therapeutic properties and various species have been recognised as a prominent source of traditional medicine. The medicinal properties of plants are normally derived from various secondary metabolites, which may also be important for plant protection under stressful environmental conditions [4, 5]. Thus, medicinal plants may be potential phytoremediating agents, although this application is still underexplored.

Although phytoremediation techniques have been implemented in some countries, it is still considered new in Malaysia. In developed countries such as the United States, phytotechnologies have the possibility to clean 30,000 of the contaminated waste sites, while in Asian countries such as Bangladesh, India and Pakistan, this method has been used to clean up pollutants mainly from sewage water and industrial wastes [6]. A review on phytoremediation techniques applied in some selected countries has been published recently by Sharma and Pandey [6]. In Malaysia numerous phytoremediation-related studies are still being conducted at the laboratory level or on small-field scale for research purposes. Large field-scale phytoremediation work has not been reported yet. As a country that is endowed with immense plant resources, it is conceivable that at least some of the local plant species can be used for treating contaminated soil and water bodies.

This report aims to gather updated information on the environmental status in Malaysia and provide an assessment of the potential use of medicinal plants in phytoremediation in the country. Safety issues that may arise from using phytoremediating medicinal plants for subsequent human use or consumption are also discussed.

ENVIRONMENTAL QUALITY IN MALAYSIA

As a rapidly developing country, Malaysia is facing enormous environmental challenges. Activities in manufacturing, agro-based industries, land development and transportation release many kinds of pollutants to the environment. Prevention and control of pollution is a great challenge for the nation. Realising the importance of good environmental quality, the Department of Environment (DOE) was formed under the Ministry of Science, Technology and Environment to manage environmental-related issues [7]. Environmental Quality Act 1974 was introduced and subjected to several amendments in 1985 [8]. To date, many guidelines have been set to monitor the quality of air, water, groundwater and coastal areas in the country [9].

The level of air quality is monitored based on several parameters. This includes carbon monoxide, nitrogen dioxide, ozone, sulphur dioxide, particulate matter and heavy metals. The air pollution problems in Malaysia stem from not only local human activities, but also a series of haze problems from a neighbouring country that occur during a certain period of the year [10, 11]. In June 2013, Malaysia experienced a short but serious haze problem, with one district in the Southern region of Peninsular Malaysia recording the air pollution index of more than 500 [11].

In 2013 the percentage of clean rivers in Malaysia was reduced by 1 % [11]. The groundwater from agricultural and industrial sites is still contaminated when assessed based on the parameters in the National Guidelines for Raw Drinking Water Quality [9, 11]. The levels of total coliform, phenol and metals such as arsenic, iron and manganese are found to exceed the safe limits stated in the guidelines.

In the coastal area in 2010, assessment of marine water quality showed that mercury and cadmium were 30.5% and 18.5% respectively higher than the permitted levels in the Malaysian Water Quality and Standards, i.e. 0.5 µg/L and 2 µg/L respectively for Class E (mangrove, estuarine and river-mouth water) [9, 12]. Mercury is a highly toxic metal and its presence even in small quantities may bring serious toxic effects to living organisms [13]. Similarly, the concentration of

copper in coastal water also poorly met the standard of 2.9 µg/L for Class E in 2011 [14]. Besides metals, oil and grease, total suspended solids and *Eschericia coli* are the source of pollutants in the water bodies. The presence of various pollutants in the environment heightens the need for remediation. From the latest Environmental Quality Report, the number of sampling points categorised as 'polluted' increased from nine stations in 2012 to 11 stations in 2013 [11].

CURRENT APPROACHES FOR POLLUTION MANAGEMENT IN MALAYSIA

Environmental issues in Malaysia necessitate serious attention, although the problem is not as severe as those in some other industrialised countries. For different types of pollutants, different management strategies have been adopted. Currently, the conventional physical and chemical treatments are widely used to treat pollutants in Malaysia.

The agricultural sector is one of the biggest industries in the country that produce various organic and inorganic pollutants. Most agricultural wastes are treated using the pond system and chemical degradation [15]. On the other hand, petroleum-based pollutants generated by many heavy industries are often treated with soil vapour extraction, a technique that removes harmful vaporised chemicals such as volatile organic compounds [16]. Other petroleum-based pollutants are removed using the containment method to prevent the spread of contaminants. Soil vapour extraction and containment methods are also applicable for chlorinated hydrocarbons produced from non-petroleum-based industries [16]. Currently, research on the use of 'biostructure' to treat wastewater from petrochemical industries has been started with continuous improvements in various aspects including the use of modelling and statistical approach [17].

Other methods such as incineration, solidification and secure landfill disposal are normally used to manage certain types of hazardous wastes. Crude landfill technique, for instance, has been used for the disposal of solid wastes. However, it may increase the chances of pollutants spreading to adjacent areas through leaching and vaporisation. Thus, to reduce this problem, sanitary landfill was suggested as a better way for solid waste management [18].

Heavy metals are also considered as the main pollutants in the environment. Industries such as petroleum refining, wood-processing, smelting and metal plating produce wastes containing heavy metals that are commonly treated with chemical means such as precipitation, ion exchange, reverse osmosis, electro dialysis and ultrafiltration [19, 20]. For less harmful and visible pollutants such as trashes in the rivers, gross pollutant traps have already been applied, for example in the Klang river [21].

Overall, the aforementioned physico-chemical methods are often very costly, complicated and sometimes ineffective. Due to environmental concerns and the urge to reduce cost, natural remediation has become an alternative way to treat various pollutants. Microbes, fungi and plants are organisms normally involved in bioremediation processes. Although it is still at an early phase, phytoremediation technique has now been incorporated as part of the pollution management strategies in Malaysia.

PHYTOREMEDIATION IN MALAYSIA

In Malaysia most of the phytoremediation and related work reported over the past ten years was based on studies conducted in the laboratory. Most studies have focused on evaluating the ability of plants to take up pollutants, with emphasis on determining the levels of pollutants in various plant tissues. Bioremediation studies conducted on the actual contaminated sites are still

lacking [22]. This could be due to the need to consider various factors such as plants species and environmental conditions prior to the scale up of lab-based experiments to the field-based phytoremediation.

Nonetheless, fundamental experiments conducted to date have revealed the capacity of various plants to take up pollutants, especially heavy metals. These studies could be the stepping stones for future phytoremediation research. Table 1 shows a number of representative studies carried out in Malaysia, which investigated the phytoremediation potential of various plant species.

Table 1. Studies of phytoremediation potential of Malaysian plant species with emphasis on medicinal plants

Type of pollutants	Plant species used	Polluted conditions simulated in laboratory	Experiments using pollutants sampled from contaminated sites	Reference
Heavy metals from soil	<i>Centella asiatica</i> *	√		[23]
Heavy metals from sewage sludge	<i>Orthosiphon stamineus</i> *	√		[24]
	<i>Acacia mangium</i> *	√		[25]
Heavy metals from sawdust sludge	<i>Pluchea indica</i> *	√		[26]
	<i>Jatropha curcas</i> *	√		[27]
Lead-contaminated soil	<i>Hibiscus cannabinus</i> *	√		[28]
Aqueous medium containing copper (II)		√		[29]
Diesel pollutants in synthetic wastewater	<i>Salvinia molesta</i> *	√		[30]
Hydrocarbon-contaminated soil	<i>Paspalum vaginatum</i> *	√		[31]
Chromium from electroplating waste	<i>Nymphaea spontanea</i> *	√		[32]
Heavy metals from agricultural soil in Cameron Highlands and Sepang	<i>Solanum melongena</i> *, <i>Ipomoea batatas</i> *, <i>Allium cepa</i> *		√	[33]
Heavy metals from petroleum refinery effluents on west coast of Peninsular Malaysia	<i>Eichhornia crassipes</i> *		√	[34]
Leachate of contaminated landfill from Burung Island			√	[35]

Table 1. (Continued)

Type of pollutants	Plant species used	Polluted conditions simulated in laboratory	Experiments using pollutants sampled from contaminated sites	Reference
Aquaculture wastewater from fish pond in Semanggol, Perak	<i>Eichhornia crassipes</i> *, <i>Pistia stratiotes</i> *		√	[36]
Textile wastewater from Senawang Industrial Estate, Negeri Sembilan	<i>Chlorella vulgaris</i> *		√	[37]
Heavy metals from Chini Lake	<i>Lepironia articulate</i> , <i>Pandanus helicopus</i> , <i>Scirpus grossus</i> *, <i>Cabomba furcata</i> , <i>Nelumbo nucifera</i> *		√	[38]
PAH from North-South Expressway in Johor	<i>Ficus microcarpa</i> *, <i>Ixora coccinea</i> *, <i>Baphia nitida</i> *		√	[39]
Heavy metals from tin tailings	<i>Cyperus rotundus</i> *, <i>Imperata cylindrical</i> *, <i>Nelumbo nucifera</i> *, <i>Phragmites australis</i> *, <i>Pteris vittata</i> *		√	[40]
Leachate of sanitary landfill in Puchong	<i>Moringa oleifera</i> *		√	[41]

* Plants with documented medicinal values

PROPERTIES AND CRITERIA OF MEDICINAL PLANTS IN RELATION TO PHYTOREMEDIATION

Besides their traditional uses, medicinal and aromatic plants have important economic values in many industries such as pharmaceuticals, food, cosmetics and ornaments. Medicinal plants exhibit therapeutic properties due to the presence of bioactive compounds derived from secondary metabolites such as phenolics, terpenoids and compounds containing sulphur and nitrogen [42]. Phenolic compounds, for example, are good solubilisers and metal chelators for plants in contaminated areas [43, 44]. Phenolic compounds can be released as plant root exudates containing organic acids such as lactates and acetates [45]. These compounds can facilitate bioremediation of pollutants, provided that other environmental factors such as pH, temperature and soil conditions are also suitable for the process to happen [46].

The mechanism of pollutant uptake and accumulation varies depending on the type of plant tissues. Pollutants normally enter plants through foliage or root system prior to undergoing oxidation or storage in other compartments such as vacuoles [47]. In response to pollutants, plants usually increase the production of reactive oxygen species [48]. However, high levels of these species are harmful; thus, antioxidants are produced to alleviate the cellular oxidative stress [49, 50].

Since secondary metabolites produced by medicinal plants normally contribute to various biological roles, this could be a way for plants to adapt to the polluted environment [4]. Secondary metabolites could contribute to the protection of plant against toxin stress and could be involved in the detoxification of some toxic metals [51]. The ability of certain plants to survive in a contaminated area suggests that they may be able to tolerate or even hyperaccumulate pollutants [52]. Table 2 shows the roles of some secondary metabolites in phytoremediation.

Table 2. Roles of some secondary metabolites as phytoremediating agents

Compound	Role in phytoremediation	Plants investigated	Reference
Phenolics	Aluminium chelator	<i>Zea mays</i> *	[53]
	Lead and copper chelator	<i>Brassica juncea</i> *	[54]
	Cadmium chelator	<i>Hypericum perforatum</i> * <i>Matricaria recutita</i> *	[55]
	Nickel chelator	<i>Matricaria chamomilla</i> *	[56]
	Biodegradation of polychlorinated biphenyls and polyaromatic hydrocarbons	<i>Morus rubra</i> *	[57]
	Biodegradation of polyaromatic hydrocarbons	<i>Miscanthus giganteus</i>	[58]
Terpenoids	Induction of biodegradation of polychlorinated biphenyls in bacteria	<i>Mentha spicata</i> *	[59]
Sulphur- or nitrogen-containing compounds	Cadmium detoxification	<i>Arabidopsis thaliana</i> *	[60]

* Plants with documented medicinal values

Apart from the roles of secondary metabolites, plant species and environmental conditions are important factors to ensure the success of phytoremediation process. For some susceptible plants, their medicinal properties may be affected due to exaggerated growth and development and alteration of their chemical composition under polluted conditions [61]. Normally, plants for bioremediation have to be robust and able to survive under a stressful environment. In addition, their ability to take up pollutants in a reasonable time frame is also important. Such characteristics as rapid growth and development resulting in height and abundant branches and leaves that lead to the production of high plant biomass under polluted conditions indicate the fitness or suitability of the plants for bioremediation [62]. Medicinal plants such as *Heliantus annuus* and *Pteris vittata* are good phytoremediators as they are fast-growing species, less prone to diseases and have the ability to accumulate heavy metals in plant tissues [63, 64].

Currently, plant tissue-culture technology is available to assist researchers in obtaining basic information related to phytoremediation in a shorter time, facilitating the investigation of suitable conditions for plant growth and optimum production of secondary metabolites for remediation

purposes [65]. Thus, the knowledge from studies based on cultured tissues may be applied when growing plants at field sites [66].

HEALTH CONCERNS FOR MEDICINAL PLANTS USED IN PHYTOREMEDIATION

There are more than 6,000 species of Malaysian plants with known medicinal values. Tongkat Ali (*Eurycoma longifolia*), Kacip Fatimah (*Labisia pumila*), Misai kucing (*Orthosiphon stamineus*), Hempedu bumi (*Andrographis paniculata*), Dukung anak (*Phyllanthus niruri* Linn) and Pegaga (*Centella asiatica*) are among the common species that have been traditionally used to promote healthy body functions and cure diseases such as diabetes, hypertension and sex-related problems [67]. A decade ago, studies on medicinal plants in Malaysia were scarce [68]. However, this field has been slowly expanding with increasing researches conducted by various agencies in the country. Research on medicinal plants that previously focused on the search of bioactive compounds for drug development has now expanded to modern phytotechnologies including phytofortification and phytoremediation [69]. In phytofortification, the accumulation of essential elements such as selenium, zinc and iron in the edible parts of medicinal plants makes them suitable as a source of supplementary nutrition [70, 71, 72]. Their ability to take up pollutants, on the other hand, has made them suitable for bioremediation purposes [73].

From another point of view, the ability of certain medicinal plants to accumulate pollutants has provoked safety concerns among consumers. As highlighted by Bagdat and Eid [74], several species of herbal plants normally used in food preparation, such as mint, lavender, thyme, pot marigold, hollyhock, garden sorrel and black nightshade, also have the capacity to take up metals. This is a big concern among consumers as herbs for cooking will be directly consumed without any extraction process. The problem may be less serious when medicinal plants grown on contaminated sites are subjected to further extraction and purification steps before their active ingredients are used for human consumption. For example, essential oil products are normally free from pollutants after the extraction process [75]. The problem will arise when people have no idea that the plants they use for medicinal purposes are contaminated.

Several important guidelines have been published by the World Health Organisation, covering the whole spectrum of procedures for herbal medicine preparation including aspects of safety, quality, agricultural practices and manufacturing of medicinal plants [76]. The aforementioned aspects are important for sustainable herbal market worldwide [77]. Malaysia also has its own national pharmaceutical control bureau to ensure that therapeutic substances approved for the local market are in high quality and safe [78]. In 2001 a national policy on traditional medicine and alternative or complementary medicine was launched and its licensing was enacted under the control of Drugs and Cosmetics Regulations 1984 [77]. Generally, materials prepared will be subjected to quality control analysis including toxicological, pharmacological and pharmacokinetic studies, while materials for the manufacturing process will be followed by clinical studies [79].

Nonetheless, the implementation of the regulations needs to be strengthened, especially among manufacturers. A study by Ang and Lee [80] revealed that 26% of the Tongkat Ali Hitam (*Eurycoma longifolia*) products contained mercury exceeding 0.5 ppm, the accepted level for traditional medicine, and these products were not registered with the Drug Control Authority. This may be an isolated case, but it has raised serious concern as the cultivation and use of medicinal

plants has to be done by taking into consideration the potential hazard to humans and the environment [81].

MEDICINAL PLANTS: FUTURE PROSPECTS FOR PHYTOREMEDIATION AND CHALLENGES

Although phytoremediation incorporates the ability of plants to remove pollutants from different sources, many studies nowadays have been emphasising on phytoremediation of heavy metals and organic pollutants from soil and water. There is lack of attention towards other pollutants such as air-polluting toxic gases despite their prevalence in the environment. Future research should investigate the ability of medicinal plants to take up both organic and inorganic pollutants. Furthermore, field-scale phytoremediation should be intensified with the goal of evaluating the effectiveness of the technology at the real contaminated sites.

In addition, many species currently tested for phytoremediation have certain medicinal properties. However, the correlation between the ability of plant to remove pollutants and the involvement of bioactive compounds in this process requires more concrete scientific evidence. Since the main issue in bioremediation is the time consumption, the introduction of transgenic plants with relevant phenotypes, the acceleration of remediation with the addition of microbes, and the combination of biological and chemical methods can all be attempted to identify a more time-efficient solution [82, 83].

Furthermore, the negative effects of consuming plant-based medicine could be avoided if consumers only use the products that have been approved by recognised bodies or agencies. For raw plant usage, consumers should choose plants from low-risk sources, for example medicinal plants harvested from unpolluted sites. It is preferable to use plants that are not accumulating pollutants in the parts that will be eaten later. In a study conducted using kenaf, lead was highly accumulated in the root, followed by stem and seed capsule, exceeding the safe level in food, which is 2 mg/kg. However, it was not detected in the leaves; hence it can be used for cattle feed [28]. However, for human it must be confirmed that a metal level in plants is safe for usage. Some species of plants such as *Pteris vittata* also have the ability to absorb and evaporate pollutants into the atmosphere [84, 85]. It was reported that *Pteris vittata* produces harmful compounds to animals. However, some of the local people in India have used this plant for wound healing or treatment of cold, cough and fever [86]. Considering the priority of human safety, we believe that the best practice is to use plants that are free from contamination to prevent poisoning or further complications from the pollutants.

Taken together, phytoremediation using medicinal plants have an immense potential in Malaysia. Although there are challenges that need to be tackled, it is not impossible to implement this technique if all parties involved could work it out collaboratively.

CONCLUSIONS

In implementing clean technologies for environmental sustainability, phytoremediation is a method of choice for removing pollutants. Available resources in Malaysia including vast varieties of herbal and medicinal plants may be used in remediating organic and inorganic pollutants. However, more studies are needed to identify promising plant species and optimum environmental conditions suitable for phytoremediation. Further efforts are also needed to make this technique applicable in the field scale. If phytoremediation is successfully applied, cost reduction and clean

environmental conditions could be achieved. With that, the full potential of Malaysian medicinal plants, not only as traditional medicine but also as phytoremediation agents, can be exploited.

ACKNOWLEDGMENTS

We thank Universiti Teknologi Malaysia and the Ministry of Education, Malaysia for providing the Fundamental Research Scheme Grant (7845.4F180) for this study.

REFERENCES

1. E. Pilon-Smits, "Phytoremediation", *Ann. Rev. Plant Biol.*, **2005**, *56*, 15-39.
2. N. Rascio and F. Navari-Izzo, "Heavy metal hyperaccumulating plants: How and why do they do it? And what makes them so interesting?", *Plant Sci.*, **2011**, *180*, 169-181.
3. S. Talukdar and S. Bhardwaj, "Bioremediation of heavy metals using metal hyperaccumulator plants", in "Fungi as Bioremediators" (Ed. E. M. Goltapeh, Y. R. Danesh and A. Varma), Springer, New York, **2013**, pp.467-480.
4. A. C. Singer, D. E. Crowley and I. P. Thompson, "Secondary plant metabolites in phytoremediation and biotransformation", *Trends Biotechnol.*, **2003**, *21*, 123-130.
5. A. Mithofer, B. Schulze and W. Boland, "Biotic and heavy metal stress response in plants: Evidence for common signals", *FEBS Lett.*, **2004**, *566*, 1-5.
6. P. Sharma and S. Pandey, "Status of phytoremediation in world scenario", *Int. J. Environ. Bioremed. Biodegrad.*, **2014**, *2*, 178-191.
7. N. Mohammad, "Environmental law and policy practices in Malaysia: An empirical study", *Aust. J. Basic Appl. Sci.*, **2011**, *5*, 1248-1260.
8. M. Mustafa, "The environmental quality Act 1974: A significant legal instrument for implementing environmental policy directives of Malaysia", *IJUM Law J.*, **2011**, *19*, 1-34.
9. Department of Environment Malaysia, "Official portal of Department of Environment", **2015**, <http://www.doe.gov.my/portalv1/en> (Accessed: May 2015).
10. Environmental Quality Report, **2012**, Department of Environment, Ministry of Natural Resources and Environment, Malaysia.
11. Environmental Quality Report, **2013**, Department of Environment, Ministry of Natural Resources and Environment, Malaysia.
12. Environmental Quality Report, **2010**, Department of Environment, Ministry of Natural Resources and Environment, Malaysia.
13. M. C. Houston, "The role of mercury and cadmium heavy metals in vascular disease, hypertension, coronary heart disease, and myocardial infarction", *Altern. Therap. Health Med.*, **2007**, *13*, 128-133.
14. Environmental Quality Report, **2011**, Department of Environment, Ministry of Natural Resources and Environment, Malaysia.
15. A. R. Abdullah, "Environmental pollution in Malaysia: Trends and prospects", *Trends Anal. Chem.*, **1995**, *14*, 191-198.
16. C. Y. Yin, S. Abdul-Talib, G. Balamurugan and K. S. Lian, "Contaminated land remediation technologies: Current usage and applicability in Malaysia", *The Ingenieur*, **2006**, *32*, 21-24.
17. M. S. Zaini, N. Ismail, C. K. Lim, C. H. Neoh, C. Y. Lam, A. Aris, Z. A. Majid, F. A. Manan and Z. Ibrahim, "Optimisation of biostructure for the adsorption of petrochemical wastewater using statistical approach", *Clean Technol. Environ. Policy*, **2015**, *17*, 249-256.

18. L. A. Manaf, M. A. A. Samah and N. I. M. Zukki, "Municipal solid waste management in Malaysia: Practices and challenges", *Waste Manag.*, **2009**, 29, 2902-2906.
19. N. Ahalya, T. V. Ramachandra and R. D. Kanamadi, "Biosorption of heavy metals", *Res. J. Chem. Environ.*, **2003**, 7, 71-78.
20. M. A. Barakat, "New trends in removing heavy metals from industrial wastewater", *Arab. J. Chem.*, **2011**, 4, 361-377.
21. N. A. Zakaria, A. Ab. Ghani, R. Abdullah, L. M. Sidek, A. H. Kassim and A. Ainan, "MSMA-A new urban stormwater management manual for Malaysia", Proceedings of 6th International Conference on Hydro-Science and Engineering, **2004**, Brisbane, Australia.
22. Ab. A. Latiff, A. Karim, M. B. Ridzuan, D. Yeoh and Y. T. Hung, "Heavy metal removal by crops from land application of sludge", in "Environmental Bioengineering: Handbook of Environmental Engineering" (Ed. L. K. Wang, J. H. Tay, S. T. L. Tay and Y. T. Hung), Vol. 11, Humana Press, Totowa (NJ), **2010**, pp.211-232.
23. C. K. Yap, M. R. M. Fitri, Y. Mazyhar and S. G. Tan, "Effects of metal-contaminated soils on the accumulation of heavy metals in different parts of *Centella asiatica*: A laboratory study", *Sains Malaysiana*, **2010**, 39, 347-352.
24. A. Abdu, N. Aderis, H. Abdul-Hamid, N. M. Majid, S. Jusop, D. S. Karam and K. Ahmad, "Using *Orthosiphon stamineus* B. for phytoremediation of heavy metals in soils amended with sewage sludge", *Amer. J. Appl. Sci.*, **2010**, 8, 323-331.
25. N. M. Majid, M. M. Islam and L. Mathew, "Heavy metal uptake and translocation by mangium (*Acacia mangium*) from sewage sludge contaminated soil", *Aust. J. Crop Sci.*, **2012**, 6, 1228-1235.
26. N. M. Majid, M. M. Islam, Y. Riasmi and A. Abdu, "Assessment of heavy metal uptake and translocation by *Pluchea indica* L. from sawdust sludge contaminated soil", *J. Food Agric. Environ.*, **2012**, 10, 849-855.
27. N. M. Majid, M. M. Islam and Y. Riasmi, "Heavy metal uptake and translocation by *Jatropha curcas* L. in sawdust sludge contaminated soils", *Aust. J. Crop Sci.*, **2012**, 6, 891-898.
28. W. M. Ho, L. H. Ang and D. K. Lee, "Assessment of Pb uptake, translocation and immobilization in kenaf (*Hibiscus cannabinus* L.) for phytoremediation of sand tailings", *J. Environ. Sci. (China)*, **2008**, 20, 1341-1347.
29. C. M. Hasfalina, R. Z. Maryam, C. A. Luqman and M. Rashid, "Adsorption of copper (II) from aqueous medium in fixed-bed column by kenaf fibres", *APCBEE Procedia*, **2012**, 3, 255-263.
30. I. A. Albaldawi, F. Suja, S. R. S. Abdullah and M. Idris, "Preliminary test of hydrocarbon exposure on *Salvinia molesta* in phytoremediation process", *Revelat. Sci.*, **2011**, 1, 52-56.
31. S. N. A. Sanusi, S. R. S. Abdullah and M. Idris, "Preliminary test of phytoremediation of hydrocarbon contaminated soil using *Paspalum vaginatum* sw.", *Aust. J. Basic Appl. Sci.*, **2012**, 6, 39-42.
32. T. P. Choo, C. K. Lee, K. S. Low and O. Hishamuddin, "Accumulation of chromium (VI) from aqueous solutions using water lilies (*Nymphaea spontanea*)", *Chemosphere*, **2006**, 62, 961-967.
33. B. S. Ismail, K. Farihah and J. Khairiah, "Bioaccumulation of heavy metals in vegetables from selected agricultural areas", *Bull. Environ. Contam. Toxicol.*, **2005**, 74, 320-327.
34. Z. Ismail and A. M. Beddri, "Potential of water hyacinth as a removal agent for heavy metals from petroleum refinery effluents", *Water Air Soil Pollut.*, **2009**, 199, 57-65.

35. C. O. Akinbile, M. S. Yusoff and L. M. Shian, "Leachate characterization and phytoremediation using water hyacinth (*Eichhornia crassipes*) in Pulau Burung, Malaysia", *Bioremed. J.*, **2012**, *16*, 9-18.
36. C. O. Akinbile and M. S. Yusoff, "Assessing water hyacinth (*Eichhornia crassipes*) and lettuce (*Pistia stratiotes*) effectiveness in aquaculture wastewater treatment", *Int. J. Phytoremed.*, **2012**, *14*, 201-211.
37. S. L. Lim, W. L. Chu and S. M. Phang, "Use of *Chlorella vulgaris* for bioremediation of textile wastewater", *Bioresour. Technol.*, **2010**, *101*, 7314-7322.
38. M. Ebrahimipour and I. Mushrifah, "Heavy metal concentrations (Cd, Cu and Pb) in five aquatic plant species in Tasik Chini, Malaysia", *Environ. Geol.*, **2008**, *54*, 689-698.
39. A. Azhari, M. N. Dalimin and S. T. Wee, "Polycyclic Aromatic Hydrocarbons (PAHs) from vehicle emission in the vegetation of highway roadside in Johor, Malaysia," *Int J. Environ. Sci. Devel.*, **2011**, *2*, 465-468.
40. M. A. Ashraf, M. J. Maah and I. B. Yusoff, "Assessment of phytoextraction efficiency of naturally grown plant species at the former tin mining catchment", *Fresenius Environ. Bull.*, **2012**, *21*, 523-533.
41. E. S. M. Ameen, S. A. Muyibi and M. I. Abdulkarim, "Microfiltration of pretreated sanitary landfill leachate," *The Environmentalist*, **2011**, *31*, 208-215.
42. K. G. Ramawat, S. Dass and M. Mathur, "The chemical diversity of bioactive molecules and therapeutic potential of medicinal plants", in "Herbal Drugs: Ethnomedicine to Modern Medicine" (Ed. K.G. Ramawat), Springer, Berlin, **2009**, pp.7-32.
43. A. Michalak, "Phenolic compounds and their antioxidant activity in plants growing under heavy metal stress", *Polish J. Environ. Studies*, **2006**, *15*, 523-530.
44. J. Psotova, J. Lasovsky and J. Vicar, "Metal-chelating properties, electrochemical behavior, scavenging and cytoprotective activities of six natural phenolics", *Biomed. Pap. Med. Fac. Univ. Palacký Olomouc Czech. Repub.*, **2003**, *147*, 147-153.
45. D. L. Jones, "Organic acids in the rhizosphere – A critical review", *Plant Soil*, **1998**, *205*, 25-44.
46. G. Máthé-Gáspár and A. Anton, "Phytoremediation study: Factors influencing heavy metal uptake of plants", *Acta Biol. Szeged.*, **2005**, *49*, 69-70.
47. J. A. C. Verkleij, A. Golan-Goldhirsh, D. M. Antosiewicz, J. P. Schwitzguébel and P. Schröder, "Dualities in plant tolerance to pollutants and their uptake and translocation to the upper plant parts", *Environ. Exp. Bot.*, **2009**, *67*, 10-22.
48. P. L. Gratão, A. Polle, P. J. Lea and R. A. Azevedo, "Making the life of heavy metal-stressed plants a little easier", *Funct. Plant Biol.*, **2005**, *32*, 481-494.
49. I. M. Møller, P. E. Jensen and A. Hansson, "Oxidative modifications to cellular components in plants", *Ann. Rev. Plant Biol.*, **2007**, *58*, 459-481.
50. P. Sharma, A. B. Jha, R. S. Dubey and M. Pessarakli, "Reactive oxygen species, oxidative damage, and antioxidative defense mechanism in plants under stressful conditions", *J. Bot.*, **2012**, *2012*, Art. ID 217037.
51. S. Goyal, C. Lambert, S. Cluzet, J. M. Mérillon and K. Ramawat, "Secondary metabolites and plant defence", in "Plant Defence: Biological Control" (Ed. J. M. Mérillon and K. G. Ramawat), Springer, Dordrecht, **2012**, pp.109-138.
52. P. K. Padmavathamma and L. Y. Li, "Phytoremediation technology: Hyper-accumulation metals in plants", *Water Air Soil Pollut.*, **2007**, *184*, 105-126.

53. R. Tolra, J. Barcelo and C. Poschenrieder, "Constitutive and aluminium-induced patterns of Phenolic compounds in two maize varieties differing in aluminium tolerance", *J. Inorg. Biochem.*, **2009**, *103*, 1486-1490.
54. S. Shobha and S. Alok, "Phyto-extraction of lead and cadmium from a contaminated soil by Indian mustard plant", *Res. J. Chem. Environ.*, **2011**, *15*, 345-348.
55. E. Masarovicova and K. Kralova, "Plant-heavy metal interaction: Phytoremediation, biofortification and nanoparticles", in "Advances in Selected Plant Physiology Aspects" (Ed. G. Montanaro and B. Dichio), InTech., Rijeka (Croatia), **2012**, pp.75-102.
56. J. Kovacik, B. Klejdus and M. Backor, "Phenolic metabolism of *Matricaria chamomilla* plants exposed to nickel", *J. Plant Physiol.*, **2009**, *166*, 1460-1464.
57. R. S. Hegde and J. S. Fletcher, "Influence of plant growth stage and season on the release of root phenolics by mulberry as related to development of phytoremediation technology", *Chemosphere*, **1996**, *32*, 2471-2479.
58. D. Techer, P. Laval-Gilly, S. Henry, A. Bennisroune, P. Formanek, C. Martinez-Chois, M. D'Innocenzo, F. Muanda, A. Dicko, K. Rejsek and J. Falla, "Contribution of *Miscanthus x giganteus* root exudates to the biostimulation of PAH degradation: An in vitro study", *Sci. Total Environ.*, **2011**, *409*, 4489-4495.
59. E. S. Gilbert and D. E. Crowley, "Plant compounds that induce polychlorinated biphenyl biodegradation by *Arthrobacter* sp. strain B1B", *Appl. Environ. Microbiol.*, **1997**, *63*, 1933-1938.
60. S. Lee, J. S. Moon, T. S. Ko, D. Petros, P. B. Goldsbrough and S. S. Korban, "Overexpression of Arabidopsis phytochelatin synthase paradoxically leads to hypersensitivity to cadmium stress", *Plant Physiol.*, **2003**, *131*, 656-663.
61. S. A. Nasim and B. Dhir, "Heavy metals alter the potency of medicinal plants", in "Reviews of Environmental Contamination and Toxicology" (Ed. D. M. Whitacre), Springer, New York, **2010**, pp.139-149.
62. M. N. V. Prasad and H. M. de O. Freitas, "Metal hyperaccumulation in plants – Biodiversity prospecting for phytoremediation technology", *Electron. J. Biotechnol.*, **2003**, *6*, 285-321.
63. A. R. Rivelli, S. De Maria, M. Puschenreiter and P. Gherbin, "Accumulation of cadmium, zinc, and copper by *Helianthus annuus* L.: Impact on plant growth and uptake of nutritional elements", *Int. J. Phytoremed.*, **2012**, *14*, 320-334.
64. G. M. Kertulis-Tartar, L. Q. Ma, C. Tu and T. Chirenje, "Phytoremediation of an arsenic-contaminated site using *Pteris vittata* L.: A two-year study", *Int. J. Phytoremed.*, **2006**, *8*, 311-322.
65. J. L. Couselo, E. Corredoira, A. M. Vieitez and A. Ballester, "Plant tissue culture of fast growing trees for phytoremediation research", in "Plant Cell Culture Protocols, Methods in Molecular Biology" (Ed. V. M. Loyola-Vargas and N. Ochoa-Alejo), Humana Press, New York, **2012**, pp.247-263.
66. P. M. Doran, "Application of plant tissue cultures in phytoremediation research: Incentives and limitations", *Biotechnol. Bioeng.*, **2009**, *103*, 60-76.
67. M. A. Khatun, M. Harun-Or-Rashid and M. Rahmatullah, "Scientific validation of eight medicinal plants used in traditional medicinal systems of Malaysia: A review", *Amer.-Euras. J. Sustain. Agric.*, **2011**, *5*, 67-75.
68. I. Jantan, "Medicinal plant research in Malaysia: Scientific interests and advances", *J. Sains Kesihatan Malaysia*, **2004**, *2*, 27-46.

69. K. Kralova and E. Masarovicova, "Plants for the future", *Ecol. Chem. Eng.*, **2006**, *13*, 1179-1207.
70. Y. G. Zhu, E. A. Pilon-Smits, F. J. Zhao, P. N. Williams and A. A. Meharg, "Selenium in higher plants: Understanding mechanisms for biofortification and phytoremediation", *Trends Plant Sci.*, **2009**, *14*, 436-442.
71. Y. Zuo and F. Zhang, "Iron and zinc biofortification strategies in dicot plants by intercropping with gramineous species: A review", *Agron. Sustain. Devel.*, **2009**, *29*, 63-71.
72. P. J. White and M. R. Broadley, "Physiological limits to zinc biofortification of edible crops", *Front. Plant Sci.*, **2011**, *2*, 80 (doi: 10.3389/fpls.2011.00080).
73. M. L. Guerinot and D. E. Salt, "Fortified foods and phytoremediation. Two sides of the same coin", *Plant Physiol.*, **2001**, *125*, 164-167.
74. R. B. Bagdat and E. M. Eid, "Phytoremediation behaviour of some medicinal and aromatic plants to various pollutants", *J. Field Crops Central Res. Inst. Ankara*, **2007**, *16*, 1-10.
75. V. Zheljazkov and D. Jekov, "Heavy metal content in some essential oils and plant extracts", *Acta Horticulturae (ISHS)*, **1996**, *426*, 427-434.
76. World Health Organization, "National Policy on Traditional Medicine and Regulation of Herbal Medicines—Report of a WHO Global Survey", **2015**, <http://apps.who.int/medicinedocs/es/d/Js7916e/9.6.html> (Accessed: May 2015).
77. O. F. Kunle, H. O. Egharevba and P. O. Ahmadu, "Standardization of herbal medicines—A review", *Int. J. Biodivers. Conserv.*, **2012**, *4*, 101-112.
78. Ministry of Health Malaysia, "Official portal of National Pharmaceutical Control Bureau", **2015**, <http://portal.bpfk.gov.my/index.cfm?menuid=4> (Accessed: May 2015).
79. J. A. Jamal, "Malay traditional medicine: An overview of scientific and technological progress", *Asia-Pac. Tech Monit.*, **2006**, Nov.-Dec., 37-49.
80. H. H. Ang and K. L. Lee, "Contamination of mercury in Tongkat Ali Hitam herbal preparations", *Food Chem. Toxicol.*, **2006**, *44*, 1245-1250.
81. E. Masarovicova and K. Kralova, "Medicinal plants: Past, nowadays, future", *Acta Horticult.*, **2007**, *49*, 19-27.
82. Y. Ma, M. N. Prasad, M. Rajkumar and H. Freitas, "Plant growth promoting rhizobacteria and endophytes accelerate phytoremediation of metalliferous soils", *Biotechnol. Adv.*, **2011**, *29*, 248-258.
83. S. Cherian and M. M. Oliveira, "Transgenic plants in phytoremediation: Recent advances and new possibilities", *Environ. Sci. Technol.*, **2005**, *39*, 9377-9390.
84. M. Sakakibara, A. Watanabe, M. Inoue, S. Sano and T. Kaise, "Phytoextraction and phytovolatilization of arsenic from As-contaminated soils by *Pteris vittata*", *Proc. Ann. Int. Conf. Soils Sediments Water Energy*, **2007**, *12*, Art. 26.
85. Y. G. Zhu and B. P. Rosen, "Perspectives for genetic engineering for the phytoremediation of arsenic-contaminated environments: From imagination to reality?", *Curr. Opin. Biotechnol.*, **2009**, *20*, 220-224.
86. V. Karthik, K. Raju, M. Ayyanar, K. Gowrishankar and T. Sekar, "Ethnomedicinal uses of pteridophytes in Kolli Hills, Eastern Ghats of Tamil Nadu, India", *J. Nat. Prod. Plant Resour.*, **2011**, *1*, 50-55.

Full Paper

Fibonacci p -sequences in groups

Ömür Deveci * and Metin Avcı

Department of Mathematics, Faculty of Science and Letters, Kafkas University, 36100 Kars, Turkey

* Corresponding author, e-mail: odeveci36@hotmail.com; metinavci36@gmail.com

Received: 6 June 2014 / Accepted: 25 August 2015 / Published: 30 September 2015

Abstract: The Fibonacci p -sequence modulo m is studied. The Fibonacci p -orbit and basic Fibonacci p -orbit of a group are defined, and then the lengths of periods of these orbits are examined. Furthermore, the Fibonacci p -lengths and basic Fibonacci p -lengths of polyhedral groups $(2, 2, 2)$, $(n, 2, 2)$, $(2, n, 2)$ and $(2, 2, n)$ for $n \geq 3$ are obtained.

Keywords: linear recurrence sequences, Fibonacci p -sequences, Fibonacci p -orbit

INTRODUCTION

Linear recurrence sequences appear in modern research in many fields, from mathematics, physics, computer science, architecture to nature and art [1-21]. The study of recurrence sequences in groups began with the earlier work of Wall [22], who investigated the ordinary Fibonacci sequence in cyclic groups. The concept was extended to some special linear recurrence sequences by several authors [23-35]. In this paper we extend the theory to Fibonacci p -sequences.

The Fibonacci p -sequence $\{F_p(n)\}$ for any given $p (p = 1, 2, 3, L)$ is defined [36, 37] by the following recurrence equation:

$$F_p(n) = F_p(n-1) + F_p(n-p-1) \quad (1)$$

for $n > p$, where $F_p(0) = 0, F_p(1) = L = F_p(p) = 1$.

The Fibonacci p -matrix Q_p was given by Stakhov [36] as follows:

$$Q_p = \begin{bmatrix} 1 & 0 & 0L & 0 & 1 \\ 1 & 0 & 0L & 0 & 0 \\ 0 & 1 & 0L & 0 & 0 \\ \mathbf{ML} & \mathbf{O} & \mathbf{L} & \mathbf{MM} & \\ 0L & 0 & 1 & 0 & 0 \\ 0 & 0L & 0 & 1 & 0 \end{bmatrix}_{(p+1) \times (p+1)} \quad (2)$$

Also, he showed that

$$Q_p^n = \begin{bmatrix} F_p(n+1) & F_p(n-p+1) & L & F_p(n-1) & F_p(n) \\ F_p(n) & F_p(n-p) & L & F_p(n-2) & F_p(n-1) \\ M & M & M & M & M \\ F_p(n-p+2) & F_p(n-2p+2) & L & F_p(n-p) & F_p(n-p+1) \\ F_p(n-p+1) & F_p(n-2p+1) & L & F_p(n-p-1) & F_p(n-p) \end{bmatrix}_{(p+1) \times (p+1)} \quad (3)$$

It is well known that a sequence is periodic if, after a certain point, it consists only of repetitions of a fixed subsequence. The number of elements in the repeating subsequence is the period of the sequence. For example, the sequence $a, b, c, d, b, c, d, b, c, d, L$ is periodic after the initial element a and has period 3. A sequence is simply periodic with period k if the first k elements in the sequence form a repeating subsequence. For example, the sequence $a, b, c, d, a, b, c, d, a, b, c, d, L$ is simply periodic with period 4.

FIBONACCI p -SEQUENCES MODULO m

Reducing the Fibonacci p -sequence $\{F_p(n)\}$ modulo m , we obtain the following repeating sequence:

$$\{F_p^{(m)}(n)\} = \{F_p^{(m)}(0), F_p^{(m)}(1), F_p^{(m)}(2), L, F_p^{(m)}(p), F_p^{(m)}(p+1), L, F_p^{(m)}(i), L\},$$

where $F_p^{(m)}(i) = F_p(i) \pmod{m}$. It has the same recurrence relation as in (1).

Theorem 1. $\{F_p^{(m)}(n)\}$ is a simple periodic sequence.

Proof. Let $S = \{(x_1, x_2, L, x_{p+1}) \mid 0 \leq x_i \leq m-1\}$. Then we have $|S| = m^{p+1}$ being finite; that is, for any $j \geq 0$, there exists $i \geq j$ such that $F_p^{(m)}(i+p) \equiv F_p^{(m)}(j+p)$, $F_p^{(m)}(i+p-1) \equiv F_p^{(m)}(j+p-1)$, L , $F_p^{(m)}(i+1) \equiv F_p^{(m)}(j+1)$ and $F_p^{(m)}(i) \equiv F_p^{(m)}(j)$. From the definition of the Fibonacci p -sequence we have $F_p(n-p-1) = F_p(n) - F_p(n-1)$. Then we can easily get that $F_p^{(m)}(i-1) \equiv F_p^{(m)}(j-1)$, $F_p^{(m)}(i-2) \equiv F_p^{(m)}(j-2)$, L , $F_p^{(m)}(i-j+1) \equiv F_p^{(m)}(1)$, and $F_p^{(m)}(i-j+1) \equiv F_p^{(m)}(0)$, which implies that $\{F_p^{(m)}(n)\}$ is a simple periodic sequence.

Let the notation $l_p(m)$ denote the length of the period of the sequence $\{F_p^{(m)}(n)\}$. For given a matrix $A = [a_{ij}]$ of integers, $A \pmod{m}$ means that the entry of A is a reduced modulo m , i.e. $A \pmod{m} = (a_{ij} \pmod{m})$. Let k be a prime and let $\langle Q_p \rangle_{k^u} = \{Q_p^i \pmod{k^u} \mid i \geq 0\}$. Since $\det Q_p = (-1)^p$, the set $\langle Q_p \rangle_{k^u}$ is a cyclic group. We denote the order of $\langle Q_p \rangle_{k^u}$ by $|\langle Q_p \rangle_{k^u}|$. From (3), it clear that $l_p(k^u) = |\langle Q_p \rangle_{k^u}|$.

Example 1. We have $\{F_2^{(5)}(n)\} = \{0, 1, 1, 1, 2, 3, 4, 1, 4, 3, 4, 3, 1, 0, 3, 4, 4, 2, 1, 0, 2, 3, 3, 0, 3, 1, 1, 4, 0, 1, 0, 0, 1, 1, \dots\}$, and then repeat. So, we get $l_2(5) = 31$.

Theorem 2. Let t be the largest positive integer and let k be a prime such that $l_p(k) = l_p(k^t)$. Then $l_p(k^\alpha) = k^{\alpha-t} \cdot l_p(k)$ for every $\alpha \geq t$.

Proof. Let q be a positive integer. Since $Q_p^{l_p(k^{q+1})} \equiv I \pmod{k^{q+1}}$, we can write $Q_p^{l_p(k^{q+1})} \equiv I \pmod{k^q}$. Then we show that $l_p(k^{q+1})$ is divisible by $l_p(k^q)$. Also, writing $Q_p^{l_p(k^q)} = I + (a_{ij}^{(q)} \cdot k^q)$, we obtain, by the binomial expansion,

$$Q_p^{l_p(k^q) \cdot k} = \left(I + (a_{ij}^{(q)} \cdot k^q) \right)^k = \sum_{i=0}^k \binom{k}{i} (a_{ij}^{(q)} \cdot k^q)^i \equiv I \pmod{k^{q+1}}.$$

This shows that $l_p(k^{q+1})$ divides $l_p(k^q) \cdot k$. Therefore, $l_p(k^{q+1}) = l_p(k^q)$ or $l_p(k^{q+1}) = l_p(k^q) \cdot k$, and the latter holds if and only if there is an $a_{ij}^{(q)}$ which is not divisible by k . Since $l_p(k^t) \neq l_p(k^{t+1})$, there is an $a_{ij}^{(t+1)}$ which is not divisible by k ; thus, $l_p(k^{t+1}) \neq l_p(k^{t+2})$. To complete the proof, we may use an inductive method on t .

Theorem 3. If m has the prime factorisation: $m = \prod_{i=1}^t k_i^{e_i}$, ($t \geq 1$), then $l_p(m) = \text{lcm} [l_p(k_i^{e_i})]$.

Proof. The statement ' $l_p(k_i^{e_i})$ is the length of the period of $\{F_p^{(k_i^{e_i})}(n)\}$ ' implies that the sequence $\{F_p^{(k_i^{e_i})}(n)\}$ repeats only after blocks of length $u \cdot l_p(k_i^{e_i})$ ($u \in \mathbb{N}$), and the statement ' $l_p(m)$ is the length of the period $\{F_p^{(m)}(n)\}$ ' implies that $\{F_p^{(k_i^{e_i})}(n)\}$ repeats after $l_p(m)$ terms for all values i . Thus, $l_p(m)$ is of the form $u \cdot l_p(k_i^{e_i})$ for all values of i , and since any such number gives a period of $\{F_p^{(m)}(n)\}$, we easily obtain that $l_p(m) = \text{lcm} [l_p(k_i^{e_i})]$.

Definition 1. Let $l_p^{(a_0, a_1, \dots, a_p)}(m)$ denote the period of the integer-valued recurrence relation $x_n = x_{n-1} + x_{n-p+1}$ for $n > p$, $x_0 = a_0, x_1 = a_1, \dots, x_p = a_p$ when each entry is a reduced modulo m .

Theorem 4. If $a_0, a_1, \dots, a_p, b_0, b_1, \dots, b_p, m \in \mathbb{N}$ is such that $\text{gcd}(a_0, a_1, \dots, a_p, m) = 1$ and $\text{gcd}(b_0, b_1, \dots, b_p, m) = 1$, then

$$l_p^{(a_0, a_1, \dots, a_p)}(m) = l_p^{(b_0, b_1, \dots, b_p)}(m).$$

Proof. Let $X_n = \begin{bmatrix} x_{n+p} \\ x_{n+p-1} \\ \vdots \\ M \\ \vdots \\ x_{n+1} \\ x_n \end{bmatrix}$. Then it is clear that $X_n = (Q_p)^n \cdot X_0$. Since the integers modulo m form

a finite set of equivalence classes, there exist integers n and r such that $(Q_p)^{n+r}$ is congruent elementwise to $(Q_p)^r$ modulo m if p is an even integer and that $(Q_p)^{n+r+1}$ is congruent elementwise to $(Q_p)^r$ modulo m . if p and n are odd integers. Since $\det Q_p = (-1)^p$, $(Q_p)^n$ or $(Q_p)^{n+1}$ is a

$(p+1) \times (p+1)$ identity matrix. Thus, it is verified that $X_n \equiv X_0 \pmod{m}$ or $X_{n+1} \equiv X_0 \pmod{m}$. So the proof is complete.

FIBONACCI p -SEQUENCE AND BASIC FIBONACCI p -SEQUENCE IN GROUPS

Let G be a finite j -generator group and let X be the subset of G^j such that $(x_0, x_1, \dots, x_{j-1}) \in X$ if and only if G is generated by x_0, x_1, \dots, x_{j-1} . We call $(x_0, x_1, \dots, x_{j-1})$ a generating j -tuple for G .

Definition 2. For a p -tuple $(x_0, x_1, \dots, x_{p-1}) \in X$, we define Fibonacci p -orbit $F_p^{(x_0, x_1, \dots, x_{p-1})}(G) = \{a_i\}$ by

$$a_0 = x_0, a_1 = x_1, \dots, a_{p-1} = x_{p-1}, a_p = x_{p-1}, a_{n+p} = a_{n-1} \cdot a_{n+p-1}, n \geq 1.$$

The classic Fibonacci p -sequence in a cyclic group $C = \langle x \rangle$ can be written as $F_p^{(x, x, \dots, x)}(C)$.

Theorem 5. A Fibonacci p -orbit of a finite group is simply periodic.

Proof. Let n be the order of G . Since there are $n^{(p+1)}$ distinct $(p+1)$ -tuples of elements of G , at least one of the $(p+1)$ -tuples appears twice in a Fibonacci p -orbit of G . Because of the repetition, Fibonacci p -orbit is periodic.

Since the Fibonacci p -orbit is periodic, there exist natural numbers u and v , with $u > v$, such that

$$a_{u+1} = a_{v+1}, a_{u+2} = a_{v+2}, \dots, a_{u+p+1} = a_{v+p+1}.$$

By definition of the Fibonacci p -orbit, it is clear that

$$a_u = (a_{u+p+1}) \cdot (a_{u+p})^{-1} \text{ and } a_v = (a_{v+p+1}) \cdot (a_{v+p})^{-1}.$$

Then we may write $a_u = a_v$, and hence

$$a_{u-v} = a_{v-v} = a_0, a_{u-v+1} = a_{v-v+1} = a_1, \dots, a_{u-v+p} = a_{v-v+p} = a_p,$$

which implies that the Fibonacci p -orbit is simply periodic.

Let the notation $LF_p^{(x_0, x_1, \dots, x_{p-1})}(G)$ denote the length of the period of the Fibonacci p -orbit $F_p^{(x_0, x_1, \dots, x_{p-1})}(G)$. It is said to be the Fibonacci p -length with respect to the generating p -tuple $(x_0, x_1, \dots, x_{p-1})$.

To examine the concept more fully we study the action of the automorphism group $\text{Aut } G$ of G on the Fibonacci p -orbit $F_p^{(x_0, x_1, \dots, x_{p-1})}(G)$, $(x_0, x_1, \dots, x_{p-1}) \in X$. Now $\text{Aut } G$ consists of all isomorphisms $\theta : G \rightarrow G$, and if $\theta \in \text{Aut } G$ and $(x_0, x_1, \dots, x_{p-1}) \in X$, then $(x_0\theta, x_1\theta, \dots, x_{p-1}\theta) \in X$.

For a subset $A \subseteq G$ and $\theta \in \text{Aut } G$, the image of A under θ is

$$A\theta = \{a\theta : a \in A\}.$$

Lemma 1. Let $(x_0, x_1, \dots, x_{p-1}) \in X$ and let $\theta \in \text{Aut } G$. Then

$$\left(F_p^{(x_0, x_1, \dots, x_{p-1})}(G)\right)\theta = F_p^{(x_0\theta, x_1\theta, \dots, x_{p-1}\theta)}(G).$$

Proof: Let $F_p^{(x_0, x_1, L, \dots, x_{p-1})}(G) = \{a_i\}$. Since $\{a_i\}\theta = \{a_i\theta\}$ and $a_{i+p}\theta = (a_{i-1}a_{i+p-1})\theta = a_{i-1}\theta a_{i+p-1}\theta$, we have the conclusion.

Each generating p -tuple $(x_0, x_1, L, \dots, x_{p-1}) \in X$ maps to $|\text{Aut } G|$ distinct elements of X under the action of elements of $\text{Aut } G$. Hence there are

$$d_p(G) = |X|/|\text{Aut } G|$$

non-isomorphic generating p -tuples for G [27]. The notation $d_p(G)$ was introduced by Hall [38].

Suppose ω of the elements of $\text{Aut } G$ maps $F_p^{(x_0, x_1, L, \dots, x_{p-1})}(G)$ into itself. Then there are $|\text{Aut } G|/\omega$ distinct Fibonacci p -orbits $F_p^{(x_0\theta, x_1\theta, L, \dots, x_{p-1}\theta)}(G)$ for $\theta \in \text{Aut } G$.

Definition 3. For a p -tuple $(x_0, x_1, L, \dots, x_{p-1}) \in X$, the basic Fibonacci p -orbit $\overline{F}_p^{(x_0, x_1, L, \dots, x_{p-1})}(G)$ of the basic period m is a sequence of group elements $b_0, b_1, b_2, L, \dots, b_n, L$ for which, given an initial (seed) set $b_0 = x_0, b_1 = x_1, L, \dots, b_{p-1} = x_{p-1}, b_p = x_{p-1}$, each element is defined by

$$b_{n+p} = b_{n-1} \cdot b_{n+p-1}, \quad n \geq 1,$$

where $m \geq 1$ is the least integer, with

$$b_0 = b_m\theta, b_1 = b_{m+1}\theta, L, \dots, b_{p-1} = b_{m+p-1}\theta, b_p = b_{m+p}\theta,$$

for some $\theta \in \text{Aut } G$. Since G is a finite p -generator group and $b_m, b_{m+1}, L, \dots, b_{m+p-1}$ generates G , it follows that θ is uniquely determined. Clearly, the basic Fibonacci p -orbit $\overline{F}_p^{(x_0, x_1, L, \dots, x_{p-1})}(G)$ contains m elements.

Let the notation $L\overline{F}_p^{(x_0, x_1, L, \dots, x_{p-1})}(G)$ denote the basic length of the period of the basic Fibonacci p -orbit $\overline{F}_p^{(x_0, x_1, L, \dots, x_{p-1})}(G)$. It is said to be the basic Fibonacci p -length with respect to the generating p -tuple $(x_0, x_1, L, \dots, x_{p-1})$.

Theorem 6. Let G be a finite group and $(x_0, x_1, L, \dots, x_{p-1}) \in X$. If $L\overline{F}_p^{(x_0, x_1, L, \dots, x_{p-1})}(G) = n$ and $\overline{F}_p^{(x_0, x_1, L, \dots, x_{p-1})}(G) = m$, then m divides n and there are n/m elements of $\text{Aut } G$ which map $F_p^{(x_0, x_1, L, \dots, x_{p-1})}(G)$ into themselves.

Proof: Since

$$F_p^{(x_0, x_1, L, \dots, x_{p-1})}(G) = \overline{F}_p^{(x_0, x_1, L, \dots, x_{p-1})}(G) \cup \overline{F}_p^{(x_0\theta, x_1\theta, L, \dots, x_{p-1}\theta)}(G) \cup \overline{F}_p^{(x_0\theta^2, x_1\theta^2, L, \dots, x_{p-1}\theta^2)}(G) \cup L$$

and

$$L\overline{F}_p^{(x_0, x_1, L, \dots, x_{p-1})}(G) = L\overline{F}_p^{(x_0\theta, x_1\theta, L, \dots, x_{p-1}\theta)}(G),$$

we have $n = m\lambda$, where λ is the order of the automorphism $\theta \in \text{Aut } G$. Thus, it is verified that $1, \theta, \theta^2, L, \dots, \theta^{\lambda-1}$ map $F_p^{(x_0, x_1, L, \dots, x_{p-1})}(G)$ into themselves.

APPLICATIONS

For application, we obtain the lengths of the periods of the Fibonacci p -orbits and the basic Fibonacci p -orbits of polyhedral groups $(2, 2, 2), (n, 2, 2), (2, n, 2)$ and $(2, 2, n)$ for $n \geq 3$.

Definition 4. The polyhedral group (l, m, n) for $l, m, n > 1$ is defined by the presentation

$$\langle x, y, z : x^l = y^m = z^n = xyz = e \rangle$$

or

$$\langle x, y : x^l = y^m = (xy)^n = e \rangle.$$

The polyhedral group (l, m, n) is finite if and only if the number

$$\mu = lmn \left(\frac{1}{l} + \frac{1}{m} + \frac{1}{n} - 1 \right) = mn + nl + lm - lmn$$

is positive, i.e. in the case $(2, 2, n)$, $(2, 3, 3)$, $(2, 3, 3)$, $(2, 3, 4)$, $(2, 3, 5)$. Its order is $2lmn/\mu$. Using Tietze transformations we may show that $(l, m, n) \cong (m, n, l) \cong (n, l, m)$. More information on these groups can be found in the work by Coxeter and Moser [39].

In this section we obtain the Fibonacci p -lengths and the basic Fibonacci p -lengths of the polyhedral groups $(2, 2, 2)$, $(n, 2, 2)$, $(2, n, 2)$ and $(2, 2, n)$ for $n \geq 3$ as applications of the results obtained.

Theorem 7. i. $LF_2^{(x,y)}((2, 2, 2)) = \overline{LF}_2^{(x,y)}((2, 2, 2)) = 7$.

ii. $LF_3^{(x,y,z)}((2, 2, 2)) = \overline{LF}_3^{(x,y,z)}((2, 2, 2)) = 15$.

Proof. i. The orbit $F_2^{(x,y)}((2, 2, 2))$ is $x, y, y, xy, x, xy, e, x, y, y, L$. So we get $LF_2^{(x,y)}((2, 2, 2)) = \overline{LF}_2^{(x,y)}((2, 2, 2)) = 7$ since $x\theta = x$ and $y\theta = y$, where θ is the identity transform.

ii. The orbit $F_3^{(x,y,z)}((2, 2, 2))$ is $x, y, z, z, y, e, z, e, y, y, x, x, z, x, e, x, y, z, z, L$. So we get $LF_3^{(x,y,z)}((2, 2, 2)) = \overline{LF}_3^{(x,y,z)}((2, 2, 2)) = 15$ since $x\theta = x$, $y\theta = y$ and $z\theta = z$, where θ is the identity transform.

Theorem 8. The lengths of the Fibonacci p -orbits and the basic lengths of the Fibonacci p -orbits of the polyhedral groups $(n, 2, 2)$, $(2, n, 2)$ and $(2, 2, n)$ for $n \geq 3$ are:

i. The Fibonacci 2-lengths and the basic Fibonacci 2-lengths in the 2-generator cases are:

i'. $LF_2^{(x,y)}((n, 2, 2)) = 7$ and $\overline{LF}_2^{(x,y)}((n, 2, 2)) = 14$.

$$\text{ii'}. LF_2^{(x,y)}((2, n, 2)) = LF_2^{(x,y)}((2, 2, n)) = \begin{cases} \frac{7n}{2}, & n \equiv 0 \pmod{4}, \\ 7n, & n \equiv 2 \pmod{4}, \\ 14n, & \text{otherwise} \end{cases} \quad \text{and}$$

$$\overline{LF}_2^{(x,y)}((2, n, 2)) = \overline{LF}_2^{(x,y)}((2, 2, n)) = \begin{cases} \frac{7n}{2}, & n \equiv 0 \pmod{4}, \\ \frac{7n}{2}, & n \equiv 2 \pmod{4}, \\ 7n, & \text{otherwise.} \end{cases}$$

ii. The Fibonacci 3-lengths and the basic Fibonacci 3-lengths in the 3-generator cases are:

$$LF_3^{(x,y,z)}((G_n)) = \begin{cases} \frac{15n}{2}, & n \equiv 0 \pmod{4}, \\ 15n, & n \equiv 2 \pmod{4}, \\ 30n, & \text{otherwise} \end{cases} \quad \text{and} \quad \overline{LF}_3^{(x,y,z)}((G_n)) = \begin{cases} \frac{15n}{2}, & n \equiv 0 \pmod{4}, \\ \frac{15n}{2}, & n \equiv 2 \pmod{4}, \\ 15n, & \text{otherwise.} \end{cases}$$

Here G_n ($n \geq 3$) is one the groups $(n, 2, 2)$, $(2, n, 2)$ and $(2, 2, n)$ in the 3-generator cases.

Proof. i.i'. The orbit $F_2^{(x,y)}((n, 2, 2))$ is $x, y, y, xy, x^{-1}, xy, e, x^{-1}, x^2y, x^2y, xy, x, xy, e, x, y, y, L$. So we get $LF_2^{(x,y)}((n, 2, 2)) = 7$ and $\overline{LF}_2^{(x,y)}((n, 2, 2)) = 14$ since $x\theta = x^{-1}$ and $y\theta = x^2y$, where θ is the inner automorphism induced by conjugation by xy .

i.ii'. Firstly, let us consider the group $(2, n, 2)$. The orbit $F_2^{(x,y)}((2, n, 2))$ is

$$x, y, y, xy, x, yx, y^{-2}, y^2x, y^{-1}, y^{-3}, y^5x, y^4x, yx, y^4, x, y, y^5, xy^5, xy^4, yx, y^{-6}, y^2x, y^{-1}, y^{-7}, y^9x, y^8x, yx, y^8, x, y, y^9, L.$$

Using the above, the sequence becomes

$$a_0 = x, a_1 = y, a_2 = y, L, \\ a_{7+14i} = y^2x, a_{8+14i} = y^{-1}, a_{9+14i} = y^{-3-4i}, L, \\ a_{14+14i} = x, a_{15+14i} = y, a_{16+14i} = y^{5+4i}, L,$$

where $i \geq 0$. So we need the smallest $i \in N$ such that $4i = nu_1$ for $u_1 \in N$.

If $n \equiv 0 \pmod{4}$, $i = \frac{n}{4}$. Thus, $LF_2^{(x,y)}((2, n, 2)) = 14 \cdot \frac{n}{4} = \frac{7n}{2}$ and $\overline{LF}_2^{(x,y)}((2, n, 2)) = \frac{7n}{2}$ since $x\theta = x$ and $y\theta = y$, where θ is the identity transform.

If $n \equiv 2 \pmod{4}$, $i = \frac{n}{2}$. Thus, $LF_2^{(x,y)}((2, n, 2)) = 14 \cdot \frac{n}{2} = 7n$ and $\overline{LF}_2^{(x,y)}((2, n, 2)) = \frac{7n}{2}$ since $x\theta = x$ and $y\theta = y^{-1}$, where θ is the inner automorphism induced by conjugation by x .

If $n \equiv 1 \pmod{4}$ or $n \equiv 3 \pmod{4}$, $i = n$. Thus, $LF_2^{(x,y)}((2, n, 2)) = 14n$ and $\overline{LF}_2^{(x,y)}((2, n, 2)) = 7n$ since $x\theta = x$ and $y\theta = y^{-1}$, where θ is the inner automorphism induced by conjugation by x .

Secondly, let us consider the group $(2, 2, n)$. The orbit $F_2^{(x,y)}((2, 2, n))$ is of the following form:

$$a_0 = x, a_1 = y, a_2 = y, L, \\ a_{7+14i} = y(xy)^{4i+3}, a_{8+14i} = y(xy)^{4i+2}, a_{9+14i} = y, L, \\ a_{14+14i} = (xy)^{4i+4}x, a_{15+14i} = (xy)^{4i+3}x, a_{16+14i} = y, L,$$

where $i \geq 0$. So we need the smallest $i \in N$ such that $4i = nu_2$ for $u_2 \in N$.

If $n \equiv 0 \pmod{4}$, $i = \frac{n}{4}$. Thus, $LF_2^{(x,y)}((2, 2, n)) = 14 \cdot \frac{n}{4} = \frac{7n}{2}$ and $\overline{LF}_2^{(x,y)}((2, 2, n)) = \frac{7n}{2}$ since $x\theta = x$ and $y\theta = y$, where θ is the identity transform.

If $n \equiv 2 \pmod{4}$, $i = \frac{n}{2}$. Thus, $LF_2^{(x,y)}((2, 2, n)) = 14 \cdot \frac{n}{2} = 7n$ and $\overline{LF}_2^{(x,y)}((2, 2, n)) = \frac{7n}{2}$ since $x\theta = yxy$ and $y\theta = y$, where θ is the inner automorphism induced by conjugation by y .

If $n \equiv 1 \pmod{4}$ or $n \equiv 3 \pmod{4}$, $i = n$. Thus, $LF_2^{(x,y)}((2, 2, n)) = 14n$ and $\overline{LF}_2^{(x,y)}((2, 2, n)) = 7n$ since $x\theta = yxy$ and $y\theta = y$, where θ is the inner automorphism induced by conjugation by y .

ii. Firstly, let us consider the group $(n, 2, 2)$. The orbit $F_3^{(x,y,z)}((n, 2, 2))$ is $x, y, z, z, xz, x^{-2}, x^2z, x^{-2}, x^3z, xz, x, x^{-1}, x^4z, x^{-3}, x^{-2}, x^{-3}, x^7z, x^4z, x^2z, zx, x^8, zx^4, x^6, zx^7, xz, x^{-5}, x, zx^8, x^9, x^4, x^5, zx^{13}, zx^4, z, x^5z, x^{-18}, x^{14}z, x^{-14}, x^{19}z, xz, x^{13}, x^{-1}, x^{20}z, x^{-19}, x^{-6}, x^{-7}, x^{27}z, x^8z, x^2z, zx^5, x^{32}, zx^{24}, x^{26}, zx^{31}, xz, x^{-25}, x, zx^{32}, x^{33}, x^8, x^9, zx^{41}, zx^8, z, L$.

Using the above, the sequence becomes:

$$a_0 = x, a_1 = y, a_2 = z, a_3 = z, L, \\ a_{15+30i} = x^{-3-4i}, a_{16+30i} = x^{8(i+1)^2-4(i+1)+3}z, a_{17+30i} = x^{4i+4}z, a_{18+30i} = x^2z, L, \\ a_{30+30i} = x^{5+4i}, a_{31+30i} = zx^{8(i+1)^2+4(i+1)+1}, a_{32+30i} = zx^{4i+4}, a_{33+30i} = z, L,$$

where $i \geq 0$. So we need the smallest $i \in N$ such that $4i = nu_3$ for $u_3 \in N$.

If $n \equiv 0 \pmod{4}$, $i = \frac{n}{4}$. Thus, $LF_3^{(x,y,z)}((n, 2, 2)) = 30 \cdot \frac{n}{4} = \frac{15n}{2}$ and $\overline{LF_3^{(x,y,z)}}((n, 2, 2)) = \frac{15n}{2}$ since $x\theta = x, y\theta = y$ and $z\theta = z$, where θ is the identity transform.

If $n \equiv 2 \pmod{4}$, $i = \frac{n}{2}$. Thus, $LF_3^{(x,y,z)}((n, 2, 2)) = 30 \cdot \frac{n}{2} = 15n$ and $\overline{LF_3^{(x,y,z)}}((n, 2, 2)) = \frac{15n}{2}$ since $x\theta = x^{-1}, y\theta = x^3z$ and $z\theta = x^2z$, where θ is the inner automorphism induced by conjugation by xz .

If $n \equiv 1 \pmod{4}$ or $n \equiv 3 \pmod{4}$, $i = n$. Thus, $LF_3^{(x,y,z)}((n, 2, 2)) = 30n$ and $\overline{LF_3^{(x,y,z)}}((n, 2, 2)) = 15n$ since $x\theta = x^{-1}, y\theta = x^3z$ and $z\theta = x^2z$, where θ is the inner automorphism induced by conjugation by xz .

Now, let us consider the group $(2, n, 2)$. The orbit $F_3^{(x,y,z)}((2, n, 2))$ is of the following form:

$$a_0 = x, a_1 = y, a_2 = z, a_3 = z, L, \\ a_{15+30i} = y^{16i^2+20i+4}x, a_{16+30i} = y^{-16i^2-20i-7}, a_{17+30i} = y^{16i^2+28i+9}x, a_{18+30i} = xy, L, \\ a_{30+30i} = xy^{16i^2+36i+20}, a_{31+30i} = y^{16i^2+36i+21}, a_{32+30i} = xy^{16i^2+44i+29}, a_{33+30i} = xy, L,$$

where $i \geq 0$. So we need the smallest $i \in N$ such that $16i^2 + 36i = nu_4$ for $u_4 \in N$.

If $n \equiv 0 \pmod{4}$, $i = \frac{n}{4}$. Thus, $LF_3^{(x,y,z)}((2, n, 2)) = 30 \cdot \frac{n}{4} = \frac{15n}{2}$ and $\overline{LF_3^{(x,y,z)}}((2, n, 2)) = \frac{15n}{2}$ since $x\theta = x, y\theta = y$ and $z\theta = z$, where θ is the identity transform.

If $n \equiv 2 \pmod{4}$, $i = \frac{n}{2}$. Thus, $LF_3^{(x,y,z)}((2, n, 2)) = 30 \cdot \frac{n}{2} = 15n$ and $\overline{LF_3^{(x,y,z)}}((2, n, 2)) = \frac{15n}{2}$ since $x\theta = y^{-2}x, y\theta = y^{-1}$ and $z\theta = z$, where θ is the inner automorphism induced by conjugation by z .

If $n \equiv 1 \pmod{4}$ or $n \equiv 3 \pmod{4}$, $i = n$. Thus, $LF_3^{(x,y,z)}((2, n, 2)) = 30n$ and $\overline{LF_3^{(x,y,z)}}((2, n, 2)) = 15n$ since $x\theta = y^{-2}x, y\theta = y^{-1}$ and $z\theta = z$, where θ is the inner automorphism induced by conjugation by z .

Finally, let us consider the group $(2, 2, n)$. The orbit $F_3^{(x,y,z)}((2, 2, n))$ is of the following form:

$$a_0 = x, a_1 = y, a_2 = z, a_3 = z, L, \\ a_{15+30i} = z^{8i^2+20i+10}x, a_{16+30i} = y, a_{17+30i} = z^{8i^2+16i+5}, a_{18+30i} = z^{-1}, L, \\ a_{30+30i} = xz^{8i^2+28i+20}, a_{31+30i} = y, a_{32+30i} = z^{-8i^2-24i-15}, a_{33+30i} = z, L,$$

where $i \geq 0$. So we need the smallest $i \in N$ such that $4i^2 + 4i = nu_5$ for $u_5 \in N$.

If $n \equiv 0 \pmod{4}$, $i = \frac{n}{4}$. Thus, $LF_3^{(x,y,z)}((2,2,n)) = 30 \cdot \frac{n}{4} = \frac{15n}{2}$ and $\overline{LF}_3^{(x,y,z)}((2,2,n)) = \frac{15n}{2}$ since $x\theta = x$, $y\theta = y$ and $z\theta = z$, where θ is the identity transform.

If $n \equiv 2 \pmod{4}$, $i = \frac{n}{2}$. Thus, $LF_3^{(x,y,z)}((2,2,n)) = 30 \cdot \frac{n}{2} = 15n$ and $\overline{LF}_3^{(x,y,z)}((2,2,n)) = \frac{15n}{2}$ since $x\theta = z^2x$, $y\theta = y$ and $z\theta = z^{-1}$, where θ is the inner automorphism induced by conjugation by y .

If $n \equiv 1 \pmod{4}$ or $n \equiv 3 \pmod{4}$, $i = n$. Thus, $LF_3^{(x,y,z)}((2,2,n)) = 30n$ and $\overline{LF}_3^{(x,y,z)}((2,2,n)) = 15n$ since $x\theta = z^2x$, $y\theta = y$ and $z\theta = z^{-1}$, where θ is the inner automorphism induced by conjugation by y .

ACKNOWLEDGMENT

This project (Project no. 2013-FEF-72) was supported by the Commission for the Scientific Research Projects of Kafkas University.

REFERENCES

1. P. G. Becker, "k-Regular power series and Mahler-type functional equations", *J. Number Theory*, **1994**, 49, 269-286.
2. W. Bosma and C. Kraaikamp, "Metrical theory for optimal continued fractions", *J. Number Theory*, **1990**, 34, 251-270.
3. G. B. Djordjević and H. M. Srivastava, "Some generalizations of the incomplete Fibonacci and the incomplete Lucas polynomials", *Adv. Stud. Contemp. Math.*, **2005**, 11, 11-32.
4. G. B. Djordjević and H. M. Srivastava, "Some generalizations of certain sequences associated with the Fibonacci numbers", *J. Indonesian Math. Soc.*, **2006**, 12, 99-112.
5. S. Falcon and A. Plaza, "k-Fibonacci sequences modulo m ", *Chaos Solitons Fract.*, **2009**, 41, 497-504.
6. A. S. Fraenkel and S. T. Klein, "Robust universal complete codes for transmission and compression", *Discrete Appl. Math.*, **1996**, 64, 31-55.
7. N. D. Gogin and A. A. Myllari, "The Fibonacci-Padovan sequence and MacWilliams transform matrices", *Program. Comput. Soft.*, **2007**, 33, 74-79.
8. D. Kalman, "Generalized Fibonacci numbers by matrix methods", *Fibonacci Quart.*, **1982**, 20, 73-76.
9. G. R. Kaluge, "Penggunaan Fibonacci dan Josephus problem dalam algoritma enkripsi transposisi+substitusi", *Makalah IF3058 Kriptografi - Sem. II Tahun 2010/2011*.
10. E. Kilic and A. P. Stakhov, "On the Fibonacci and Lucas p -numbers, their sums, families of bipartite graphs and permanents of certain matrices", *Chaos Solitons Fract.*, **2009**, 40, 2210-2221.
11. B. K. Kirchoof and R. Rutishauser, "The phyllotaxy of costus (costaceae)", *Bot. Gaz.*, **1990**, 151, 88-105.
12. D. M. Mandelbaum, "Synchronization of codes by means of Kautz's Fibonacci encoding", *IEEE Trans. Inform. Theory*, **1972**, 18, 281-285.
13. M. S. El Naschie, "Deriving the essential features of the standard model from the general theory of relativity", *Chaos Solitons Fract.*, **2005**, 24, 941-946.

14. M. S. El Naschie, "Stability analysis of the two-slit experiment with quantum particles", *Chaos Solitons Fract.*, **2005**, *26*, 291-294.
15. R. G. E. Pinch, "Recurrent sequences modulo prime powers", Proceedings of 3rd IMA Conference on Crptography and Coding, **1991**, Cirencester, United Kingdom, pp.297-310.
16. V. W. de Spinadel, "The family of metallic means", *Vis. Math.*, **1999**, *1*, No.3 (<http://members.tripod.com/vismath1/spinadel/>).
17. V. W. de Spinadel, "The metallic means family and forbidden symmetries", *Int. Math. J.*, **2002**, *2*, 279-288.
18. W. Stein, "Modeling the evolution of stelar architecture in vascular plants", *Int. J. Plant Sci.*, **1993**, *154*, 229-263.
19. D. Tasci and E. Kilic, "On the order-k generalized Lucas numbers", *Appl. Math. Comput.*, **2004**, *155*, 637-641.
20. N. Tuglu, E. G. Kocer and A. P. Stakhov, "Bivariate Fibonacci like p-polynomials", *Appl. Math. Comput.*, **2011**, *217*, 10239-10246.
21. F. Yilmaz and D. Bozkurt, "The generalized order-k Jacobsthal numbers", *Int. J. Contemp. Math. Sci.*, **2009**, *4*, 1685-1694.
22. D. D. Wall, "Fibonacci series modulo m ", *Amer. Math. Monthly*, **1960**, *67*, 525-532.
23. H. Aydin and R. Dikici, "General Fibonacci sequences in finite groups", *Fibonacci Quart.*, **1998**, *36*, 216-221.
24. C. M. Campbell and P. P. Campbell, "The Fibonacci length of certain centro-polyhedral groups", *J. Appl. Math. Comput.*, **2005**, *19*, 231-240.
25. C. M. Campbell, H. Doostie and E. F. Robertson, "Fibonacci length of generating pairs in groups", in "Applications of Fibonacci Numbers" (Ed. G. E. Bergum A. N. Philippou and A. F. Horadam), Vol. 3, Kluwer Academic Publishers, Dordrecht, **1990**, pp.27-35.
26. O. Deveci, "The k-nacci sequences and the generalized order- k Pell sequences in the semi-direct product of finite cyclic groups", *Chiang Mai J. Sci.*, **2013**, *40*, 89-98.
27. O. Deveci and E. Karaduman, "On the basic k-nacci sequences in finite groups", *Discrete Dyn. Nat. Soc.*, **2011**, *2011*, Art. ID 639476.
28. O. Deveci and E. Karaduman, "The generalized order- k Lucas sequences in finite groups", *J. Appl. Math.*, **2012**, *2012*, Art. ID 464580.
29. O. Deveci and E. Karaduman, "The Pell sequences in finite groups", *Util. Math.*, **2015**, *96*, 263-276.
30. O. Deveci, "The Pell-Padovan sequences and the Jacobsthal-Padovan sequences in finite groups", *Util. Math.*, in press.
31. O. Deveci and Y. Akuzum, "The recurrence sequences via Hurwitz matrices", *Sci. Annals "Al. I. Cuza" Univ. Iasi*, in press.
32. H. Doostie and M. Hashemi, "Fibonacci lengths involving the Wall number $k(n)$ ", *J. Appl. Math. Comput.*, **2006**, *20*, 171-180.
33. S. W. Knox, "Fibonacci sequences in finite groups", *Fibonacci Quart.*, **1992**, *30*, 116-120.
34. K. Lü and J. Wang, "k-Step Fibonacci sequence modulo m ", *Util. Math.*, **2006**, *71*, 169-178.
35. E. Ozkan, H. Aydin and R. Dikici, "3-Step Fibonacci series modulo m ", *Appl. Math. Comput.*, **2003**, *143*, 165-172.
36. A. P. Stakhov, "A generalization of the Fibonacci Q -matrix", *Rep. Natl. Acad. Sci. Ukraine*, **1999**, *9*, 46-49.

37. A. P. Stakhov and B. Rozin, "Theory of Binet formulas for Fibonacci and Lucas p-numbers", *Chaos Solitons Fract.*, **2006**, 27, 1162-1177.
38. P. Hall, "The Eulerian functions of a group", *Quart. J. Math.*, **1936**, 7, 134-151.
39. H. S. M. Coxeter and W. O. J. Moser, "Generators and Relations for Discrete Groups", 3rd Edn., Springer, Berlin, **1972**, pp.67-68.

© 2015 by Maejo University, San Sai, Chiang Mai, 50290 Thailand. Reproduction is permitted for noncommercial purposes.

Full Paper

Doubly censored mixture of two Rayleigh distributions: Properties and applications

Navid Feroze^{1,*}, Tabassum Naz Sindhu², Muhammad Aslam^{2,3} and Wasif Yaseen⁴

¹ Department of Statistics, Government Post Graduate College Muzaffarabad, Azad Kashmir, Pakistan

² Department of Statistics, Quaid-i-Azam University 45320, Islamabad 44000, Pakistan

³ Department of Statistics, Riphah International University, Islamabad, Pakistan

⁴ National College of Business Administration and Economics, Lahore, Pakistan

* Corresponding author, e-mail: navidferoz@gmail.com

Received: 3 November 2013 / Accepted: 16 August 2015 / Published: 6 October 2015

Abstract: The Bayes estimation of the parameters of single and mixture of Rayleigh distributions under double censoring is discussed. The informative and non-informative priors under squared error loss function and k-loss function are assumed for the posterior estimation. The posterior risks, associated with each estimator are used to compare the performance of different estimators using the simulated and real life data sets.

Keywords: inverse transformation method, mixture model, double censoring, loss functions, Bayes estimator

INTRODUCTION

In survival analysis data are always subject to censoring. The right censoring is the most common type of the censoring. In right censoring the survival time is smaller than the observed right censoring time. However, in some cases the data are subjected to left as well as right censoring. In case of left censoring, an analyst can only have the information that the survival time is larger than or equal to the observed left censoring time. A more difficult censoring scheme is established when both the initial and final times are interval-censored. Such a situation is referred as double censoring and the data with both left and right censored observations are known as doubly censored data.

The analysis of the doubly censored data for simple (single) distribution has been performed by many authors. Fernandez [1] studied the maximum likelihood prediction based on type-II doubly censored samples from exponential distribution. Fernandez [2] investigated Bayesian estimation

based on censored samples from Pareto populations. Khan et al. [3] discussed predictive inference from a two-parameter Rayleigh life model using doubly censored samples. Kim and Song [4] considered Bayesian estimation of parameters of generalised exponential distribution using doubly censored samples. Khan et al. [5] performed the sensitivity analysis of predictive modelling for responses from three-parameter Weibull model using doubly censored sample of cancer patients. Pak et al. [6] proposed an estimation of Rayleigh scale parameter under doubly type-II censoring from imprecise data.

In statistics a mixed model is signified as a convex fusion of other probability distributions. It can be used to model a full statistical population with subpopulations, where the components of mixture probability densities are the probability densities of the subpopulations. The mixed model may appropriately be used to the model data set, where the subsets of the whole data set own different properties that can best be modelled separately. They can be more mathematically manageable as the individual mixture components are more easily dealt with than the overall mixture density. The families of mixture distributions have many applications in different fields such as fisheries, botany, agriculture, economics, psychology, medicine, finance, electrophoresis, geology, communication theory and zoology.

Soliman [7] obtained estimators for the finite mixture of Rayleigh model on the basis of progressively censored data. Sultan et al. [8] analysed some properties of the mixture of two inverse Weibull distributions. Saleem and Aslam [9] presented a comparison of the maximum likelihood estimates with the Bayesian estimates under uniform and Jeffreys' priors for the parameters of the Rayleigh mixture. Kundu and Howalder [10] discussed the Bayesian estimation and prediction of the inverse Weibull distribution for type-II censored data. Saleem et al. [11] investigated the Bayesian properties of the mixture of Power function distribution using the complete and censored samples. Shi and Yan [12] studied the two-parameter exponential distribution under type-I censoring to obtain empirical Bayes estimates. Eluebaly and Bouguila [13] discussed a Bayesian approach to explore the finite generalised Gaussian mixed models which include several standard mixtures extensively used in signal and image processing applications such as Gaussian and Laplace. Sultan and Moisher [14] developed an approximate Bayes estimation of the parameters and reliability function of the two-component mixture of inverse Weibull distributions under type-II censoring. The other contributions regarding Bayesian analysis of the mixed models can be seen from the work of Kazmi et al. [15], Ali et al. [16], Ali et al. [17], Feroze and Aslam [18], Feroze and Aslam [19], Feroze and Aslam [20], Sindhu et al. [21] and Sindhu et al. [22].

METHODS

This section contains the introduction of the model and the likelihood function, along with the derivation of posterior distributions, Bayes estimators and posterior risks. The prior elicitation is also discussed.

Proposed Mixed Model and Likelihood Function

The probability density function of the Rayleigh distribution with rate parameter λ_i is:

$$f_i(x_{ij}) = 2x_{ij}\lambda_i^2 \exp(-x_{ij}^2\lambda_i^2), \quad 0 < x_{ij} < \infty, \quad \lambda_i^2 > 0, \quad i = 1,2 \text{ and } j = 1,2,\dots,n_i. \quad (1)$$

This function can be obtained by putting $\lambda^2 = 1/\theta^2$ in the probability density function used by Saleem and Aslam [9].

The cumulative distribution function of the distribution is

$$F_i(x_{ij}) = 1 - \exp(-\lambda_i^2 x_{ij}^2), \quad 0 < x_{ij} < \infty, \quad \lambda_i^2 > 0, \quad i = 1, 2 \text{ and } j = 1, 2, \dots, n_i. \quad (2)$$

Saleem and Aslam [9] used the distribution function for a mixture of two-component densities. The same kind of mixture distribution with mixing weights $(p_1, 1 - p_1)$ can be written as

$$f(x) = p_1 f_1(x) + (1 - p_1) f_2(x), \quad 0 < p_1 < 1. \quad (3)$$

Again considering the cumulative distribution function for the mixed model used by Saleem and Aslam [9], the cumulative distribution function for mixture distribution can be written as

$$F(x) = p_1 F_1(x) + (1 - p_1) F_2(x). \quad (4)$$

Identifiability is a necessary condition for a model to produce precise inferences. Teicher [23] pioneered the study of identifiability of finite mixture distributions and showed that the class of scale parameters of the mixed models is identifiable. As we also use the scale parameters of the mixed model with a special case of Rayleigh distribution, the model is identifiable and we can use it for analysis.

The graphs of single and mixture of Raleigh models under different parametric values are presented in Figures 1 and 2 respectively. They tend to be more peaked for larger values of the parameters.

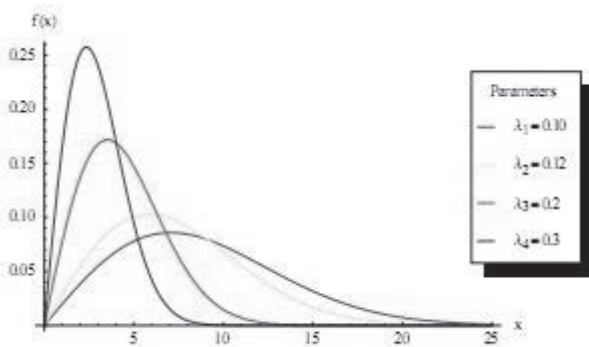


Figure 1. Graphs of single Raleigh distribution under different parametric values

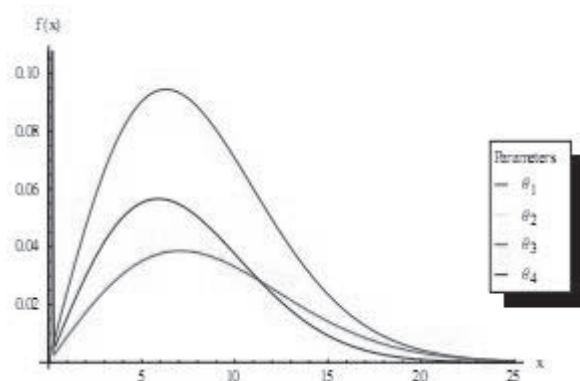


Figure 2. Graphs of mixture of Raleigh distributions under different parametric values

$$\begin{aligned} \theta_1 &= (p_1 = 0.45, \lambda_1 = 0.1, \lambda_2 = 0.12), \\ \theta_2 &= (p_1 = 0.45, \lambda_1 = 10, \lambda_2 = 12), \\ \theta_3 &= (p_1 = 0.45, \lambda_1 = 0.1, \lambda_2 = 12), \\ \theta_4 &= (p_1 = 0.45, \lambda_1 = 10, \lambda_2 = 0.12) \end{aligned}$$

Likelihood function under doubly censored samples using single Rayleigh distribution

Consider a random sample of size ‘n’ from a Rayleigh distribution, and let x_r, \dots, x_s be the ordered observations that can only be observed. The remaining ‘r – 1’ smallest observations and the ‘n – s’ largest observations are assumed to be censored. Then the likelihood function for type-II doubly censored sample $x = (x_r, \dots, x_s)$ as used by Feroze and Aslam [24] can be written as

$$L(\lambda|x) = \frac{n!}{(r-1)!(n-s)!} [F(x_r|\lambda)]^{r-1} [1 - F(x_s|\lambda)]^{n-s} \prod_{i=r}^s f(x_i|\lambda)$$

$$L(\lambda|x) \propto [1 - e^{-\lambda^2 x_r^2}]^{r-1} [e^{-\lambda^2 x_s^2}]^{n-s} \prod_{i=r}^s \lambda^2 e^{-\lambda^2 x_i^2}$$

After simplifications, it becomes

$$L(\lambda | \mathbf{x}) \propto \sum_{j=0}^{r-1} (-1)^j \binom{r-1}{j} \lambda^{2m} e^{-\lambda^2 \left(\sum_{i=r}^s x_i^2 + (n-s)x_s^2 + j\lambda r^2 \right)} \tag{5}$$

where $m = n - s - r + 1$.

Likelihood function under doubly censored samples using mixed Rayleigh distributions

Consider a random sample of size ‘ n ’ from the Rayleigh distribution, and let x_r, x_{r+1}, \dots, x_s be the ordered observations that can only be observed. The remaining ‘ $r - 1$ ’ smallest observations and the ‘ $n - s$ ’ largest observations are assumed to be censored. Now, based on causes of failure, the failed items are assumed to come either from subpopulation 1 or from subpopulation 2, so the $x_{1r_1}, \dots, x_{1s_1}$ and $x_{2r_2}, \dots, x_{2s_2}$ failed items come from the first and second subpopulations respectively. The rest of the observations which are less than x_r and greater than x_s are assumed to be censored from each component, where $x_s = \max(x_{1s_1}, x_{2s_2})$ and $x_r = \min(x_{1r_1}, x_{2r_2})$. Therefore, the numbers of failed items, $m_1 = s_1 - r_1 + 1$ and $m_2 = s_2 - r_2 + 1$, can be observed from the first and second subpopulations respectively. The remaining $n - (s - r + 2)$ items are assumed to be censored observations and $s - r + 2$ are the uncensored items, where $r = r_1 + r_2$, $s = s_1 + s_2$ and $m = m_1 + m_2$. Then assuming the causes of failure of the left censored items are identified, the likelihood function for type-II doubly censored sample, $\mathbf{x} = \left\{ (x_{1r_1}, \dots, x_{1s_1}), (x_{2r_2}, \dots, x_{2s_2}) \right\}$, as done by Feroze and Aslam [20], can be written as

$$L(\lambda_1, \lambda_2, p_1 | \mathbf{x}) \propto p_1^{s_1} (1 - p_1)^{s_2} \left\{ F_1(x_{(r_1)}, \lambda_1) \right\}^{n-1} \left\{ F(x_{(r_2)}, \lambda_2) \right\}^{r_2-1} \left\{ 1 - F(x_s, \lambda_1, \lambda_2) \right\}^{n-s} \left\{ \prod_{i=r_1}^{s_1} f_1(x_{1(i)}, \lambda_1) \right\} \left\{ \prod_{i=r_2}^{s_2} f_2(x_{2(i)}, \lambda_2) \right\} \tag{6}$$

$$L(\lambda_1, \lambda_2, p_1 | \mathbf{x}) \propto \sum_{k_1=0}^{r_1-1} \sum_{k_2=0}^{r_2-1} \sum_{k_3=0}^{n-s} (-1)^{k_1+k_2} \binom{r_1-1}{k_1} \binom{r_2-1}{k_2} \binom{n-s}{k_3} p_1^{n-s-k_3+s_1} (1 - p_1)^{s_2+k_3} \times \lambda_1^{2m_1} \lambda_2^{2m_2} \exp \left\{ -\lambda_1^2 \left(\Omega(x_{1j}) \right) \right\} \exp \left\{ -\lambda_2^2 \left(\Omega(x_{2j}) \right) \right\} \tag{7}$$

where $\Omega(x_{1j}) = \sum_{i=r_1}^{s_1} x_{1(i)}^2 + (n - s - k_3)x_{(s)}^2 + kx_{(r_1)}^2$, $\Omega(x_{2j}) = \sum_{i=r_2}^{s_2} x_{2(i)}^2 + k_3x_{(s)}^2 + kx_{(r_2)}^2$,

$m_1 = s_1 - r_1 + 1$ and $m_2 = s_2 - r_2 + 1$.

Bayes Estimation

This section covers the Bayesian analysis of single and mixture of Rayleigh distributions under uniform and Nakagami priors.

Bayesian estimation for single model using uniform and Nakagami priors

The uniform prior proposed by Laplace [25] for the parameter of the Raleigh distribution is

$$f(\lambda) \propto 1, \lambda > 0. \tag{8}$$

The posterior distribution under uniform prior using the likelihood function in equation (5) can be obtained as

$$\pi(\lambda | \mathbf{x}) \propto \sum_{j=0}^{r-1} (-1)^j \binom{r-1}{j} \lambda^{2m} e^{-\lambda^2 \left(\sum_{i=r}^s x_i^2 + (n-s)x_s^2 + jx_r^2 \right)} \quad (9)$$

The Nakagami distribution proposed by Nakagami [26] is used as a prior distribution for the rate parameter λ , with the hyper-parameters a and b given by

$$f(\lambda) = \frac{2a^a}{\Gamma(a)b^a} \lambda^{2a-1} \exp\left(-\frac{\lambda^2 a}{b}\right), \quad a, b > 0, \lambda > 0. \quad (10)$$

The posterior distribution under Nakagami prior using the likelihood function in equation (5) can be obtained as

$$\pi(\lambda | \mathbf{x}) \propto \sum_{j=0}^{r-1} (-1)^j \binom{r-1}{j} \lambda^{2m+2a-1} e^{-\lambda^2 \left(\sum_{i=r}^s x_i^2 + (n-s)x_s^2 + jx_r^2 + a/b \right)} \quad (11)$$

The graphs of the posterior distribution under uniform and Nakagami priors for doubly censored single Rayleigh distribution under different parametric values using a simulated sample of size $n = 40$ are presented in Figures 3 and 4 respectively. Again, the graphs for posterior distributions tend to be more peaked for larger values of the parameters. Similarly, the curves of posterior distribution under Nakagami prior are more peaked than those under uniform prior. In the case of Nakagami prior, the elicited values of hyper-parameters are used in the graphs.

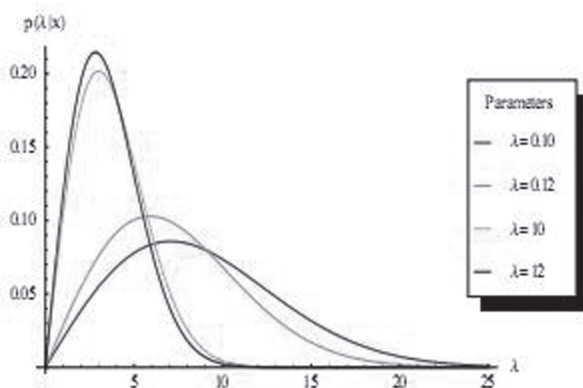


Figure 3. Graphs of posterior distribution under uniform prior

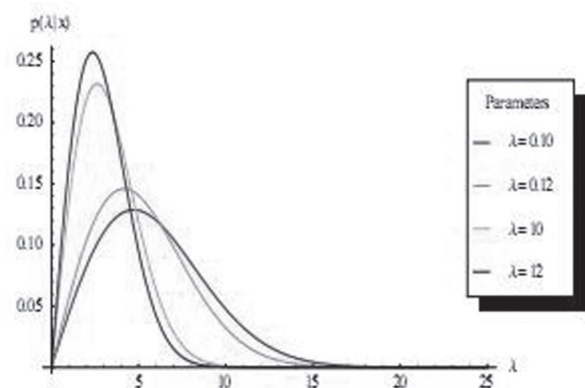


Figure 4. Graphs of posterior distribution under Nakagami prior

Bayesian estimation for mixed model using uniform and Nakagami priors

The uniform prior for the vector $\Theta = (\lambda_1, \lambda_2, \rho_1)$ of the mixed model can be assumed as $g(\Theta) \propto 1$. (12)

By multiplying equation (12) with equation (7), the joint posterior density for the vector Θ given the data, becomes

$$\pi(\Theta | \mathbf{x}) \propto \sum_{k_1=0}^{r_1-1} \sum_{k_2=0}^{r_2-1} \sum_{k_3=0}^{n-s} \prod_{i=1}^2 (-1)^{k_1+k_2} \binom{r_1-1}{k_1} \binom{r_2-1}{k_2} \binom{n-s}{k_3} p_1^{n-s-k_3+s_1} \times (1-p_1)^{s_2+k_3} \lambda_i^{2m_i} \exp\{-\lambda_i^2 \Omega(x_{ij})\} \quad (13)$$

For the Bayes estimation using Nakagami prior, let us assume that the parameters λ_i ($i = 1, 2$) and p_1 are independent random variables, and then we consider the following priors for different parameters. The prior for the rate parameters λ_i for $i = 1, 2$ is assumed as the Nakagami distribution with the hyper-parameters a_i and b_i given by

$$f_{\lambda_i}(\lambda_i) = \frac{2a_i^{a_i}}{\Gamma(a_i)b_i^{a_i}} \lambda_i^{2a_i-1} \exp\left(\frac{-\lambda_i^2 a_i}{b_i}\right), \quad a_i, b_i > 0 \quad (14)$$

The prior for p_1 is assumed to be the beta distribution, whose density is given by

$$f_p(p_1) = \frac{\Gamma(c_1 + d_1)}{\Gamma(c_1)\Gamma(d_1)} p_1^{c_1-1} (1-p_1)^{d_1-1}, \quad c_1, d_1 > 0 \quad (15)$$

From equations (14) and (15), we propose the following joint prior density of the vector $\Theta = (\lambda_1, \lambda_2, p_1)$:

$$g(\Theta) \propto \lambda_i^{2a_i-1} \exp\left(\frac{-\lambda_i^2 a_i}{b_i}\right) p_1^{c_1-1} (1-p_1)^{d_1-1}, \quad 0 < p_1 < 1, a_i > 0, b_i > 0, c_1 > 0, d_1 > 0 \quad (16)$$

By multiplying equation (16) with equation (7), the joint posterior density for the vector Θ , given the data, becomes

$$\begin{aligned} \pi(\Theta | x) \propto & \sum_{k_1=0}^{r_1-1} \sum_{k_2=0}^{r_2-1} \sum_{k_3=0}^{n-s} \prod_{i=1}^2 (-1)^{k_1+k_2} \binom{r_1-1}{k_1} \binom{r_2-1}{k_2} \binom{n-s}{k_3} p_1^{n-s-k_3+s_1+c_1-1} (1-p_1)^{s_2+k_3+d_1-1} \\ & \times \lambda_i^{2(a_i+m_i)-1} \exp\left\{-\lambda_i^2 \left(\frac{a_i}{b_i} + \Omega(x_{ij})\right)\right\} \end{aligned} \quad (17)$$

The marginal distributions of λ_i ($i = 1, 2$) and p_1 can be obtained by integrating the nuisance parameters.

Figures 5 and 6 show the graphs of the marginal posterior distributions for both components under uniform prior, using a simulated sample of size $n = 40$. As observed in the case of single posterior models, the marginal posterior distributions tend to be more peaked for larger values of the parameters. Similarly, the curves of marginal posterior distributions under Nakagami prior are more peaked than those under uniform prior.

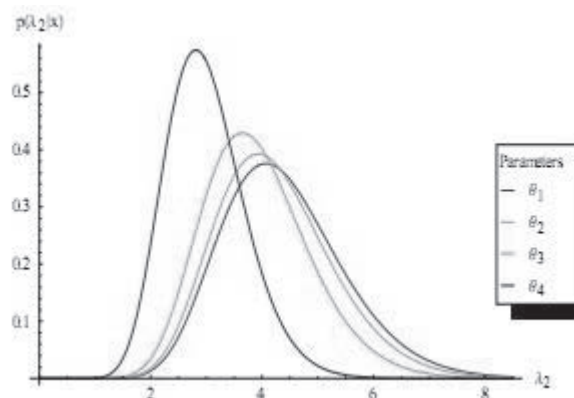
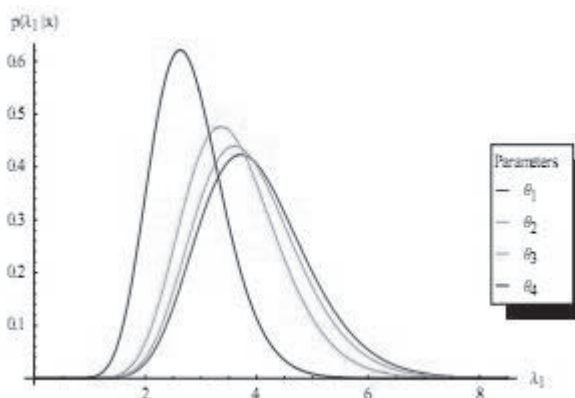


Figure 5. Graphs of marginal posterior distribution for first component under uniform prior
 $[\theta_1 = (p_1 = 0.45, \lambda_1 = 0.1, \lambda_2 = 0.12); \theta_2 = (p_1 = 0.45, \lambda_1 = 10, \lambda_2 = 12); \theta_3 = (p_1 = 0.45, \lambda_1 = 0.1, \lambda_2 = 12); \theta_4 = (p_1 = 0.45, \lambda_1 = 10, \lambda_2 = 0.12)]$

Figure 6. Graphs of marginal posterior distribution for second component under uniform prior
 $[\theta_1 = (p_1 = 0.45, \lambda_1 = 0.1, \lambda_2 = 0.12); \theta_2 = (p_1 = 0.45, \lambda_1 = 10, \lambda_2 = 12); \theta_3 = (p_1 = 0.45, \lambda_1 = 0.1, \lambda_2 = 12); \theta_4 = (p_1 = 0.45, \lambda_1 = 10, \lambda_2 = 0.12)]$

Bayes Estimation of Vector of Parameters Θ

The Bayesian point estimation is linked to a loss function in general, signifying the loss occurring when the estimate $\hat{\theta}$ differs from true parameter θ . As there is no specific rule of thumb that helps us to decide the appropriate loss function to be used, the squared error loss function (SELF) is used in this paper as it serves as standard loss. It is well known that under the SELF, the Bayes estimator of a function of the parameters is the posterior mean of the loss function and the risk is the posterior variance. It is defined as $l(\hat{\theta}, \theta) = (\theta - \hat{\theta})^2$. It was initially used in estimation problems when the unbiased estimator of θ was being considered. Another reason for its attractiveness is its relationship to the least squares theory. The use of SELF makes the calculations simpler.

The K-loss function (KLF), proposed by Wasan [27] and defined as $l(\hat{\theta}, \theta) = (\hat{\theta} - \theta)^2 / \hat{\theta}\theta$, is well fitted for a measure of inaccuracy for an estimator of a scale parameter of the distribution defined as $R^+ = (0, \infty)$. Under KLF, the Bayes estimates and posterior risks are defined as $\hat{\theta} = \sqrt{E(\theta | \mathbf{x}) / E(\theta^{-1} | \mathbf{x})}$ and $\rho(\hat{\theta}) = 2 \left\{ \sqrt{E(\theta | \mathbf{x}) E(\theta^{-1} | \mathbf{x})} - 1 \right\}$ respectively. Recently Ali [28] used this loss function and also suggested a modified KLF.

In the Bayesian estimation in the case of single Rayleigh model, the Bayes estimator and posterior risk using SELF under uniform prior are respectively presented as

$$\hat{\lambda}_{(SELF)} = \frac{\sum_{j=0}^{r-1} (-1)^j \binom{r-1}{j} \Gamma(m+1) \left(\sum_{i=r}^s x_i^2 + (n-s)x_s^2 + jx_r^2 \right)^{-(m+1)}}{\sum_{j=0}^{r-1} (-1)^j \binom{r-1}{j} \Gamma(m+1/2) \left(\sum_{i=r}^s x_i^2 + (n-s)x_s^2 + jx_r^2 \right)^{-(m+1/2)}}$$

$$\rho(\hat{\lambda}_{(SELF)}) = \frac{\sum_{j=0}^{r-1} (-1)^j \binom{r-1}{j} \Gamma(m+3/2) \left(\sum_{i=r}^s x_i^2 + (n-s)x_s^2 + jx_r^2 \right)^{-(m+3/2)}}{\sum_{j=0}^{r-1} (-1)^j \binom{r-1}{j} \Gamma(m+1/2) \left(\sum_{i=r}^s x_i^2 + (n-s)x_s^2 + jx_r^2 \right)^{-(m+1/2)}} - \left(\hat{\lambda}_{(SELF)} \right)^2$$

The Bayes estimators and posterior risks under Nakagami prior and KLF can be obtained with little modifications.

In the Bayesian estimation in the case of mixture of Rayleigh models, the respective marginal distribution of each parameter is used to derive the Bayes estimators and posterior risks for λ_1 , λ_2 and p_1 under SELF and KLF. The Bayes estimators of λ_1 , λ_2 and p_1 under SELF, assuming Nakagami prior, are given as

$$\hat{\lambda}_{1(SELF)} = N^{-1} \sum_{k_1=0}^{r_1-1} \sum_{k_2=0}^{r_2-1} \sum_{k_3=0}^{n-s} (-1)^{k_1+k_2} \binom{r_1-1}{k_1} \binom{r_2-1}{k_2} \binom{n-s}{k_3} \frac{B(A_1, A_2) \Gamma(a_1 + m_1 + 1/2) \Gamma(a_2 + m_2)}{2 \{a_1 / b_1 + \Omega(x_{1j})\}^{(a_1+m_1+1/2)} 2 \{a_2 / b_2 + \Omega(x_{2j})\}^{(a_2+m_2)}}$$

$$\hat{\lambda}_{2(SELF)} = N^{-1} \sum_{k_1=0}^{r_1-1} \sum_{k_2=0}^{r_2-1} \sum_{k_3=0}^{n-s} (-1)^{k_1+k_2} \binom{r_1-1}{k_1} \binom{r_2-1}{k_2} \binom{n-s}{k_3} \frac{B(A_1, A_2) \Gamma(a_1 + m_1) \Gamma(a_2 + m_2 + 1/2)}{2 \{a_1 / b_1 + \Omega(x_{1j})\}^{(a_1+m_1)} 2 \{a_2 / b_2 + \Omega(x_{2j})\}^{(a_2+m_2+1/2)}}$$

$$\hat{p}_{1(SELF)} = N^{-1} \sum_{k_1=0}^{r_1-1} \sum_{k_2=0}^{r_2-1} \sum_{k_3=0}^{n-s} (-1)^{k_1+k_2} \binom{r_1-1}{k_1} \binom{r_2-1}{k_2} \binom{n-s}{k_3} \frac{B(A_1+1, A_2) \Gamma(a_1+m_1) \Gamma(a_2+m_2)}{2\{a_1/b_1+\Omega(x_{1j})\}^{(a_1+m_1)} 2\{a_2/b_2+\Omega(x_{2j})\}^{(a_2+m_2)}}$$

The posterior risks of λ_1 , λ_2 and p_1 are given as

$$\rho(\hat{\lambda}_{1(SELF)}) = N^{-1} \sum_{k_1=0}^{r_1-1} \sum_{k_2=0}^{r_2-1} \sum_{k_3=0}^{n-s} (-1)^{k_1+k_2} \binom{r_1-1}{k_1} \binom{r_2-1}{k_2} \binom{n-s}{k_3} \frac{B(A_1, A_2) \Gamma(a_1+m_1+1) \Gamma(a_2+m_2)}{2\{a_1/b_1+\Omega(x_{1j})\}^{(a_1+m_1+1)} 2\{a_2/b_2+\Omega(x_{2j})\}^{(a_2+m_2)}} - (\hat{\lambda}_{1(SELF)})^2$$

$$\rho(\hat{\lambda}_{2(SELF)}) = N^{-1} \sum_{k_1=0}^{r_1-1} \sum_{k_2=0}^{r_2-1} \sum_{k_3=0}^{n-s} (-1)^{k_1+k_2} \binom{r_1-1}{k_1} \binom{r_2-1}{k_2} \binom{n-s}{k_3} \frac{B(A_1, A_2) \Gamma(a_1+m_1) \Gamma(a_2+m_2+1)}{2\{a_1/b_1+\Omega(x_{1j})\}^{(a_1+m_1)} 2\{a_2/b_2+\Omega(x_{2j})\}^{(a_2+m_2+1)}} - (\hat{\lambda}_{2(SELF)})^2$$

$$\rho(\hat{p}_{1(SELF)}) = N^{-1} \sum_{k_1=0}^{r_1-1} \sum_{k_2=0}^{r_2-1} \sum_{k_3=0}^{n-s} (-1)^{k_1+k_2} \binom{r_1-1}{k_1} \binom{r_2-1}{k_2} \binom{n-s}{k_3} \frac{B(A_1+2, A_2) \Gamma(a_1+m_1) \Gamma(a_2+m_2)}{2\{a_1/b_1+\Omega(x_{1j})\}^{(a_1+m_1)} 2\{a_2/b_2+\Omega(x_{2j})\}^{(a_2+m_2)}} - (\hat{p}_{1(SELF)})^2$$

where N^{-1} is formulised as

$$N^{-1} = \sum_{k_1=0}^{r_1-1} \sum_{k_2=0}^{r_2-1} \sum_{k_3=0}^{n-s} (-1)^{k_1+k_2} \binom{r_1-1}{k_1} \binom{r_2-1}{k_2} \binom{n-s}{k_3} \frac{B(A_1, A_2) \Gamma(a_1+m_1) \Gamma(a_2+m_2)}{2\{a_1/b_1+\Omega(x_{1j})\}^{(a_1+m_1)} 2\{a_2/b_2+\Omega(x_{2j})\}^{(a_2+m_2)}}$$

$$A_1 = n - s - k_3 + s_1 + c_1 \text{ and } A_2 = s_2 + k_3 + d_1.$$

Similarly, expressions for Bayes estimators and their posterior risks under KLF and uniform prior can be obtained with little modifications.

Elicitation

In Bayesian analysis the elicitation of opinion is an important step. It helps us to easily understand the expert’s opinions. In statistical inference the hyper-parameters of a prior distribution are determined by the characteristics of a certain predictive distribution proposed by an expert. In this study we focus on a method of elicitation based on prior predictive distribution. The elicitation of the hyper-parameters from the prior $p(\lambda)$ is a complex task. The prior predictive distribution is used for the elicitation of the hyper-parameters, which is compared with the experts' judgement about this distribution, and then the hyper-parameters are chosen in such a way so as to make the judgment agree as closely as possible with the given distribution. More detail on this may be obtained from the work of Grimshaw et al. [29], O’Hagan et al. [30], Jenkinson [31] and Leon et al. [32]. Aslam [33] suggested the method of elicitation that compares the prior predictive distribution with the expert’s assessments about the distribution involved and then chooses the hyper-parameters that make the assessment agree closely with the member of the family. This method has also been used by Kazmi et al. [15]. The prior predictive distribution is derived using the following formula:

$$p(y) = \int_{\Theta} p(y|\Theta)p(\Theta)d\Theta$$

For the elicitation for single Rayleigh model under Nakagami distribution, the prior predictive distribution using Nakagami prior is

$$p(y) = 2(ab^{-1})^a \frac{ya}{(y^2 + ab^{-1})^{(a+1)}}, y > 0 \tag{18}$$

For the elicitation of the two hyper-parameters, two intervals are considered. From equation (18), the experts' probabilities/assessments are supposed to be 0.10 for each case. The two integrals for equation (18) are considered with the following limits of values of random variable 'Y': (0, 10) and (10, 20) respectively. For the elicitation of the hyper-parameters a and b , these two equations are solved simultaneously through a computer program developed in SAS package using the command of PROC SYSLIN. Thus, the values of the hyper-parameters obtained by applying this methodology are 0.010348 and 0.735261 respectively.

For the elicitation for mixture of Rayleigh models under Nakagami distribution, the prior predictive distribution using Nakagami prior is

$$p(y) = 2(a_1 b_1^{-1})^{a_1} \frac{y a_1 c_1}{(c_1 + d_1)(y^2 + a_1 b_1^{-1})^{(a_1+1)}} + 2(a_2 b_2^{-1})^{a_2} \frac{y a_2 d_1}{(c_1 + d_1)(y^2 + a_2 b_2^{-1})^{(a_2+1)}}, y > 0 \quad (19)$$

For the elicitation of the six hyper-parameters, six different intervals are considered. From equation (19), the expert's probabilities/assessments are supposed to be 0.10 for each case. The six integrals for equation (19) are considered with the following limits of values of random variable 'Y': (0, 10), (10, 20), (20, 30), (30, 40), (40, 50) and (50, 60) respectively. For the elicitation of the hyper-parameters a_1, a_2, b_1, b_2, c_1 and d_1 , these six equations are solved simultaneously through a computer program developed in SAS package using the command of PROC SYSLIN. Thus, the values of the hyper-parameters obtained by applying this methodology are 0.000231, 0.012109, 0.52114, 4.99325, 0.52130 and 0.14790 respectively.

RESULTS AND DISCUSSION

A simulation study was carried out to investigate the performance of Bayes estimates under a tenfold choice of parametric values, different sample sizes, and different values of mixing parameter. We took random samples of sizes $n = 20, 40$ and 80 from single and two-component mixture of Rayleigh distributions with tenfold choice of the parameters. The choice of censoring time was made in such a way that the censoring rate in the resultant sample was approximately 20%. The processes for the generation of data from the single and mixed models are discussed in the following sections.

Simulation

In the case of single Rayleigh model the parametric space is considered as $\lambda \in (0.1, 10)$. The data are generated using the following steps.

- Step 1: Draw samples of size 'n' from Rayleigh model using inverse transformation technique by taking the generator $x = \sqrt{-\lambda^{-2} \ln(1-u)}$, where 'u' is a uniform random variable.
- Step 2: Determine the test termination points on the left and right, i.e. the values of x_r (test termination point from left) and x_s (test termination point from right).
- Step 3: The observations which are less than x_r and greater than x_s are considered to be censored.
- Step 4: Use the observations which are greater than or equal to x_r and less than or equal to x_s for the analysis.
- Step 5: Repeat steps 1- 4 ten thousand times and calculate the average of the estimates.

It should be noted that the values of x_r and x_s are assumed to be such that an equal number of values are censored from left and right, i.e 10% from each side.

In the case of mixture of Rayleigh models, the parametric space is considered as $(\lambda_1, \lambda_2) \in \{(0.1, 0.12), (10, 12), (0.1, 12), (10, 0.12)\}$, $p_1 = 0.45$. To generate the mixture data we make use of probabilistic mixing with probabilities p_1 and $(1 - p_1)$. A uniform number u is generated n times and if $u < p_1$, the observation is taken randomly from F_1 (Rayleigh distribution with parameter λ_1), otherwise from F_2 (Rayleigh distribution with parameter λ_2). To implement censored samplings, we consider that the $x_{1r_1}, \dots, x_{1s_1}$ and $x_{2r_2}, \dots, x_{2s_2}$ failed items come from the first and second subpopulations respectively. The values of x_r and x_s are assumed to be such that an equal number of values are censored from left and right, i.e. 10% from each side. The simulated data sets are obtained using the following steps:

- Step 1: Draw samples of size 'n' from each component of the mixture model using inverse transformation technique by taking the generator $x = \sqrt{-\lambda^{-2} \ln(1-u)}$, where 'u' is a uniform random variable.
- Step 2: Generate a uniform random number u , corresponding to each observation.
- Step 3: If $u \leq p_1$, take the observation from the first subpopulation; if $u > p_1$, take the observation from the second subpopulation.
- Step 4: Determine the test termination points on the left and right, i.e. the values of x_r (test termination point from left) and x_s (test termination point from right).
- Step 5: The observations which are less than x_r and greater than x_s are considered to be censored from each component.
- Step 6: Use the observations which are greater than or equal to x_r and less than or equal to x_s for the analysis.
- Step 7: Repeat steps 1 - 6 ten thousand times and calculate the average of the estimates.

Table 1 represents the Bayes estimates and corresponding posterior risks for doubly censored single Rayleigh model. From this table, it can be seen that estimated values of the parameters converge to the true values of the parameters, and the amount of the corresponding posterior risk decreases with increase in sample size. As the amount of posterior risks associated with the estimates under Nakagami prior is smaller than that under uniform prior, so the performance of Nakagami prior is better than uniform prior. On the other hand, the performance of SELF is better than KLF when the parametric values are small, while in the case of larger values of the parameter, the performance of KLF is better than SELF.

Numerical results of the simulation study, presented in Tables 2-5, reveal interesting properties of the proposed Bayes estimators for the mixture of Rayleigh models. The estimated values of the parameters converge to the true values of the parameters, and the amounts of posterior risks tend to decrease by increasing the sample size. Another interesting point concerning the posterior risks of the estimates of λ_1 and λ_2 is that increasing (or decreasing) the proportion of component in the mixture decreases (or increases) the amount of posterior risks for the estimates of λ_1 .

The Bayes estimates of the lifetime parameters are either over- or underestimated. The estimates of the mixing parameter (p_1) also have mixed behaviour: sometimes overestimated and other times underestimated. The performance of Nakagami prior seems better than uniform prior as the associated magnitude of posterior risks is smaller in the case of Nakagami prior. In comparing the loss functions, it is assessed that the magnitude of posterior risks under SELF is smaller than that under KLF for a smaller choice of true parametric values, i.e. for $(\lambda_1, \lambda_2) = (0.1, 0.12)$. On the other hand, for quite larger values of parameters, i.e. for $(\lambda_1, \lambda_2) = (10, 12)$ and for significantly

different values of parameters, i.e. for $(\lambda_1, \lambda_2) = (0.1, 12)$ and $(10, 0.12)$, the KLF produces better results. It should also be mentioned here that the SELF in the majority of cases produces better convergence than the KLF.

Table 1. Bayes estimators and posterior risks (in brackets) under uniform prior and Nakagami prior for single model using $\lambda \in (0.1, 10)$

n	Uniform prior				Nakagami prior			
	SELF		KLF		SELF		KLF	
	$\lambda = 0.10$	$\lambda = 10$						
20	0.10664 (0.00051)	11.41053 (4.47964)	0.10540 (0.08900)	10.72593 (0.08795)	0.10550 (0.00050)	10.88324 (4.27545)	0.10427 (0.08647)	10.23027 (0.08394)
40	0.10855 (0.00023)	10.93152 (2.48177)	0.10440 (0.04732)	10.66980 (0.04397)	0.10375 (0.00023)	10.42546 (2.45224)	0.10394 (0.04572)	10.17586 (0.04344)
80	0.10329 (0.00012)	10.47666 (1.10186)	0.10252 (0.02175)	10.44836 (0.02387)	0.10221 (0.00012)	10.10949 (1.07332)	0.10145 (0.02151)	10.08218 (0.02325)

Table 2. Bayes estimators and posterior risks (in brackets) under uniform prior for mixed model using $(\lambda_1, \lambda_2, p_1) = (0.1, 0.12, 0.45)$ and $(10, 12, 0.45)$

n	SELF					
	$\hat{\lambda}_1$	$\hat{\lambda}_2$	\hat{p}_1	$\hat{\lambda}_1$	$\hat{\lambda}_2$	\hat{p}_1
20	0.107209 (0.000503)	0.132703 (0.000564)	0.515202 (0.013700)	11.086576 (4.321071)	13.549166 (4.923963)	0.517763 (0.013560)
40	0.100505 (0.000230)	0.130256 (0.000314)	0.509777 (0.007576)	10.567887 (2.488090)	13.461262 (2.797394)	0.502870 (0.007513)
80	0.103622 (0.000118)	0.127356 (0.000167)	0.502084 (0.003912)	9.912993 (1.088862)	13.026748 (1.624447)	0.484931 (0.003864)
KLF						
20	0.102959 (0.087594)	0.129129 (0.072430)	0.497539 (0.133359)	10.221412 (0.084839)	12.865358 (0.070344)	0.502526 (0.131133)
40	0.106241 (0.046633)	0.128014 (0.038191)	0.487087 (0.071148)	10.014874 (0.044080)	12.850151 (0.038230)	0.493996 (0.071735)
80	0.094853 (0.021888)	0.123316 (0.020362)	0.484133 (0.034902)	10.285132 (0.023584)	12.557065 (0.020691)	0.475643 (0.037357)

Table 3. Bayes estimators and posterior risks (in brackets) under uniform prior for mixed model using $(\lambda_1, \lambda_2, p_1) = (0.10, 12, 0.45)$ and $(10, 0.12, 0.45)$

n	SELF					
	$\hat{\lambda}_1$	$\hat{\lambda}_2$	\hat{p}_1	$\hat{\lambda}_1$	$\hat{\lambda}_2$	\hat{p}_1
20	0.098497 (0.000316)	14.214270 (4.921202)	0.552917 (0.012464)	12.212382 (4.343465)	0.117154 (0.000331)	0.420005 (0.012162)
40	0.091638 (0.000135)	13.945293 (2.401793)	0.543338 (0.006765)	12.073530 (2.219332)	0.119216 (0.000160)	0.432426 (0.006444)
80	0.095115 (0.000067)	13.649684 (1.193893)	0.534044 (0.003386)	11.518744 (1.119705)	0.121828 (0.000077)	0.450936 (0.003253)
KLF						
20	0.092387 (0.068477)	13.492645 (0.055819)	0.541278 (0.100292)	11.771346 (0.068494)	0.108699 (0.054418)	0.436242 (0.152270)
40	0.096671 (0.033686)	13.246342 (0.026147)	0.528118 (0.052829)	11.638419 (0.033122)	0.121915 (0.026645)	0.440904 (0.083827)
80	0.098805 (0.016265)	12.535256 (0.013083)	0.520105 (0.027307)	11.569858 (0.016581)	0.124054 (0.013209)	0.445349 (0.042834)

Table 4. Bayes estimators and posterior risks (in brackets) under uniform prior for mixed model using $(\lambda_1, \lambda_2, p_1) = (0.1, 0.12, 0.45)$ and $(10, 12, 0.45)$

n	SELF					
	$\hat{\lambda}_1$	$\hat{\lambda}_2$	\hat{p}_1	$\hat{\lambda}_1$	$\hat{\lambda}_2$	\hat{p}_1
20	0.104076 (0.000479)	0.127713 (0.000558)	0.498425 (0.013229)	10.82959 (4.256710)	12.9605 (4.8388)	0.497084 (0.013244)
40	0.099427 (0.000223)	0.12652 (0.000306)	0.48622 (0.007231)	10.12890 (2.39442)	12.88640 (2.71684)	0.479166 (0.007305)
80	0.099036 (0.000114)	0.125807 (0.000161)	0.478841 (0.003865)	9.61493 (1.05203)	12.67810 (1.58376)	0.462094 (0.003820)
KLF						
20	0.101884 (0.086648)	0.123181 (0.069120)	0.480102 (0.129905)	10.11040 (0.083902)	12.73760 (0.068839)	0.481255 (0.12979)
40	0.101669 (0.045012)	0.123008 (0.037679)	0.471869 (0.070063)	9.85076 (0.043278)	12.45580 (0.037003)	0.474996 (0.069297)
80	0.090768 (0.021446)	0.121778 (0.019760)	0.470942 (0.034345)	9.91883 (0.022678)	12.11990 (0.019891)	0.468498 (0.036650)

Table 5. Bayes estimators and posterior risks (in brackets) under uniform prior for mixed model using $(\lambda_1, \lambda_2, p_1) = (0.10, 12, 0.45)$ and $(10, 0.12, 0.45)$

n	SELF					
	$\hat{\lambda}_1$	$\hat{\lambda}_2$	\hat{p}_1	$\hat{\lambda}_1$	$\hat{\lambda}_2$	\hat{p}_1
20	0.095619 (0.000301)	13.67980 (4.868910)	0.534912 (0.012036)	11.92930 (4.278770)	0.112064 (0.000325)	0.403231 (0.011879)
40	0.090655 (0.000131)	13.54530 (2.343030)	0.51823 (0.006457)	11.5720 (2.13578)	0.114125 (0.000155)	0.412042 (0.006265)
80	0.090905 (0.000065)	13.48370 (1.148460)	0.509322 (0.003346)	11.17240 (1.08183)	0.118567 (0.000075)	0.42970 (0.003216)
KLF						
20	0.0914225 (0.067737)	12.87110 (0.053268)	0.522308 (0.097694)	11.64350 (0.067737)	0.10762 (0.053254)	0.417776 (0.15071)
40	0.092511 (0.032515)	12.72830 (0.025796)	0.511618 (0.052023)	11.44770 (0.032519)	0.118174 (0.025790)	0.423946 (0.080978)
80	0.09455 (0.015937)	12.37891 (0.012696)	0.505934 (0.026871)	11.15780 (0.015944)	0.119735 (0.012698)	0.438659 (0.042023)

Real Data Analysis

We analysed a real data set to illustrate the methodology discussed in the previous section. In order to show the usefulness of the proposed mixture distribution, we applied the results to the survival times (in years) of a set of cancer patients given chemotherapy treatment. The details of this data can be seen from Bekker et al. [34] and the references cited therein. We used the Kolmogorov-Smirnov and chi-square tests to see whether the data follow the Rayleigh distribution. These tests, with p-values of 0.2170 and 0.2681 respectively, indicate that the data follow the Rayleigh distribution at 5% level of significance. The original data consisted of 46 values regarding survival times (in years) of cancer patients given chemotherapy treatment. A uniform number ‘ u ’ was generated for each of the 46 values. If $u < p_1$, the observation was allotted to F_1 (the Rayleigh distribution with parameter λ_1 , i.e. the first component of the mixture); otherwise to F_2 (from the Rayleigh distribution with parameter λ_2 , i.e. the second component of the mixture). The observations allotted to the first and second components of the mixture were considered as population-I and population-II respectively. The observations which were less than 0.047 (i.e. x_r) and greater than 3.978 (i.e. x_s) were assumed to be censored from left and right respectively from each population. The remaining doubly censored data from population-I and population-II are presented in Table 6. The values of x_r and x_s were assumed to be such that an equal number of values were censored from left and right, i.e. 10% from each side. The Bayes estimates were obtained assuming non-informative and informative priors under SELF and KLF.

Tables 7-8 contain the Bayesian estimation of parameters of the single and mixture of Rayleigh distributions under real-life data set. The findings from the real-life analysis are in close

agreement with those from the simulation study. It should be noted that the estimates under SELF and Nakagami prior are associated with smaller amounts of posterior risks.

Table 6. Doubly-censored, real-life data of the mixture regarding survival times (in years) of cancer patients given chemotherapy treatment

Population-I	Population-II
0.197, 0.534, 0.115, 0.296, 0.121, 0.466, 0.529, 1.447, 0.863, 0.132, 0.395, 0.696, 2.825, 3.658, 3.978, 3.743, 2.343, 2.178, 0.540, 4.003, 1.553, 1.485, 2.83, 2.416	0.260, 1.099, 0.501, 0.458, 0.641, 0.334, 0.570, 0.164, 0.203, 0.282, 0.047, 1.271, 1.589, 1.326, 0.841, 2.444

Table 7. Bayes estimators and posterior risks (in brackets) for single Rayleigh model using real data set

Uniform prior		Nakagami prior	
SELF	KLF	SELF	KLF
0.386117 (0.002481)	0.383239 (0.035318)	0.382462 (0.002451)	0.377970 (0.035057)

Table 8. Bayes estimators and posterior risks (in brackets) for mixed Rayleigh models using real data set

Prior $p_1 = 0.45$	SELF			KLF		
	$\hat{\lambda}_1$	$\hat{\lambda}_2$	\hat{p}_1	$\hat{\lambda}_1$	$\hat{\lambda}_2$	\hat{p}_1
Uniform prior	0.381184 (0.002447)	0.756889 (0.007935)	0.535297 (0.006711)	0.378104 (0.034814)	0.723677 (0.031677)	0.532335 (0.053736)
Nakagami prior	0.377204 (0.002420)	0.722023 (0.007572)	0.516536 (0.006537)	0.373998 (0.034429)	0.716491 (0.030999)	0.509802 (0.053186)

CONCLUSIONS

In this article the Bayesian inference of the single and mixture of Rayleigh models under type-II double censoring has been considered assuming informative and non-informative priors. The simulation study has displayed some interesting properties of the Bayes estimates. It is noted in each case that the posterior risks of estimates of lifetime parameters are reduced as the sample size increases. The performance of the Nakagami prior in each case (single or mixed model) is found to be better than the uniform prior. On the other hand, the performance of SELF is better for a smaller choice of parametric values, while for larger values of parameter the performance of KLF is better. This property is also the same in the case of single and mixed models. A real-life example further strengthens the findings from the simulation study. The study can further be extended by considering some other censoring techniques and by using some more flexible probability distributions.

REFERENCES

1. A. J. Fernandez, "On maximum likelihood prediction based on type II doubly censored exponential data", *Metrika*, **2000**, 50, 211-220.
2. A. J. Fernandez, "Bayesian estimation based on trimmed samples from Pareto populations", *Comput. Stat. Data Anal.*, **2006**, 51, 1119-1130.
3. H. M. R. Khan, S. B. Provost and A. Singh, "Predictive inference from a two-parameter Rayleigh life model given a doubly censored sample", *Commun. Stat. Theory Methods*, **2010**, 39, 1237-1246.
4. C. Kim and S. Song, "Bayesian estimation of the parameters of the generalized exponential distribution from doubly censored samples", *Stat. Papers*, **2010**, 51, 583-597.
5. H. M. R. Khan, A. Albatineh, S. Alshahrani, N. Jenkins and N. U. Ahmed, "Sensitivity analysis of predictive modeling for responses from the three-parameter Weibull model with a follow-up doubly censored sample of cancer patients", *Comput. Stat. Data Anal.*, **2011**, 55, 3093-3103.
6. A. Pak, G. A. Parham and M. Saraj, "On estimation of Rayleigh scale parameter under doubly type-II censoring from imprecise data", *J. Data Sci.*, **2013**, 11, 305-322.
7. A. A. Soliman, "Estimators for the finite mixture of Rayleigh model based on progressively censored data", *Commun. Stat. Theory Methods*, **2006**, 35, 803-820.
8. K. S. Sultan, M. A. Ismail and A. S. Al-Moisheer, "Mixture of two inverse Weibull distributions: Properties and estimation", *Comput. Stat. Data Anal.*, **2007**, 51, 5377-5387.
9. M. Saleem and M. Aslam, "Bayesian analysis of the two-component mixture of the Rayleigh distribution assuming the Uniform and the Jeffreys' priors", *J. Appl. Stat. Sci.*, **2008**, 16, 105-113.
10. D. Kundu and H. Howlader, "Bayesian inference and prediction of the inverse Weibull distribution for type-II censored data", *Comput. Stat. Data Anal.*, **2010**, 54, 1547-1558.
11. M. Saleem, M. Aslam and P. Economou, "On the Bayesian analysis of the mixture of power function distribution using the complete and the censored sample", *J. Appl. Stat.*, **2010**, 37, 25-40.
12. Y. Shi and W. Yan, "The EB estimation of scale-parameter for two-parameter exponential distribution under the type-I censoring life test", *J. Phys. Sci.*, **2010**, 14, 25-30.
13. T. Eluebaly and N. Bougila, "Bayesian learning of finite generalized Gaussian mixture models on images", *Signal Proc.*, **2011**, 91, 801-820.
14. K. S. Sultan and A. S. Al-Moisheer, "Approximate Bayes estimation of the parameters and reliability function of a mixture of two inverse Weibull distributions under type-2 censoring", *J. Stat. Comput. Simul.*, **2013**, 83, 1900-1914.
15. S. M. A. Kazmi, M. Aslam, S. Ali and N. Abbas, "Selection of suitable prior for the Bayesian mixture of a class of lifetime distributions under type-I censored datasets", *J. Appl. Stat.*, **2013**, 40, 1639-1658.
16. S. Ali, M. Aslam and S. M. A. Kazmi, "On the Bayesian analysis of the mixture of Laplace distribution using the censored data under different loss functions", *Model Assist. Stat. Appl.*, **2012**, 7, 209-227.
17. S. Ali, M. Aslam and S. M. A. Kazmi, "Choice of suitable informative prior for the scale parameter of the mixture of Laplace distribution", *Electron. J. Appl. Stat. Anal.*, **2013**, 6, 32-56.
18. N. Feroze, M. Aslam and M. Saleem, "Statistical properties of two component mixture of Topp Leone distribution under a Bayesian approach", *Int. J. Intell. Technol. Appl. Stat.*, **2013**, 6, 65-99.

19. N. Feroze and M. Aslam, "On Bayesian estimation and predictions for two-component mixture of Gompertz distribution", *J. Modern Appl. Stat. Meth.*, **2013**, 12, 269-292.
20. N. Feroze and M. Aslam, "Bayesian analysis of doubly censored lifetime data using two component mixture of Weibull distribution", *J. Natn. Sci. Found. Sri Lanka*, **2014**, 42, 325-334.
21. T. N. Sindhu, M. Aslam and N. Feroze, "Statistical inference for mixed Burr type II distribution using a Bayesian framework", *Int. J. Stat. Econ.*, **2014**, 13, 90-107.
22. T. N. Sindhu, N. Feroze and M. Aslam, "Preference of prior for Bayesian analysis of the mixed Burr type x distribution under type I censored samples", *Pakistan J. Stat. Operat. Res.*, **2014**, 10, 17-39.
23. H. Teicher, "Identifiability of mixtures", *Ann. Math. Stat.*, **1961**, 32, 244-248.
24. N. Feroze and M. Aslam, "Bayesian analysis of Gumbel type II distribution under doubly censored samples using different loss functions", *Caspian J. Appl. Sci. Res.*, **2012**, 1, 1-10.
25. P. S. Laplace, "Theorie Analytique des Probabilités", Ve. Courcier, Paris, **1812**.
26. M. Nakagami, "The m-distribution: A general formula of intensity distribution of rapid fading", in "Statistical Methods in Radio Wave Propagation" (Ed. W. C. Hoffman), Pergamon Press, New York, **1960**, pp.3-36.
27. M. T. Wasan, "Parametric Estimation", McGraw-Hill, New York, **1970**.
28. S. Ali, "On the Bayesian estimation of weighted Lindley distribution", *J. Stat. Comput. Simul.*, **2015**, 85, 855-880.
29. S. D. Grimshaw, B. J. Collings, W. A. Larsen and C. R. Hurt, "Eliciting factor importance in a designed experiment", *Technometrics*, **2001**, 43, 133-146.
30. A. O'Hagan, C. E. Buck, A. Daneshkhah, J. R. Eiser, P. H. Garthwaite, D. J. Jenkinson, J. E. Oakley and T. Rakow, "Uncertain Judgements: Eliciting Expert Probabilities", John Wiley and Sons, Chichester, **2006**.
31. D. Jenkinson, "The elicitation of probabilities: A review of the statistical literature", BEEP Working Paper, Department of Probability and Statistics, University of Sheffield, Scotland, **2005**.
32. J. C. Leon, F. J. Vazquez-Polo and R. L. Gonzalez, "Elicitation of expert opinion in benefit transfer of environmental goods", *Environ. Resour. Econ.*, **2003**, 26, 199-210.
33. M. Aslam, "An application of prior predictive distribution to elicit the prior density", *J. Stat. Theory Appl.*, **2003**, 2, 70-83.
34. A. Bekker, J. J. J. Roux and P. J. Mosteit, "A generalization of the compound Rayleigh distribution: Using a Bayesian method on cancer survival times", *Commun. Stat. Theory Meth.*, **2000**, 29, 1419-1433.

Full Paper

Numerical modelling of local scour caused by submerged jets

Sangdo An¹, Hyeyun Ku^{2,*} and Pierre Y. Julien³

¹Korea Water Resources Corporation, 200 Sintanjin-ro, Daedeok-gu, Daejeon 306-711, South Korea

²Department of Civil Engineering, Seoul National University, 1 Gwanak-ro, Gwanak-gu, Seoul 151-744, South Korea

³Department of Civil Engineering, Colorado State University, Fort Collins 80526-1372, Colorado, USA

* Corresponding author, e-mail: hyeyun.ku@gmail.com

Received: 1 June 2014 / Accepted: 14 October 2015 / Published: 17 October 2015

Abstract: The local scour downstream of an apron caused by submerged jets issuing from a sluice gate is investigated by means of Flow-3D computational fluid dynamics code. The performance of the numerical model based on renormalisation group $k-\varepsilon$ turbulence scheme and large-eddy simulation (LES) technique is evaluated by comparison with laboratory experiments. Various empirical formulas are coupled with the Flow-3D model to accurately simulate the bedload transport rate. The simulated evolution profiles of local scour are also compared with laboratory experiments. The simulation results show considerable numerical discrepancies between the renormalisation group $k-\varepsilon$ and the LES closure scheme. The Flow-3D model by the LES closure scheme coupled with an appropriate bedload transport formula successfully captures the bed deformation. The simulation results provide a good quantitative means of predicting the formation of both the local scour and the sand dune caused by submerged jets. The present work highlights the potential of the numerical simulation technique and the empirical bedload formulas for the investigation of local scour.

Keywords: computational fluid dynamics, local scour, sediment transport, Flow-3D, environmental engineering

INTRODUCTION

Scour in the river environment has received much attention in the engineering field. Hydraulic structures such as dams, sea walls and bridge piers which completely or partially obstruct water flow induce changes in the hydraulic characteristics of the flow. For instance flow acceleration as a result of vertical expansion or contraction in the river causes strong turbulence and channel degradation or aggradation leading to a new equilibrium status [1-2]. In the vicinity of a

hydraulic structure, increase in the transport sediment load may directly result in a local scour. In some cases the scour holes may lead to failure of the hydraulic structure in coastal areas and rivers [3]. Because scouring has been recognised as one of the major causes of collapse of hydraulic structures, prediction of scour development around them is of great importance not only for ensuring their safety, but also for ensuring their effective long-term maintenance.

Many hydraulic structures (e.g. reservoirs and dams) have been constructed and managed in South Korea with the objectives of controlling flood and storing agricultural water. Downstream of a reservoir and dam, bed scour may be formed by plunging jets and submerged jets of periodically released water. To prevent the formation of local scour resulting from jets, currents, waves or eddies, stilling basins and bed protection methods such as horizontal mats or large rock riprap are widely employed. However, in most cases the flow still remains highly turbulent, resulting in local scour of the seabed or streambed downstream of the hydraulic structure. In some cases it may require constructing a bed protection to minimise and move further the scour holes, thus decreasing the risk of a hydraulic structure failure [2]. Figure 1 shows local scour downstream of the concert apron of a low-head dam constructed in South Korea. A multi-beam echo sounder and side-scan sonar system were used to measure the depth and extent of scour holes.

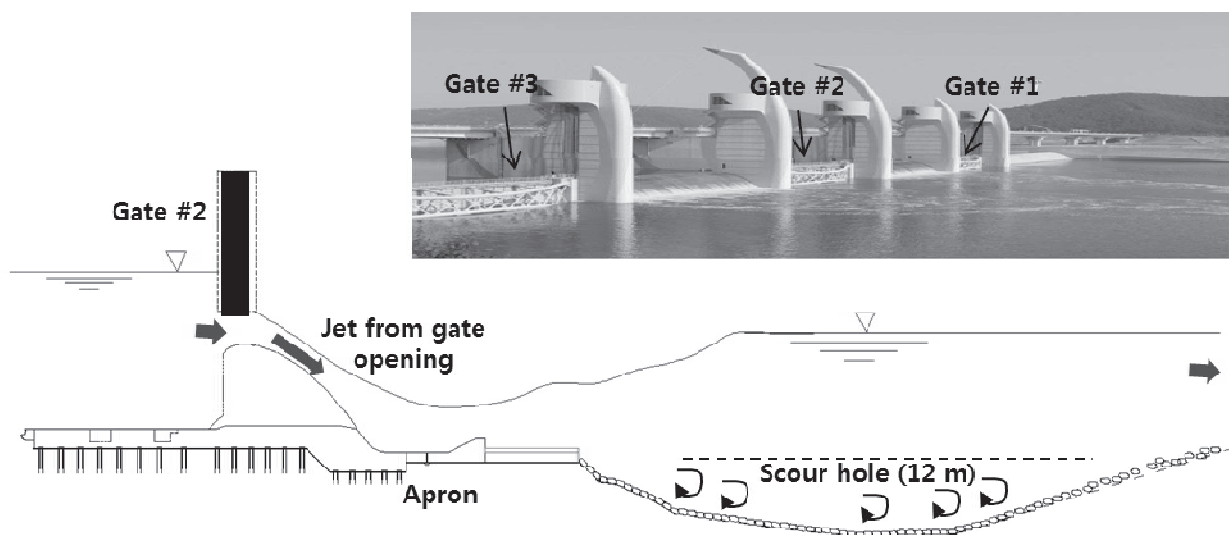


Figure 1. A schematic diagram of local scour downstream of a low-head dam in South Korea based on the bathymetric survey by means of a side-scan sonar system

Many experimental studies have focused on local scour downstream of hydraulic structures such as bed sills in an estuary [4, 5], underflow sluice gates [6] and grade-control structures [7]. Various numerical models for predicting bed changes have been used. One-dimensional sediment transport models have been most often applied to the long-time simulation of reach-scale bed changes [8, 9]. Two-dimensional depth-averaged models, which are widely used in the engineering practice, have been employed so far for local scour modelling [10, 11]. Efforts to simulate local scour with more complicated three-dimensional turbulence closure models have increased since the scouring and sedimentation processes are actually three-dimensional in nature [12, 13]. Direct numerical simulations of the sediment transport forced by steady currents or waves have been performed [14, 15], but they are computationally too intensive and thus generally have not been applied to field-scale applications [16]. In recent years numerical models based on computational

fluid dynamics have been applied to practical sedimentation engineering problems and have shown the good results in predicting the bed deformation in rivers [17-19]. The scour process caused by plunging or submerged jets released from large dams is associated with strong vortexes induced by three-dimensional highly turbulent flows. In this case a three-dimensional numerical model is recommended for the simulation of local scour.

In this study we mainly focus on understanding the local scour process by employing the computational fluid dynamics code, Flow-3D, which is a non-hydrostatic numerical model [20]. We firstly demonstrate the applicability of the code for predicting the shape and depth of a local scour hole by comparing numerical results with those from laboratory experiments reported in the literature [4-7]. An assessment and comparison of turbulence closure schemes using various empirical formulas for bedload sediment transport are then performed. We expect that this study can finally be used to justify the potential of the Flow-3D code after coupling with proper empirical formulas for studying local scour at the field scale.

NUMERICAL MODEL DESCRIPTION

Fluid Flow Model

In this study we employed the Flow-3D code, which is the non-hydrostatic numerical model [20]. The non-hydrostatic numerical simulation constitutes a technological improvement for the movement of sediment particles because hydrostatic models cannot accurately predict the fluid flow and sediment transport in the region where 3-dimensional flows strongly occur [21]. The governing equations solved in Flow-3D are: (1) 3-D Reynolds-averaged Navier-Stokes equations for fluid flow with Boussinesq approximation, (2) the continuity equation and (3) the transport equation for each scalar (e.g. sediment concentration) variable [20]. These equations are given in tensor notations by

$$\frac{\partial u_i}{\partial t} + u_j \frac{\partial u_i}{\partial x_j} = -\frac{1}{\rho_r} \frac{\partial p}{\partial x_i} + \frac{\partial}{\partial x_j} \left(\nu \frac{\partial u_i}{\partial x_j} - \overline{u_i u_j} \right) + g_i \frac{\rho - \rho_r}{\rho_r}, \quad (1)$$

$$\frac{\partial u_i}{\partial x_i} = 0 \quad (2)$$

$$\frac{\partial \phi}{\partial t} + \frac{\partial}{\partial x_i} (u_i \phi) = \frac{\partial}{\partial x_i} \left(\Gamma \frac{\partial \phi}{\partial x_i} - \overline{u_i \phi} \right) \quad (3)$$

where u_i = mean velocity components in a Cartesian coordinate system (x, y, z) , t = time, ρ = density which can be calculated as a function of sediment concentration, ρ_r = reference density, p = total pressure, ν = fluid kinematic viscosity, $-\overline{u_i u_j}$ = Reynolds stresses, g_i = gravitational acceleration components in each direction, Γ = molecular diffusivity of arbitrary scalar ϕ , and $-\overline{u_i \phi}$ = turbulent fluxes of scalar ϕ . The overbar denotes the averaging of fluctuating quantities.

Turbulence Model

The Reynolds stresses ($\overline{u_i u_j}$) can be generally modelled using the turbulent viscosity hypothesis [22]:

$$-\overline{u_i u_j} = \nu_t \left(\frac{\partial u_i}{\partial x_j} + \frac{\partial u_j}{\partial x_i} \right) - \frac{2}{3} k \delta_{ij}, \quad (4)$$

where ν_t = turbulent (eddy) viscosity, δ_{ij} = Kronecker delta and k = turbulent kinetic energy. In this study we first employed the renormalisation-group (RNG) $k - \varepsilon$ closure scheme [23], in which the eddy viscosity is defined as

$$\nu_t = c_\mu k^2 / \varepsilon, \quad (5)$$

where c_μ = empirical constant and ε = turbulence kinetic energy dissipation rate. In (5) the turbulence kinetic energy (k) and its dissipation rate (ε) are obtained from the following transport equations [20]:

$$\frac{\partial k}{\partial t} + u_j \frac{\partial k}{\partial x_j} = \frac{\partial}{\partial x_j} \left(\frac{\nu_t}{\sigma_k} \frac{\partial k}{\partial x_j} \right) + P + G - \varepsilon, \quad (6)$$

$$\frac{\partial \varepsilon}{\partial t} + u_j \frac{\partial \varepsilon}{\partial x_j} = \frac{\partial}{\partial x_j} \left(\frac{\nu_t}{\sigma_\varepsilon} \frac{\partial \varepsilon}{\partial x_j} \right) + c_{1\varepsilon} \frac{\varepsilon}{k} (P + c_{3\varepsilon} G) - c_{2\varepsilon} \frac{\varepsilon^2}{k}, \quad (7)$$

where P and G are defined as

$$P = \nu_t \left(\frac{\partial u_i}{\partial x_j} + \frac{\partial u_j}{\partial x_i} \right) \frac{\partial u_i}{\partial x_j}, \quad (8)$$

$$G = g_i \frac{\nu_t}{Sc_i} \frac{1}{\rho_r} \frac{\partial \rho}{\partial x_i}. \quad (9)$$

The parameter values in (5)-(7) obtained from the literature are: $c_\mu = 0.085$, $c_{1\varepsilon} = 1.42$, $c_{3\varepsilon} = 0.2$, $\sigma_k = 1.39$ and $\sigma_\varepsilon = 1.39$. In the RNG model, $c_{2\varepsilon}$ is a function of the shear rate given [23] by

$$c_{2\varepsilon} = 1.83 + \frac{c_\mu \eta^3 (1 - \eta / \eta_o)}{1 + \beta \eta^3}, \quad (10)$$

where $\eta_o = 4.38$, $\beta = 0.015$, $\eta = S k / \varepsilon$ and $S = \sqrt{2 S_{ij} S_{ij}}$, S_{ij} representing the strain rate tensor given by

$$S_{ij} = \frac{1}{2} \left(\frac{\partial u_i}{\partial x_j} + \frac{\partial u_j}{\partial x_i} \right). \quad (11)$$

This study also employed the large-eddy simulation (LES) technique, which provides more detailed information about the interfacial turbulence between bottom and ambient fluids. The LES technique resolves large eddies directly but uses a subgrid-scale turbulence model for small eddies [24].

Sediment Scour Model

Particle dynamics

Most previous studies employed the advection-diffusion relationship (equation 3) to describe the transport of suspended sediment [25-29]. They assumed that particle inertia could be ignored and thus only the mechanism of advection and diffusion affected the transport of suspended sediment. However, some researchers showed that this approach could not fully describe the motion of suspended sediment [30]. In the Flow-3D model a more accurate simulation is obtained by incorporating particle dynamics into the code [16]. The drift velocity of sediment is computed based

on momentum balances for each sediment fraction and fluid-sediment mixture, given in vector forms as:

$$\frac{\partial u_{s,i}}{\partial t} + \bar{u} \cdot \nabla u_{s,i} = -\frac{1}{\rho_{s,i}} \nabla p + F - \frac{K_i}{f_{s,i} \rho_{s,i}} u_{r,i}, \quad (12)$$

$$\frac{\partial \bar{u}}{\partial t} + \bar{u} \cdot \nabla \bar{u} = -\frac{1}{\bar{\rho}} \nabla p + F, \quad (13)$$

where F is ratio of fluid volume to one computational cell (for example, $F = 1$ indicates that the computational cell is filled with fluid), K_i and $f_{s,i}$ are drag function and volume fraction of sediment respectively, $u_{s,i}$ is velocity of sediment fraction i , \bar{u} and $\bar{\rho}$ are mean velocity and density of fluid-sediment mixture respectively, and $u_{r,i}$ is relative velocity given by

$$u_{r,i} = u_{s,i} - u_f. \quad (14)$$

The mean density $\bar{\rho}$ is defined as:

$$\bar{\rho} = \sum_{i=1}^N f_{s,i} \rho_{s,i} + \left(1 - \sum_{i=1}^N f_{s,i}\right) \rho_f \quad (15)$$

where $\rho_{s,i}$ and ρ_f are densities of sediment fraction i and fluid respectively, and N is number of sediment fractions. Subtracting (13) from (12) gives

$$\frac{\partial u_{drift,i}}{\partial t} + \bar{u} \cdot \nabla u_{drift,i} = \left(\frac{1}{\bar{\rho}} - \frac{1}{\rho_{s,i}}\right) \nabla p - \frac{K_i}{f_{s,i} \rho_{s,i}} u_{r,i}. \quad (16)$$

The drift velocity $u_{drift,i}$ is defined as:

$$u_{drift,i} = u_{s,i} - \bar{u}. \quad (17)$$

In (14), $u_{r,i}$ is computed by assuming that the advection term is very small due to the small gradient in drift velocity and the slow motion of sediment in near-steady state at the scale of the computational time:

$$u_{r,i} = \frac{\nabla p}{\bar{\rho} K_i} (\rho_{s,i} - \rho_f) f_{s,i}, \quad (18)$$

where K_i denotes the drag function involving form drag and Stokes drag:

$$K_i = \frac{3 f_{s,i}}{4 d_{s,i}} \left(C_{D,i} \|u_{r,i}\| + 24 \frac{\mu_f}{\rho_f d_{s,i}} \right), \quad (19)$$

where $C_{D,i}$ and $d_{s,i}$ indicate drag coefficient and diameter of sediment species respectively, and μ_f is fluid viscosity. The mean flow velocity \bar{u} is determined by computing the velocities of all of the phases:

$$\bar{u} = \left(1 - \sum_{j=1}^N f_{s,j}\right) u_f + \sum_{j=1}^N f_{s,j} u_{s,j}. \quad (20)$$

The drift becomes essentially an additional mechanism of sediment transport in the mixture flows with advection and turbulent diffusion.

Entrainment

Entrainment involves the processes of particle pick-up and re-suspension near the bed surface. This needs to be computed in the saltation region (i.e. packed sediment domain). In the model the entrainment of packed sediment is calculated using an empirical model [31]. The entrainment lift velocity of sediment fraction i is the volumetric flux of sediment defined as

$$u_{lift,i} = \alpha_i n_s d_*^{0.3} (\tau_{*,i} - \tau_{*,c,i})^{1.5} \sqrt{\frac{\|g\| d_{s,i} (\rho_{s,i} - \rho_f)}{\rho_f}}, \quad (21)$$

where $\tau_{*,i}$ is the local Shields parameter on the bed surface, obtained based on the ratio of hydrodynamic forces to the particle submerged weight, given by

$$\tau_{*,i} = \frac{\tau_o}{\|g\| d_{s,i} (\rho_{s,i} - \rho_f)}. \quad (22)$$

In the Shields parameter, τ_o is the local boundary shear stress and d_* is the dimensionless mean particle diameter defined as

$$d_* = d_{50} \left[\frac{\rho_f (\rho_{s,i} - \rho_f) \|g\|}{\mu_m} \right]^{\frac{1}{3}}, \quad (23)$$

where d_{50} and μ_m are the local mean particle size and the viscosity of a mixture respectively. The critical value of the Shields parameter $\tau_{*,c,i}$ corresponds to the beginning of motion of sediment particle. In this model $\tau_{*,c,i}$ describes incipient motion on a flat horizontal surface and is computed by the Shields-Rouse equation [32] given by

$$\tau_{*,c,i} = \frac{0.1}{R_{*,i}^{2/3}} + 0.054 \left[1 - \exp\left(-\frac{R_{*,i}^{0.52}}{10}\right) \right] \quad (24)$$

where R_* is the Rouse-Reynolds number, defined as

$$R_{*,i} = \frac{\sqrt{0.1(\rho_{s,i} - \rho_f)\rho_f \|g\| d_{s,i}^3}}{\mu_f}. \quad (25)$$

In the case of a sloping bed surface, $\tau_{*,c,i}$ should be modified according to the local slope of the bed and the shear force direction. In this study the approach suggested by Soulsby [33], which is similar to the those of Brooks [34] and Julien [35], was employed to account for the effect of the bed slope on sediment transport. The adjusted critical Shields parameter is given by

$$\tau'_{*,c,i} = \tau_{*,c,i} \frac{\cos\psi \sin\beta + \sqrt{\cos^2\beta \tan^2\varphi_i - \sin^2\psi \sin^2\beta}}{\tan\varphi_i}, \quad (26)$$

where β is the computed angle between the normal to the bed surface and the gravitational acceleration vector g , φ_i is the angle of repose of sediment fraction i , and ψ is the angle between the flow and the upslope direction (Figure 2). If the flow goes up the slope (i.e. $\psi = 0$), (26) then reduces to the formulation of Bormann and Julien [7]:

$$\tau'_{*,c,i} = \tau_{*,c,i} \frac{\sin(\varphi_i + \beta)}{\sin\varphi_i}. \quad (27)$$

If the flow goes directly down the slope (i.e. $\psi = 180^\circ$), (26) reduces to

$$\tau'_{*c,i} = \tau_{*c,i} \frac{\sin(\varphi_i - \beta)}{\sin \varphi_i} \tag{28}$$

When the flow is directed laterally across the slope (i.e. $\psi \pm 90^\circ$), (26) becomes identical to the formulation of Lane [36]:

$$\tau'_{*c,i} = \tau_{*c,i} \cos \beta \left(1 - \frac{\tan^2 \beta}{\tan^2 \varphi_i} \right)^{1/2} \tag{29}$$

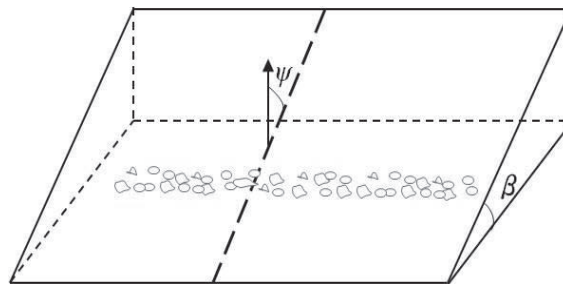


Figure 2. Angles of bedload transport: β is angle between the normal to bed surface and the gravitational vector, and ψ is angle between the flow and the upslope direction.

Bedload transport

Non-cohesive bed particles begin to move when the shear stress on the bed material exceeds the critical shear stress. Generally, finer sediment such as silt and clay is easily entrained and suspended, whereas sand and gravel particles roll and slide in the bed layer or bedload. Most of the bedload transport formulas suggested in the literature were empirically developed. Many of them relate the transport rate to the average shear stress in excess of the critical shear stress. A numerical modelling of small-scale turbulence affecting bedload transport requires an extremely fine mesh size and accurate bed surveys that may be almost impossible to actually perform in field-scale applications. To overcome these problems, an empirical formula may be used to estimate the effects of small-scale turbulence on bedload transport. Table 1 shows the bedload formulas used for this purpose.

Table 1. Bedload transport formulas

Author	Formula
Engelund and Fredsøe [37]	$q_{*i} = 18.74(\tau_{*i} - \tau_{*c,i})[\tau_{*i}^{1/2} - 0.7\tau_{*c,i}^{1/2}]$
Meyer-Peter and Müller [38]	$q_{*i} = 8(\tau_{*i} - \tau_{*c,i})^{1.5}$
Nielsen [39]	$q_{*i} = 12(\tau_{*i} - \tau_{*c,i})^{1.5} \sqrt{\tau_{*i}}$

The bedload transport of sediment is quantified by the bedload flux $q_{bv,i}$ that refers to the volume of sediment per unit width per unit time within the bed layer, and is rewritten using the dimensionless bedload flux q_{*i} [40]:

$$q_{bv,i} = q_{*,i} \sqrt{\left(\frac{\rho_{s,i} - \rho_f}{\rho_f} \right) \|g\| d_{s,i}^3} \quad (30)$$

The Flow-3D model adjusts the time-step size so that the fluid does not flow across more than one cell in one computational time step, δt , which is referred to as a Courant stability criterion [41], defined as:

$$\delta t < 0.45 \cdot \min \left(\frac{V_f \delta x_i}{A_x u}, \frac{V_f \delta y_j}{A_y v}, \frac{V_f \delta z_k}{A_z w} \right) \quad (31)$$

where V_f and A are, respectively, fractional volume and area open to flow in the FAVOR method [42]. In Flow-3D, if the automatic time-step is selected, the model adjusts the time step to be as large as possible while keeping the stability criteria.

MODEL APPLICATION

Problem Configuration and Simulation Cases

A series of numerical simulations were performed under conditions that corresponded to a laboratory experimental flume set-up for submerged jet scour [6]. This experiment studied the development of a scour hole and sand dune by submerged jets as shown in Figure 3.

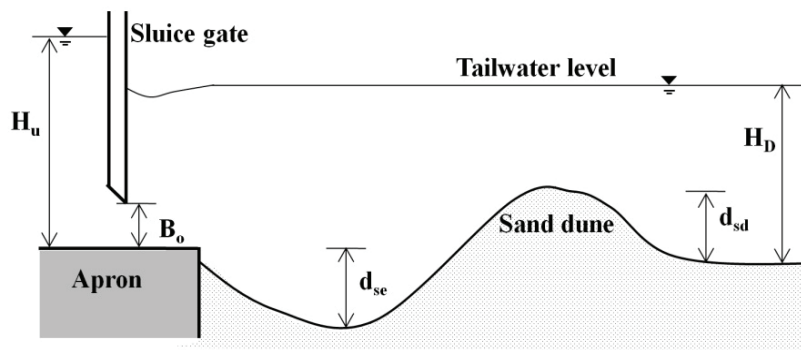


Figure 3. Schematic of scour hole and sand dune development due to turbulent jet

The computational domain was configured in an identical manner with the experimental dimensions (i.e. 406 cm in length, 60 cm in width and 60 cm in height). The erodible bed consisted of 0.4 m of open channel at the end of the rigid apron. The jet flowed out from the sluice gate opening and flowed over the erodible bed consisting of coarse sand (mean particle size (d_{50}) = 0.76 mm, density (ρ_s) = 2,650 kg/m³, porosity (p_o) = 0.43, and angle of repose (φ) = 29°). The gate opening (B_o) was fixed at 2.0 cm and the jet inlet velocity was 1.56 m/s.

The computational domain for the submerged jet scour simulations with the specified boundary conditions is illustrated in Figure 4. In the laterally-averaged simulation, the computational grid size in the x -direction was uniformly set at $\Delta x = 16$ mm, whereas the fine grid-spacing ranging between 0.02-0.005 mm was used in the z -direction to increase the simulation speed without significant loss of accuracy. For 3-D simulation, the computational grid was extended in a

lateral (y) direction. Considering the computational constraints, a coarser grid size ($\Delta y = 12$ mm) was used in the lateral direction. The domain was comprised of approximately 750,000 cells.

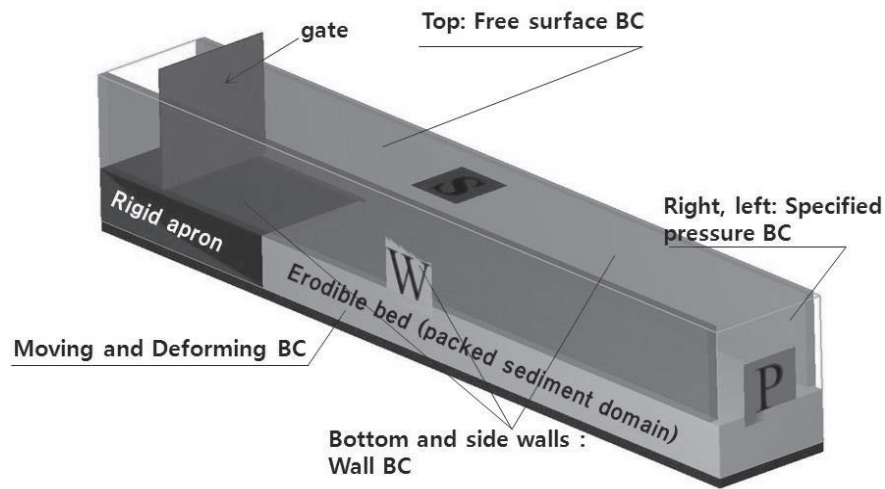


Figure 4. Computational domain depicting erodible region and boundary conditions (BCs) for the simulations corresponding to experiment [6]. W, P and S indicate wall, pressure and symmetry boundary conditions respectively.

The wall boundary is specified as non-tangential stress areas with no-slip condition. At the walls, k and ε were computed using a logarithmic law of wall function [41] given by

$$k = \frac{u_*^2}{\sqrt{c_\mu}}, \varepsilon = \frac{u_*^3}{\kappa y_o}, \quad (32)$$

where u_* = shear velocity, κ = von Kármán constant and y_o = the normal distance from the boundary wall to the location of tangential velocity. The packed sediment domain was set as a moving and deforming boundary. It could be deformed only by entrainment or bedload transport. The change in the surface of the packed erodible bed was computed using the current sediment concentration. When the computed sediment concentration in a cell exceeded the packing fraction of the sediment, it meant that all sediment settled down to the bottom and increased the thickness of the packed bed. A volume-of-fluid function was used to track fluid-sediment interfaces [43]. At the free surface no flux conditions were imposed and tangential stresses were zero since all velocity derivatives including velocity components outside the surface were assumed to be zero. The volume-of-fluid function was used to track the location of the free surface in a Eulerian mesh cell. For the inlet and outlet boundaries, the pressure boundary condition with hydrostatic pressure distribution was used to represent the water depth at the downstream end of the erodible bed and upstream end of the flume. The suspended sediment flux and the bedload flux at the inlet were zero since clear water flowed out from the inlet boundary and flowed over the rigid apron without any bedload transport before hitting the sand bed. All conditions for numerical simulations are summarised in Table 2. The numerical simulations were performed on a personal computer with 3.2GHz Quad-core(i7) and 4GB memory. We used the shared-memory parallel version of Flow-3D code allowing for efficient parallelism. We performed the numerical simulations until a steady state was reached, i.e. approximately 10 hours for a 2-D simulation and 1 day for a 3-D simulation.

Table 2. Summary of simulation cases

Case no.	Bed material (sand)				Domain set-up			Numerical option		
	d_{50} (mm)	ρ_s (kg/m ³)	Porosity	p_o	B_o (cm)	H_U (cm)	H_D (cm)	Dimensionality	Turbulence model	Bedload formula
1	0.76	2650	0.43	29	2.0	41.1	29.1	2-D	RNG $k-\varepsilon$	Meyer-Peter and Müller [38]
2								2-D	LES	Meyer-Peter and Müller [38]
3								2-D	LES	Engelund and Fredsøe [37]
4								2-D	LES	Nielsen [39]
5								3-D	LES	Meyer-Peter and Müller [38]

Development of Local Scour

Velocity vectors near the scour hole are shown in Figure 5. They show that the strong submerged jet forms an attached bed-jet on the packed sediment region and induces a recirculating flow region rotating in a counterclockwise direction with flow separation at the top of the sand dune.

In Figure 6 the ratios of U/U_0 are plotted against the corresponding non-dimensional distance x/B_o , where U and U_0 are the depth-maximum horizontal velocity at position x and the inlet jet velocity below the sluice gate respectively. Values of U and U_0 are obtained by the simulations in this study and from experiment investigations in the literature [6].

The jet inlet velocity U_0 was computed to be 1.47 m/s, close to the experimental value of 1.56 m/s. In the rigid apron region the simulation results are very close to the experimental data but show a higher maximum velocity in the far downstream region.

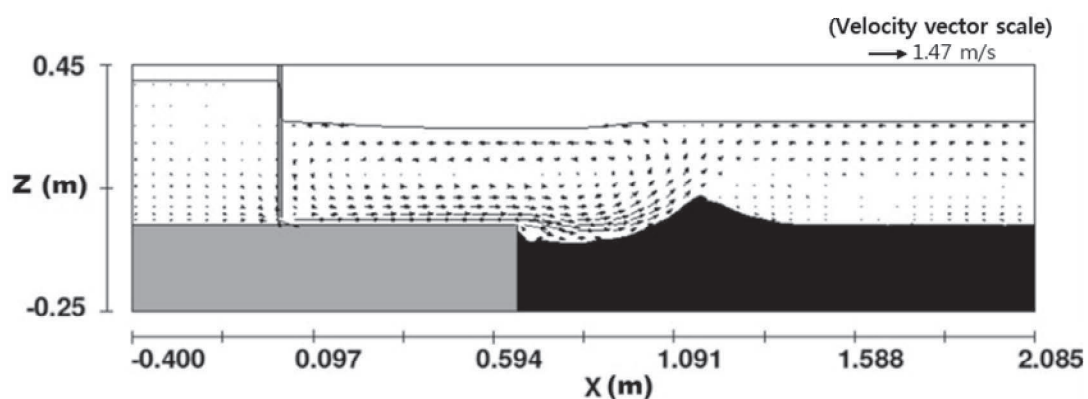


Figure 5. Velocity vectors and scour hole after 3600 sec (Case 5) near equilibrated scour depth of $d_{se} = 0.055$ m

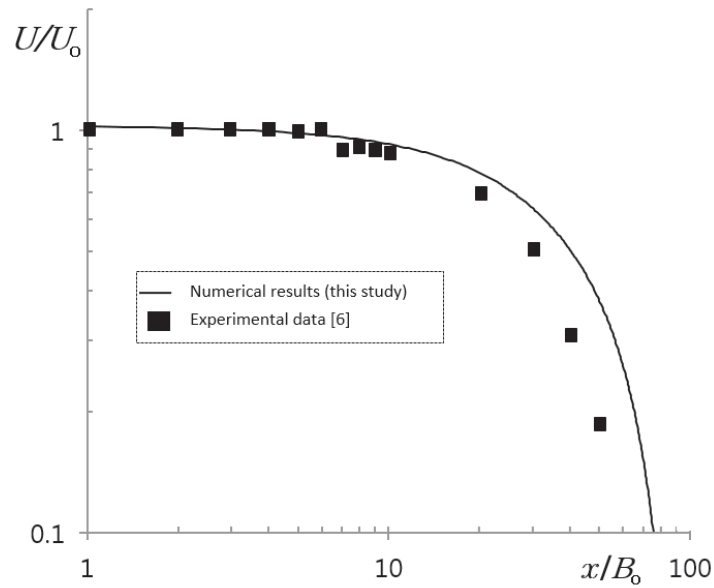


Figure 6. Depth-maximum velocity change along non-dimensional distance x/B_0 (x = distance in x-direction and B_0 = value of gate opening)

Figure 7 shows the performance of the numerical model using two different turbulence closure schemes, i.e. the RNG $k-\epsilon$ and the LES schemes, in comparison with the laboratory experiment. Significantly different results were obtained between the two numerical schemes. The limitation of the RNG $k-\epsilon$ scheme in sediment deposition modelling is that it does not capture the development of any sand dune, resulting in an inaccurate velocity distribution related to the scour process. In comparison, a better description of scour and deposition is achieved using the LES technique, which successfully reproduces the results from the experiment with scour hole formation and sediment deposition. However, the location of the simulated deposition region does not agree well with experimental data: the maximum height of the deposition region, $d_{sd} = 0.053$ m, and the scour hole, $d_{se} = 0.054$ m, are underestimated by 23% and 13% respectively.

Applications of various bedload formulas were carried out to improve the predictive capabilities for the development of deposition and the scour and deposition process for this study. Overall, all formulas predicted the scour hole and deposition process rather well. However, the prediction of the aggradation in front of the scour region is still unsatisfactory as shown in Figure 8.

Figure 9 depicts the results of the three-dimensional simulation conducted for comparison with the 2-D modelling. The comparison confirms that the 3-D simulation can improve the accuracy of the reproduction of local scour and deposition processes. In this case the simulation results of case 5 provide a maximum scour depth (d_{se}) of 0.055 m and a deposition height (d_{sd}) of 0.078 m, which agrees well with the measured data from the experiment.

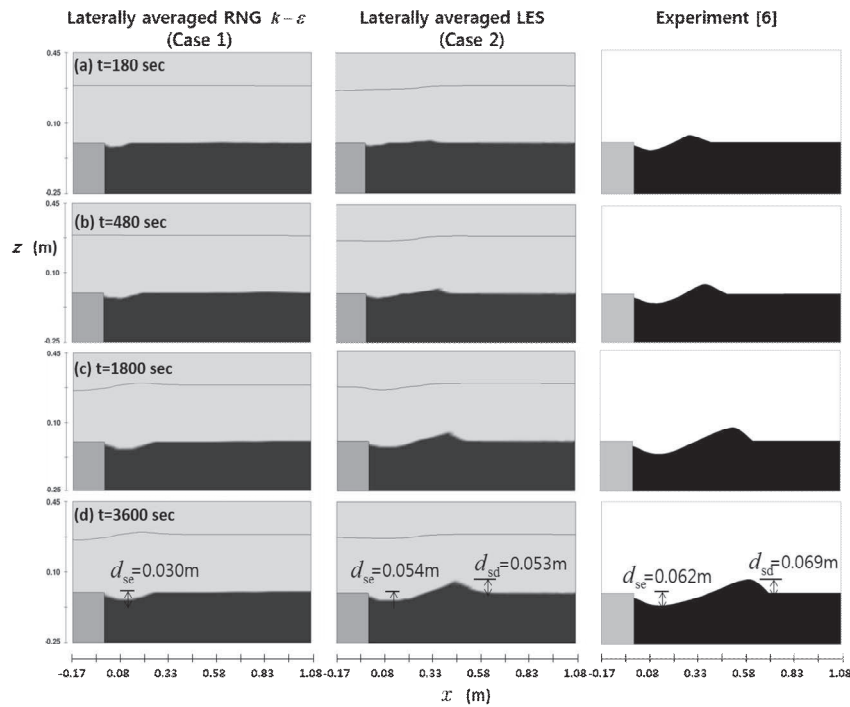


Figure 7. Temporal development of scour hole and sand dune computed using laterally averaged RNG and LES in comparison with experimental results. Computation of bedload transport is based on the Meyer-Peter and Müller formula [38].

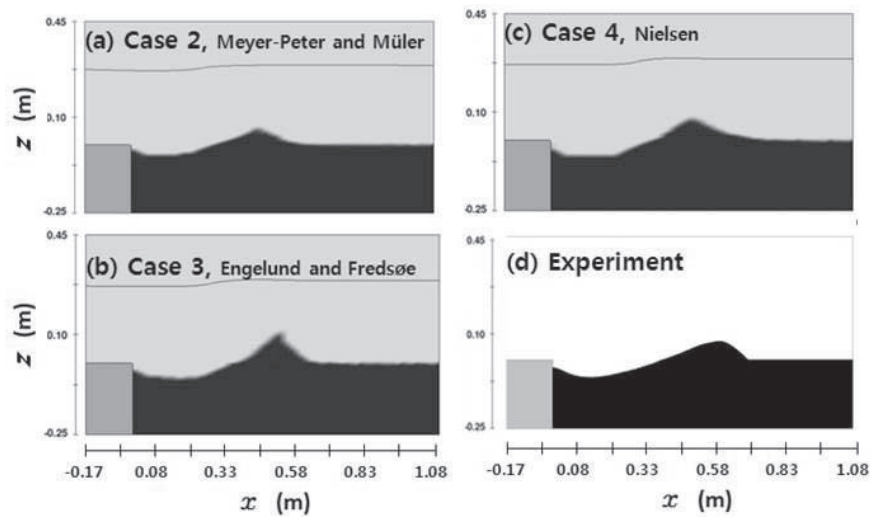
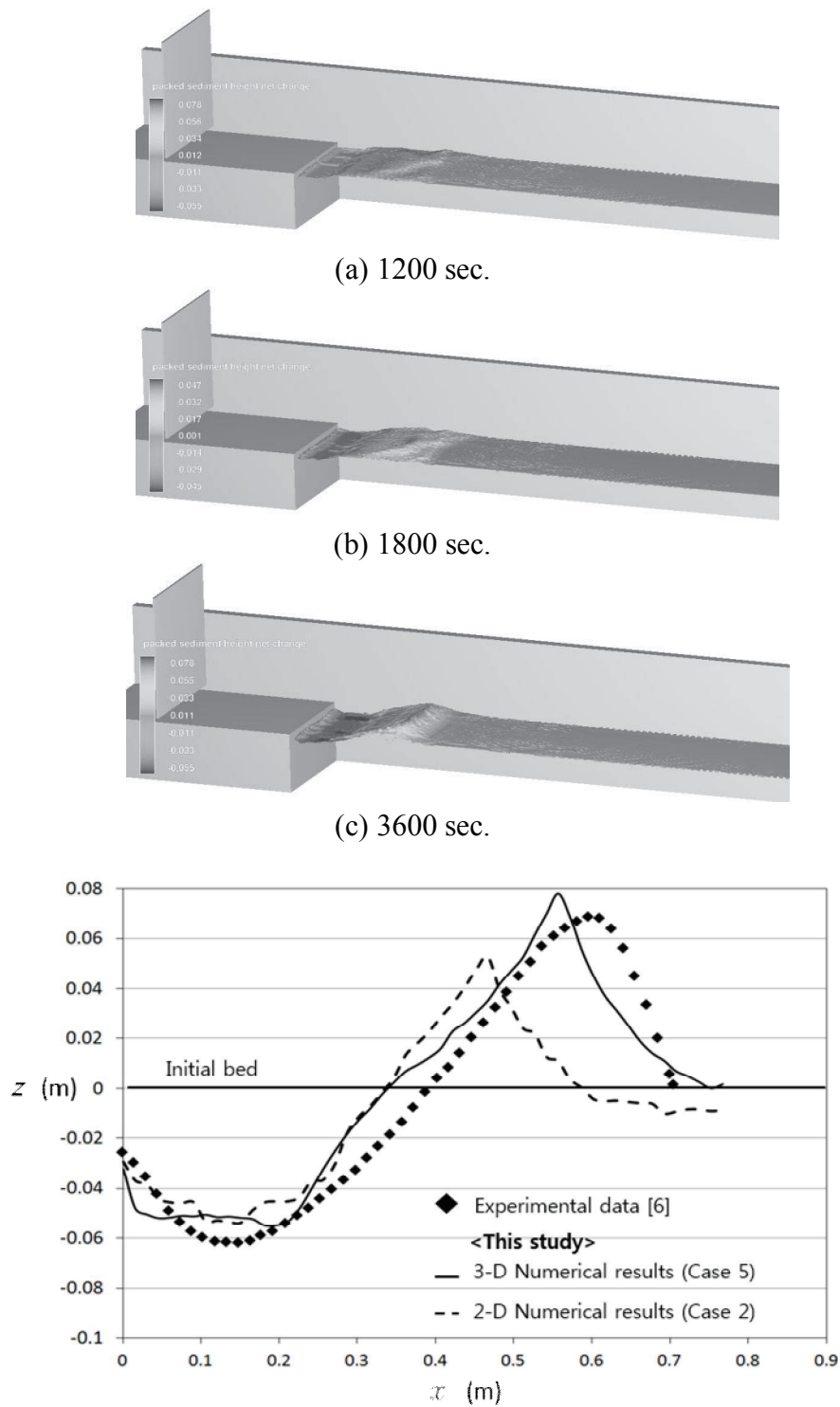


Figure 8. Comparison of bed profiles from tests using different bedload formulas with corresponding experimental data. Numerical results at $t = 3600$ sec. were used for plotting: (a)-(c) laterally-averaged LES scheme using different bedload formulas; (d) measured data from experiment [6]



(d) Plot of simulation and experimental data at 3600 sec.

Figure 9. 3-D estimation of bed elevation by LES scheme with Meyer-Peter and Müller formula [38] (case 5) and comparison with case 2 and with experimental data [6]

CONCLUSIONS

Two different turbulence closure schemes, viz. RNG $k-\varepsilon$ and LES have been tested for local scour modelling. The simulation results have shown considerable discrepancies between the two techniques. They clearly demonstrate that the RNG $k-\varepsilon$ closure scheme within the Reynolds-averaged Navier-Stokes framework cannot correctly reproduce the formation of a scour hole and

sand dune. In contrast, a more accurate reproduction of the shapes of both the scour hole and the sand dune is obtainable by employing the LES technique. However, both the direct numerical simulations and the LES schemes are prohibitive for field application because they are computationally very intensive. In this study we have also compared various empirical bedload formulas that can be coupled with the LES scheme, and which can reduce computational time without significant loss in performance. Overall, all formulas are found to predict the depth of the scour hole rather well.

The 2-D simulation accuracy in the prediction of aggradation in front of the scour region is unsatisfactory. A more accurate simulation of sediment transport and bed change is achieved by employing a 3-D model, which successfully captures both the scour hole and the sand dune growth and development.

REFERENCES

1. P. Y. Julien, "River Mechanics", 1st Edn., Cambridge University Press, Cambridge, **2002**, Ch.9.
2. G. J. C. M. Hoffmans and H. J. Verheij, "Scour Manual", CRC Press, Boca Raton, **1997**, Ch. 1.
3. R. Whitehouse, "Scour at Marine Structures: A Manual for Practical Application", Thomas Telford, London, **1998**, Ch. 1.
4. S. Dey and R. V. Raikar, "Scour below a high vertical drop", *J. Hydraul. Eng.*, **2007**, *133*, 564-568.
5. R. Gaudio and A. Marion, "Time evolution of scouring downstream of bed sills", *J. Hydraul. Res.*, **2003**, *41*, 271-284.
6. S. S. Chatterjee and S. N. Ghosh, "Submerged horizontal jet over erodible bed", *J. Hydraul. Div.*, **1980**, *106*, 1765-1782.
7. N. E. Bormann and P. Y. Julien, "Scour downstream of grade-control structures", *J. Hydraul. Eng.*, **1991**, *117*, 579-594.
8. W. Wu, D. Vieira and S. Wang, "One-dimensional numerical model for nonuniform sediment transport under unsteady flows in channel networks", *J. Hydraul. Eng.*, **2004**, *130*, 914-923.
9. R. Ferguson and M. Church, "A critical perspective on 1-D modeling of river processes: Gravel load and aggradation in lower Fraser River", *Water Resour. Res.*, **2009**, *45*, W11424.
10. B. M. Sumer, R. J. S. Whitehouse and A. Tørum, "Scour around coastal structures: A summary of recent research", *Coastal Eng.*, **2001**, *44*, 153-190.
11. W. Wu, R. Marsooli and Z. He, "Depth-averaged two-dimensional model of unsteady flow and sediment transport due to noncohesive embankment break/breaching", *J. Hydraul. Eng.*, **2012**, *138*, 503-516.
12. H. D. Smith and D. L. Foster, "Modeling of flow around a cylinder over a scoured bed", *J. Waterway Port Coast. Ocean Eng.*, **2005**, *131*, 14-24.
13. X. Liu and M. García, "Three-dimensional numerical model with free water surface and mesh deformation for local sediment scour", *J. Waterway Port Coast. Ocean Eng.*, **2008**, *134*, 203-217.
14. K. Bhaganagar and T.-J. Hsu, "Direct numerical simulations of flow over two-dimensional and three-dimensional ripples and implication to sediment transport: Steady flow", *Coast. Eng.*, **2009**, *56*, 320-331.
15. M. W. Schmeckle and J. M. Nelson, "Direct numerical simulation of bedload transport using a local, dynamic boundary condition", *Sedimentol.*, **2003**, *50*, 279-301.

16. S. An, P. Y. Julien and S. K. Venayagamoorthy, "Numerical simulation of particle-driven gravity currents", *Environ. Fluid Mech.*, **2012**, 12, 495-513.
17. N. Ruether and N. R. B. Olsen, "Towards the prediction of free-forming meander formation using 3D computational fluid dynamics", Proceedings of Annual Conference on Hydraulic Engineering: Flow Simulation in Hydraulic Engineering, **2006**, Dresden, Germany, pp.31-38.
18. Z. Xie, "Theoretical and numerical research on sediment transport in pressurised flow conditions", *PhD Thesis*, **2011**, University of Nebraska, USA.
19. C. Nitatwichit, Y. Khunatorn and N. Tippayawong, "Computational analysis and visualisation of wind-driven naturally ventilated flows around a school building", *Maejo Int. J. Sci. Technol.*, **2008**, 2, 240-254.
20. S. D. An, "Interflow dynamics and three-dimensional modeling of turbid density currents in Imha Reservoir, South Korea", *PhD Thesis*, **2011**, Colorado State University, USA.
21. O. B. Fringer, M. Gerritsen and R. L. Street, "An unstructured-grid, finite-volume, nonhydrostatic, parallel coastal ocean simulator", *Ocean Model.*, **2006**, 14, 139-173.
22. S. B. Pope, "Turbulent Flows", Cambridge University Press, Cambridge, **2000**, pp.359-365.
23. V. Yakhot, S. A. Orszag, S. Thangam, T. B. Gatski and C. G. Speziale, "Development of turbulence models for shear flows by a double expansion technique", *Phys. Fluids*, **1992**, 4, 1510-1520.
24. W. Rodi, G. Constantinescu and T. Stoesser, "Large-Eddy Simulation in Hydraulics", CRC Press, London, UK, **2013**, Ch.2.
25. A. O. Demuren and W. Rodi, "Calculation of flow and pollutant dispersion in meandering channels", *J. Fluid Mech.*, **1986**, 172, 63-92.
26. W. A. Thomas, W. H. McAnally and US Army Waterways Experiment Station, "User's Manual for the Generalized Computer Program Systems, Open Channel Flow and Sedimentation, TABS-2: Main Text", Department of the Army, Waterways Experiment Station, Corps of Engineers, Vicksburg (MS), **1985**, Ch.1.
27. L. C. Van Rijn, "Mathematical modeling of suspended sediment in nonuniform flows", *J. Hydraul. Eng.*, **1986**, 112, 433-455.
28. W. Wu, W. Rodi and T. Wenka, "3D numerical modeling of flow and sediment transport in open channels", *J. Hydraul. Eng.*, **2000**, 126, 4-15.
29. W. Wu, "CCHE2D-2.1, sediment transport model", Technical report no. NCCHE-TR- 2001-3, National Center for Computational Hydroscience and Engineering, University of Mississippi, **2001**, Ch.1.
30. G. Wang, X. Fu, Y. Huang and G. Huang, "Analysis of suspended sediment transport in open-channel flows: Kinetic-model-based simulation", *J. Hydraul. Eng.*, **2008**, 134, 328-339.
31. D. R. Mastbergen and J. H. Van Den Berg, "Breaching in fine sands and the generation of sustained turbidity currents in submarine canyons", *Sedimentol.*, **2003**, 50, 625-637.
32. J. Guo, "Hunter rouse and shields diagram", Proceedings of 13th IAHR-APD Congress, Vol.2, **2002**, Singapore, pp.1096-1098.
33. R. Soulsby, "Dynamics of Marine Sands", Thomas Telford, London, **1997**, pp.107-119.
34. N. H. Brooks, "Mechanics of streams with movable beds of fine sands", *Trans. ASCE*, **1958**, 123, 525-549.
35. P. Y. Julien, "Erosion and Sedimentation", 2nd Edn., Cambridge University Press, Cambridge, UK, **2010**, Ch.7.

36. E. W. Lane, "Progress report on studies on the design of stable channels by the Bureau of reclamation", *Proc. Am. Soc. Civ. Eng.*, **1953**, 79, 246-261.
37. F. Engelund and J. Fredsøe, "A sediment transport model for straight alluvial channels", *Nordic Hydrol.*, **1976**, 7, 293-306.
38. E. Meyer-Peter and R. Muller, "Formulas for bedload transport", Report, 2nd Meeting of International Association of Hydraulic Research, **1948**, Stockholm, Sweden, pp.39- 64.
39. P. Nielsen, "Coastal Bottom Boundary Layers and Sediment Transport", World Scientific, Singapore, **1992**, pp.112-113.
40. J. Brethour and J. Burnham, "Modeling Sediment Erosion and Deposition with the FLOW-3D Sedi-mentation and Scour Model", Flow Science Inc., Santa Fe, **2010**.
41. D. Vanneste, "Experimental and numerical study of wave-induced porous flow in rubble-mound breakwaters", *PhD Thesis*, **2012**, Ghent University, Belgium.
42. C. W. Hirt, "Volume-fraction techniques: Powerful tools for wind engineering", *J. Wind Eng. Ind. Aerodyn.*, **1993**, 46-47, 327-338.
43. C. W. Hirt and B. D. Nichols, "Volume of fluid (VOF) method for the dynamics of free boundaries", *J. Comput. Phys.*, **1981**, 39, 201-225.

© 2015 by Maejo University, San Sai, Chiang Mai, 50290 Thailand. Reproduction is permitted for noncommercial purposes.

Report

Chemical constituents of Oolong tea produced in Thailand and their correlation with infusion colour

Theerapong Theppakorn

School of Agro-Industry, Mae Fah Luang University, Chiang Rai 57100, Thailand

E-mail: theerapong@mfu.ac.th

Received: 14 June 2014 / Accepted: 8 November 2015 / Published: 10 November 2015

Abstract: Constituents expected to influence the colour of tea infusion, namely total polyphenols, total catechins, eight individual catechins, theaflavins and chlorophylls were determined in 28 samples of Oolong tea manufactured in Thailand. The colours attributes (L^* , a^* , b^* , hue angle and absorbance at 420 nm) of the infusions were measured and the correlation between the constituents and infusion colours was determined. The correlation analysis indicates that theaflavins and chlorophylls strongly correlate with infusion colours but total polyphenols and total catechins do not. Theaflavins correlate negatively with L^* and positively with a^* and b^* . Chlorophylls correlate positively with the L^* but negatively with a^* , b^* and hue angle. Chlorophylls and theaflavins were found to be the most important constituents contributing to the colour of Oolong tea manufactured in Thailand.

Keywords: chemical constituents of tea, tea infusion colour, Oolong tea, Thailand

INTRODUCTION

Tea (*Camellia sinensis* L.) is one of the most consumed beverages across the world. It can be categorised based on the degree of fermentation: green tea (unfermented), Oolong tea (partially fermented) and black tea (fully fermented). Green tea is heated to avoid enzymatic oxidation in a fermentation process. Oolong tea is semi-fermented to permit a level of partial enzymatic oxidation. Black tea is the most thoroughly oxidised enzymatically. Green tea has been regarded as a rich source of catechins, which include (-)-gallocatechin (GC), (-)-epigallocatechin (EGC), (+)-catechin (C), (-)-epicatechin (EC), (-)-epigallocatechin gallate (EGCG), (-)-gallocatechin gallate (GCG), (-)-epicatechin gallate (ECG) and (-)-catechin gallate (CG) [1]. These compounds account for the colour, aroma and taste of green tea. During fermentation, catechins undergo oxidation and polymerisation, resulting in the formation of two groups of colour compounds: theaflavins (TF) and thearubigins (TR). The former group is golden-yellow while the latter group is reddish-brown. These

two groups of compounds impart the colour characteristics for Oolong and black tea infusions [2, 3]. The consumption of tea has been linked to its health benefits due to the presence of catechins, TF and TR. Because of this, many studies have been focused on the determination of polyphenols in green and black teas [4-7] and in Oolong teas [8-10].

The quality of tea is normally assessed by a tea taster. Tea tasting focuses on the appearance of the leaf, the aroma, both before and after the leaves are infused, the flavour and the colour of the infusion. Among these, the infusion colour is one of the most important attributes that is affected by chemical compounds in different kinds of tea. Green tea infusion generally contains no TF or TR and the desired colour of green tea is greenish or yellowish green [11]. The green colour is mainly due to the chlorophyll content. Since chlorophylls are not water soluble, the greenness of the tea infusion may come from other related coloured components such as chlorophyllides, the water-soluble green pigments derived from chlorophylls through the catalysis of chlorophyllase [12]. The red-brown colour is the main shade of black tea infusion, resulting mainly from TR which are formed in the fermentation process [13]. Oolong tea infusion is generally a dark greenish colour in the lightly fermented type and a yellowish-brown colour in the moderately to heavily fermented type. The colour-determining compounds in Oolong tea are comprised of several components such as chlorophylls and their degradation products, catechins and small amounts of TF and TR, depending on the degree of fermentation [11].

Compounds affecting the colour of tea infusion have been investigated in many studies. Borah and Bhuyan [14] indicated that the colour and colour change should be measured to assess tea quality during the process of fermentation. Liang et al. [15] showed that chemical compounds and colour differences in black tea infusions were correlated significantly with the sensory quality assessed by tea tasters. Wang et al. [16] reported that chlorophyll is released from tea leaves during steeping and it could contribute to the greenness of tea. Among the flavonoids (catechins and flavonols) detected in green tea infusions, quercetin was shown to be the most important compound contributing to the greenness of green tea infusions [16]. Kim et al. [17] reported that the green tea infusion colour was affected by heat during tea processing. The colour indicator L^* decreased while indicators a^* and b^* increased with an increase in heating temperature. This result was also related to the oxidation of catechins and degradation of chlorophyll under hot condition.

The quality of tea is influenced by many factors such as cultivar, harvest season, age of plant, climate, environmental condition and processing condition [18-20]. The colour of tea infusions can vary, leading to colour differences between different producers and different samples of tea. In Thailand tea is cultivated in the northern part of the country in the provinces of Chiang Rai and Chiang Mai (accounting for 93% of tea production in Thailand). Among the 3 types of tea, Oolong tea has the highest price in Thai tea market. Normally, it is produced from young green shoots of two Chinese sub-varieties: cv. 'Oolong no. 12' and cv. 'Oolong no. 17'. The chemical constituents affecting the shade of infusion colour of Oolong tea manufactured in Thailand have not been determined so far. The purpose of the present study is to determine some chemical constituents of Oolong tea produced in Thailand and explore their relationship with the infusion colour of the tea.

MATERIALS AND METHODS

Tea Samples, Chemicals and Reagents

Twenty-eight Oolong tea samples were collected from tea factories in Chiang Rai province. All Oolong teas were produced from *Camellia sinensis* var. *sinensis*.

Folin-Ciocalteu's phenol reagent, gallic acid, acetonitrile, acetone, trifluoroacetic acid, ethanol and methanol (HPLC grade) were purchased from Fluka (Switzerland). Anhydrous sodium carbonate was purchased from Merck (Germany). Isobutyl methyl ketone, Flavognost reagent (diphenylboric acid 2-aminoethyl ester) and 4-methyl-2-pentanone were purchased from Sigma-Aldrich (Switzerland). All chemical standards (GC, EGC, C, EC, EGCG, caffeine, GCG, ECG and CG) were purchased from Sigma-Aldrich (USA).

Determination of Moisture Content

Tea samples (~5 g, weighed to the nearest 0.001 g) were placed in a moisture can and heated in an oven at $103\pm 2^\circ\text{C}$ for at least 16 hr to constant weight. The percentage of moisture content and dry matter (%DM) in the samples were then calculated from the weight difference [21].

Sample Extraction

Each ground tea sample (~2 g, weighed to the nearest 0.001g) was extracted with distilled water (200 mL) at 95°C . The extraction mixture was constantly stirred with a magnetic stirrer. After 10 min., the extraction mixture was filtered through Whatman No. 4 filter paper. The residue was washed with distilled water (3x10 mL). The tea solution was cooled to room temperature and adjusted to 250 mL with distilled water.

Determination of Total Polyphenol

The total polyphenol (TP) content was determined by spectrophotometry with gallic acid as standard [22]. The tea solution was diluted 50-fold with distilled water. To a 1.0 mL sample of the diluted solution, 5.0 mL of Folin-Ciocalteu's reagent (10% v/v) and then 4.0 mL sodium carbonate (7.5% w/v) were added. The mixture was mixed and left to stand at room temperature for 60 min. before the absorbance at 765 nm was measured. The concentration of polyphenols in the sample was derived from a standard curve of gallic acid (10-100 $\mu\text{g/mL}$). The TP was expressed as gallic acid equivalents (GAE) in g/100 g dry weight.

Determination of Individual Catechins and Total Catechins

Individual catechins and total catechin (TC) content were determined by ISO method [23] as modified by Theppakorn and Wongsakul [24]. The individual standard solutions of GC, EGC, C, EC, EGCG, GCG, ECG and CG were prepared by dissolution in methanol to generate a stock concentration of 1,000 $\mu\text{g/mL}$. The mixed stock standard solution was prepared by mixing an equal volume of each stock standard. Working standard solutions (0.2-100 $\mu\text{g/mL}$) were prepared by diluting and filtering the mixed stock solution through a 0.45- μm PTFE filter. The HPLC analysis of standards and samples was conducted on a Water 966 high performance liquid chromatograph with a vacuum degasser, quaternary pump, auto-sampler, thermostatted column compartment and photo diode array detector. The column used was a Platinum EPS C18 reverse phase, 3 μm (53x7mm), and operated at 30°C . The mobile phase (flow rate = 2 mL/min.) was water/acetonitrile (87:13)

containing 0.05% (v/v) trifluoroacetic acid. The absorption wavelength was 210 nm and the injection volume was 20 μ L. Individual catechins were identified by comparing their retention times and UV spectra in the 190-400 nm range with the standards and quantified using a caffeine calibration curve, together with the consensus relative response factors with respect to caffeine as shown below. The total TC content was obtained by summation of individual catechins.

$$\text{Individual catechin content (g/100g DW)} = \frac{(A_s - b) \times \text{RRF}_{\text{std}}}{m} \times \frac{V_s \times \text{DF}}{W_s \times 10,000} \times \frac{100}{\% \text{DM}}$$

where

- DW = dry weight;
 A_s = peak area of individual catechin in sample;
 b = peak area at point of interception on y-axis of caffeine calibration curve;
 RRF_{std} = relative response factor of individual catechin with respect to caffeine;
 m = slope of caffeine calibration curve;
 V_s = sample extraction volume (mL);
 DF = dilution factor;
 W_s = sample weight (g);
 %DM = percentage of dry matter of sample.

Determination of Chlorophylls

The content of chlorophylls was determined as follows. About 0.2 g of the ground tea sample was extracted by vortex-mixing with 50 mL of 80% (v/v) acetone for 2 min. and filtered. The extracted solution was analysed spectrophotometrically at the wavelength of 663 nm (for chlorophyll a) and 645 nm (for chlorophyll b). The contents of chlorophyll a, chlorophyll b and total chlorophyll were calculated according to the formula [25]:

$$\text{Chlorophyll a } (C_a, \text{ mg/g}) = \frac{(12.7A_{663} - 2.95A_{645}) \times 50}{W \times 1000}$$

$$\text{Chlorophyll b } (C_b, \text{ mg/g}) = \frac{(22.9A_{645} - 4.67A_{663}) \times 50}{W \times 1000}$$

$$\text{Chlorophyll total } (C_t, \text{ mg/g}) = C_a + C_b$$

(W = weight (g) of tea sample; A_{663} and A_{645} = absorbance at 663 and 645 nm respectively)

Determination of TF

The TF content was determined by the Flavognost method [26]. A tea infusion was made with 375 mL of boiling water and 9 g of tea. After shaking for 10 min., the infusion was filtered through rough cotton wool and allowed to cool to room temperature, and then 10 mL were pipetted into 10 mL of isobutyl methyl ketone. The mixture was shaken for 10 min. and allowed to stand until the layers separated. Two mL of the upper layer, followed by 4 mL of ethanol and 2 mL of Flavognost reagent (2 g of diphenylboric acid-2-aminoethyl ester dissolved in 100 mL of ethanol) were pipetted into a test tube. The contents were mixed and the colour was allowed to develop for 15 min. The absorbance at 625 nm was read against the isobutyl methyl ketone /ethanol (1:1 v/v) blank and used for the following formula:

$$\text{TF content } (\mu\text{mol/g}) = \frac{A_{625} \times 47.9 \times 100}{\% \text{DM}}$$

Colour Analysis of Tea Infusion

By spectrophotometer

A ground tea sample (2 g) was extracted with boiling water (100 mL) for 5 min. and then filtered through Whatman No.1 filter paper. The absorbance of the filtrate at 420 nm was measured with a spectrophotometer with distilled water as blank [25].

By colorimeter

A tea sample (5 g) was brewed with hot water (95°C, 200 mL) for 5 min. and filtered. The CIE $L^*a^*b^*$ (CIELAB) of the tea infusion was measured with a Minolta CR400 colorimeter using standard cuvettes after a proper calibration. Each colour value (L^* , a^* , b^* and hue angle) was measured in triplicate.

Data Analysis

All tests were carried out in triplicate and mean \pm SD values are presented. The chemical compositions were correlated with the colour parameters of tea infusions. A linear regressive analysis was carried out using SPSS 16.0 for Windows.

RESULTS AND DISCUSSION

Chemical Constituents

Table 1 shows the chemical constituents of interest of 28 Oolong teas produced in Thailand. The TP content, varying between 10.97-18.01 g GAE/100g DW, is in the range of that found in green tea [27, 28]. Catechins are the main polyphenolic compounds in fresh tea leaves and in general the total catechin content in green tea products is significantly higher than that in partially or fully fermented teas [29]. Catechins are colourless and water soluble and contribute to the bitterness and astringency of green tea [11]. My results indicate that catechins are also the major polyphenolic constituents of Oolong teas (approximately 70% of TP). I found that all Oolong tea samples contained GC, EGC, C, EC, EGCG, GCG and ECG but no CG, EGC (3.38%) and EGCG (2.85%) being the 2 predominant catechins based on the mean content. These findings are similar to those of Kerio et al. [30].

Due to the partial fermentation in Oolong tea processing, catechins are partially oxidised, mainly to TF, which are a group of major pigments that give a yellow-orange colour in fermented tea. The TF content in Oolong teas in Table 1 varies between 0.50-1.60 μ moles/g. In black teas it varies between 14.75-26.38 μ moles/g [31] and 9.84-20.70 μ mole/g [32]. However, many studies have shown that fermentation time, temperature and tea variety strongly affect the TF content in black tea [2, 33, 34]. Another important colouring matter in Oolong tea is the chlorophyll, which gives a green or yellowish-green hue to the tea infusion. From Table 1, the chlorophyll a content (0.42 \pm 0.13 mg/g) is higher than that of chlorophyll b (0.22 \pm 0.08 mg/g). Chlorophyll a is dark green and chlorophyll b is yellowish-green in colour.

There is no specific fermentation stage during Oolong tea manufacture in Thailand. The partial oxidation of tea polyphenols takes place during the withering and leaf handling stages, in which the tea shoots are partially bruised by mechanical handling, leading to an enzymatic oxidation of tea polyphenols. The major purpose of the withering and leaf handling is to eliminate moisture and promote the enzymatic hydrolysis of glycoside aroma precursors, which releases volatile flavour compounds without accelerating the oxidation of tea polyphenols. As can be seen from the results of

TC and TF, Oolong teas produced in Thailand are slightly fermented, undergoing a restricted level of enzymatic oxidation.

Table 1. Some chemical constituents of 28 samples of Oolong tea produced in Thailand

No.	TP (GAE, g/100g)	TC (g/100g)	Individual catechin content (g/100g)								TF (μ mol/g)	Chlorophyll (mg/g)		
			GC	EGC	C	EC	EGCG	GCG	ECG	CG		a	b	Total
1	16.29±0.87	9.70	1.18	3.77	0.59	1.03	2.38	0.37	0.38	nd	0.79±0.04	0.32±0.03	0.14±0.19	0.47±0.02
2	15.43±0.77	9.36	1.19	3.92	0.40	0.76	2.12	0.42	0.55	nd	0.59±0.02	0.55±0.07	0.27±0.03	0.82±0.01
3	18.01±0.01	10.34	1.34	3.53	0.60	1.00	2.68	0.72	0.47	nd	0.53±0.01	0.54±0.05	0.25±0.06	0.78±0.01
4	15.90±0.17	11.67	1.29	3.79	0.86	1.09	3.41	0.61	0.62	nd	0.50±0.01	0.46±0.04	0.26±0.05	0.72±0.02
5	15.39±0.40	9.38	1.13	3.29	0.53	0.84	2.75	0.38	0.46	nd	0.54±0.02	0.52±0.04	0.27±0.03	0.79±0.01
6	12.44±0.45	9.59	1.18	3.26	0.61	0.92	2.63	0.53	0.46	nd	0.60±0.04	0.51±0.04	0.26±0.02	0.77±0.01
7	16.17±0.84	11.58	1.68	4.15	0.72	1.20	2.71	0.61	0.51	nd	0.61±0.01	0.48±0.03	0.26±0.06	0.75±0.02
8	14.86±0.33	13.27	1.80	5.33	0.76	1.30	2.97	0.65	0.46	nd	0.54±0.01	0.59±0.02	0.34±0.10	0.94±0.01
9	15.47±0.60	10.60	1.44	3.52	0.71	1.18	2.66	0.49	0.60	nd	0.51±0.01	0.59±0.09	0.34±0.08	0.93±0.05
10	14.62±0.87	9.28	1.21	4.57	0.60	1.11	1.31	0.37	0.11	nd	0.79±0.01	0.39±0.06	0.19±0.09	0.58±0.03
11	15.03±0.27	10.61	1.32	3.18	4.59	0.62	0.90	nd	nd	nd	0.65±0.01	0.38±0.08	0.17±0.06	0.55±0.02
12	11.75±0.01	9.60	1.15	3.12	0.60	0.88	2.80	0.56	0.49	nd	0.52±0.01	0.45±0.13	0.23±0.05	0.68±0.02
13	11.19±0.51	9.94	1.19	3.22	0.68	0.94	2.77	0.60	0.54	nd	0.65±0.03	0.50±0.01	0.24±0.07	0.74±0.01
14	13.89±0.05	11.97	1.19	3.66	0.76	1.21	3.71	0.65	0.79	nd	0.58±0.02	0.40±0.02	0.20±0.03	0.61±0.01
15	15.36±0.02	6.66	0.93	1.75	0.61	0.67	1.91	0.41	0.38	nd	0.63±0.02	0.52±0.06	0.26±0.01	0.79±0.01
16	10.97±0.35	9.37	1.20	3.09	0.67	0.90	2.61	0.45	0.45	nd	0.63±0.01	0.59±0.06	0.32±0.01	0.91±0.01
17	14.85±0.28	7.95	1.28	2.37	0.66	0.85	2.04	0.34	0.41	nd	0.68±0.02	0.30±0.03	0.16±0.04	0.46±0.01
18	15.05±0.18	8.26	1.51	5.18	0.53	1.04	nd	nd	nd	nd	0.61±0.01	0.65±0.05	0.34±0.04	0.99±0.02
19	11.05±0.39	9.32	1.18	3.01	0.67	0.93	2.53	0.56	0.44	nd	0.54±0.01	0.61±0.02	0.33±0.01	0.94±0.01
20	15.04±0.45	5.01	0.24	0.66	1.46	1.48	nd	nd	1.17	nd	1.22±0.02	0.25±0.01	0.12±0.01	0.38±0.01
21	16.08±0.04	10.50	1.02	2.82	0.71	1.11	3.38	0.53	0.93	nd	1.06±0.04	0.17±0.01	0.06±0.06	0.22±0.04
22	14.83±0.05	10.85	1.32	3.11	0.75	1.07	3.53	0.31	0.76	nd	0.59±0.01	0.34±0.01	0.22±0.06	0.56±0.01
23	16.29±0.24	13.31	1.11	4.11	0.75	1.29	4.55	0.50	1.00	nd	1.60±0.01	0.31±0.04	0.12±0.06	0.43±0.06
24	12.92±0.52	12.23	0.80	2.77	0.63	0.95	5.27	0.79	1.02	nd	0.59±0.04	0.33±0.02	0.09±0.03	0.41±0.01
25	17.64±0.70	9.65	1.04	5.23	0.57	1.08	1.21	0.47	0.05	nd	0.69±0.02	0.29±0.05	0.09±0.01	0.38±0.01
26	16.73±0.30	12.25	0.87	2.93	0.69	1.00	4.94	0.82	1.00	nd	0.94±0.01	0.31±0.04	0.13±0.02	0.44±0.01
27	16.02±0.07	11.39	0.99	3.18	0.65	0.96	4.17	0.78	0.66	nd	0.83±0.01	0.21±0.02	0.25±0.02	0.46±0.01
28	17.64±0.46	7.55	0.77	2.15	0.64	0.91	2.21	0.41	0.46	nd	0.78±0.03	0.25±0.06	0.25±0.03	0.36±0.01
Min.	10.97	5.01	0.24	0.66	0.40	0.62	0.90	0.31	0.05	nd	0.50	0.17	0.06	0.22
Max.	18.01	13.31	1.80	5.33	4.59	1.48	5.27	0.82	1.17	nd	1.60	0.65	0.34	0.99
Mean	14.89	10.04	1.16	3.38	0.82	1.01	2.85	0.53	0.58	nd	0.71	0.42	0.22	0.64
SD	1.92	1.89	0.29	1.01	0.76	0.19	1.07	0.15	0.27	nd	0.24	0.13	0.08	0.21

Note: Values are expressed as means ± standard deviation (SD) from triplicate analysis; TP= total polyphenols; TC= total catechins; GC= (-)-gallocatechin; EGC= (-)-epigallocatechin; C= (+)-catechin; EC= (-)-epicatechin; EGCG= (-)-epigallocatechin gallate; GCG= (-)-gallocatechin gallate; ECG= (-)-epicatechin gallate; CG= (-)-catechin gallate; TF= total theaflavins; nd= not detected.

Infusion Colour

Table 2 shows values of L*, a*, b*, hue angle and A₄₂₀ of the liquor of Oolong tea samples. The L* value represents the degree of lightness: the higher it is, the lighter is the colour. The a* value indicates redness when positive and greenness when negative, while the b* value reflects yellowness when positive and blueness when negative. Generally the infusion colour of Oolong tea varies from green to greenish yellow to golden yellow, depending on the fermentation time. The hue angle is often used to express the green colour [35]. The increase in hue angle corresponds to an increase in greenness and a reduction in yellowness. The absorbance at 420 nm is used in China to assess the colour quality of tea: a high absorbance value is preferred for a good quality.

Table 2. L*, a*, b*, hue angle and absorbance at 420 nm of infusions of Oolong tea samples

No.	L*	a*	b*	Hue angle	A ₄₂₀
1	35.41±0.08	0.24±0.02	2.83±0.04	85.11±0.40	0.18±0.03
2	29.75±1.38	0.46±0.04	4.52±0.39	84.19±0.57	0.19±0.04
3	33.91±0.31	0.11±0.08	2.83±0.34	87.70±1.45	0.19±0.16
4	26.92±0.55	1.01±0.07	5.96±0.44	80.30±1.13	0.19±0.02
5	24.17±0.42	1.29±0.09	8.65±0.54	81.50±0.69	0.21±0.01
6	26.04±0.40	1.45±0.11	9.34±1.05	81.13±1.11	0.31±0.01
7	34.20±0.23	0.05±0.09	3.63±0.18	89.35±1.40	0.24±0.02
8	34.53±0.10	-0.09±0.04	1.62±0.21	93.38±1.33	0.14±0.01
9	33.90±0.33	-0.08±0.05	3.84±0.35	91.22±0.84	0.29±0.04
10	34.47±0.49	0.03±0.09	2.23±0.13	89.22±2.22	0.17±0.01
11	34.25±0.04	-0.01±0.10	3.17±0.32	90.22±1.95	0.24±0.03
12	34.27±0.10	-0.11±0.06	2.81±0.12	92.19±1.22	0.20±0.02
13	35.00±0.18	-0.01±0.07	2.43±0.05	90.31±1.69	0.17±0.01
14	34.81±0.01	0.05±0.05	3.18±0.04	89.07±0.87	0.22±0.01
15	35.48±0.02	-0.09±0.09	3.64±0.16	91.31±1.32	0.2±0.01
16	35.32±0.10	-0.04±0.04	3.79±0.11	90.58±0.64	0.21±0.01
17	35.85±0.09	0.17±0.14	4.33±0.23	87.81±1.80	0.28±0.04
18	36.56±0.13	-0.21±0.03	3.42±0.09	93.44±0.63	0.25±0.02
19	36.36±0.12	-0.14±0.10	3.18±0.09	92.54±1.81	0.23±0.01
20	23.96±2.24	1.14±0.45	13.09±4.17	85.14±0.57	0.26±0.06
21	16.19±1.76	2.77±0.64	21.72±1.67	82.81±1.11	0.24±0.01
22	18.59±1.93	1.36±0.34	13.16±3.71	84.06±0.39	0.14±0.03
23	18.51±2.23	1.81±0.32	16.94±1.37	83.93±0.60	0.20±0.01
24	20.78±0.23	1.68±0.14	11.45±0.42	80.51±0.32	0.15±0.03
25	22.94±0.52	1.68±0.06	10.03±0.22	81.66±0.55	0.19±0.03
26	27.10±0.79	0.92±0.09	7.13±0.25	82.63±0.70	0.16±0.01
27	28.62±0.18	0.89±0.06	6.35±0.25	82.09±0.26	0.19±0.01
28	29.30±0.77	0.82±0.11	6.99±0.69	83.32±0.75	0.26±0.03
Min.	16.19	-0.21	1.62	80.30	0.14
Max.	36.56	2.77	21.72	93.44	0.31
Mean	29.90	0.61	6.51	86.67	0.21
SD	6.19	0.77	4.86	4.27	0.04

Note: Values are expressed as means ± SD (n=3).

Correlation between Chemical Constituents and Infusion Colour

Correlation analysis of the 28 Oolong teas revealed that their TP content did not correlate well with L*, a*, b* or A₄₂₀ values but was significantly related with the hue angle (r = 0.391) (Table 3). In Thai Oolong tea catechins comprise approximately 70% of the TP content and about 10% of the dry weight (Table 1). Correlation analysis showed that the TC content did not correlate with any measured colour parameters. Correlation of the most abundant catechin (EGC) also gives a similar result. This may be because all catechins appear to be colourless in water (as observed with the aqueous solutions of authentic compounds), hence their negligible influence the infusion colour. However, some individual catechins (GC, ECG and EGCG) are fairly related to some measured colour parameters. Although the oxidation products of catechins have been reported to increase the redness and yellowness of tea infusions [16], their influence on the colour of freshly brewed Oolong tea infusion seems to be minimal when compared to other compounds.

The correlation analysis in this study shows that the TF content negatively correlates with L* (r = -0.505) and positively correlates with a* (r = 0.508) and b* (r = 0.644). However, it does not correlate with hue angle and A₄₂₀. Interestingly, chlorophylls, the green pigments in tea leaf, strongly correlate with the infusion colour. Chlorophyll a, b and total positively correlate with L* (r = 0.581, 0.584 and 0.603) but negatively correlate with a* (r = -0.636, -0.647 and -0.663), b* (r = -0.602, -0.622 and -0.632) and hue angle (r = -0.612, -0.562 and -0.614). As can be clearly seen from Table 3, TF and chlorophylls show significant correlation with the infusion colour. These findings indicate that TF and chlorophylls may be the most important compounds affecting the infusion colour of Thai Oolong tea.

Table 3. Linear correlation coefficients between some constituents and infusion colour of Oolong tea samples

Constituent	Parameters of infusion colour				
	L*	a*	b*	Hue angle	A ₄₂₀
Total polyphenols (TP)	-0.273	0.293	0.224	0.391*	-0.141
Total catechins (TC)	-0.211	0.17	0.079	-0.145	0.204
GC	0.433*	-0.452*	-0.464*	0.479**	-0.097
EGC	0.15	-0.147	-0.253	0.168	-0.024
C	0.079	-0.112	0.057	0.145	0.018
EC	-0.27	0.22	0.135	-0.036	0.008
EGCG	-0.387*	0.364	0.278	-0.401*	0.274
GCG	-0.09	0.13	-0.031	-0.236	0.079
ECG	-0.579**	0.514**	-0.592	-0.422*	0.189
CG	-	-	-	-	-
Total theaflavins (TF)	-0.505**	0.508**	0.644**	-0.3	0.173
Chlorophyll a	0.581**	-0.636**	-0.602**	-0.612**	-0.099
Chlorophyll b	0.584**	-0.647**	-0.622**	-0.562**	-0.167
Total chlorophylls	0.603**	-0.663**	-0.632**	-0.614**	-0.129

* Correlation is significant at the 0.05 level.

** Correlation is significant at the 0.01 level.

CONCLUSIONS

This study provides the relationship between the relevant constituents and the infusion colour of Oolong teas produced in Thailand. The results indicate that they seem to undergo only a mild fermentation and their infusion colour is determined mainly by the chlorophylls and theaflavins formed by partial fermentation during the tea processing.

ACKNOWLEDGEMENT

The author warmly thanks the Tea Institute, Mae Fah Luang University for support.

REFERENCES

1. M. G. Ferruzzi and R. J. Green, "Analysis of catechins from milk-tea beverages by enzyme assisted extraction followed by high performance liquid chromatography", *Food Chem.*, **2006**, *99*, 484-491.
2. T. Muthumani and R. S. S. Kumar, "Influence of fermentation time on the development of compounds responsible for quality in black tea", *Food Chem.*, **2007**, *101*, 98-102.
3. Y. Kim, K. L. Goodner, J. D. Park, J. Choi and S. T. Talcott, "Changes in antioxidant phytochemicals and volatile composition of *Camellia sinensis* by oxidation during tea fermentation", *Food Chem.*, **2011**, *129*, 1331-1342.
4. Y. Liang, J. Lu, L. Zhang, S. Wu and Y. Wu, "Estimation of black tea quality by analysis of chemical composition and colour difference of tea infusions", *Food Chem.*, **2003**, *80*, 283-290.
5. V. Sharma, A. Gulati, S. D. Ravindranath and V. Kumar, "A simple and convenient method for analysis of tea biochemicals by reverse phase HPLC", *J. Food Compos. Anal.*, **2005**, *18*, 583-594.
6. D. Wang, J. Lu, A. Miao, Z. Xie and D. Yang, "HPLC-DAD-ESI-MS/MS analysis of polyphenols and purine alkaloids in leaves of 22 tea cultivars in China", *J. Food Compos. Anal.*, **2008**, *21*, 361-369.
7. G. Alaerts, J. Van Erps, S. Pieters, M. Dumarey, A. M. van Nederkassel, M. Goodarzi, J. Smeyers-Verbeke and Y. V. Heyden, "Similarity analyses of chromatographic fingerprints as tools for identification and quality control of green tea", *J. Chromatogr. B*, **2012**, *910*, 61-70.
8. Y. Chen, Y. Jiang, J. Duan, J. Shi, S. Xue and Y. Kakuda, "Variation in catechin contents in relation to quality of 'Huang Zhi Xiang' Oolong tea (*Camellia sinensis*) at various growing altitudes and seasons", *Food Chem.*, **2010**, *119*, 648-652.
9. Y. Wang, Q. Li, Q. Wang, Y. Li, J. Ling, L. Liu, X. Chen and K. Bi, "Simultaneous determination of seven bioactive components in Oolong tea *Camellia sinensis*: Quality control by chemical composition and HPLC fingerprints", *J. Agric. Food Chem.*, **2012**, *60*, 256-260.
10. K. Wang, F. Liu, Z. Liu, J. Huang, Z. Xu, Y. Li, J. Chen, Y. Gong and X. Yang, "Analysis of chemical components in Oolong tea in relation to perceived quality", *Int. J. Food Sci. Technol.*, **2010**, *45*, 913-920.
11. V. S. P. Chaturvedula and I. Prakash, "The aroma, taste, color and bioactive constituents of tea", *J. Med. Plants Res.*, **2011**, *5*, 2110-2124.
12. N. Ogura, M. Ueno, M. Matsunaga, T. Sato and H. Nakagawa, "Chlorophyllase activities and color changes of fresh green leaves on blanching", *Nippon Nogeik. Kaishi*, **1987**, *61*, 451-456 (in Japanese).

13. E. A. H. Roberts and R. F. Smith, "The phenolic substances of manufactured tea. IX.—The spectrophotometric evaluation of tea liquors", *J. Sci. Food Agric.*, **1963**, 14, 689-700.
14. S. Borah and M. Bhuyan, "Non-destructive testing of tea fermentation using image processing", *Brit. Inst. J. Nondestr. Test.*, **2003**, 45, 55-58.
15. Y. Liang, J. Lu, L. Zhang, S. Wu and Y. Wu, "Estimation of tea quality by infusion colour difference analysis", *J. Sci. Food Agric.*, **2005**, 85, 286-292.
16. L. F. Wang, S. C. Park, J. O. Chung, J. H. Baik and S. K. Park, "The compounds contributing to the greenness of green tea", *J. Food Sci.*, **2004**, 69, S301-S305.
17. E. S. Kim, Y. R. Liang, J. Jin, Q. F. Sun, J. L. Lu, Y. Y. Du and C. Lin, "Impact of heating on chemical compositions of green tea liquor", *Food Chem.*, **2007**, 103, 1263-1267.
18. Y. S. Lin, Y. J. Tsai, J. S. Tsay and J. K. Lin, "Factors affecting the levels of tea polyphenols and caffeine in tea leaves", *J. Agric. Food Chem.*, **2003**, 51, 1864-1873.
19. R. Cooper, D. J. Morr e and D. M. Morr e, "Medicinal benefits of green tea: Part I. Review of non-cancer health benefits", *J. Altern. Complement. Med.*, **2005**, 11, 521-528.
20. P. O. Owuor, M. Obanda, H. E. Nyirenda and W. L. Mandala, "Influence of region of production on clonal black tea chemical characteristics", *Food Chem.*, **2008**, 108, 263-271.
21. ISO 1573:1980, "Tea—Determination of loss in mass at 103 degrees C", International Organization for Standardization, Geneva, **1980**.
22. ISO 14502-1:2005, "Determination of substances characteristic of green and black tea—Part 1: Content of total polyphenols in tea—Colorimetric method using Folin–Ciocalteu reagent", International Organization for Standardization, Geneva, **2005**.
23. ISO 14502-2:2005, "Determination of substances characteristic of green and black tea—Part 2: Content of catechins in green tea—Method using high-performance liquid chromatography", International Organization for Standardization, Geneva, **2005**.
24. T. Theppakorn and S. Wongsakul, "Optimization and validation of the HPLC-base method for the analysis of gallic acid, caffeine and 5 catechins in green tea", *Naresuen Univ. J.*, **2012**, 20, 1-11.
25. Tea Institute of Chinese Academy of Agricultural Sciences, "Experiment Handbook of Tea Tree Physiology and Tea Leaves Biochemistry", Press of Chinese Agriculture, Beijing, **1983**.
26. P. J. Hilton and R. Palmer-Jones, "Relationship between the flavanol composition of fresh tea shoots and the theaflavin content of manufactured tea", *J. Sci. Food Agric.*, **1973**, 24, 813-818.
27. K. M. M. Alam, M. S. Uddin, M. A. M. Chowdhury and M. A. Motalib, "Qualitative evaluation of ten major marketed brands of tea in Bangladesh", *Plant Arch.*, **2011**, 11, 173-177.
28. S. Jayasekera, A. L. Molan, M. Garg and P. J. Moughan, "Variation in antioxidant potential and total polyphenol content of fresh and fully-fermented Sri Lankan tea", *Food Chem.*, **2011**, 125, 536-541.
29. S. M. Karori, F. N. Wachira, J. K. Wanyoko and R. M. Ngure, "Antioxidant capacity of different types of tea products", *Afr. J. Biotechnol.*, **2007**, 6, 2287-2296.
30. L. C. Kerio, F. N. Wachira, J. K. Wanyoko and M. K. Rotich, "Total polyphenols, catechin profiles and antioxidant activity of tea products from purple leaf coloured tea cultivars", *Food Chem.*, **2013**, 136, 1405-1413.
31. P. O. Owuor, M. Obanda, H. E. Nyirenda, N. I. K. Mphangwe, L. P. Wright and Z. Apostolides, "The relationship between some chemical parameters and sensory evaluations for

plain black tea (*Camellia sinensis*) produced in Kenya and comparison with similar teas from Malawi and South Africa”, *Food Chem.*, **2006**, 97, 644-653.

32. M. Obanda, P. O. Owuor, R. Mang'oka and M. M. Kavoi, “Changes in thearubigin fractions and theaflavin levels due to variations in processing conditions and their influence on black tea liquor brightness and total colour”, *Food Chem.*, **2004**, 85, 163-173.
33. M. Obanda, P. O. Owuor and R. Mang'oka, “Changes in the chemical and sensory quality parameters of black tea due to variations of fermentation time and temperature”, *Food Chem.*, **2001**, 75, 395-404.
34. P. O. Owuor and M. Obanda, “Comparative responses in plain black tea quality parameters of different tea clones to fermentation temperature and duration”, *Food Chem.*, **2001**, 72, 319-327.
35. M. H. Lau, J. Tang and B. G. Swanson, “Kinetics of textural and color changes in green asparagus during thermal treatments”, *J. Food Eng.*, **2000**, 45, 231-236.

© 2015 by Maejo University, San Sai, Chiang Mai, 50290 Thailand. Reproduction is permitted for noncommercial purposes.

Full Paper

Assessing readability of Thai text using support vector machines

Yaw-Huei Chen and Patcharanut Daowadung*

Department of Computer Science and Information Engineering, National Chiayi University, Chiayi City 60004, Taiwan (R.O.C.)

* Corresponding author, e-mail: s0970384@mail.ncyu.edu.tw

Received: 13 February 2014 / Accepted: 3 November 2015 / Published: 16 November 2015

Abstract: The readability of a document is a measure of how easily the document can be read and understood. To select appropriate reading materials for children, techniques that can automatically assess readability are required. The objective of this study is to develop a machine-learning-based technique to assess the readability of Thai text. The experimental corpus, which was divided into training data and test data, consisted of articles selected from the textbooks of primary schools in Thailand. Documents in the corpus were first segmented into terms and then represented by feature vectors. Different combinations of feature sets including term frequencies of selected terms, shallow features and language model features were tested in the experiments. Classification and regression models were learned from the training data using support vector machines. Experimental results confirm that the proposed term-selection method can identify effective term frequency features for assessing the readability of Thai text.

Keywords: Thai readability, term frequency, feature selection, support vector machines

INTRODUCTION

Reading has an important role in learning for children because it can help them acquire knowledge and develop new ideas. However, articles with complex grammatical structure or difficult words may be overly complicated for children to comprehend. Children should read materials that are suitable to their reading ability. A task confronting schoolteachers is to choose appropriate reading materials for their students. The number of Thai articles available online is continuously increasing. This extensive number of digital Thai articles certainly improves the availability of reading materials for children, but it also increases the workload of the teacher in selecting suitable articles. The readability level of an article indicates how easily an article can be read and understood; therefore, it is reasonable to use the readability level as a major criterion to

select appropriate reading materials for primary school students. Thus, we require an effective technique for assessing the readability of Thai text so that teachers can easily select appropriate reading materials.

Various techniques for assessing readability have been developed in the past, including both formula-based [1, 2] and machine-learning-based techniques [3, 4]. The majority of these techniques focus on English text. In Thai language the text is written without explicit word boundary delimiters, sentence endings or capital letters. For example, the word ‘คนขับรถ’ (kon-khup-rod) may refer to ‘a driver’ as a noun, ‘a man drives a car’ as a sentence, or a compound noun depending on the context where the word occurs. Word segmentation is a necessary pre-processing step in Thai text processing. Because of the fundamental difference between Thai and English, techniques developed for assessing readability of English text may not be effective for assessing the readability of Thai text.

In this paper a machine-learning-based technique is developed to assess the readability of Thai text. The proposed method predicts the reading levels of documents using support vector machines (SVM). Various features including term frequency features (TF), shallow features (SL) and language model features (LM) are extracted from the documents and are tested for their effectiveness for assessing readability. The documents are classified into six grade levels for students in primary school. A multiclass feature selection method is proposed to select the terms used for computing TF. In the experiments we selected 720 articles from the textbooks of primary schools in Thailand to form an experimental corpus. Feature selection methods based on mutual information and chi-square test were first evaluated and then different combinations of the feature sets were tested for assigning reading levels to the documents. The experimental results confirm that the proposed multiclass term-selection method can identify effective TF for assessing the readability of Thai text.

RELATED WORK

Readability formulas consisting of SL such as the average number of syllables per word and average number of words per sentence in a document were frequently used in early studies to predict the readability levels of the documents [2, 5, 6]. These formulas are usually simple and easy to calculate. However, complex words and long sentences do not always render a document difficult to read and therefore a simple readability formula cannot accurately predict the readability level of a document.

In addition to SL, word frequency is another common feature used for measuring readability. Chall and Dale [1] estimated the readability of a document using a combination of average sentence length and percentage of words occurring in a list of 3,000 familiar words identified manually. A document that contains fewer words in the common word list is likely to be more difficult. Stenner [7] combined the word frequency and sentence length features to generate a regression equation for predicting the difficulty of reading material. Heilman et al. [8] assessed reading difficulty using lexical features based on the frequencies of 5,000 common words in the training corpus and grammatical features derived from context-free grammar parses of sentences. They concluded that the combination of grammatical and lexical features was most effective. Chen et al. [9] calculated the term frequency and inverse document frequency of selected terms as features and applied SVM to assess the readability of Chinese text. The effectiveness of these methods depends primarily on the corpus from which the word list, the frequency information and the grammatical features are derived.

Statistical language models compute the probability of the next word from the previous $n - 1$ words. Si and Callan [10] used unigram models to measure the reading difficulty of science web pages. Collins-Thompson and Callan [11] focused on using smoothed unigram-language models to predict the grade level of web documents; this approach demonstrated superior performance to traditional methods. Language modelling techniques have also been used to assess the readability of non-English texts. For example, Sato et al. [12] devised a character unigram model to measure the readability of Japanese text because each Kanji character in Japanese can be considered a single term.

With the ever-increasing computing power of modern computers, researchers have acquired the ability to use machine-learning-based techniques to assess the readability of documents. For example, Schwarm and Ostendorf [13] utilised SVM to combine features from traditional reading-level measures, parse trees and statistical language models for assessing the reading level. Vajjala and Meurers [14] tested various syntactic and lexical features on a corpus created from two web sources: Weekly Reader and BBC Bitesize. They found that a combination of development measures from second language acquisition research and traditional readability features significantly improved the performance of the classifiers. Francois and Miltsakaki [15] compared readability formulas with machine-learning-based methods for assessing the readability of French text. The best result was obtained when they used a combination of traditional readability features and new features derived from languages models, parse tree-based predictors and other measures.

PROPOSED METHOD

The problem of readability assessment has been studied for several languages. However, research on Thai readability remains in its initial stage. Preliminary experiments in our previous study indicated that using SVM to analyse the term frequency and inverse document frequency values of selected terms in Thai text is promising in classifying documents for primary school students [16]. Because the feature set used in a machine-learning-based approach is critical to the performance of a learned-text classifier, we propose to compare the effectiveness of prediction models with different feature sets which are derived from SL, LM and TF of selected terms. A machine-learning-based approach is applied to produce the prediction models for assessing the readability of Thai text. The proposed method consists of the tasks of Thai word segmentation and pre-processing, feature selection, feature value computation, and prediction model generation.

Thai Word Segmentation and Pre-processing

Owing to the lack of explicit word boundaries in Thai written text, word segmentation has a significant role in extracting terms for Thai language processing. Dictionary-based techniques and machine-learning-based algorithms are two well-known approaches for Thai word segmentation [17]. The former segments input text strings into words based on terms defined in a dictionary, which must contain an extensive number of terms for this approach to perform well. The latter learns a classification model from a training corpus to predict whether a character in the input text string is a word beginning. The performance of the classification model depends on the quality and size of the training corpus, where word boundaries are clearly identified.

In this study LexTo (Thai Lexeme Tokenizer) [18] was applied to segment text strings into words using both the longest matching and dictionary-based techniques; the former solves the ambiguity problem by selecting the longest matched word in the dictionary. LexTo provides a source code of the program and a dictionary (i.e. Lexitron [19]) containing approximately 40,000

words. Because the performance of the word segmentation program can be improved by increasing the size of the dictionary, we added 5,000 proper names, organisations and places as new words into the dictionary. We also removed punctuation, numeric characters, special symbols and Thai number characters from the corpus.

Feature Selection

Feature selection is the process of selecting a subset of terms in the training data such that values computed from these terms can be used as features more effectively in the text classification. Several term-selection methods have been studied for text categorisation [20]. We compared mutual information and chi-square test as the feature selection methods for this study. Mutual information measures the importance of the presence or absence of term t in a document for prediction on class c . In a two-class classification problem mutual information is computed using equation (1), where N is the total number of documents and N_{ij} is the number of documents that contain term t ($i = 1$) or do not contain term t ($i = 0$) and are in class c ($j = 1$) or are not in class c ($j = 0$) [21]. For example, N_{11} is the number of documents that contain term t and are in class c . Note that ‘.’ represents both ‘0’ and ‘1’, and therefore $N_{.1} = N_{01} + N_{11}$ is the total number of documents in class c .

$$MI = \frac{N_{11}}{N} \log_2 \frac{NN_{11}}{N_{.1}N_{.1}} + \frac{N_{01}}{N} \log_2 \frac{NN_{01}}{N_{.0}N_{.1}} + \frac{N_{10}}{N} \log_2 \frac{NN_{10}}{N_{.1}N_{.0}} + \frac{N_{00}}{N} \log_2 \frac{NN_{00}}{N_{.0}N_{.0}} \quad (1)$$

The chi-square test measures the independence of two events: the occurrence of the term and the occurrence of the class. In a two-class classification problem, the chi-square test value is computed using Equation (2), where N and N_{ij} are defined as in Equation (1) [21].

$$\chi^2 = \frac{N(N_{11}N_{00} - N_{10}N_{01})^2}{(N_{11} + N_{01})(N_{11} + N_{10})(N_{10} + N_{00})(N_{01} + N_{00})} \quad (2)$$

Because these feature selection methods are only suitable for two-class classification problems, we devised a new method to select the features for multiclass-classification problems. For each term, a one-against-all approach was employed to calculate the goodness measures of the term as a feature for k binary classifiers, where k is the number of classes in the training data. The i th binary classifier is trained with documents in the i th class as positive and all other documents as negative. For each classifier, we sorted the goodness measures of all the terms and assigned order numbers to the terms. Therefore, every term received an order number for each classifier. We chose the best order number in the k classifiers as the representing order number of the term. Then we sorted the representing order numbers and used the sorted list of terms for feature selection. Note that ties were broken arbitrarily when sorting the terms. A fixed number of terms were selected as features from the top of the sorted list. We conducted experiments to determine the feature selection method for calculating the goodness measures to be used in the experiments.

Feature Value Computation

Three different sets of features were used: SL, LM and TF. Because the Thai language has no explicit word boundaries, sentence endings or capital letters, many SL such as the average number of words per sentence, average number of sentences per paragraph and average number of syllables per word are difficult to extract. Therefore, as indicated in Table 1, we adopted features from Coh-

Metrix-Port [3] as our SL; these include the average length per word, percentage of some connectives and percentage of words in word lists for different grade levels defined by the Office of the Basic Education Commission of Thailand.

Table 1. SL used in the proposed method

Number	Feature
1	Average word length
2	Ratio of ‘และ’ (and)
3	Ratio of ‘หรือ’ (or)
4	Ratio of ‘ถ้า’ (if)
5	Ratio of other connectives (i.e. ‘แต่’ (but), ‘แต่กระนั้น’ (yet), ‘แม้’ (although), ‘แม้ว่า’ (even), ‘แต่ที่ว่า’ (whereas), ‘ที่ว่า’ (albeit) and ‘แต่ที่ว่า’ (however))
6	Ratio of words in word list of Grade 1
7	Ratio of words in word list of Grade 2
8	Ratio of words in word list of Grade 3
9	Ratio of words in word list of Grade 4
10	Ratio of words in word list of Grade 5
11	Ratio of words in word list of Grade 6

To compare the different aspects of Thai readability assessment, we used n -gram language models to assign probability measures to the word strings at each reading level. For any given text, each language model was evaluated through its perplexity defined by Equation (3), where $P(t | c)$ is the conditional probability of a word sequence of length m : $t = w_1, \dots, w_m$ relative to class c . Because a lower perplexity indicates a higher probability, we can use the perplexity as a feature in the readability assessment task [13].

$$perplexity = P(t | c)^{-\frac{1}{m}} \tag{3}$$

Unigram, bigram and trigram were the language models that we used for capturing the term frequency and collocation information in the text. For a test document, we generated a perplexity value from each language model that was trained on documents in one of the six grade levels. Therefore, as shown in Table 2, there were eighteen perplexity values in the language model feature set.

Table 2. Language model feature set

Number	Perplexity
1	Generated by unigram model trained on Grade 1 text
2	Generated by unigram model trained on Grade 2 text
3	Generated by unigram model trained on Grade 3 text
4	Generated by unigram model trained on Grade 4 text
5	Generated by unigram model trained on Grade 5 text
6	Generated by unigram model trained on Grade 6 text
7	Generated by bigram model trained on Grade 1 text
8	Generated by bigram model trained on Grade 2 text
9	Generated by bigram model trained on Grade 3 text
10	Generated by bigram model trained on Grade 4 text
11	Generated by bigram model trained on Grade 5 text
12	Generated by bigram model trained on Grade 6 text
13	Generated by trigram model trained on Grade 1 text
14	Generated by trigram model trained on Grade 2 text
15	Generated by trigram model trained on Grade 3 text
16	Generated by trigram model trained on Grade 4 text
17	Generated by trigram model trained on Grade 5 text
18	Generated by trigram model trained on Grade 6 text

The term frequency measure, which is proportional to the number of occurrences of a term in a document, can be used to evaluate the importance of the term to the document in a collection. We used a sublinear term frequency scaling method to compute the term frequency measure in Equation (4), where $wf_{t,d}$ is the modified term frequency value of term t in document d and $tf_{t,d}$ is the number of occurrences of term t in document d [21].

$$wf_{t,d} = \begin{cases} 1 + \log tf_{t,d} & \text{if } tf_{t,d} > 0 \\ 0 & \text{otherwise} \end{cases} \quad (4)$$

Prediction Model Generation

SVM is a supervised learning classification method that attempts to identify a maximum-margin hyper plane between two classes [22]. SVM works well on a large feature space in terms of both the accuracy of the classification results and the efficiency of training and classification algorithms. Moreover, SVM has generated good classifiers for many different types of datasets [23]. Because SVM is a binary classifier, it must be extended for solving multiclass-classification problems. In a one-against-one approach all possible $k(k - 1)/2$ two-class classifiers are first

generated from a training set of k classes; then the class label of a test document can be determined using a voting strategy [24]. We used LIBSVM [25] to build the multiclass classifiers based on different combinations of feature sets. However, because the readability was divided into six reading levels corresponding to the six grades in primary school, the readability levels were continuous and exhibited a natural order. This ordinal-regression problem can be solved using new SVM formulations that are modified from two-class classification approaches [26, 28]. In the experiments we evaluated both multiclass-classification and ordinal-regression approaches.

EXPERIMENTS AND RESULTS

This section describes the environment, corpus and results of the experiments on the feature selection methods and feature sets. Both multiclass-classification and ordinal-regression learning techniques were evaluated in the experiments.

Experimental Environment

We developed JAVA-based programs to assess the readability of Thai articles. The applications were installed on a Windows-based PC with an Intel Core 2 Quad CPU and 8 GB of RAM. Thai words were segmented using the LexTo application. The corpus was stored in a MySQL database. LIBSVM, a machine-learning toolkit, was used for learning and testing the SVM prediction models [25]. A program modified from LIBSVM was used for performing ordinal regression in the experiments [27]. SRILM, a language modelling toolkit, was used for building and applying the n -gram models to the generation of LM [29].

Corpus

The corpus was selected from textbooks in six core subjects, namely ‘occupations and technology’, ‘social studies, religion and culture’, ‘health and physical education’, ‘Thai language’, ‘arts’, and ‘science’, which are mandatory courses for primary school students in Thailand. The articles were retrieved from textbooks in paper and digital formats. The *trueplookpanya* website provided content for all six subjects. *Max Education* provided content for Grades 4-6 of all six subjects, whereas another website provided articles in the subject of the Thai language. The articles were captured either by entering the texts manually or by copying the texts electronically.

One of the challenges in training and testing models for assessing readability is to correctly assign a reading level to the documents in the corpus. Originally, there were 1,080 articles retrieved from the textbooks. We invited five primary school teachers, each with more than ten years of teaching experience, to assess the reading levels of the articles. Only articles that were labelled with the same reading level by all five teachers were selected for inclusion in the corpus. We selected 720 articles to form the final corpus, where all the grade levels were equally represented with the same number of documents. The distribution of the 720 documents in the corpus is presented in Table 3.

Table 3. Distribution of articles in the corpus

Grade	Number of documents	Number of words
1	120	22,844
2	120	39,298
3	120	40,973
4	120	44,866
5	120	91,540
6	120	93,553

Experiments on TF

Because even a small corpus may contain many thousands of unique terms, the learning algorithms must evaluate an enormous number of feature values when using TF. The dimensionality of the feature space can be reduced by employing feature selection methods to determine the most discriminative terms for classification and regression. To determine the number of terms to be used as features, we compared two feature selection criteria: mutual information and chi-square. For each term, we applied the one-against-all approach to determine the order of the term in each classifier according to the feature selection criterion. Then we selected the best order number in the six classifiers as the representing order number of the term. Finally, we sorted the representing order numbers of all terms and selected the terms from the top of the sorted list. The modified term frequency of the selected terms calculated from Equation (4) was used as the feature for training and testing the prediction models. Note that the feature values were scaled to the interval of numbers between 0 and 1 for both the training and test data in all the experiments.

The experimental results of the SVM-based approaches with linear kernel functions for multiclass classification and ordinal regression are presented in Tables 4 and 5 respectively. The performance of randomly selected terms is also included as baseline comparison. In the experiments the mutual information method generated the highest accuracy in all cases except for the ‘5,000 terms’ in the ordinal-regression approach. Therefore, we selected mutual information as the feature selection criterion for the TF in the remaining experiments. The experimental results also showed that the multiclass-classification model provided superior performance compared to the ordinal-regression model. A reason for the inferior performance of the latter may lie in the reading levels assigned to the documents. Because these levels were manually rated, the evaluation may be imprecise and the difference in reading difficulty among levels may vary, which can cause performance degradation in the ordinal-regression model. Another possible reason for the resulting performance may be due to the lack of parameter adjustment. However, the experiments indicated that both multiclass-classification and ordinal-regression models had the highest or near-highest accuracy values when the number of terms was 4,000. Therefore, we used the 4,000-term frequency features in the experiments on feature set combination.

Table 4. Accuracy of different feature selection criteria for multiclass classification

Number of terms	Mutual information	Chi-square	Random
100	41.389%	40.000%	22.083%
200	44.722%	39.722%	27.639%
300	46.111%	41.944%	29.583%
400	45.278%	44.167%	30.972%
500	46.111%	42.083%	33.056%
600	45.694%	43.889%	35.556%
700	46.528%	45.417%	32.222%
800	46.528%	45.833%	33.750%
900	47.222%	45.417%	34.583%
1000	46.528%	45.694%	36.111%
2000	47.361%	47.083%	38.056%
3000	49.167%	47.500%	42.222%
4000	50.278%	47.917%	44.028%
5000	49.444%	48.472%	45.000%

Table 5. Accuracy of different feature selection criteria for ordinal regression

Number of terms	Mutual information	Chi-square	Random
100	37.778%	34.861%	20.694%
200	37.361%	35.972%	24.583%
300	37.500%	35.139%	25.417%
400	37.083%	35.278%	28.472%
500	36.944%	34.444%	29.722%
600	39.167%	36.944%	30.000%
700	36.528%	36.111%	28.472%
800	36.250%	37.778%	29.861%
900	36.528%	36.111%	30.000%
1000	38.472%	35.694%	31.806%
2000	40.000%	37.778%	32.639%
3000	42.778%	39.028%	34.722%
4000	41.667%	39.861%	36.389%
5000	41.111%	42.361%	38.611%

Experiments on SL

SL have been used in many traditional readability formulas [1-3, 5, 6]. In these experiments we investigated the performance of shallow features for assessing Thai text readability. The SL listed in Table 1, which include average word length, ratio of some connectives and ratio of words in word lists for different grades, were used as features for the SVM-based learning algorithms for multiclass classification and ordinal regression. Table 6 presents the average results of the experiments which used a 5-fold cross validation in terms of accuracy, mean absolute error, and squared correlation coefficient. The accuracy values of both the multiclass-classification and ordinal-regression models using SL were inferior to those of the models using TF as shown in Tables 4 and 5. The number of SL used in the experiments was very limited, which may have caused the inferior performance. However, it is difficult to extract additional SL owing to the characteristics of Thai text.

Table 6. Performance of 11 SL

	Accuracy	Mean absolute error	Squared correlation coefficient
Multiclass classification	29.306%	1.20694	0.31503
Ordinal regression	32.080%	1.09167	0.46422

Experiments on LM

To compare the different aspects of textual properties on the performance of Thai text readability assessment, we used n -gram language models to predict the probability that a particular word sequence would occur in an article. The language models were created with language modelling toolkit SRILM [29]. To avoid over-fitting by less informative terms in the corpus, we retained only the 400 terms with the highest mutual information and replaced the remaining terms with 'unknown' tags. Table 7 presents the average accuracy obtained from the 5-fold experiments. The performance of the LM was even poorer than that of the SL in these experiments.

Table 7. Performance of the 18 LM

	Accuracy	Mean absolute error	Squared correlation coefficient
Multiclass classification	27.361%	1.53056	0.21621
Ordinal regression	17.222%	1.95555	0.10219

Experiments on Combination of Feature Sets

We evaluated SL, LM and TF for both SVM-based multiclass-classification and ordinal-regression approaches. In these experiments various combinations of feature sets were also tested, viz. SL+LM, TF+SL, TF+LM, TF+SL+LM, and the set of TF of all terms. For these tests, the TF set contained 4,000 terms as suggested by the aforementioned experiments.

The experimental results are presented in Table 8. Among the eight feature sets, the LM had the lowest accuracy values for multiclass classification and ordinary regression. This result indicates

that LM alone are not sufficient for assessing Thai text readability. However, the performance of the combined feature set SL+LM was superior to either the single feature set SL or LM. This outcome is similar to the conclusions drawn from other studies [10, 13]. As indicated in Table 8, prediction models with TF outperformed those without these features and the multiclass-classification model outperformed the ordinal-regression model. The addition of SL and/or LM did not improve the accuracy of the model, while the TF exhibited effective predictive capabilities for assessing the readability of Thai text. We also noticed that using all 14,205 terms as features (all terms) produced the best performance with lowest mean absolute error and highest squared correlation coefficient in the ordinal-regression model and good performance in the multiclass-classification model.

Table 8. Comparison of feature sets

Feature set	No. of features	Multiclass classification			Ordinal regression		
		Accuracy	Mean absolute error	Squared correlation coefficient	Accuracy	Mean absolute error	Squared correlation coefficient
SL	11	29.306%	1.20694	0.31503	32.080%	1.09167	0.46422
LM	18	27.361%	1.53056	0.21621	17.222%	1.95555	0.10219
TF	4000	50.278%	0.73611	0.60536	41.667%	0.79028	0.60575
SL+LM	29	31.528%	1.12917	0.33831	37.083%	0.99305	0.49733
TF+SL	4011	50.417%	0.72222	0.61741	42.500%	0.77917	0.61873
TF+LM	4018	50.139%	0.72639	0.61408	42.083%	0.78056	0.61551
TF+SL+LM	4029	50.972%	0.70972	0.62303	40.972%	0.79028	0.62355
All terms*	14205	49.306%	0.74028	0.60628	44.861%	0.70694	0.64837

* Set of TF of all terms

Experiments on Feature Sets with Different Numbers of Terms

Because the feature sets with a smaller number of features could generate comparative performance in less time, we tested the models with different numbers of terms as features in the subsequent experiments. Figures 1 and 2 illustrate the accuracy of the multiclass-classification and ordinal-regression models respectively with different numbers of terms. It can be observed that the four tested feature sets, i.e. TF, TF+SL, TF+LM and TF+SL+LM, generate similar accuracies in both Figures. Therefore, TF alone seem to be sufficient for assessing the readability of Thai text.

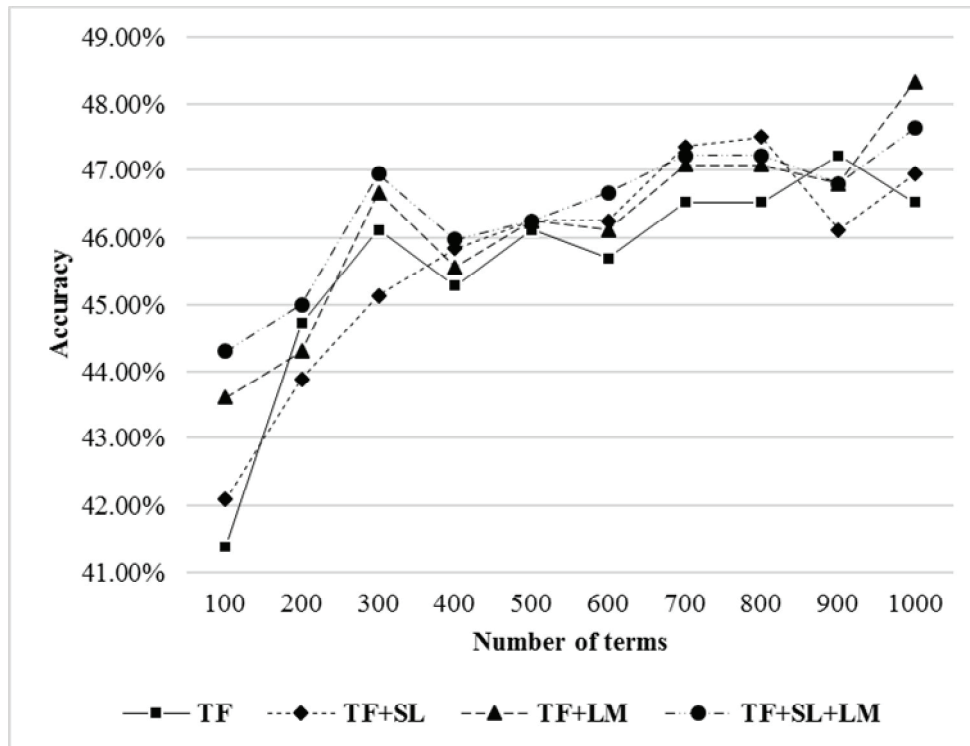


Figure 1. Accuracy for multiclass classification

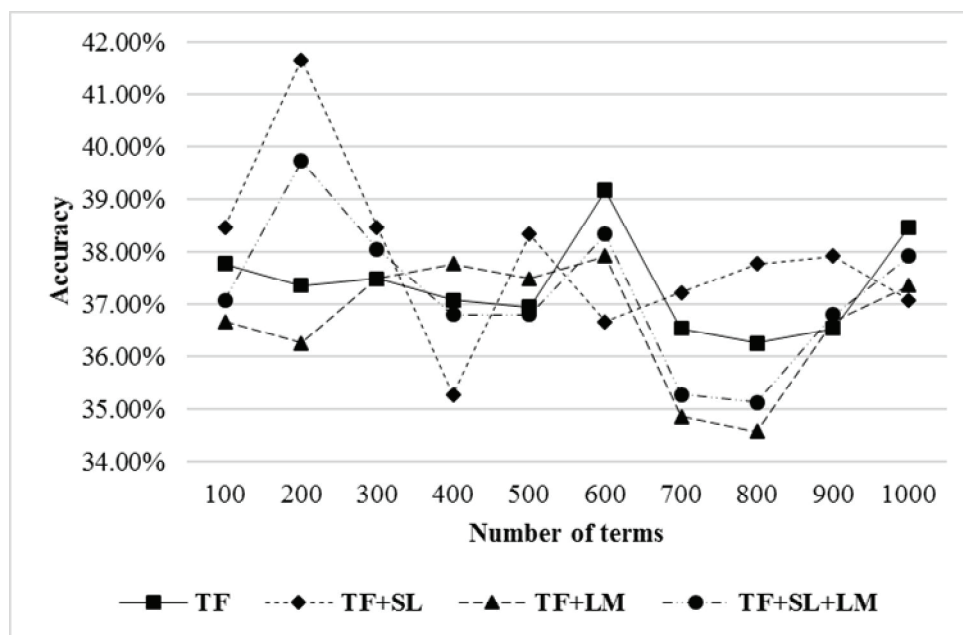


Figure 2. Accuracy for ordinal regression

DISCUSSION

SL have been used successfully for assessing the readability of English text, but their performance is not good for Thai text because we could extract only eleven SL. Although LM are expensive to compute, it did not perform well in the experiments. The combined feature set SL+LM provided an improvement in performance compared to either single feature set SL or LM, which is consistent with the results of previous studies [10, 13]. The experimental results suggested that the TF set performed well for all the models and the combined feature set TF+SL+LM did not provide

noticeable improvement in performance. Because the terms were sorted by the proposed feature selection method, a relatively small number of terms were enough for generating the TF set for the classifier and we could process these TF very efficiently. In addition, it was demonstrated that the multiclass classification provided a higher accuracy compared to the ordinal regression in every experiment. Therefore, the multiclass-classification model with TF selected by the proposed feature selection method should be capable of effectively assessing the readability of Thai text.

There are still areas in the proposed method that require further investigation. For example, the quantity and quality of the training data which are crucial to the success of the supervised learning can be improved by increasing the number of documents from other sources (e.g. annotated web pages). Moreover, other types of features such as topic information may be capable of improving the performance. We expect to achieve superior accuracy in the future using new features such as name entity, discourse features and topic information. Based on the proposed method, a software tool using a larger training data could be developed for accessing the readability level of Thai text and teachers could easily use this tool to select suitable reading materials for primary school students.

CONCLUSIONS

The machine-learning-based method introduced in this study can effectively assess the readability of Thai text. Term frequency values generated from a small number of terms which are selected by the proposed feature selection method can form the term frequency feature set of a good classification model for accessing the readability. The performance of the term frequency feature set is superior to either a single shallow feature set or language model feature set and is comparable to combinations of feature sets. Additionally, the classification model with the term frequency feature set is computationally more efficient in comparison to other models.

ACKNOWLEDGEMENT

This work was supported in part by the National Science Council under Grant No. NSC102-2511-S-415-009.

REFERENCES

1. J. S. Chall and E. Dale, "Readability Revisited: The New Dale-Chall Readability Formula", Brookline Books, Cambridge (MA), **1995**.
2. R. Flesch, "A new readability yardstick", *J. Appl. Psychol.*, **1948**, 32, 221-233.
3. S. Aluisio, L. Specia, C. Gasperin and C. Scarton, "Readability assessment for text simplification", Proceedings of NAACL HLT 2010 5th Workshop on Innovative Use of NLP for Building Educational Applications, **2010**, Los Angeles, USA, pp.1-9.
4. S. E. Petersen and M. Ostendorf, "A machine learning approach to reading level assessment", *Comput. Speech Lang.*, **2009**, 23, 89-106.
5. J. P. Kincaid, R. P. Fishburne, Jr., R. L. Rogers and B. S. Chissom, "Derivation of new readability formulas (automated readability index, Fog count and Flesch reading ease formula) for navy enlisted personnel", Research Report, **1975**, Institute for Simulation and Training, University of Central Florida, USA.
6. G. H. McLaughlin, "SMOG grading: A new readability formula", *J. Reading*, **1969**, 12, 639-646.

7. A. J. Stenner, "Measuring reading comprehension with the Lexile framework", Proceedings of 4th North American Conference on Adolescent/Adult Literacy, **1996**, Washington, DC, USA.
8. M. Heilman, K. Collins-Thompson and M. Eskenazi, "An analysis of statistical models and features for reading difficulty prediction", Proceedings of 3rd Workshop on Innovative Use of NLP for Building Educational Applications, **2008**, Columbus, USA, pp.71-79.
9. Y.-H. Chen, Y.-H. Tsai and Y.-T. Chen, "Chinese readability assessment using TF-IDF and SVM", Proceedings of International Conference on Machine Learning and Cybernetics, **2011**, Guilin, China, pp.705-710.
10. L. Si and J. Callan, "A statistical model for scientific readability", Proceedings of 10th International Conference on Information and Knowledge Management, **2001**, Atlanta, USA, pp.574-576.
11. K. Collins-Thompson and J. Callan, "Predicting reading difficulty with statistical language models", *J. Am. Soc. Inform. Sci. Technol.*, **2005**, 56, 1448-1462.
12. S. Sato, S. Matsuyoshi and Y. Kondoh, "Automatic assessment of Japanese text readability based on a textbook corpus", Proceedings of 6th International Conference on Language Resources and Evaluation, **2008**, Marrakech, Morocco, pp.654-660.
13. S. E. Schwarm and M. Ostendorf, "Reading level assessment using support vector machines and statistical language models", Proceedings of 43rd Annual Meeting of Association for Computational Linguistics, **2005**, Ann Arbor, USA, pp.523-530.
14. S. Vajjala and D. Meurers, "On improving the accuracy of readability classification using insights from second language acquisition", Proceedings of 7th Workshop on Building Educational Applications Using NLP, **2012**, Montreal, Canada, pp.163-173.
15. T. Francois and E. Miltsakaki, "Do NLP and machine learning improve traditional readability formulas?", Proceedings of 1st Workshop on Predicting and Improving Text Readability for Target Reader Populations, **2012**, Montreal, Canada, pp.49-57.
16. P. Daowadung and Y.-H. Chen, "Using word segmentation and SVM to assess readability of Thai text for primary school students", Proceedings of 8th International Joint Conference on Computer Science and Software Engineering, **2011**, Nakhon Pathom, Thailand, pp.170-174.
17. C. Haruechaiyasak, S. Kongyoung and M. Dailey "A comparative study on Thai word segmentation approaches", Proceedings of 5th International Conference on Electrical Engineering/ Electronics, Computer, Telecommunications and Information Technology, **2008**, Krabi, Thailand, Vol. 1, pp.125-128.
18. NECTEC, "LexTo: Thai lexeme tokenizer", **2007**, <http://www.sansarn.com/lexto/> (Accessed: December 2013).
19. S. Klaithin, P. Chootrakool and K. Kosawat, "LEXiTRON-Pro editor: An integrated tool for developing Thai pronunciation dictionary", Proceedings of International Multiconference on Computer Science and Information Technology, **2010**, Wisla, Poland, pp.429-433.
20. Y. Yang and J. O. Pedersen, "A comparative study on feature selection in text categorization", Proceedings of 14th International Conference on Machine Learning, **1997**, Nashville, USA, pp.412-420.
21. C. D. Manning, P. Raghavan and H. Schutze, "Introduction to Information Retrieval", Cambridge University Press, Cambridge, **2008**.
22. C. Cortes and V. Vapnik, "Support-vector networks", *Mach. Learn.*, **1995**, 20, 273-297.
23. M. Reif, F. Shafait, M. Goldstein, T. Breuel and A. Dengel, "Automatic classifier selection for non-experts", *Pattern Anal. Appl.*, **2014**, 17, 83-96.

24. C.-W. Hsu and C.-J. Lin, “A comparison of methods for multiclass support vector machines”, *IEEE Trans. Neural Netw.*, **2002**, 13, 415-425.
25. C.-C. Chang and C.-J. Lin, “LIBSVM: A library for support vector machines”, *ACM Trans. Intell. Syst. Technol.*, **2011**, 2, no. 27.
26. W. Chu and S. S. Keerthi, “Support vector ordinal regression”, *Neural Comput.*, **2007**, 19, 792-815.
27. H.-T. Lin and L. Li, “Reduction from cost-sensitive ordinal ranking to weighted binary classification”, *Neural Comput.*, **2012**, 24, 1329-1367.
28. F. Xia, L. Zhou, Y. Yang and W. Zhang, “Ordinal regression as multiclass classification,” *Int. J. Intell. Ctrl. Syst.*, **2007**, 12, 230-236.
29. A. Stolcke, “SRILM—An extensible language modeling toolkit”, Proceedings of 7th International Conference on Spoken Language Processing, **2002**, Denver, USA, pp.901-904.

© 2015 by Maejo University, San Sai, Chiang Mai, 50290 Thailand. Reproduction is permitted for non-commercial purposes.

Full Paper

Effects of *Musa* (ABB group) prebiotic and *Bacillus subtilis* S11 probiotic on growth and disease resistance of cultivated Pacific white shrimp (*Litopenaeus vannamei*)

Ratchana Boonmee¹ and Sirirat Rengpipat^{1,2,*}

¹ Programme in Biotechnology, Faculty of Science, Chulalongkorn University, Bangkok 10330, Thailand

² Department of Microbiology, Faculty of Science, Chulalongkorn University, Bangkok 10330, Thailand

* Corresponding author. E-mail: srengpipat@gmail.com

Received: 26 June 2014/ Accepted: 14 November 2015/ Published: 17 November 2015

Abstract: Extract of ripe banana (BN) with a prebiotic activity score of 1.77 were demonstrated to support the growth of probiotic *Bacillus subtilis* S11 (BS11). BN and BS11, separate and combined, were then fed to the Pacific white shrimp (*Litopenaeus vannamei*) over 90 days in the rainy season and in the dry (hot) season. In both seasons, the highest production was found in shrimp fed with BS11 plus 10% BN. After challenging with *Vibrio harveyi* 639, the lowest cumulative mortality was found in shrimp fed with BS11 and 10% BN in the rainy season, indicating a higher shrimp production following the synbiotic use of the BS11 probiotic combined with the BN prebiotic.

Keywords: Pacific white shrimp, *Litopenaeus vannamei*, probiotic, *Bacillus subtilis* S11, prebiotic, *Musa* (ABB group), banana

INTRODUCTION

The farming of Pacific white shrimp (*Litopenaeus vannamei*) has recently become a major economic industry in Thailand. However, from 2013 onwards the industry has faced a severe blow due to outbreaks of acute hepatopancreatic necrosis disease [1]. *Bacillus subtilis* S11 (BS11) has been proposed as a probiotic bacterium for the black tiger shrimp (*Penaeus monodon*) [2, 3] and also for the Pacific white shrimp [4] due to the bacterium's ability to survive the passage through the gastrointestinal tract of these shrimp and enhance the growth and defense against pathogens including *Vibrio harveyi*.

The inclusion of inulin-derived fructo-oligosaccharide (FOS) into regular animal feed has also been shown to have a broad antibacterial effect against such pathogens as *Escherichia coli*, *Salmonella* spp., *Clostridium* spp., enterobacteria, eubacteria and coliforms [5]. Inulin and

oligofructose have been reported to occur in several fruits including the banana, in which inulin content of 0.3-0.7% of fresh weight were reported [6]. Conversion of inulin to oligofructose normally occurs through controlled partial enzymatic hydrolysis which resembles that of the processing of chicory roots [7]. The most popular banana cultivar in Thailand, *Musa* (ABB group) or Kluai Namwa in Thai, is a hybrid of *Musa acuminata* Colla and *M. balbisiana* Colla [8]. Both of the parental plants typically contain a considerable amount of dietary fibre [8], which has been claimed to have a prebiotic activity that promotes the growth of bacteria within the small intestine leading to the colon and provides potential health benefits [9,10].

In this study the use of a probiotic coupled with a prebiotic, an approach known as synbiotics, is undertaken in order to evaluate the effects of the BS11 probiotic and *Musa* (ABB group) prebiotic supplemented to the regular feed on the growth and disease resistance of the Pacific white shrimp

MATERIALS AND METHODS

Bacterial Strains

BS11 was isolated from the gastrointestinal tract of *Penaeus monodon* caught from the Gulf of Thailand as previously described [2, 3] and shown to be a good probiotic for *Litopenaeus vannamei* [4]. *Vibrio harveyi* 639, a pathogenic bacterium, also isolated from *P. monodon* that had died from luminescent disease, was kindly provided by the Shrimp Culture Research Centre, Charoen Pokphand Feedmill, Samutsakorn, Thailand. The bacterium was cultured in tryptic soya agar (TSA), tryptic soya broth (TSB) with 1.5% (w/v) agar supplemented with 2% (w/v) NaCl, or in thiosulphate-citrate-bile-salt-sucrose agar (TCBS) and was used for inducing *V. harveyi* infection in the shrimp. All culture media were purchased from Difco (USA).

Escherichia coli ATCC 25922 and *Bifidobacterium animalis* subsp. *lactis* BB12 were provided by the Department of Microbiology and the Department of Food Science, Faculty of Science, Chulalongkorn University respectively. Lactic acid bacteria (LAB), namely *Lactobacillus* (*Lb.*) *acidophilus* IAM 10074, *Lb. casei* subsp. *casei* IAM 1045, *Lb. fermentum* IAM 1148, *Lactococcus* (*Lc.*) *lactis* subsp. *cremoris* IAM 1150 and *Lc. lactis* subsp. *lactis* IAM 1198 were obtained from Riken Bioresource Centre, Japan.

Preparation of *Musa* (ABB group) Extract

The ripe (yellow skin) fruits of *Musa* (ABB group) were peeled and sliced. The sliced flesh (10 g) was homogenised in 100 mL of hot water (100°C) and left to stand for 10 min. Suspended particles were removed by centrifugation at 10160 g and 4°C for 10 min., and the supernatant was harvested [11] and used as the ripe banana extract (BN) in subsequent experiments. Larger scales of BN preparation was performed as desired and kept at 4°C before use.

Prebiotic Activity Score

Prebiotic activity score (PAS) was determined as previously reported [12]. In brief, an overnight culture of *B. animalis* subsp. *lactis* BB12, *Lb. acidophilus* IAM 10074, *Lb. casei* subsp. *casei* IAM 1045, *Lb. fermentum* IAM 1148, *Lc. lactis* subsp. *cremoris* IAM 1150 and *Lc. lactis* subsp. *lactis* IAM 1198 were transferred at 1% (v/v) in triplicate into individual tubes containing manually prepared lactobacillus de Man, Rogosa and Sharpe broth without dextrose (mMRS-D) (10 mL) supplemented with either 1% (w/v) glucose, 1% (w/v) inulin, or 1% (w/v) BN. The tubes were then incubated at 37°C under an anaerobic condition in candle jars [13]. An overnight culture of

either BS11 or *E. coli* ATCC 25922 (0.1 mL) was transferred in triplicate into culture tubes containing manually prepared TSB without dextrose (mTSB-D) (10 mL) and also into the same broth but with either 1% (w/v) glucose, 1% (w/v) inulin or 1% (w/v) BN and incubated aerobically at 37°C [13]. After 24 hr of incubation, samples were harvested and enumerated on MRS agar (Difco, USA) for LAB and on TSA for BS11 and *E. coli*. All chemicals for manually prepared culture media were obtained from Merck (Germany). Inulin was from Sigma-Aldrich (USA).

The PAS was determined using the following formula [12]:

$$\text{PAS} = \frac{P_{P_{24}} - P_{P_0}}{P_{g_{24}} - P_{g_0}} - \frac{E_{P_{24}} - E_{P_0}}{E_{g_{24}} - E_{g_0}}$$

where P_p and P_g are the probiotic log colony forming units (CFU)/mL when grown on the prebiotic and glucose respectively; E_p and E_g are the enteric log CFU/mL when grown on the prebiotic and glucose respectively; and the subscript numbers represent the culture time (0 and 24 hr). By definition, substrates with a high PAS support a good growth of the probiotic bacteria, with cell densities (CFU/mL) comparable with BS11 grown on mTSB-D with glucose.

Preparation of Shrimp Feed

Commercial feed (Charoen Pokphand Foods Public Co., Thailand) was used as the regular feed and then supplemented with the probiotic and/or prebiotic before use. The feed mixed with BN at 10%, 20% and 30% (v/w) (designated as 10%BN-, 20%BN- and 30%BN-feeds respectively) were prepared. BS11 was cultured in TSB at 30°C with shaking at 200 rpm for 24 hr and then washed three times with sterile normal saline solution by centrifuging at 10160 g and 4°C for 10 min. The cell pellet was harvested and mixed into the feed. The wet cells were thoroughly mixed with the regular feed at a ratio of 1:3 respectively (~2.5% of bacteria by weight) and designated as BS11-feed. In addition, the BS11 was co-supplemented into the 10%, 20% and 30% BN-feeds (designated as BS11&10%BN-, BS11&20%BN- and BS11&30%BN-feeds respectively). Each mixture was spread out, dried in an oven for 1-2 hr at 37°C and then stored in a clean plastic bag at 4°C until use. Each batch was examined for viable BS11 cells (CFU/g).

Cultivation of Shrimp

The post-larvae of the Pacific white shrimp (*Litopenaeus vannamei*), aged 20 days after hatching, were obtained from a commercial shrimp farm in Pathumthani province and acclimatised in an aerated tank with a closed recirculating water system (containing 25 mg/L NaCl) at 30°C until they reached 1-2 g in weight. They were then transferred into a 200-L high-density polyethylene culture tank (0.64 x 1.05 x 0.56 m). Suspended solids were removed with a filtering unit consisting of three layers: sand at the bottom, oyster-shells in the middle and fibre filler on the top. Water was transferred into the filter unit by an air-lift pump and passed through the unit by gravity into the culture tank. All the culture tanks were placed outdoors under a roof and sun-shade net cover. A total of eight different feeding regimes, viz. the regular feed (control) and the BS11-, 10%BN-, 20%BN-, 30%BN-, BS11&10%BN-, BS11&20%BN- and BS11&30%BN-feeds were evaluated. Each treatment was performed in triplicate using 30 shrimp in each tank. The shrimp were fed three times daily at 09.00 am, 1.00 pm and 6.00 pm at 10% of their net body weight. This set of experiment was performed twice, one in the rainy season and one in the hot season. The shrimp body weight and survival, total bacteria, BS11 and *Vibrio* spp. counts from the cultivation tank and

intestines of moribund shrimp, together with total haemocyte count (THC) and phenoloxidase (PO) activity of live shrimp were monitored before and after challenging with *V. harveyi* 639.

Water samples (100 mL) were collected from the centre of each tank every 15 days and their pH, alkalinity, dissolved oxygen, salinity, temperature, and ammonium and nitrite contents were monitored as described previously [14].

***Vibrio harveyi* Challenge**

Vibrio harveyi 639 was cultured in TSB with 2% (w/v) NaCl or on TCBS and used for inducing the infection. After feeding for 90 days, the shrimp in each treatment were exposed to pathogenic *V. harveyi* 639 at $\sim 10^7$ CFU/mL by immersion in tank water. Ten shrimp were randomly transferred to each 40-L water tank (three tanks per treatment). The remaining shrimp were kept and fed with the same regime as before. No water was exchanged between the tanks thereafter for 3 days. During the trial, the number of live shrimp was measured and the moribund shrimp were removed every 24 hr, and from this the cumulative mortality was recorded. The hepatopancreas and intestine were dissected from each moribund shrimp and examined for the presence of *V. harveyi* 639 initially by isolation on TCBS agar, and subsequent identification as *V. harveyi* was performed as previously described [15].

Defense Parameters from Shrimp Hemolymph

Shrimp haemolymph (100 μ L) was collected from the ventral-sinus using a 26-gauge needle and a 1-mL syringe containing 200 μ L of anticoagulant solution (10% w/v sodium citrate). A 20- μ L drop of the mixture was placed in a haemocytometer and the THC determined under a light microscope at 400 x magnification.

After collecting the haemolymph and pelleting the cells by centrifugation at 800 g and 4°C for 10 min., the pellet was washed and collected in ice-cold cacodylate buffer (Sigma-Aldrich, USA) at pH 7.0 and then homogenised with a sonicator for 10 sec. The homogenate was centrifuged at 16000 g and 4°C for 20 min. to obtain the hemocyte lysate supernatant. The PO activity of the supernatant was measured spectrophotometrically at 490 nm using L-3,4-dihydroxyphenylalanine (Sigma-Aldrich, USA) as the substrate as described previously [4, 16, 17]. One unit of enzyme activity was defined as an increase in absorbance per min. per μ g protein [18]. The protein content in the hemocyte lysate supernatant was measured by Bradford's method [19] using bovine serum albumin (Sigma-Aldrich, USA) as standard.

Statistical Analysis

The data on shrimp growth, survival and disease resistance are presented as mean \pm standard deviation (SD). The significance of differences between means was tested by analysis of variance and Duncan's multiple range tests with accepted significance at $p < 0.05$ level [20].

RESULTS AND DISCUSSION

Prebiotic Activity Score

BS11 grown in mTSB-D with 1% inulin or 1% BN has a reasonably high PAS of 1.42 ± 0.20 and 1.77 ± 0.35 respectively, with 1.25-fold higher growth in BN- than inulin-supplemented mTSB-D, but this is not statistically significant (Figure 1). In contrast, *B. animalis* subsp. *lactis* BB12 growth in mMRS-D with 1% inulin is markedly lower than that in mMRS-D with 1% BN giving a low PAS of -0.18 ± 0.08 and -0.36 ± 0.02 respectively. The inability of *B. animalis* subsp.

lactis BB12 to grow well in the presence of inulin or BN is in agreement with that previously reported for a different strain of *B. bifidum* NCI on inulin-S with a PAS of -1.11 ± 0.08 [12]. Among the other tested LAB, the highest PAS of 1.94 ± 0.40 and 1.97 ± 0.43 in mMRS-D with 1% inulin and 1% BN respectively was detected in *Lc. lactis* subsp. *cremoris* IAM 1150. These are 1.4- and 1.1-fold higher than PAS for BS11 on the media supplemented with inulin and BN respectively. None of the other tested LAB grew as well in mMRS-D with 1% BN compared to that with 1% inulin (PAS < 1), except for *Lc. lactis* subsp. *cremoris* IAM 1150. However, the LAB evaluated in this study seem to grow well in the presence of inulin but not in the presence of BN (Figure 1). Similar to that reported previously [12], the PAS is observed to be dependent on both the bacterial strain and the prebiotic type/dose. Apparently, BN can replace inulin and support BS11 growth.

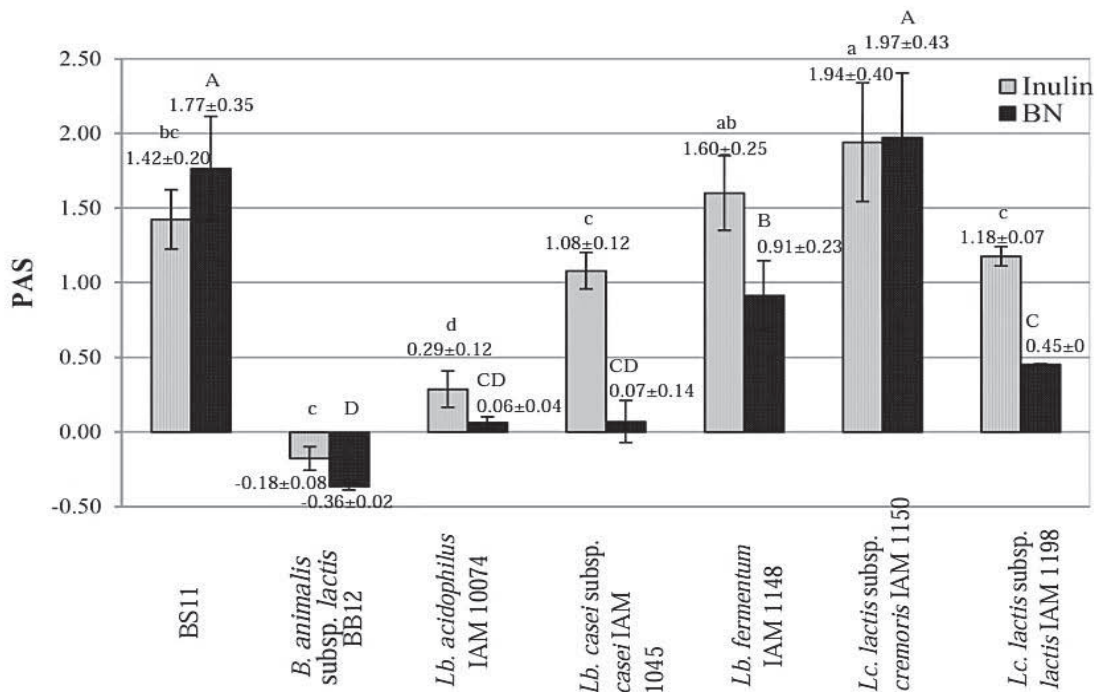


Figure 1. PAS of BS11 grown in mTSB-D and various LAB grown in mMRS-D supplemented with either 1% inulin or 1% BN as a prebiotic. Data are shown as mean ± SD from triplicate analysis, and means with different lowercase letters (for inulin) or uppercase letters (for BN) are significantly different ($P < 0.05$).

Effects of BS11- and BN-Feeds on Shrimp Weight, Survival and Production

The weights of *L. vannamei* among the eight treatments were not significantly different after 30 days of culture in the rainy season (Figure 2a). The average water quality in all treatments (4-6 mg/L dissolved oxygen, 25-29 mg/L salinity, pH 7.5-8.4, 0-0.50 mg/L ammonia, 80-150 ppm alkalinity and 0-0.50 mg/L nitrite) was within safe limits for shrimp culture [21]. The temperature varied only slightly, ranging between 29.0-31.0°C in the rainy season. The water quality in all treatments in the hot season was similar, except for a narrower pH range (7.36-8.25) and broader temperature range (28.5-35.5°C), which included a markedly high climate temperature of up to 41.5°C between 11am-1pm for a one-week period after 30 days of culture. This elevated temperature was likely to have induced significant heat stress in the surviving shrimp.

After 90 days of culture in the rainy season, the highest average shrimp weight (15.7 ± 0.75 g) was found in those fed with 20%BN-feed, which was significantly higher than that in the control

(Figure 2a). In contrast, the shrimp survival after 90 days of culturing with feed supplemented with BS11&10%BN ($95.6 \pm 3.9\%$) or BS11&20%BN ($94.4 \pm 5.1\%$) were significantly greater than that of the control (Figure 2c). Thus, there appears to be a marked synbiotic function of the BS11 probiotic and BN prebiotic on the shrimps' survival but not on their weight. The highest average shrimp production occurred in shrimp fed with BS11&10%BN-feed (380.9 ± 36.2 g), which was significantly higher than that in the control (Figure 2e).

In the trials performed in the hot season the highest increase in the average shrimp weight after 90 days of culture was observed in shrimp fed with BS11&20%BN-feed (15.7 ± 0.74 g) (Figure 2b). On the other hand, the highest shrimp survival was detected in shrimp fed with BS11-feed ($81.1 \pm 11.7\%$) (Figure 2d). A lower survival was found in the hot season than in the rainy season, apparently due to the high water temperature fluctuations in the hot season, which is above the optimum temperature for shrimp growth (28-30°C). This may also account for a larger variance seen in the average values in the hot season than in the rainy season. Likewise, the net average production in the hot season was lower than in the rainy season, with the highest production level in the hot season being found in shrimp fed with the BS11&10%BN-feed (291.1 ± 0.44 g) (Figure 2f). However, this is still 1.3-fold lower than the best production level found in the rainy season. The results are in agreement with the known effects of temperature stress, which can increase the shrimp's susceptibility to pathogens, limit growth and reduce survival rate and production [22, 23].

The higher net production of shrimp fed with BS11&10%BN-feed than with BS11-feed implies the possibility of a synbiotic effect of the combination of the BS11 probiotic and the BN prebiotic on production. In both seasons a reduced shrimp production level was found mostly when shrimp were fed only with BN-feed and this is significantly different from those fed with BS11- and BS11&BN-feeds (Figures 2e and 2f). This is in agreement with previous reports that the prebiotic function of FOS did not affect the weight gain and survival of the Pacific white shrimp [24], whilst Bio-Mos[®] and β -1,3-D-glucan did not affect the growth of the western king prawn *P. latisulcatus* [25]. In contrast, mannan oligosaccharides at 3.0 g/kg were found to significantly enhance the weight and survival of *P. semisulcatus* PL [26], whilst short chain FOS significantly enhanced the survival and weight of juvenile white shrimp in a dose-dependent manner [27]. In addition, the survival of Indian white shrimp larvae (M₁-M₃) after administration of inulin (Raftilline ST) + Easy DHA Selco[®]-enriched *Artemia* was significantly higher than that fed with either Easy DHA Selco[®]-enriched *Artemia* or inulin-enriched *Artemia* [28].

Without the prebiotic function of BN, the probiotic BS11 alone seems to significantly enhance the shrimp production level (Figures 2e and 2f), consistent with its previously reported probiotic properties [8] including growth enhancement, induction of healthy appearance [29, 30] and increased survival [31, 32]. It is probable that BS11 can produce some anti-microbial substances that negatively affect other pathogens [2, 3] and/or it can produce useful enzymes or metabolites to increase the uptake of useful nutrients, provide a competitive exclusion effect on pathogens and provide some benefits to indigenous induction [2, 3, 25, 33]. Many other *Bacillus* spp. have previously been reported to act as good probiotic candidates for Pacific white shrimp by supplementation into the diet [34-36] or culture water [31, 37]. Here, prebiotic (BN) feeds are demonstrated to confer benefits on the BS11 growth and may improve gastrointestinal microflora of the host as described previously [9, 24, 38].

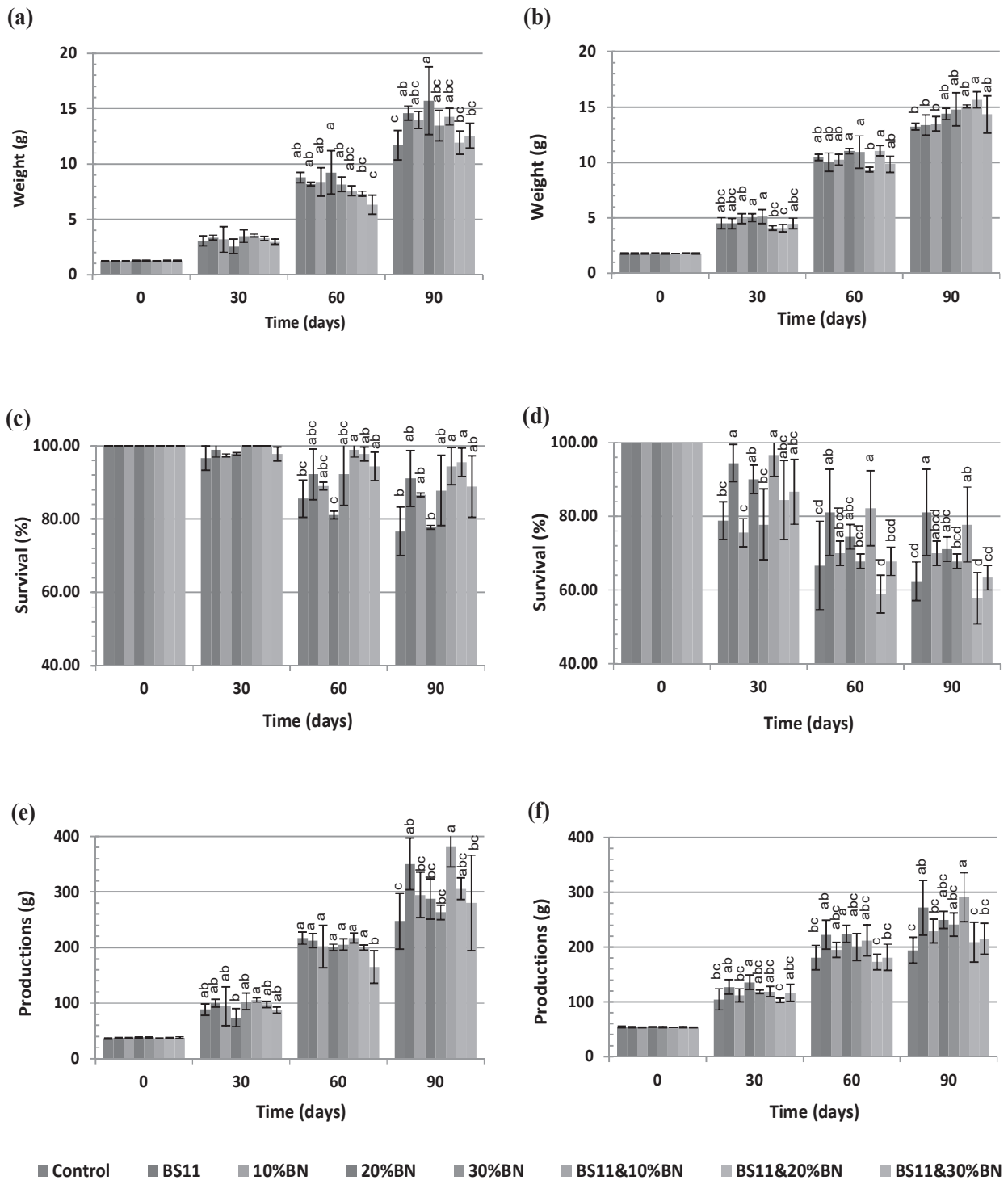


Figure 2. Average live (wet) weights (a, b), survival (c, d) and production (e, f) of *L. vannamei* during 90-day culture period when fed with regular feed (control) or with BS11-, 10%BN-, 20%BN-, 30%BN-, BS11&10%BN-, BS11&20%BN- or BS11&30%BN-supplemented feeds in rainy season (a, c, e) and hot season (b, d, f). Data are shown as mean \pm SD from triplicate analysis, and means with different letters are significantly different between treatments within the respective time points.

The total bacterial and *Vibrio* spp. counts in the culture water of all treatments ranged between $\sim 4 \times 10^5$ - $\sim 3 \times 10^7$ and $\sim 2 \times 10^2$ - $\sim 2 \times 10^4$ CFU/mL respectively in rainy season, and between $\sim 3 \times 10^4$ - $\sim 10^6$ and $\sim 1 \times 10^3$ - $\sim 2 \times 10^4$ CFU/mL respectively in hot season. As expected,

BS11 was only found in the culture water from tanks of shrimp fed with BS11-supplemented feeds and was at $\sim 7 \times 10^2$ - $\sim 2 \times 10^3$ CFU/mL in rainy season and $\sim 9 \times 10^2$ - $\sim 3 \times 10^3$ CFU/mL in hot season.

Challenge Test and Defense Parameters from Shrimp Hemolymph

From Figures 3a and 3b, the THCs in shrimp fed with different supplemented feeds before and after being challenged by *V. harveyi* 639 are numerically higher than those in shrimp fed with regular feed in both seasons, but are only significantly higher in shrimp fed with BS11- and BS11&10%BN-feeds. The reduction in THC after being challenged with *V. harveyi* 639 for all eight treatments ranges between 36-56% and 52-64% in the rainy and hot seasons respectively. The lowest THC reduction is observed in shrimp fed with BS11&10%BN-feed in both seasons, whereas the highest THC reduction is found in shrimp fed with regular feed. The control shrimp give the lowest average THC after *V. harveyi* 639 challenge, at 1.6- and 2.0-fold lower than those from shrimp fed with BS11&10%BN- and BS11-feeds respectively in the rainy season (Figure 3a), and at 1.4- and 2.3-fold lower in the hot season (Figure 3b).

From Figures 3c and 3d, the highest reduction in hemocyte PO activity (84% and 70% in rainy and hot seasons respectively) after challenge with *V. harveyi* are observed in shrimp fed with regular feed, whilst BS11- and BS11&10%BN-feeds give 55-68% and 51-63% reduction in rainy and hot seasons respectively. The lowest average hemocyte PO activity after *V. harveyi* 639 challenge occurs in the control shrimp, being more than 2.0-fold lower than that in the BS11&10%BN- and BS11-feeds in both seasons.

From Figures 3e and 3f, mortality is evident from the first day onwards in all the treatments after challenge with *V. harveyi* 639. However, the shrimp fed with control feed suffer a significantly higher mortality from day 2 and reach 90% mortality 3 days after *V. harveyi* exposure in rainy season and 42% in hot season. The improved shrimp survival, taken to imply disease resistance as compared to control, is clearly evident in the shrimp fed with all BN- and BS11-feeds, with the highest survival of 66.7% in those fed with BS11&10%BN-feed in rainy season, 90.0% survival in those fed with 20%BN- or 30%BN-feeds in hot season, and 86.7% survival in those fed with BS11&10%BN-feed. BS11-, BN- or BS11&BN-feed thus gives an enhanced survival after an external *V. harveyi* exposure. In agreement with these results, a decreased shrimp mortality after infection with *V. parahaemolyticus* was previously reported in shrimp that were fed with feed containing *V. alginolyticus* UTM 102, *B. subtilis* UTM126, *Roseobacter gallaeciensis* SLV03 and *Pseudomonas aestumarina* SLV22 [36]. Overall, a lower mortality was observed in the hot season during the 3-day exposure period to *V. harveyi* than in the rainy season. This may well reflect the $\sim 10^3$ CFU/mL lower viable *Vibrio* spp. levels in shrimp water in the hot season compared with those in the rainy season.

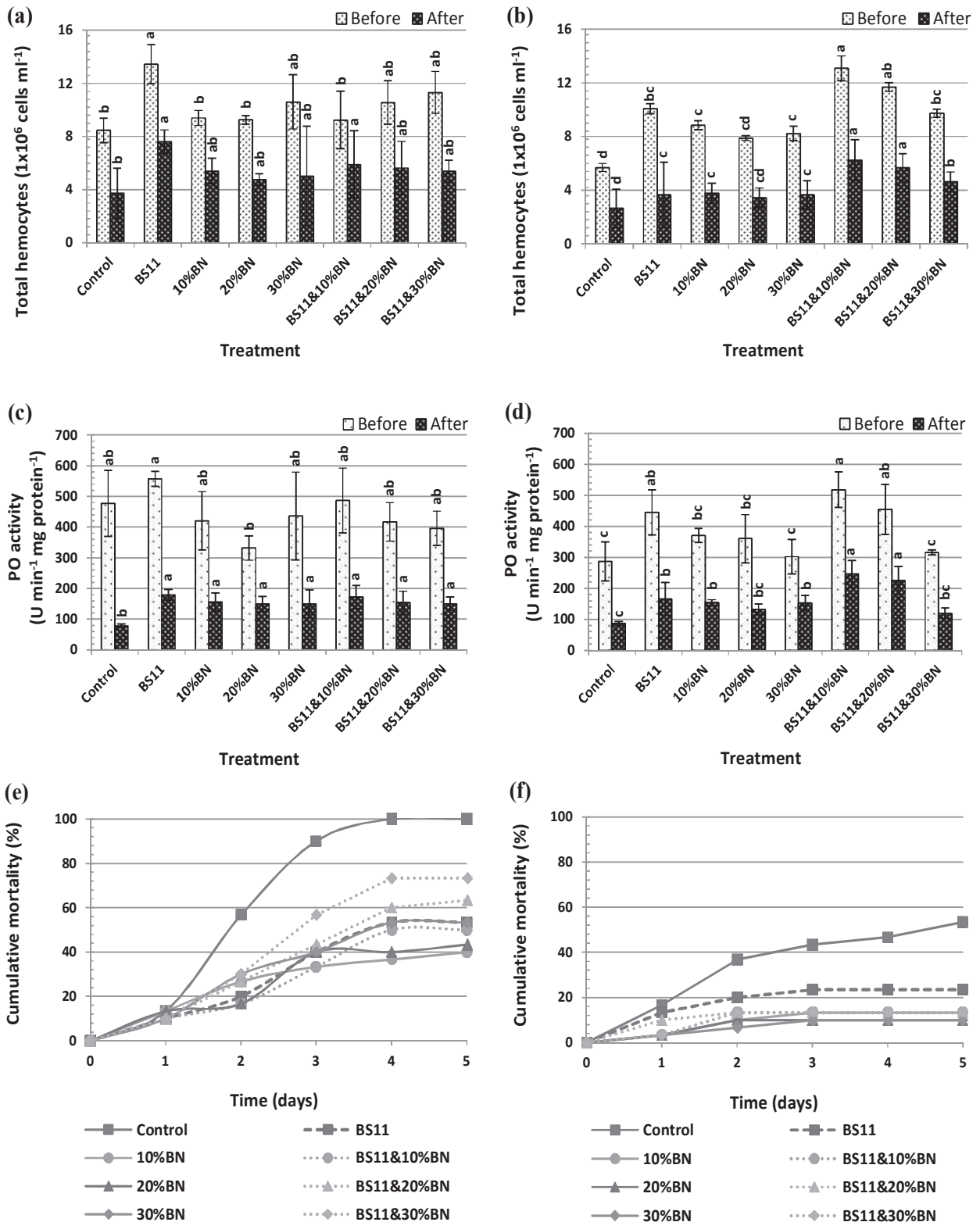


Figure 3. Mean shrimp THC (a, b) and PO activities (c, d) before and after challenge for 3 days by *Vibrio harveyi* 639, and shrimp cumulative mortality (e, f) during 3-day challenge for shrimp fed with regular feed (control) or BS11-, 10%BN-, 20%BN-, 30%BN-, BS11&10%BN-, BS11&20%BN- or BS11&30%BN-supplemented feeds in rainy season (a, c, e) and hot season (b, d, f). Data are shown as mean \pm SD, derived from nine shrimp. Different letters represent significant difference among treatments before or after challenge by *Vibrio harveyi* 639.

The *Vibrio* counts in the intestines of the moribund shrimp from all the treatments after challenge with *V. harveyi* 639 for 3 days ranged between $3.9-8.2 \times 10^7$ CFU/g in the rainy season and $3 \times 10^5 - 1.15 \times 10^7$ CFU/g in the hot season, which were significantly higher than those before *V. harveyi* challenge. Lower *Vibrio* counts from the intestines of shrimp fed with BS11-feed than with normal or BN-feeds were noted. The decrease in total *Vibrio* counts in the intestines of BS11-fed shrimp in this study agrees with previous results on shrimp fed with probiotic *Halomonas* sp. B12 [39], although it does not exactly match the shrimp mortality rates observed here.

CONCLUSIONS

A synbiotic effect using *Bacillus subtilis* S11 probiotic bacteria and banana prebiotic on enhancing the production and luminous vibriosis resistance of the Pacific white shrimp, *Litopenaeus vannamei*, has been demonstrated. The results from this study support the possibility of using *Bacillus subtilis* S11 and/or banana prebiotic as alternatives to antibiotics in the shrimp farming process, which could lead to a more sustainable and environmentally friendly industry as well as a healthier food product of higher economic value.

ACKNOWLEDGEMENTS

The authors sincerely thank Robert Butcher for revising the manuscript and providing many valuable suggestions and comments. This research was supported by the Thai Government Stimulus Package 2 (TKK 2555) under the Project for the Establishment of a Comprehensive Centre for Education Research Promotion and by the National Research University Project of Thailand, Office of the Higher Education Commission (FW643A) and partially by Chulalongkorn University 90th Anniversary fund (Ratchadaphisek Somphot Endowment Fund).

REFERENCES

1. FAO, "Report of the FAO/MARD Technical Workshop on Early Mortality Syndrome (EMS) or Acute Hepatopancreatic Necrosis Syndrome (AHPENS) of Cultured Shrimp (under TCP/VIE/3304), Hanoi, Viet Nam, 2013", FAO, Rome, 2013.
2. S. Rengpipat, W. Phianphak, S. Piyatiratitivorakul and P. Menasveta, "Effect of a probiotic bacterium on black tiger shrimp *Penaeus monodon* survival and growth", *Aquaculture*, 1998, 167, 301-313.
3. S. Rengpipat, S. Rukpratanporn, S. Piyatiratitivorakul and P. Menasveta, "Immunity enhancement in black tiger shrimp (*Penaeus monodon*) by a probiont bacterium (*Bacillus* S11)", *Aquaculture*, 2000, 191, 271-278.
4. P. Sapcharoen and S. Rengpipat, "Effects of the probiotic *Bacillus subtilis* (BP11 and BS11) on the growth and survival of Pacific white shrimp, *Litopenaeus vannamei*", *Aquacult. Nutr.*, 2013, 19, 946-954.
5. L. S. Boeckner, M. I. Schnepf and B. C. Tugland, "Inulin: A review of nutritional and health implications", *Adv. Food Nutr. Res.*, 2001, 43, 1-63.
6. J. van loo, P. Coussement, L. de Leenheer, H. Hoebregs and G. Smits, "On the presence of inulin and oligofructose as natural ingredients in the western diet", *Crit. Rev. Food Sci. Nutr.*, 1995, 35, 525-552.
7. E. J. Vandamme and D. G. Derycke, "Microbial inulinases: Fermentation process, properties, and applications", *Adv. Appl. Microbiol.*, 1983, 29, 139-176.

8. W. H. Haslinda, L. H. Cheng, L. C. Chong and A. A. N. Aziah, "Chemical composition and physicochemical properties of green banana (*Musa acuminata* X *balbisiana* Colla cv. Awak) flour", *Int. J. Food Sci. Nutr.*, **2009**, *60*, 232-239.
9. G. R. Gibson, H. M. Probert, J. van Loo, R. A. Rastall and M. B. Roberfroid, "Dietary modulation of the human colonic microbiota: Updating the concept of prebiotics", *Nutr. Res. Rev.*, **2004**, *17*, 259-275.
10. E. A. Flickinger, J. V. Loo and G. C. Fahey, "Nutritional responses to the presence of inulin and oligofructose in the diets of domesticated animals: A review", *Crit. Rev. Food Sci. Nutr.*, **2003**, *43*, 19-60.
11. L. Wei, J. Wang, X. Zheng, D. Teng, Y. Yang, C. Cai, T. Feng and F. Zhang, "Studies on the extracting technical conditions of inulin from Jerusalem artichoke tubers", *J. Food Eng.*, **2007**, *79*, 1087-1093.
12. J. Huebner, R. L. Wehling and R. W. Hutkins, "Functional activity of commercial prebiotics", *Int. Dairy J.*, **2007**, *17*, 770-775.
13. R. M. Atlas, "Handbook of Microbiological Media for the Examination of Food", 4th Edn., CRC Press Taylor and Francis, Boca Raton (FL), **2010**, p.1554.
14. J. D. H. Strickland and T. R. Parsons, "A Practical Handbook of Seawater Analysis", 2nd Edn., Alger Press, Ottawa, **1972**.
15. P. Baumann and R. H. W. Schubert, "Vibrionaceae", in "Bergey's Manual of Systematic Bacteriology, Vol. 1", (Ed. N.A. Krieg and J.G. Holt), William and Wilkins, Baltimore, **1984**, pp.516-549.
16. K. Söderhäll, "Fungal cell wall β -1,3-glucans induce clotting and phenoloxidase attachment to foreign surfaces of crayfish hemocyte lysate", *Dev. Comp. Immunol.*, **1981**, *5*, 565-573.
17. V. J. Smith and K. Söderhäll, "A comparison of phenoloxidase activity in the blood of marine invertebrates", *Dev. Comp. Immunol.*, **1991**, *15*, 251-261.
18. K. Söderhäll and T. Unestam, "Activation of serum prophenoloxidase in arthropod immunity. The specificity of cell wall glucan activation and activation by purified fungal glycoproteins of crayfish phenoloxidase", *Can. J. Microbiol.*, **1979**, *25*, 406-414.
19. M. M. Bradford, "A rapid and sensitive method for the quantitation of microgram quantities of protein utilizing the principle of protein-dye binding", *Anal. Biochem.*, **1976**, *72*, 248-254.
20. K. A. Council, "SAS Introductory Guide for Personal Computers", Version 6 Edn., SAS Institute, Cary (NC), **1985**.
21. P. Menasveta, P. Aranyakanonda, S. Rungsapa and N. Moree, "Maturation and larviculture of penaeid prawns in closed recirculating seawater system", *Aquacult. Eng.*, **1989**, *8*, 357-368.
22. A. D. Re, F. Díaz, E. Ponce-Rivas, I. Giffard, M.-E. Muñoz-Marquez and H. M. Sigala-Andrade, "Combined effect of temperature and salinity on the thermotolerance and osmotic pressure of juvenile white shrimp *Litopenaeus vannamei* (Boone)", *J. Therm. Biol.*, **2012**, *37*, 413-418.
23. D. Cottin, B. Shillito, T. Chertemps, A. Tanguy, N. Léger and J. Ravaux, "Identification of differentially expressed genes in the hydrothermal vent shrimp *Rimicaris exoculata* exposed to heat stress", *Mar. Genomics*, **2010**, *3*, 71-78.
24. P. Li, G. S. Burr, D. M. Gatlin III, M. E. Hume, S. Patnaik, F. L. Castille and A. L. Lawrence, "Dietary supplementation of short-chain fructooligosaccharides influences gastrointestinal microbiota composition and immunity characteristics of Pacific white shrimp, *Litopenaeus vannamei*, cultured in a recirculating system", *J. Nutr.*, **2007**, *137*, 2763-2768.
25. N. V. Hai, R. Fotedar and N. Buller, "Selection of probiotics by various inhibition test methods for use in the culture of western king prawns, *Penaeus latisulcatus* (Kishinouye)", *Aquaculture*, **2007**, *272*, 231-239.

26. M. A. Genc, M. Aktas, E. Genc and E. Yilmaz, “Effects of dietary mannan oligosaccharide on growth, body composition and hepatopancreas histology of *Penaeus semisulcatus* (de Haan 1844)”, *Aquacult. Nutr.*, **2007**, *13*, 156-161.
27. Z. Zhou, Z. Ding and L. V. Huiyuan, “Effects of dietary short-chain fructooligosaccharides on intestinal microflora, survival, and growth performance of juvenile white shrimp, *Litopenaeus vannamei*”, *J. World Aquacult. Soc.*, **2007**, *38*, 296-301.
28. S. H., Hoseinifar, P. Zare and D. L. Merrifield, “The effects of inulin on growth factors and survival of the Indian white shrimp larvae and postlarvae (*Fenneropenaeus indicus*)”, *Aquacult. Res.*, **2010**, *41*, 348-352.
29. Y. B. Wang, “Effect of probiotics on growth performance and digestive enzyme activity of the shrimp *Penaeus vannamei*”, *Aquaculture*, **2007**, *269*, 259-264.
30. L. Verschuere, G. Rombaut, P. Sorgeloos and W. Verstraete, “Probiotic bacteria as biological control agents in aquaculture”, *Microbiol. Mol. Biol. Rev.*, **2000**, *64*, 655-671.
31. I. E. Luis-Villaseñor, M. E. Macías-Rodríguez, B. Gómez-Gil, F. Ascencio-Valle and Á. I. Campa-Córdova, “Beneficial effects of four *Bacillus* strains on the larval cultivation of *Litopenaeus vannamei*”, *Aquaculture*, **2011**, *321*, 136-144.
32. X.-X. Zhou, Y.-B. Wang and W.-F. Li, “Effect of probiotic on larvae shrimp (*Penaeus vannamei*) based on water quality, survival rate and digestive enzyme activities”, *Aquaculture*, **2009**, *287*, 349-353.
33. M. Maeda and I. C. Liao, “Effect of bacterial population on the growth of a prawn larva, *Penaeus monodon*”, *Bull. Natl. Res. Inst. Aquacult.*, **1992**, *21*, 25-29.
34. D. Y. Tseng, P. L. Ho, S. Y. Huang, S. C. Cheng, Y. L. Shiu, C. S. Chiu and C. H. Liu, “Enhancement of immunity and disease resistance in the white shrimp, *Litopenaeus vannamei*, by the probiotic, *Bacillus subtilis* E20”, *Fish Shellfish Immunol.*, **2009**, *26*, 339-344.
35. J. Li, B. Tan and K. Mai, “Dietary probiotic *Bacillus* OJ and isomaltooligosaccharides influence the intestine microbial populations, immune responses and resistance to white spot syndrome virus in shrimp (*Litopenaeus vannamei*)”, *Aquaculture*, **2009**, *291*, 35-40.
36. J. L. Balcázer, T. Rojas-Luna and D. P. Cunningham, “Effect of the addition of four potential probiotic strains on the survival of pacific white shrimp (*Litopenaeus vannamei*) following immersion challenge with *Vibrio parahaemolyticus*”, *J. Invertebr. Pathol.*, **2007**, *96*, 147-150.
37. K. F. Liu, C. H. Chiu, Y. L. Shiu, W. Cheng and C. H. Liu, “Effects of the probiotic, *Bacillus subtilis* E20, on the survival, development, stress tolerance, and immune status of white shrimp, *Litopenaeus vannamei* larvae”, *Fish Shellfish Immunol.*, **2010**, *28*, 837-844.
38. Joint FAO/WHO Working Group, “Guidelines for the evaluation of probiotics in food”, Report on Drafting Guidelines for the Evaluation of Probiotics in Food, FAO/WHO, Ontario, **2002**.
39. L. Zhang, K. Mai, B. Tan, Q. Ai, C. Qi, W. Xu, W. Zhang, Z. Liufu, X. Wang and H. Ma, “Effects of dietary administration of probiotic *Halomonas* sp. B12 on the intestinal microflora, immunological parameters, and midgut histological structure of shrimp, *Fenneropenaeus chinensis*”, *J. World Aquacult. Soc.*, **2009**, *40*, 58-66.

Full Paper

Viability and probiotic properties of *Lactobacillus plantarum* TISTR 2075 in spray-dried fermented cereal extracts

Wanticha Savedboworn¹ and Penkhae Wanchaitanawong^{2,*}

¹ Department of Agro-Industry Technology and Management, Faculty of Agro-Industry, King Mongkut's University of Technology North Bangkok, Prachinburi Campus, Prachinburi Province 25230, Thailand

² Department of Biotechnology, Faculty of Agro-Industry, Kasetsart University, Bangkok 10900, Thailand

* Corresponding author, e-mail: fagipkw@ku.ac.th

Received: 14 June 2014 / Accepted: 22 September 2015 / Published: 26 November 2015

Abstract: Spray-dried cereal extracts containing probiotic *Lactobacillus plantarum* TISTR 2075 was produced. Sterile soya milk extract and Job's-tears extract fortified with sesame (1-2%) and glucose (1-20%) were fermented by *L. plantarum* TISTR 2075. After 24 hr, the strain was found to grow well both in soya milk and Job's-tears extracts with viable cells of 8.28 and 7.73 log CFU/mL respectively. Higher viable cells were observed with addition of 1% glucose and 1% sesame. Sesame was also found to significantly increase soluble calcium after fermentation due to lowered pH due to the production of organic acids. Each fermented cereal extract was then mixed with 20% maltodextrin prior to spray-drying at 130°C and 70°C (inlet and outlet air temperature respectively). After spray-drying, the survival of *L. plantarum* TISTR 2075 in spray-dried soya milk and Job's-tears extract powders was 79.0 and 85.4% respectively. The functional properties of the probiotic including pathogenic inhibition of foodborne pathogens (*Escherichia coli* O157:H7 DMST 12743 and *Salmonella typhimurium* ATCC 13311) and the tolerance to simulated gastric juice (pH 2.0) and small intestinal juice (pH 8.0) were not affected by the spray-drying process.

Keywords: probiotics, *Lactobacillus plantarum*, fermented spray-dried cereal extracts, spray-drying, probiotic properties, soluble calcium

INTRODUCTION

Recently, consumer demand for cereal-based probiotic products has increased due to a combination of high nutritive values from cereals and health benefits from probiotics. Many studies have used cereals for developing non-dairy probiotic foods since they can alleviate some of disadvantages associated with dairy products like lactose intolerance, allergy to milk protein and the

impact in cholesterol levels [1-4]. Furthermore, cereals are suitable substrates for the growth of beneficial probiotic bacteria since it contains sucrose, raffinose and stachyose used as energy sources for probiotics [2, 5-9]. For example, soya milk is a suitable substrate for the growth of lactic acid bacteria *Lactobacillus* and *Bifidobacteria* [10-13]. According to Chou et al. [14], soya milk can support the growth of *B. infantis* CCRC 14633 and *B. longum* B6 with viable cell counts of 8.5 and 7.1 log CFU/mL respectively after fermentation for 48 hr. *L. plantarum* NCIMB 8826 and *L. acidophilus* NCIMB 8821 grow well in malt, barley and barley-malt media with viable cell numbers of 8.59, 7.91 and 8.53 log CFU/mL respectively after 24 hr of fermentation [2]. Oat-based substrate can be used as a growth medium of *L. reuteri*, *L. acidophilus* and *B. bifidum* with viable cell counts of greater than 8 log CFU/mL after 30 days of storage [15]. In addition, the fermentation of cereals or vegetables by lactic acid bacteria enhances the availability of minerals such as calcium and iron, which correlate with the effect of pH reduction [11, 16]. According to Tang et al. [11], *L. acidophilus* ATCC 4962 and *L. casei* ASCC 290 exhibit the highest increase in soluble calcium after calcium-fortified soya milk is fermented for 24 hr. Also, a 2.5-fold increase in soluble calcium is observed in fermented soya milk with sucrose addition [12]. Bergqvist et al. [16] further reported that the level of soluble iron is markedly enhanced during fermentation of carrot juice by *L. pentosus* FSC 1.

In recent years, spray-drying is considered as a useful technique for preserving probiotics in dried form due to its relatively inexpensive cost and availability of the process [17-20]. Viability and stability of probiotics are a technological challenge because the probiotics bacteria are susceptible to high temperature during the spray-drying process [21]. A prerequisite for probiotic products is that a sufficiently large number (at least 10^7 CFU/g or mL) of viable probiotic bacteria survive in the final product at the time of consumption [22, 23]. In addition, it is important that the probiotic should maintain its properties after spray-drying in order to give the health beneficial effect to the host [24]. Spray-drying does not affect bacteriocin production of *L. salivarius* UCC 118 [25]. Also, spray-dried *L. plantarum* 83114 and *L. kefir* 8321 do not lose their capacity to adhere to Caco-2/TC-7 cells [26]. *L. plantarum* CFR 2191 was found to retain its acid-tolerance property up to 95% in the cell suspensions spray-dried with maltodextrin. However, a significant loss of viable cells was observed in the case of *Pediococcus acidilactici* CFR 2193 spray-dried with non-fat skimmed milk [27].

Soya bean, sesame and Job's-tears were found to enhance the viability of *L. plantarum* TISTR 2075 during exposure to simulated gastrointestinal tract conditions [28]. In the present study the ability of *L. plantarum* TISTR 2075 to use the sesame-supplemented extracts of soya bean and Job's-tears as substrate is investigated. The effect of glucose is also studied in order to obtain a high cell density. Furthermore, the effects of spray-drying on cell survival with emphasis on retention of probiotic properties, viz. gastrointestinal tract tolerance and pathogenic inhibition, are evaluated.

MATERIALS AND METHODS

Bacterial Strain and Preparation of Culture

L. plantarum TISTR 2075 isolated from fermented vegetables was obtained from Microbiological Resource Centre, Thailand Institute of Scientific and Technological Research (TISTR). The strain was preserved in de Man, Rogosa, Sharpe (MRS) broth (Merck, Germany) with

20% (v/v) glycerol at -20°C. The strain was subcultured twice in MRS broth by incubating at 37°C for 24 hr under microaerobic-static condition and then used as inoculum [29].

E. coli O157:H7 DMST 12743 and *S. typhimurium* ATCC 13311 were purchased from Department of Medical Science, Ministry of Public Health. These strains were grown in tryptic soya broth (Difco Laboratories, USA) supplemented with 0.6% yeast extract (Difco Laboratories, USA) at 37°C. Both strains were subcultured twice by incubating at 37°C for 24 hr under microaerobic-static condition and then used as indicator strains.

Preparation and Fermentation of Cereal Extracts

Cereal extracts were prepared as described by Wang et al. [30]. Dried soya bean and Job's-tears (Thai Cereals World Co., Bangkok) were washed and soaked in distilled water for 5 hr, then mixed with distilled water (cereal:water = 1:10 w/v) and sesame (Thai Cereals World Co., Bangkok) at 0%, 1% or 2% w/v. The mixture was comminuted in a blender for 3 min. and the resultant slurry was filtered twice through double-layered cheesecloth to yield the cereal extract (filtrate). Each of the extracts was dispensed into a container, added with glucose solution to make 1, 5, 10, 15 and 20% w/v concentrations and sterilised by heating at 121°C for 15 min. The sterile cereal extract was inoculated with an overnight culture of 1 *L. plantarum* TISTR 2075 to make 1% concentration (initial cell number = 10⁷ CFU/mL). Fermentation was carried out at 37°C for 24 hr and viable cell counts were performed by the standard plate count method with MRS medium containing 0.5% CaCO₃ as indicator for the acid-producing strain at 37°C. The pH was measured with a pH meter.

Spray-Drying of Fermented Cereal Extracts

Prior to spray-drying, the overnight culture of fermented cereal extracts was mixed with 20% w/v maltodextrin (MD) (DE = 10; Du ZhiXue, China). The suspension was then spray-dried with a pilot-scale spray-drier (GEA Niro A/S, Denmark) at a constant air inlet and outlet temperature of 130°C and 70°C respectively. Viable cell count was done by standard plate count.

Simulated Gastrointestinal Tract Tolerance

Simulated gastric juice at pH 2.0 was prepared by suspending pepsin from porcine gastric mucosa (P-7000, Sigma, UK) in sterile 0.5% NaCl to a final concentration of 3 g/L and adjusting to pH 2.0 with concentrated HCl [31]. Simulated small intestinal juice at pH 8.0 was prepared by suspending pancreatin USP (P-1500, Sigma, UK) in sterile 0.5% NaCl to a final concentration of 1 g/L, adding with 0.45% bile salt (Oxoid, UK) and adjusting to pH 8.0 with sterile 0.1M NaOH [32].

For the determination of tolerance to simulated gastric juice and small intestinal juices, spray-dried powder (1 g) was suspended in 0.85% NaCl (9 mL). An aliquot of 0.2 mL of the suspension was transferred to a sterile tube, mixed with sterile 0.5% NaCl (0.3 mL) and blended with 1.0 mL of the simulated gastric juice or small intestinal juice. Viable cell counts were measured after 30, 60, 90 and 180 min. or after 240 min. for the simulated gastric juice or small intestinal juice tolerance determination respectively.

Determination of Pathogenic Inhibition of Spray-Dried *L. plantarum* TISTR 2075

Each spray-dried fermented cereal extract (1% w/v) was inoculated into MRS broth and cultured at 37°C for 24 hr. The inhibitory activity against *E. coli* O157:H7 DMST 12743 and *S. typhimurium* ATCC 13311 was determined using agar well diffusion method. The overnight culture

(200 µL) of each of the two bacteria was mixed with 20 mL of molten tryptic soya agar supplemented with 0.6% yeast extract (approximately 10^6 CFU/mL) and poured into a sterile petri-dish. Wells (7-mm diameter) were punched out of the solid agar with a sterile cork borer. The overnight culture of spray-dried *L. plantarum* (50 µL) was inoculated into the wells and the plates were incubated at 37°C for 24 hr. The diameter of inhibition zones was measured. Each experiment was done in triplicate.

Enumeration of Viable Cells

The spray-dried powder (1 g) was suspended in sterile 0.85% NaCl solution (9 mL) for 1 hr at room temperature. Appropriate serial dilutions were prepared before pour plating onto MRS agar (with added 0.5% CaCO₃) and incubated at 37°C for 24 hr. The percentage of cell survival is defined as follows: survival rate (%) = $(\log N / \log N_0) \times 100$, where N represents the number of viable cells (CFU/g) after exposure and N₀ denotes the initial viable cell count (CFU/g) prior to exposure [33].

Determination of Soluble Calcium

The fermented cereal extract was centrifuged at 10,000 g for 30 min. After centrifugation, the supernatant was collected and then filtered through a 0.2-µm membrane filter (Minisarts®, Satorius, Germany) before measurement of soluble calcium content by an atomic absorption spectrophotometer (Avanta M1, GBC Scientific Equipment, USA).

Scanning Electron Microscopy

The spray-dried powder was coated with sublimated 1% osmium tetroxide for 3 hr and kept in a desiccator for a week. The rehydrated spray-dried sample was filtered through 0.2-µm sterile membrane filter (Minisarts, Sartorius, Germany). The sample adhered to the filter was first fixed with a 2.5% glutaraldehyde in sodium phosphate buffer (pH 7.2) for 12 hr. After washing three times with the phosphate buffer, the sample was fixed with 1% osmium tetroxide for 1 hr followed by washing with distilled water three times. The sample was then dehydrated by soaking with a graded series of ethanol (30, 50, 70, 90 and 100 %, the last being used three times) and drying with liquid carbon dioxide. It was then attached to a brass stub with double-sided adhesive tape, coated with a layer of gold and analysed using a scanning electron microscope (JMS 5600 LV, Jeol, Japan).

Statistical Analysis

Each result was expressed as mean ± S.D. The data were assessed using analysis of variance (ANOVA) with a level of significance at $P < 0.05$. Significant divergences among mean values were determined with Duncan's multiple range tests. All statistical analyses were performed using SPSS Software (IBM, USA), version 12.

RESULTS AND DISCUSSION

Fermentation of Cereal Extracts

As shown in Tables 1 and 2, *L. plantarum* TISTR 2075 grows well in the extracts of soya milk and Job's-tears after 24 hr of fermentation, giving viable cell numbers of 8.28 and 7.73 log CFU/mL respectively. Addition of 1% and 2% sesame improves the viable cell count by 0.02-0.12 log CFU/mL in fermented soya milk extract and 0.66 log CFU/mL in fermented Job's-tears extract.

However, there is no significant difference ($P > 0.05$) in viable cell number between 1% and 2% sesame. To obtain a higher cell number, different conc. of glucose (1-20%) were applied, whereby a slight increase in viable cell number was observed in all fermented cereal extracts. With 1% glucose addition, viable cell numbers of 8.76 log CFU/mL in fermented soya milk extract and 8.67 log CFU/mL in fermented Job's-tears extract were achieved, which were significantly higher in comparison with controls. When higher glucose concentrations were applied, there was no significant difference ($P > 0.05$) in the viable cell count. Similarly, Timbuntam et al. [34] reported that there was no significant difference in viable cell number of *Lactobacillus* spp. FCP2 grown in 3 and 13% sugarcane juice. According to Shirai et al. [35], glucose concentration of higher than 10% resulted in an extended lag phase during shrimp waste fermentation by *Lactobacillus* spp. B2. This is probably because a higher initial substrate concentration gives rise to an increase in the lag phase and a decrease in the specific growth rate due to the decrease in water activity in the system, promoted by a large amount of the water-binding substance [35, 36].

Table 1. Effects of glucose content on viability of *L. plantarum* TISTR 2075 after 24 hr fermentation in soya milk extracts

Glucose concentration (% w/v)	Viable cell count (log CFU/mL)		
	Fermented soya milk	Fermented soya milk + 1% sesame	Fermented soya milk + 2% sesame
0%	8.28 ± 0.09 ^e	8.30 ± 0.16 ^e	8.40 ± 0.11 ^e
1%	8.69 ± 0.10 ^{bcd}	8.76 ± 0.04 ^{abcd}	8.79 ± 0.04 ^{abcd}
5%	8.87 ± 0.03 ^{ab}	8.69 ± 0.14 ^{bcd}	8.64 ± 0.01 ^{cd}
10%	8.95 ± 0.04 ^a	8.79 ± 0.04 ^{abcd}	8.84 ± 0.04 ^{abc}
15%	8.79 ± 0.03 ^{abcd}	8.60 ± 0.01 ^d	8.62 ± 0.02 ^d
20%	8.84 ± 0.02 ^{abc}	8.61 ± 0.04 ^d	8.79 ± 0.21 ^{abcd}

Note: Values with different letters (a-e) are significantly different ($P < 0.05$) by Duncan's multiple range test.

Table 2. Effect of glucose content on viability of *L. plantarum* TISTR 2075 after 24 hr fermentation in Job's-tears extracts

Glucose concentration (% w/v)	Viable cell count (log CFU/mL)		
	Fermented Job's-tears extract	Fermented Job's-tears extract + 1% sesame	Fermented Job's tears extract + 2% sesame
0%	7.73 ± 0.14 ^g	8.39 ± 0.13 ^{def}	8.39 ± 0.06 ^{def}
1%	8.33 ± 0.06 ^{ef}	8.67 ± 0.12 ^{ab}	8.37 ± 0.01 ^{def}
5%	8.23 ± 0.04 ^f	8.64 ± 0.03 ^{abc}	8.48 ± 0.05 ^{cde}
10%	8.35 ± 0.05 ^{def}	8.76 ± 0.04 ^a	8.52 ± 0.08 ^{bcde}
15%	8.37 ± 0.01 ^{def}	8.63 ± 0.13 ^{abc}	8.54 ± 0.07 ^{bcd}
20%	8.36 ± 0.06 ^{def}	8.62 ± 0.13 ^{abc}	8.46 ± 0.04 ^{cde}

Note: Values with different letters (a-g) are significantly different ($P < 0.05$) by Duncan's multiple range test.

As shown in Figure 1, with the addition of 1% glucose, a decrease in pH was observed in all cereal fermentations (pH < 3.34, < 3.28 and ~ 4.4 for soya milk extract, Job's-tears extract and control respectively). However, higher glucose concentrations do not seem to have any significant effect on pH. Increasing soluble calcium (73.02-112.0 mg/L in fermented soya milk extract and 2.27-5.26 mg/L in Job's-tears extract) can be clearly observed with increased addition of glucose (1-20%). Moreover, addition of sesame (1% and 2%) significantly improves soluble calcium content in the fermented cereals (67.1-145.3 mg/L in soya milk extract and 2.65-9.42 mg/L for Job's-tears extract). Tang et al. [11] reported a significant increase in soluble calcium in the fermentation of soya milk with *L. acidophilus* ATCC 4962 and *L. casei* ASCC 290 (89.3% and 87% respectively). Lopez et al. [37] established the degradation of phytic acid and the production of lactic acid leading to greater calcium solubility in the fermentation of *Leuconostoc mesenteroides* strain 38 in whole wheat flour medium. The increase in calcium solubility is related to a lowered pH due to, among other mechanisms, the production of organic acids such as lactic and acetic acids [11, 16, 37].

Soya milk and Job's-tears extracts supplemented with 1% sesame + 1% glucose were found to be suitable substrates for the growth of *L. plantarum* TISTR 2075 and were used as culture media for further study.

Effects of Spray-Drying

After spray-drying, the viable cell counts of *L. plantarum* TISTR 2075 in spray-dried soya milk and Job's-tears extract powders were 7.18 and 7.30 log CFU/g with survival rate of 79.0 and 85.4 % respectively (Figure 2). Although the stress caused by heat and dehydration results in permanent loss of viability [38], a high survival rate is observed in this experiment. This is probably because of the protein and carbohydrate in cereal, which play an important role in protecting the cells [39]. Protein can stabilise cell membrane constituents, resulting in improvement of viability [40]. MD as carrier has the ability to retain water, stabilise enzymes and prevent cellular injuries during drying [20, 41, 42]. Moreover, incorporation of MD could be beneficial due to its relatively high glass transition values (160°C) [41] and its amorphous form preventing protein unfolding during drying [43], and could thus result in less damage to the cells during drying at high temperature and desiccated condition [44]. As shown in Figure 3, the cells were found to localise within the microparticles after rehydration in 0.85% NaCl. According to Reddy et al. [27], *L. plantarum* CFR 2191, *L. salivarius* CFR 2158 and *Pediococcus acidilactici* CFR 2193 with 10% MD displayed more than 97% survival after spray-drying at 140°C (inlet air) and 40°C (outlet air). Fu and Chen [45] and Otero et al. [46] suggested that the survival rate is species-specific and depends on the drying method and protective agents. The survival rate of the strain in spray-dried Job's-tears extract is higher than that in spray-dried soya milk extract in the present study. The former extract containing *L. plantarum* TISTR 2075 was thus selected for further study.

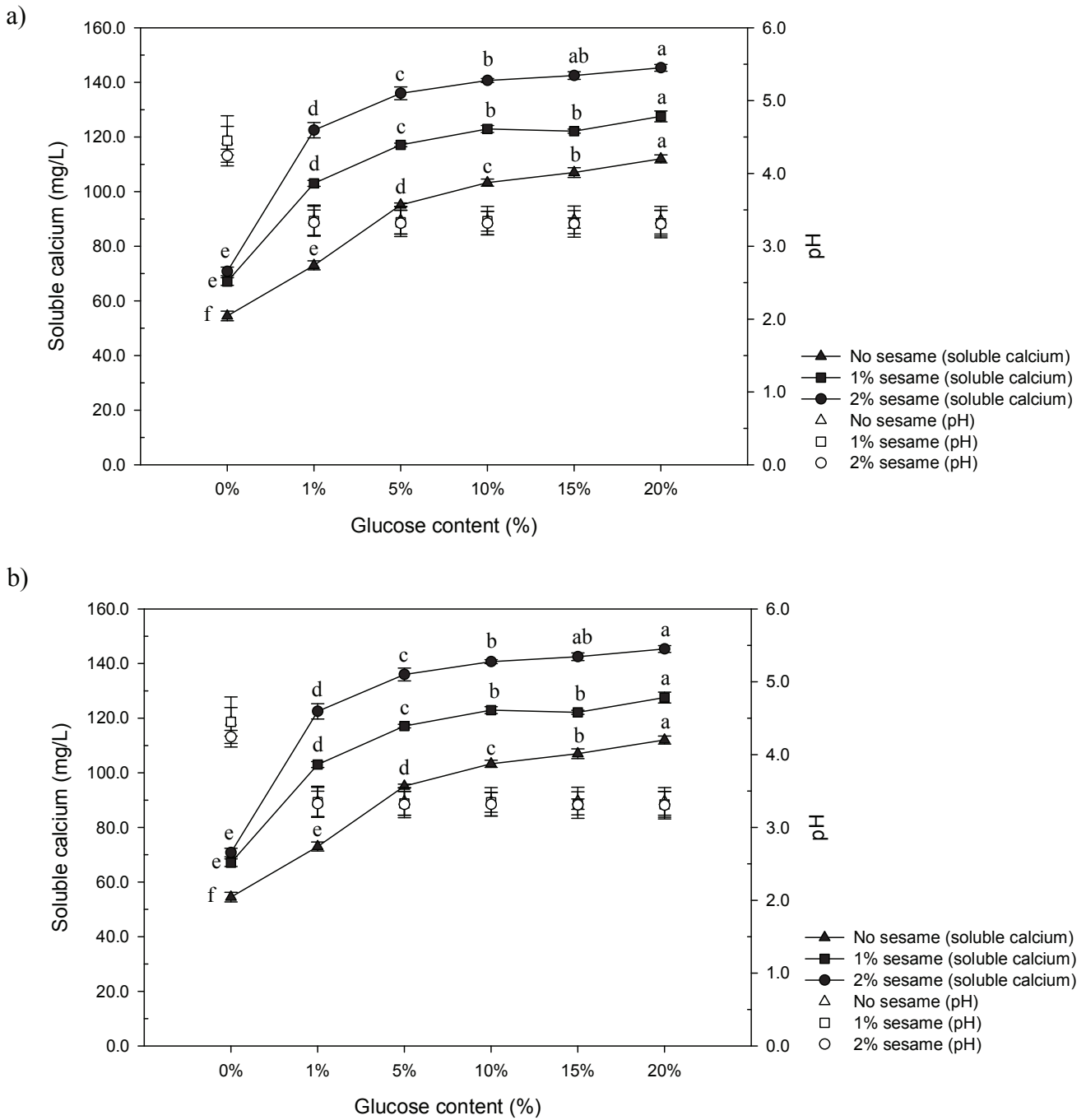


Figure 1. Effects of glucose content on pH and soluble calcium after 24-hr fermentation of: a) soya milk extract and b) Job's-tears extract. Values with different letters (a-f) in the same sesame content are significantly different ($P < 0.05$) by Duncan's multiple range test.

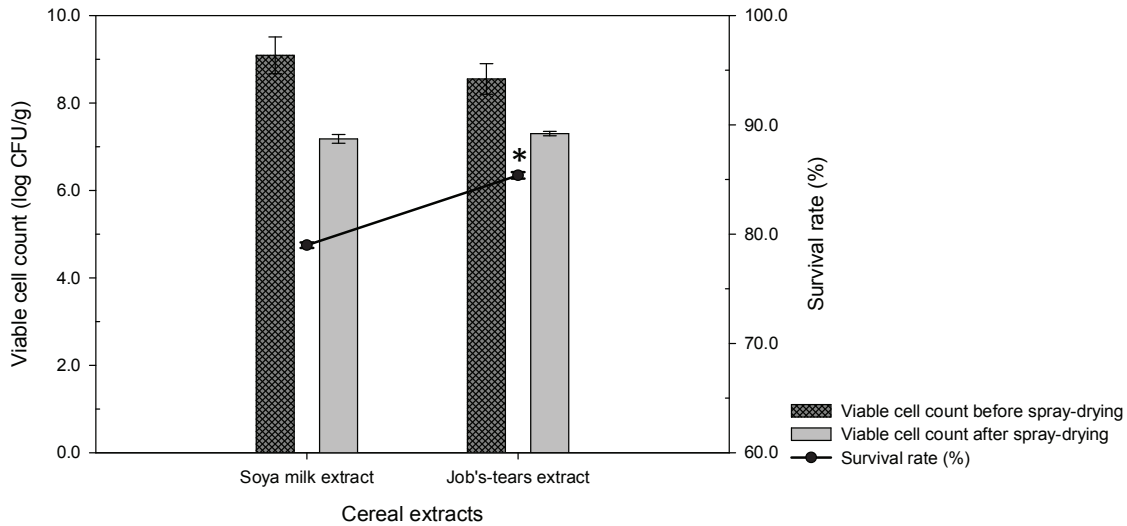
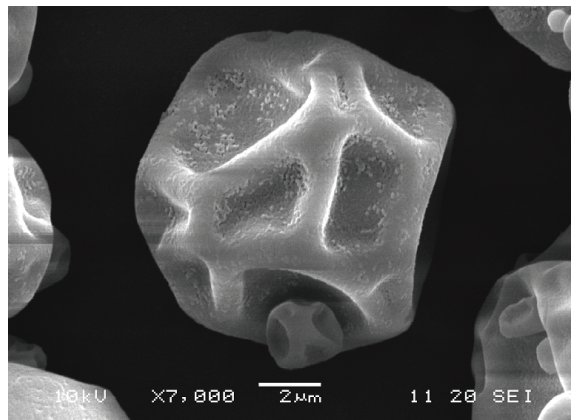


Figure 2. Viable cell counts of *L. plantarum* TISTR 2075 grown in soya milk and Job's-tears extracts before and after spray-drying. Survival rates of strain after spray-drying of cereal extracts were compared.

* $P < 0.05$ (Student's *t*-test, two tailed)

a)



b)

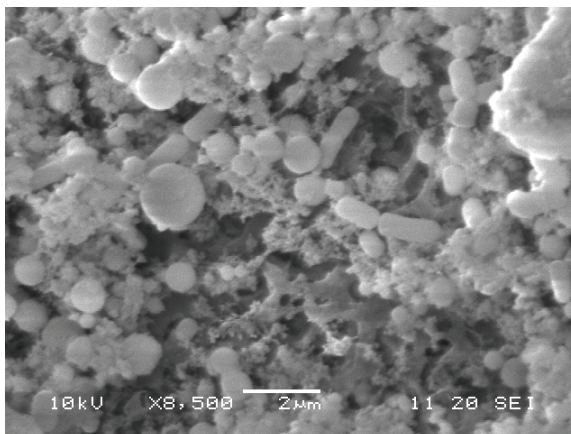


Figure 3. Scanning electron micrographs of spray-dried *L. plantarum* TISTR 2075: a) with MD and b) after rehydration in 0.85% NaCl

Probiotic Properties

Results of simulated gastric juice tolerance of *L. plantarum* TISTR 2075 in spray-dried fermented cereal extracts are shown in Table 3. The survival rate of spray-dried strain (44.3%) is not significantly different ($P > 0.05$) from that of the free cells (46.8%) at 180 min. This is in agreement with the work of Reddy et al. [27], in which the acid tolerance of *L. plantarum* CFR 2191 was found to remain at a significant level even after spray-drying. However, the survival rates of the spray-dried *L. plantarum* TISTR 2075 are significantly lower than those of the free cells after exposure for 30, 60 and 90 min. These results are in accordance with those of Miciel et al. [47], in which heat-injured cells are more prone to inactivation in stress environments such as gastrointestinal conditions and high salt.

After exposure to the simulated small intestinal juice with 0.45% bile salt for 240 min., the TISTR 2075 strain exhibited a survival rate of 82.4%, which was not different from the control (77.5%), thus indicating that its acid and bile tolerance is not affected by the spray-drying process. According to Reddy et al. [27], there is no significant difference in bile tolerance between spray-dried *L. plantarum* CFR 2191 and active cell. Serrazanetti et al. [48] suggested that the small intestinal juice tolerance of probiotic bacteria is strain dependent.

Table 3. Survival rates of spray-dried *L. plantarum* TISTR 2075 exposed to simulated gastric juice at pH 2.0

Condition	Survival rate (% \pm S.D.)			
	Exposure time			
	30 min.	60 min.	90 min.	180 min.
After spray-drying	78.72 \pm 0.93*	68.67 \pm 0.45*	60.90 \pm 1.92*	44.33 \pm 2.01
Control (free cell)	91.25 \pm 3.36	82.21 \pm 3.21	73.56 \pm 3.52	46.83 \pm 1.70

* $P < 0.05$ (Student's *t*-test, two-tailed)

Spray-dried *L. plantarum* TISTR 2075 was also found to exhibit pathogenic inhibition of *Escherichia coli* O157:H7 DMST 12743 and *Salmonella typhimurium* ATCC 13311, with inhibition zones of 12.6 \pm 0.3 and 14.4 \pm 0.4 mm respectively. These results were not significant different ($P > 0.05$) from the inhibition zones of the free cell, which were 12.2 \pm 0.2 mm. and 14.3 \pm 0.2 mm. respectively, again indicating that the pathogenic inhibition of *L. plantarum* TISTR 2075 is not affected by the spray-drying process. This agrees with the work of Gardiner et al. [25], in which spray-dried *L. salivarius* UCC 118 was found to retain its pathogenic inhibition of *Bacillus coagulans*. According to Silva et al. [24], spray-dried *L. sakei* CTC 494 and *L. salivarius* CTC 2197 were observed to retain the bacteriocinogenic activity against *Listeria innocua*, *L. monocytogenes* and *Staphylococcus aureus*.

CONCLUSIONS

Soya milk and Job's-tears extracts supplemented with sesame can be used as culture media for the growth of *Lactobacillus plantarum* TISTR 2075, giving a viable cell number above 8.6 log CFU/mL. A significant increase in calcium solubility was also observed after fermentation of the cereal extracts supplemented with 1% glucose and 1% sesame. After spray-drying, high numbers of viable cells (7.30 log CFU/g in Job's-tears extract powder and 7.18 log CFU/g in soya milk powder) could be achieved and their functional probiotic properties, viz. pathogenic inhibition of foodborne

pathogens and tolerance to simulated gastrointestinal tract conditions were not affected. These findings make possible the development of new functional cereal beverages containing probiotics.

ACKNOWLEDGEMENT

We are grateful to the Office of the Higher Education Commission, Ministry of Education for financial support.

REFERENCES

1. F. C. Prado, J. L. Parada, A. Pandey and C. R. Soccol, "Trends in non-dairy probiotic beverages", *Food Res. Int.*, **2008**, *41*, 111-123.
2. D. Bayrock and W. M. Ingledew, "Mechanism of viability loss during fluidized bed drying of baker's yeast", *Food Res. Int.*, **1997**, *30*, 417-425.
3. S. Vasudha and H. N. Mishra, "Non dairy probiotic beverages", *Int. Food Res. J.*, **2013**, *20*, 7-15.
4. M. Thirabunyanon, "Biotherapy for and protection against gastrointestinal pathogenic infections via action of probiotic bacteria", *Maejo Int. Sci. Technol.*, **2011**, *5*, 108-128.
5. R. Rozada-Sánchez, A. P. Sattur, K. Thomas and S. S. Pandiella, "Evaluation of *Bifidobacterium* spp. for the production of a potentially probiotic malt-based beverage", *Process Biochem.*, **2008**, *43*, 848-854.
6. A. L. F. Pereira, T. C. Maciel and S. Rodrigues, "Probiotic beverage from cashew apple juice fermented with *Lactobacillus casei*", *Food Res. Int.*, **2011**, *44*, 1276-1283.
7. Y. Rivera-Espinoza and Y. Gallardo-Navarro, "Non-dairy probiotic products", *Food Microbiol.*, **2010**, *27*, 1-11.
8. P. Scalabrini, M. Rossi, P. Spettoli and D. Matteuzzi, "Characterization of *Bifidobacterium* strains for use in soymilk fermentation", *Int. J. Food Microbiol.*, **1998**, *39*, 213-219.
9. I. C. Cheng, H. F. Shang, T. F. Lin, T. H. Wang, H. S. Lin and S. H. Lin, "Effect of fermented soy milk on the intestinal bacterial ecosystem", *World J. Gastroenterol.*, **2005**, *11*, 1225-1227.
10. Y. H. Pyo, T. C. Lee and Y. C. Lee, "Enrichment of bioactive isoflavones in soymilk fermented with β -glucosidase-producing lactic acid bacteria", *Food Res. Int.*, **2005**, *38*, 551-559.
11. A. L. Tang, N. P. Shan, G. Wilcox, K. Z. Walker and L. Stojanovska, "Fermentation of calcium-fortified soymilk with *Lactobacillus*: Effects on calcium solubility, isoflavone conversion, and production of organic acids", *J. Food Sci.*, **2007**, *72*, M431-M436.
12. P. Bamrungna, "Production of fermented soymilk powder containing lactic acid bacteria by spray drying", *M.Sc. Thesis*, **2009**, Kasetsart University, Thailand.
13. S. K. Yeo and M. T. Liong, "Effect of prebiotics on viability and growth characteristics of probiotics in soymilk", *J. Sci. Food Agric.*, **2010**, *90*, 267-275.
14. C. C. Chou and J. W. Hou, "Growth of *Bifidobacteria* in soymilk and their survival in the fermented soymilk drink during storage", *Int. J. Food Microbiol.*, **2000**, *56*, 113-121.
15. O. Mårtenson, R. Öste and O. Holst, "The effect of yoghurt culture on the survival of probiotic bacteria in oat-based, non-dairy products", *Food Res. Int.*, **2002**, *35*, 775-784.
16. S. W. Bergqvist, A. S. Sandberg, N. G. Carlsson and T. Andlid, "Improved iron solubility in carrot juice fermented by homo- and hetero-fermentative lactic acid bacteria", *Food Microbiol.*, **2005**, *22*, 53-61.
17. B. R. Bhandari, K. C. Patel and X. D. Chen, "Spray drying of food materials - process and product characteristics", in "Drying Technologies in Food Processing" (Ed. X. D. Chen and A. S. Mujumdar), Blackwell Publishing, West Sussex, **2008**, Ch.4.

18. E. O. Sunny-Roberts and D. Knorr, "Cellular injuries on spray-dried *Lactobacillus rhamnosus* GG and its stability during food storage", *Nutr. Food Sci.*, **2011**, *41*, 191-200.
19. A. E. C. Antunes, A. M. Liserre, A. L. A. Coelho, C. R. Menezes, I. Moreno, K. Yotsuyanagi and N. C. Azambuja, "Acerola nectar with added microencapsulated probiotic", *LWT-Food Sci. Technol.*, **2013**, *54*, 125-131.
20. B. E. Chávez and A. M. Ledebøer, "Drying of probiotics: Optimization of formulation and process to enhance storage survival", *Dry. Technol. Int. J.*, **2007**, *25*, 1193-1201.
21. T. Mattila-Sandholm, P. Myllärinen, R. Crittenden, G. Mogensen, R. Fondén and M. Saarela, "Technological challenges for future probiotic foods", *Int. Dairy J.*, **2002**, *12*, 173-182.
22. FAO/WHO, "Health and nutritional properties of probiotics in food including powder milk with live lactic acid bacteria", Report on Joint FAO/WHO Expert Consultation on Evaluation of Health and Nutritional Properties of Probiotics in Food Including Powder Milk with Live Lactic Acid Bacteria", Cordoba, Argentina, **2001**.
23. N. Ishibashi and S. Shimamura, "Bifidobacteria: Research and development in Japan", *Food Technol.*, **1993**, *47*, 126-135.
24. J. Silva, A. S. Carvalho, P. Teixeira and P. A. Gibbs, "Bacteriocin production by spray-dried lactic acid bacteria", *Lett. Appl. Microbiol.*, **2002**, *34*, 77-81.
25. G. E. Gardiner, E. O'Sullivan, J. Kelly, M. A. Auty, G. F. Fitzgerald, J. K. Collins, R. P. Ross and C. Stanton, "Comparative survival rates of human-derived probiotic *Lactobacillus paracasei* and *L. salivarius* strains during heat treatment and spray drying", *Appl. Environ. Microbiol.*, **2000**, *66*, 2605-2612.
26. M. A. Golowczyc, J. Silva, P. Teixeira, G. L. de Antoni and A. G. Abraham, "Cellular injuries of spray-dried *Lactobacillus* spp. isolated from kefir and their impact on probiotic properties", *Int. J. Food Microbiol.*, **2011**, *144*, 556-560.
27. K. B. P. K. Reddy, A. N. Madhu and S. G. Prapulla, "Comparative survival and evaluation of functional probiotic properties of spray-dried lactic acid bacteria", *Int. J. Dairy Technol.*, **2009**, *62*, 240-248.
28. W. Lapsiri and P. Wanchaitanawong, "Protective effects of soybean, sesame and Job's tears on the survival of fermented vegetable *Lactobacillus plantarum* under gastrointestinal tract conditions", *Afr. J. Microbiol. Res.*, **2012**, *6*, 3380-3389.
29. W. Lapsiri, B. Bhandari and P. Wanchaitanawong, "Viability of *Lactobacillus plantarum* TISTR 2075 in different protectants during spray drying and storage", *Dry. Technol. Int. J.*, **2012**, *30*, 1407-1412.
30. Y. C. Wang, R. C. Yu and C. C. Chou, "Growth and survival of bifidobacteria and lactic acid bacteria during the fermentation and storage of cultured soymilk drinks", *Food Microbiol.*, **2002**, *19*, 501-508.
31. H. Michida, S. Tamalampudi, S. S. Pandiella, C. Webb, H. Fukuda and A. Kondo, "Effect of cereal extracts and cereal fiber on viability of *Lactobacillus plantarum* under gastrointestinal tract conditions", *Biochem. Eng. J.*, **2006**, *28*, 73-78.
32. Y. Huang and M. C. Adams, "In vitro assessment of the upper gastrointestinal tolerance of potential probiotic dairy propionibacteria", *Int. J. Food Microbiol.*, **2004**, *91*, 253-260.
33. Y. Bao, Y. Zhang, Y. Zhang, Y. Liu, S. Wang, X. Dong, Y. Wang and H. Zhang, "Screening of potential probiotic properties of *Lactobacillus fermentum* isolated from traditional dairy products", *Food Control*, **2010**, *21*, 695-701.
34. W. Timbuntam, K. Sriroth and Y. Tokiwa, "Lactic acid production from sugar-cane juice by a newly isolated *Lactobacillus* sp.", *Biotechnol. Lett.*, **2006**, *28*, 811-814.

35. A. Senthuran, V. Senthuran, R. Hatti-Kaul and B. Mattiasson, "Lactic acid production by immobilized *Lactobacillus casei* in recycle batch reactor: A step towards optimization", *J. Biotechnol.*, **1999**, 73, 61-70.
36. K. Shirai, I. Guerrero, S. Huerta, G. Saucedo, A. Castillo, R. O. Gonzalez and G. M. Hall, "Effect of initial glucose concentration and inoculation level of lactic acid bacteria in shrimp waste ensilation", *Enzyme Microbial Technol.*, **2001**, 28, 446-452.
37. H. W. Lopez, A. Ouvry, E. Bervas, C. Guy, A. Messenger, C. Demigne and C. Remesy, "Strains of lactic acid bacteria isolated from sour doughs degrade phytic acid and improve calcium and magnesium solubility from whole wheat flour", *J. Agric. Food Chem.*, **2000**, 48, 2281-2285.
38. D. Y. Ying, S. Schwander, R. Weerakkody, L. Sanguansri, C. Gantenbein-Demarchi and M. A. Augustin, "Microencapsulated *Lactobacillus rhamnosus* GG in whey protein and resistant starch matrices: Probiotic survival in fruit juice", *J. Funct. Foods*, **2013**, 5, 98-105.
39. Y. Mille, J.-P. Obert, L. Beney and P. Gervais, "New drying process for lactic bacteria based on their dehydration behavior in liquid medium", *Biotechnol. Bioeng.*, **2004**, 88, 71-76.
40. G. Zhao and G. Zhang, "Effect of protective agents, freezing temperature, rehydration media on viability of malolactic bacteria subjected to freeze-drying", *J. Appl. Microbiol.*, **2005**, 99, 333-338.
41. B. R. Bhandari and T. Howes, "Implication of glass transition for the drying and stability of dried foods", *J. Food Eng.*, **1999**, 40, 71-79.
42. A. K. Yadav, A. B. Chaudhari and R. M. Kothari, "Enhanced viability of *Bacillus coagulans* after spray drying with calcium lactate, storage and re-hydration", *Indian J. Chem. Technol.*, **2009**, 16, 519-522.
43. R. A. DePaz, D. A. Dale, C. C. Barnett, J. F. Carpenter, A. L. Gaertner and T. W. Randolph, "Effects of drying methods and additives on the structure, function, and storage stability of subtilisin: Role of protein conformation and molecular mobility", *Enzy. Microb. Technol.*, **2002**, 31, 765-774.
44. A. Nag and S. Das, "Improving ambient temperature stability of probiotics with stress adaptation and fluidized bed drying", *J. Funct. Foods*, **2013**, 5, 170-177.
45. N. Fu and X. D. Chen, "Towards a maximal cell survival in convective thermal drying processes", *Food Res. Int.*, **2011**, 44, 1127-1149.
46. M. C. Otero, M. C. Espeche and M. E. Nader-Macias, "Optimization of the freeze-drying media and survival throughout storage of freeze-dried *Lactobacillus gasseri* and *Lactobacillus delbrueckii* subsp. *delbrueckii* for veterinarian probiotic applications", *Process Biochem.*, **2007**, 42, 1406-1411.
47. G. M. Maciel, K. S. Chaves, C. R. Grosso and M. L. Gigante, "Microencapsulation of *Lactobacillus acidophilus* La-5 by spray-drying using sweet whey and skim milk as encapsulating materials", *J. Dairy Sci.*, **2014**, 97, 1991-1998.
48. D. I. Serrazanetti, M. E. Guerzoni, A. Corsetti and R. Vogel, "Metabolic impact and potential exploitation of the stress reactions in lactobacilli", *Food Microbiol.*, **2009**, 26, 700-711.

Full Paper

Integral inequalities of Hermite-Hadamard type for the product of strongly logarithmically convex and other convex functions

Ying Wu¹, Feng Qi^{2,*} and Da-Wei Niu^{3,4}

¹College of Mathematics, Inner Mongolia University for Nationalities, Tongliao City, Inner Mongolia Autonomous Region, 028043, China

²Department of Mathematics, School of Science, Tianjin Polytechnic University, Tianjin City, 300387, China

³Department of Mathematics, East China Normal University, Shanghai City, China

⁴College of Information and Business, Zhongyuan University of Technology, Zhengzhou City, Henan Province, 450007, China

* Corresponding author, e-mail: qifeng618@gmail.com; qifeng618@hotmail.com

Received: 25 July 2014 / Accepted: 4 December 2015 / Published: 8 December 2015

Abstract: Some new integral inequalities of Hermite-Hadamard type for the product of strongly logarithmically convex functions and other convex functions such as the P -convex, quasi-convex, m -convex, (α, m) -convex and s -convex functions have been established.

Keywords: integral inequality, Hermite-Hadamard type inequality, strongly logarithmically convex function, Hölder inequality, P -convex function, quasi-convex function, m -convex function, (α, m) -convex function, s -convex function

INTRODUCTION

Throughout this paper we use the following notation:

$$R = (-\infty, \infty), \quad R_0 = [0, \infty) \quad \text{and} \quad R_+ = (0, \infty).$$

The following definitions are well known in the literature.

Definition 1. A function $f : I \subseteq R \rightarrow R$ is said to be convex on I if

$$f(\lambda x + (1-\lambda)y) \leq \lambda f(x) + (1-\lambda)f(y)$$

holds for all $x, y \in I$ and $\lambda \in [0, 1]$.

Definition 2. A function $f : I \subseteq R \rightarrow R_+$ is said to be logarithmically convex if

$$f(\lambda x + (1-\lambda)y) \leq [f(x)]^\lambda [f(y)]^{1-\lambda}$$

holds for all $x, y \in I$ and $\lambda \in [0, 1]$.

Definition 3 [1]. A function $f : I \subseteq R \rightarrow R_0$ is said to be P -convex if

$$f(\lambda x + (1 - \lambda)y) \leq f(x) + f(y)$$

holds for all $x, y \in I$ and $\lambda \in [0, 1]$.

Definition 4 [1]. A function $f : I \subseteq R \rightarrow R_0$ is said to be quasi-convex if

$$f(\lambda x + (1 - \lambda)y) \leq \max \{f(x), f(y)\}$$

holds for all $x, y \in I$ and $\lambda \in [0, 1]$.

Definition 5 [2]. For $f : [0, b] \rightarrow R$ and $m \in (0, 1]$, if

$$f(tx + m(1 - t)y) \leq tf(x) + m(1 - t)f(y)$$

is valid for all $x, y \in [0, b]$ and $t \in [0, 1]$, then we say that $f(x)$ is an m -convex function on $[0, b]$.

Definition 6 [3]. For $f : [0, b] \rightarrow R$ and $(\alpha, m) \in (0, 1]^2$, if

$$f(tx + m(1 - t)y) \leq t^\alpha f(x) + m(1 - t^\alpha)f(y)$$

is valid for all $x, y \in [0, b]$ and $t \in [0, 1]$, then we say that $f(x)$ is an (α, m) -convex function on $[0, b]$.

Definition 7 [4]. Let $s \in (0, 1]$. A function $f : [a, b] \subseteq R_0 \rightarrow R_0$ is said to be s -convex (in the second sense) if

$$f(\lambda x + (1 - \lambda)y) \leq \lambda^s f(x) + (1 - \lambda)^s f(y)$$

holds for all $x, y \in I$ and $\lambda \in [0, 1]$.

Definition 8 [5]. A function $f : [a, b] \rightarrow R$ is said to be strongly convex with modulus $c \geq 0$ if

$$f(tx + (1 - t)y) \leq tf(x) + (1 - t)f(y) - ct(1 - t)(x - y)^2$$

is valid for all $x, y \in [a, b]$ and $t \in [0, 1]$.

Definition 9 [6]. A function $f : I \subseteq R \rightarrow R_+$ is said to be strongly logarithmically convex with modulus $c \geq 0$ if

$$f(tx + (1 - t)y) \leq [f(x)]^t [f(y)]^{1-t} - ct(1 - t)(x - y)^2$$

holds for all $x, y \in I$ and $t \in [0, 1]$.

Remark 1. If a function $f : I \subseteq R \rightarrow R_+$ is strongly logarithmically convex, then it is also a strongly convex function, and so it is integrable on I .

Remark 2. For all $x \in [0, 1]$ and $0 \leq c \leq e^{-1}$, it is easy to obtain that $1 - cx \geq e^{-x}$. For all $x, y \in [0, 1]$ and $0 \leq c \leq e^{-1}$, we acquire

$$e^{[tx+(1-t)y]^2 - [t^2x^2+(1-t)^2y^2]} \leq 1 - ct(1-t)(x-y)^2 \leq 1 - \frac{ct(1-t)(x-y)^2}{e^{tx^2+(1-t)y^2}}$$

for all $t \in [0, 1]$. As a result, when $0 \leq c \leq e^{-1}$, the function $f(x) = e^{x^2}$ is a strongly logarithmically convex functions on $[0, 1]$.

In recent decades, a number of inequalities of Hermite-Hadamard type for different kinds of convex functions have been established. Some of them may be reformulated as follows.

Theorem 1 [1]. Let $f : I^{\circ} \subseteq R \rightarrow R_0$ be a P -convex mapping on I , $a, b \in I$ with $a < b$, and $f \in L([a, b])$. Then

$$\frac{1}{b-a} \int_a^b f(x) dx \leq f(a) + f(b).$$

Theorem 2 [7]. Let $f, g : [a, b] \rightarrow R_0$ be a convex functions on $[a, b] \subseteq R$ with $a < b$. Then

$$\frac{1}{b-a} \int_a^b f(x)g(x) dx \leq \frac{1}{3}M(a, b) + \frac{1}{6}N(a, b),$$

where

$$M(a, b) = f(a)g(a) + f(b)g(b) \tag{1}$$

and

$$N(a, b) = f(a)g(b) + f(b)g(a). \tag{2}$$

Theorem 3 [8]. Let $f, g : [a, b] \rightarrow R_0$ and $fg \in L([a, b])$ with $0 \leq a < b < \infty$. If f is convex and nonnegative on $[a, b]$ and g is s -convex on $[a, b]$ for some fixed $s \in (0, 1]$, then

$$\frac{1}{b-a} \int_a^b f(x)g(x) dx \leq \frac{1}{s+2}M(a, b) + \frac{1}{(s+1)(s+2)}N(a, b),$$

where $M(a, b)$ and $N(a, b)$ are defined by (1) and (2).

In recent years, some inequalities of Hermite-Hadamard type for other kinds of convex functions were established [9, 10, 11, 12, 13, 14, 15, 16, and closely related references therein]. It was reported that some kinds of Hermite-Hadamard type inequalities have applications in statistics and other mathematical sciences [17]. The goal of this paper is to establish some new integral inequalities of Hermite-Hadamard type for the product of strongly logarithmically convex functions and other convex functions such as P -convex, quasi-convex, m -convex, (α, m) -convex and s -convex functions.

INTEGRAL INEQUALITIES OF HERMITE-HADAMARD TYPE

Now we start out to establish some new integral inequalities of Hermite-Hadamard type for the product of strongly logarithmically convex functions and other convex functions.

Theorem 4. For $-\infty < a < b < \infty$, let $f, g : [a, b] \rightarrow R_+$. If f and g^q are strongly logarithmically convex functions on $[a, b]$ with modulus $c \geq 0$ for $q \geq 1$, then

$$\begin{aligned} \frac{1}{b-a} \int_a^b f(x)g(x) dx \leq & \left[f(b)G\left(\frac{f(a)}{f(b)}\right) - \frac{c(b-a)^2}{6} \right]^{1-1/q} \left\{ f(b)g^q(b)G\left(\frac{f(a)}{f(b)}\left[\frac{g(a)}{g(b)}\right]^q\right) \right. \\ & \left. - c(b-a)^2 \left[f(b)F\left(\frac{f(a)}{f(b)}\right) + g^q(b)F\left(\left[\frac{g(a)}{g(b)}\right]^q\right) \right] + \frac{c^2(b-a)^4}{30} \right\}^{1/q}, \end{aligned}$$

where

$$G(u) = \begin{cases} 1, & u = 1, \\ \frac{u-1}{\ln u}, & u \neq 1 \end{cases} \quad \text{and} \quad F(u) = \begin{cases} \frac{1}{6}, & u = 1, \\ \frac{(u+1)\ln u - 2(u-1)}{(\ln u)^3}, & u \neq 1. \end{cases} \tag{3}$$

Proof. Taking $x = ta + (1-t)b$ for $t \in [0,1]$, $v_f = \frac{f(a)}{f(b)}$ and $u = \frac{f(a)}{f(b)} \left[\frac{g(a)}{g(b)} \right]^q$, and using Hölder's inequality and the strongly logarithmic convexity of the functions f and g^q , the following is figured out:

$$\begin{aligned} & \frac{1}{b-a} \int_a^b f(x)g(x)dx = \int_0^1 f(ta + (1-t)b)g(ta + (1-t)b) dt \\ & \leq \left[\int_0^1 f(ta + (1-t)b) dt \right]^{1-1/q} \left[\int_0^1 f(ta + (1-t)b)g^q(ta + (1-t)b) dt \right]^{1/q} \\ & \leq \left\{ \int_0^1 [f'(a)f^{1-t}(b) - ct(1-t)(b-a)^2] dt \right\}^{1-1/q} \\ & \quad \times \left\{ \int_0^1 [f'(a)f^{1-t}(b) - ct(1-t)(b-a)^2] [g^{qt}(a)g^{q(1-t)}(b) - ct(1-t)(b-a)^2] dt \right\}^{1/q} \\ & = \left[f(b) \int_0^1 v_f^t dt - c(b-a)^2 \int_0^1 t(1-t) dt \right]^{1-1/q} \left\{ f(b)g^q(b) \int_0^1 u^t dt \right. \\ & \quad \left. - c(b-a)^2 \int_0^1 [f'(a)f^{1-t}(b) + g^{qt}(a)g^{q(1-t)}(b)] t(1-t) dt + c^2(b-a)^4 \int_0^1 t^2(1-t)^2 dt \right\}^{1/q} \\ & = \left[f(b)G(v_f) - \frac{c(b-a)^2}{6} \right]^{1-1/q} \left\{ f(b)g^q(b)G(u) - c(b-a)^2 [f(b)F(v_f) + g^q(b)F(v_g^q)] + \frac{c^2(b-a)^4}{30} \right\}^{1/q}. \end{aligned}$$

Theorem 4 is thus proved.

Corollary 1. Under the conditions of Theorem 4,

1) when $c = 0$, we have

$$\frac{1}{b-a} \int_a^b f(x)g(x)dx \leq f(b)g(b)G^{1-1/q} \left(\frac{f(a)}{f(b)} \right) G^{1/q} \left(\frac{f(a)}{f(b)} \left[\frac{g(a)}{g(b)} \right]^q \right);$$

2) when $c = 0$ and $q = 1$, we have

$$\frac{1}{b-a} \int_a^b f(x)g(x)dx \leq f(b)g(b)G \left(\frac{f(a)g(a)}{f(b)g(b)} \right).$$

Theorem 5. For $a, b \in R_0$ with $a < b$, let $f, g : [a, b] \rightarrow R_+$. If f is an s -convex function on $[a, b]$ for some $s \in (0,1]$ and g^q is a strongly logarithmically convex function on $[a, b]$ with modulus $c \geq 0$ for $q \geq 1$, then

$$\begin{aligned} & \frac{1}{b-a} \int_a^b f(x)g(x)dx \leq \left[\frac{f(a) + f(b)}{s+1} \right]^{1-1/q} \left\{ \left[\frac{g^q(a) - g^q(b)}{s+2} + \frac{g^q(b)}{s+1} \right] f(a) \right. \\ & \quad \left. + \left[\frac{g^q(a) - g^q(b)}{(s+1)(s+2)} + \frac{g^q(b)}{s+1} \right] f(b) - \frac{c(b-a)^2}{(s+2)(s+3)} [f(a) + f(b)] \right\}^{1/q}. \end{aligned}$$

Proof. Employing the conditions that f is s -convex and g^q is strongly logarithmically convex on $[a, b]$, let $x = ta + (1-t)b$ for $t \in [0,1]$ and $u = \left[\frac{g(a)}{g(b)} \right]^q$. Then making use of Hölder's inequality the following is generated:

$$\frac{1}{b-a} \int_a^b f(x)g(x)dx = \int_0^1 f(ta + (1-t)b)g(ta + (1-t)b) dt$$

$$\begin{aligned} &\leq \left[\int_0^1 f(ta + (1-t)b) dt \right]^{1-1/q} \left[\int_0^1 f(ta + (1-t)b) g^q(ta + (1-t)b) dt \right]^{1/q} \\ &\leq \left\{ \int_0^1 [t^s f(a) + (1-t)^s f(b)] dt \right\}^{1-1/q} \left\{ \int_0^1 [t^s f(a) + (1-t)^s f(b)] [g^{qt}(a) g^{q(1-t)}(b) \right. \\ &\quad \left. - ct(1-t)(b-a)^2] dt \right\}^{1/q} \\ &= \left[\frac{1}{s+1} [f(a) + f(b)] \right]^{1-1/q} \left\{ g^q(b) \int_0^1 [t^s u^t f(a) + (1-t)^s u^t f(b)] dt \right. \\ &\quad \left. - \frac{c(b-a)^2}{(s+2)(s+3)} [f(a) + f(b)] \right\}^{1/q}. \end{aligned}$$

Since $u^t \leq (u-1)t + 1$ for all $0 \leq t \leq 1$, we obtain

$$\int_0^1 t^s u^t dt \leq \int_0^1 t^s [(u-1)t + 1] dt = \frac{u-1}{s+2} + \frac{1}{s+1}$$

and

$$\int_0^1 (1-t)^s u^t dt \leq \int_0^1 (1-t)^s [(u-1)t + 1] dt = \frac{u-1}{(s+1)(s+2)} + \frac{1}{s+1}.$$

Accordingly,

$$\begin{aligned} \frac{1}{b-a} \int_a^b f(x) g(x) dx &\leq \left[\frac{f(a) + f(b)}{s+1} \right]^{1-1/q} \left\{ g^q(b) \int_0^1 [t^s u^t f(a) + (1-t)^s u^t f(b)] dt \right. \\ &\quad \left. - \frac{c(b-a)^2}{(s+2)(s+3)} [f(a) + f(b)] \right\}^{1/q} \\ &\leq \left[\frac{f(a) + f(b)}{s+1} \right]^{1-1/q} \left\{ g^q(b) \left[\left(\frac{u-1}{s+2} + \frac{1}{s+1} \right) f(a) \right. \right. \\ &\quad \left. \left. + \left(\frac{u-1}{(s+1)(s+2)} + \frac{1}{s+1} \right) f(b) \right] - \frac{c(b-a)^2}{(s+2)(s+3)} [f(a) + f(b)] \right\}^{1/q} \\ &= \left[\frac{f(a) + f(b)}{s+1} \right]^{1-1/q} \left\{ \left[\frac{g^q(a) - g^q(b)}{s+2} + \frac{g^q(b)}{s+1} \right] f(a) \right. \\ &\quad \left. + \left[\frac{g^q(a) - g^q(b)}{(s+1)(s+2)} + \frac{g^q(b)}{s+1} \right] f(b) - \frac{c(b-a)^2}{(s+2)(s+3)} [f(a) + f(b)] \right\}^{1/q}. \end{aligned}$$

The proof of Theorem 5 is thus complete.

Corollary 2. Under the conditions of Theorem 5,

1) if $c = 0$, then

$$\begin{aligned} \frac{1}{b-a} \int_a^b f(x) g(x) dx &\leq \frac{[f(a) + f(b)]^{1-1/q}}{(s+1)(s+2)^{1/q}} \\ &\quad \times [(s+1)f(a)g^q(a) + f(a)g^q(b) + f(b)g^q(a) + (s+1)f(b)g^q(b)]^{1/q}; \end{aligned}$$

2) if $c = 0$ and $q = 1$, we have

$$\frac{1}{b-a} \int_a^b f(x) g(x) dx \leq \frac{(s+1)f(a)g(a) + f(a)g(b) + f(b)g(a) + (s+1)f(b)g(b)}{(s+1)(s+2)};$$

3) if $c = 0, q = 1$ and $s = 1$, then

$$\frac{1}{b-a} \int_a^b f(x)g(x)dx \leq \frac{2f(a)g(a)+f(a)g(b)+f(b)g(a)+2f(b)g(b)}{6}.$$

Theorem 6. For $a, b \in R_0$ with $a < b$, let $f, g : R_0 \rightarrow R_+$. If f is an (α, m) -convex function on $[0, b/m]$ for $(\alpha, m) \in (0, 1]^2$ and g^q is a strongly logarithmically convex function on $[a, b]$ with modulus $c \geq 0$ for $q \geq 1$, then

$$\begin{aligned} \frac{1}{b-a} \int_a^b f(x)g(x)dx \leq & \left\{ \frac{1}{\alpha+1} \left[f(a) + m\alpha f\left(\frac{b}{m}\right) \right] \right\}^{1-1/q} \left\{ \left[\frac{g^q(a) - g^q(b)}{\alpha+2} + \frac{g^q(b)}{\alpha+1} \right] f(a) \right. \\ & + m \left[\frac{\alpha}{2(\alpha+1)(\alpha+2)} \left(3 + \alpha + (1+\alpha) \left[\frac{g(a)}{g(b)} \right]^q \right) \right] f\left(\frac{b}{m}\right) g^q(b) \\ & \left. - \frac{c(b-a)^2}{(\alpha+2)(\alpha+3)} \left[f(a) + \frac{m\alpha(\alpha+5)}{6} f\left(\frac{b}{m}\right) \right] \right\}^{1/q}. \end{aligned}$$

Proof. Let $x = ta + (1-t)b$ for $t \in [0, 1]$ and $u = \left[\frac{g(a)}{g(b)} \right]^q$. By making use of the (α, m) -convexity of f and the strongly logarithmic convexity of g^q , and applying Hölder's inequality, the following is brought out:

$$\begin{aligned} \frac{1}{b-a} \int_a^b f(x)g(x)dx &= \int_0^1 f(ta + (1-t)b)g(ta + (1-t)b) dt \\ &\leq \left[\int_0^1 f(ta + (1-t)b) dt \right]^{1-1/q} \left[\int_0^1 f(ta + (1-t)b)g^q(ta + (1-t)b) dt \right]^{1/q} \\ &\leq \left\{ \int_0^1 \left[t^\alpha f(a) + m(1-t^\alpha) f\left(\frac{b}{m}\right) \right] dt \right\}^{1-1/q} \\ &\quad \times \left\{ \int_0^1 \left[t^\alpha f(a) + m(1-t^\alpha) f\left(\frac{b}{m}\right) \right] \left[g^{qt}(a)g^{q(1-t)}(b) - ct(1-t)(b-a)^2 \right] dt \right\}^{1/q} \\ &= \left\{ \frac{1}{\alpha+1} \left[f(a) + m\alpha f\left(\frac{b}{m}\right) \right] \right\}^{1-1/q} \left\{ g^q(b) \int_0^1 \left[t^\alpha f(a) + m(1-t^\alpha) f\left(\frac{b}{m}\right) \right] u^t dt \right. \\ &\quad \left. - \frac{c(b-a)^2}{(\alpha+2)(\alpha+3)} \left[f(a) + \frac{m\alpha(\alpha+5)}{6} f\left(\frac{b}{m}\right) \right] \right\}^{1/q}. \end{aligned}$$

By virtue of the inequality $u^t \leq (u-1)t + 1$ for all $0 \leq t \leq 1$, we have

$$\begin{aligned} g^q(b) \int_0^1 \left[t^\alpha f(a) + m(1-t^\alpha) f\left(\frac{b}{m}\right) \right] u^t dt &\leq g^q(b) \int_0^1 \left[t^\alpha f(a) + m(1-t^\alpha) f\left(\frac{b}{m}\right) \right] [(u-1)t + 1] dt \\ &= g^q(b) \left\{ \left(\frac{u-1}{\alpha+2} + \frac{1}{\alpha+1} \right) f(a) + m \left[\frac{\alpha(3+u+\alpha+\alpha u)}{2(\alpha+1)(\alpha+2)} \right] f\left(\frac{b}{m}\right) \right\} \\ &= \left[\frac{g^q(a) - g^q(b)}{\alpha+2} + \frac{g^q(b)}{\alpha+1} \right] f(a) + m \left[\frac{\alpha(3+u+\alpha+\alpha u)}{2(\alpha+1)(\alpha+2)} \right] f\left(\frac{b}{m}\right) g^q(b). \end{aligned}$$

Theorem 6 is thus proved.

Corollary 3. Under the conditions of Theorem 6,

- 1) when $c = 0$, we have

$$\frac{1}{b-a} \int_a^b f(x)g(x)dx \leq \frac{1}{2^{1/q}(\alpha+1)(\alpha+2)^{1/q}} \left[f(a) + \alpha mf\left(\frac{b}{m}\right) \right]^{1-1/q} \times \left\{ 2[(\alpha+1)g^q(a) + g^q(b)]f(a) + \alpha m[(\alpha+3)g^q(b) + (\alpha+1)g^q(a)]f\left(\frac{b}{m}\right) \right\}^{1/q};$$

2) when $c=0$ and $q=1$, we have

$$\frac{1}{b-a} \int_a^b f(x)g(x)dx \leq \frac{2[(\alpha+1)g(a) + g(b)]f(a) + \alpha m[(\alpha+3)g(b) + (\alpha+1)g(a)]f(b/m)}{2(\alpha+1)(\alpha+2)};$$

3) when $c=0$, $q=1$ and $m=1$, we have

$$\frac{1}{b-a} \int_a^b f(x)g(x)dx \leq \frac{2[(\alpha+1)g(a) + g(b)]f(a) + \alpha[(\alpha+3)g(b) + (\alpha+1)g(a)]f(b)}{2(\alpha+1)(\alpha+2)};$$

4) when $c=0$, $q=1$ and $m=\alpha=1$, we have

$$\frac{1}{b-a} \int_a^b f(x)g(x)dx \leq \frac{[2g(a) + g(b)]f(a) + [2g(b) + g(a)]f(b)}{6}.$$

Theorem 7. For $a, b \in R$ with $a < b$, let $f, g : R \rightarrow R_+$. If f is a P -convex function on $[a, b]$ and g^q is a logarithmically convex function on $[a, b]$ for $q \geq 1$, then

$$\frac{1}{b-a} \int_a^b f(x)g(x)dx \leq [f(a) + f(b)] \left[g^q(b)G\left(\left[\frac{g(a)}{g(b)}\right]^q\right) - \frac{c(b-a)^2}{6} \right]^{1/q},$$

where $G(u)$ is defined by (3).

Proof. Taking $x = ta + (1-t)b$ for $t \in [0, 1]$ and denoting $u = \left[\frac{g(a)}{g(b)}\right]^q$ lead to

$$\begin{aligned} \frac{1}{b-a} \int_a^b f(x)g(x)dx &= \int_0^1 f(ta + (1-t)b)g(ta + (1-t)b)dt \\ &\leq \left[\int_0^1 f(ta + (1-t)b)dt \right]^{1-1/q} \left[\int_0^1 f(ta + (1-t)b)g^q(ta + (1-t)b)dt \right]^{1/q} \\ &\leq [f(a) + f(b)]^{1-1/q} \left\{ \int_0^1 [f(a) + f(b)][g^{qt}(a)g^{q(1-t)}(b) - ct(1-t)(b-a)^2]dt \right\}^{1/q} \\ &\leq [f(a) + f(b)] \left[g^q(b) \int_0^1 u' dt - \frac{c(b-a)^2}{6} \right]^{1/q} \\ &= [f(a) + f(b)] \left[g^q(b)G(u) - \frac{c(b-a)^2}{6} \right]^{1/q}. \end{aligned}$$

Theorem 7 is thus proved.

Corollary 4. Under the conditions of Theorem 7,

1) when $c=0$, we have

$$\frac{1}{b-a} \int_a^b f(x)g(x)dx \leq [f(a) + f(b)]g(b)G^{1/q}\left(\left[\frac{g(a)}{g(b)}\right]^q\right);$$

2) when $c=0$ and $q=1$, we have

$$\frac{1}{b-a} \int_a^b f(x)g(x)dx \leq [f(a) + f(b)]g(b)G\left(\frac{g(a)}{g(b)}\right).$$

Theorem 8. For $a, b \in R$ with $a < b$, let $f, g: R \rightarrow R_+$. If f is a quasi-convex function on $[a, b]$ and g^q is a logarithmically convex function on $[a, b]$ for $q \geq 1$, then

$$\frac{1}{b-a} \int_a^b f(x)g(x)dx \leq \max \{f(a), f(b)\} \left[g^q(b)G\left(\left[\frac{g(a)}{g(b)}\right]^q\right) - \frac{c(b-a)^2}{6} \right]^{1/q},$$

where $G(u)$ is defined by (3).

Proof. Let $x = ta + (1-t)b$ for $t \in [0, 1]$ and $u = \left[\frac{g(a)}{g(b)}\right]^q$. This gives

$$\begin{aligned} \frac{1}{b-a} \int_a^b f(x)g(x)dx &= \int_0^1 f(ta + (1-t)b)g(ta + (1-t)b) dt \\ &\leq \left[\int_0^1 f(ta + (1-t)b) dt \right]^{1-1/q} \left[\int_0^1 f(ta + (1-t)b)g^q(ta + (1-t)b) dt \right]^{1/q} \\ &\leq [\max \{f(a), f(b)\}]^{1-1/q} \left[\int_0^1 \max \{f(a), f(b)\} [g^{qt}(a)g^{q(1-t)}(b) - ct(1-t)(b-a)^2] dt \right]^{1/q} \\ &\leq \max \{f(a), f(b)\} \left[g^q(b)G(u) - \frac{c(b-a)^2}{6} \right]^{1/q}. \end{aligned}$$

Theorem 8 is thus proved.

Corollary 5. Under conditions of Theorem 8,

1) when $c = 0$, we have

$$\frac{1}{b-a} \int_a^b f(x)g(x)dx \leq \max \{f(a), f(b)\} g(b)G^{1/q} \left(\left[\frac{g(a)}{g(b)} \right]^q \right);$$

2) when $c = 0$ and $q = 1$,

$$\frac{1}{b-a} \int_a^b f(x)g(x)dx \leq \max \{f(a), f(b)\} g(b)G \left(\frac{g(a)}{g(b)} \right).$$

ACKNOWLEDGEMENTS

This work was partially supported by the National Nature Science Foundation of China under Grant No. 11361038 and by the Inner Mongolia Autonomous Region Natural Science Foundation Project under Grant No. 2015MS0123, China.

The authors appreciate anonymous referees for their careful corrections of and valuable comments on the original version of this paper.

REFERENCES

1. S. S. Dragomir, J. Pečarić and L. E. Persson, "Some inequalities of Hadamard type", *Soochow J. Math.*, **1995**, 21, 335-341.
2. G. Toader, "Some generalizations of the convexity", Proceedings of Colloquium on Approximation and Optimization, **1985**, Cluj-Napoca, Romania, pp.329-338.
3. V. G. Miheşan, "A generalization of the convexity", Seminar on Functional Equations, Approximation and Convexity, **1993**, Cluj-Napoca, Romania.
4. H. Hudzik and L. Maligranda, "Some remarks on s -convex functions", *Aequat. Math.*, **1994**, 48, 100-111.

5. B. T. Polyak, "Existence theorems and convergence of minimizing sequences in extremum problems with restrictions", *Soviet Math. Dokl.*, **1966**, 7, 72-75.
6. M. Z. Sarikaya and H. Yaldiz, "On Hermite Hadamard-type inequalities for strongly log-convex functions", *Int. J. Modern Math. Sci.*, **2013**, 6, 1-8.
7. B. G. Pachpatte, "On some inequalities for convex functions", RGMIA Research Report, **2003**, Vol. 6 (Suppl.), Art. No. 1.
8. U. S. Kirmaci, M. K. Bakula, M. E. Özdemir and J. Pečarić, "Hadamard-type inequalities for s -convex functions", *Appl. Math. Comput.*, **2007**, 193, 26-35.
9. R.-F. Bai, F. Qi and B.-Y. Xi, "Hermite-Hadamard type inequalities for the m - and (α, m) -logarithmically convex functions", *Filomat*, **2013**, 27, 1-7.
10. S.-P. Bai, S.-H. Wang and F. Qi, "Some Hermite-Hadamard type inequalities for n -time differentiable (α, m) -convex functions", *J. Inequal. Appl.*, **2012**, doi: 10.1186/1029-242X-2012-267.
11. L. Chun and F. Qi, "Integral inequalities of Hermite-Hadamard type for functions whose third derivatives are convex", *J. Inequal. Appl.*, **2013**, doi: 10.1186/1029-242X-2013-451.
12. F. Qi and B.-Y. Xi, "Some integral inequalities of Simpson type for GA- ε -convex functions", *Georgian Math. J.*, **2013**, 20, 775-788.
13. Y. Shuang, Y. Wang and F. Qi, "Some inequalities of Hermite-Hadamard type for functions whose third derivatives are (α, m) -convex", *J. Comput. Anal. Appl.*, **2014**, 17, 272-279.
14. B.-Y. Xi, R.-F. Bai and F. Qi, "Hermite-Hadamard type inequalities for the m - and (α, m) -geometrically convex functions", *Aequat. Math.*, **2012**, 84, 261-269.
15. B.-Y. Xi and F. Qi, "Some Hermite-Hadamard type inequalities for differentiable convex functions and applications", *Hacetatepe J. Math. Stat.*, **2013**, 42, 243-257.
16. B.-Y. Xi and F. Qi, "Some integral inequalities of Hermite-Hadamard type for convex functions with applications to means", *J. Funct. Spaces Appl.*, **2012**, 2012, Article ID 980438.
17. S. S. Dragomir and C. E. M. Pearce, "Selected Topics on Hermite-Hadamard Type Inequalities and Applications", RGMIA Monographs, Victoria University, Melbourne, **2000**.

Technical Note

Automated three-wheel rice seeding robot operating in dry paddy fields

Piyanun Ruangurai¹, Mongkol Ekpanyapong^{2,*}, Chatchai Pruetong² and Thaisiri Watwai³

¹ Faculty of Industrial Education, Rajamangala University of Technology Phra Nakhon, No. 399, Samsen Road, Dusit Sub-area, Dusit Area, Bangkok province 10300, Thailand

² Microelectronics and Embedded Systems, Asian Institute of Technology, Km. 42 Klong Luaong, Pathumthani 12120, Thailand

³ Department of Banking and Finance, Faculty of Commerce and Accountancy, Chulalongkorn University, Phayathai Road, Patumwan, Bangkok 10330, Thailand

* Corresponding author, e-mail: mongkol@ait.ac.th

Received: 22 January 2014 / Accepted: 4 December 2015 / Published: 23 December 2015

Abstract: Automated farming robots can help address the labour shortage issue in the agricultural sector. In this paper, a automated direct rice seeding robot is introduced. The machine is capable of controlling the number of rice seeds per dropping point as well as the distance between the dropping points, as well as navigating automatically in the paddy field. In a field test an accuracy of 92% for the number of seeds dropped and only an error of about 5 centimetres in the dropping location were achieved.

Keywords: direct rice seeding, agricultural machinery, robotics, rice seeding robot, embedded systems

INTRODUCTION

Rice is one of the most important economic crops in Asia. In the past rice farming required intensive human labour. However, workers throughout the region have been moving to work for higher-paying industrial jobs, leading to labour shortages in the agricultural sector. With the technology advancement, more tools have been introduced to the farmers. These tools can help address this labour-shortage problem and at the same time improve farming efficiency. Nishimura et al. [1] introduced a precision-drill seeder for the direct sowing of rice in flooded paddy fields. They used an 8-row seeder mounted on a vehicle. Their machine had two parts: the first part was the seeding part and the second part was the fertilising part. The system was operated manually. Nagasaka et al. [2] proposed an automated rice transplanter with a real-time kinematic global positioning system (RTKGPS) and a fibre optic gyro. Their objective was to develop an automated system for a precise operation on paddy fields. They used the RTKGPS to locate the position and

the fibre optic gyro sensor to measure the direction and inclination of the robot. The vehicle could move in a straight line automatically and the deviation from the desired straight path was less than 10 cm. Nagasaka et al. [3] introduced a high-precision automated, unmanned rice transplanter. The system was operated using a RTKGPS with 2-cm precision at 10Hz. They used a simple proportional controller for steering control. The transplanter was guided by a global positioning system (GPS) with a maximum deviation of 12 cm from the desired straight path and a root mean square (RMS) deviation of 5.5 cm. However, the drawback of the RTKGPS is that it requires the setting up of a base station prior to operating the system. Hence it is not practical for actual farming. Yoshinaga [4] developed a hill seeder and improved the lodging resistance of hill-seeded rice in Japan. He developed the seeder that effectively drives seeds intermittently into the puddled soil and enabled the establishment of several kinds of plants on a hill.

Apart from rice farming, there are other kinds of crop farming that have incorporated the technology for efficiency improvement. Chaorakam et al. [5] performed a field evaluation of slot openers for minimum tillage, which may help retain soil moisture, reduce time requirement and save fuel consumption for soil preparation. Noguchi and Barawid [6] introduced a farming robot which uses low-cost navigation and a real-time monitoring system. The navigation system uses a Hemisphere GPS, which is an inexpensive sensor in place of the inertial measurement unit (IMU). It provides minimum errors both in lateral and heading deviations. They also used an inexpensive GPS sensor instead of the RTKGPS and IMU sensors. With those inexpensive sensors, the robot could follow the navigation map with good accuracy, although it was less accurate than the robot with more expensive systems (RTKGPS and IMU). They used a laser scanning system to detect objects in the farm but this sensor is expensive. They also introduced a real time monitoring system to observe the status of each robot.

As a larger proportion of the labour force is moving to higher-paying jobs in manufacturing industries in the cities or suburban areas, a labour shortage in the agricultural sector in most developing countries becomes more severe and the introduction of agricultural machinery becomes increasingly important. Examples of rice farming machinery include rice harvesters and rice transplanters. However, labour is still needed for most part of rice farming even with rice transplanters. Here we introduce an automated direct rice seeding robot which is capable of controlling the number of rice seeds per dropping point as well as the distance between the dropping points, and navigates automatically in the paddy field. We propose a novel mechanic design and a mathematical model for the dynamic control of a three-wheel robot in the paddy field. Most existing agricultural machines are based on a four-wheel system. The advantage of a three-wheel robot over a four-wheel one is the ease of steering control for making turns. We apply the extended Kalman filter (EKF) algorithm for sensor fusion to an accurate tracking of our robot system and provide proportional-integral-derivative (PID)-based and proportional-derivative (PD)-based control systems for driving control and steering control respectively.

MATERIALS AND METHODS

Rice Seeding System

The rice seeding system [7] used in this study consists of two subsystems: the rice seed container as shown in Figure 1 and the ground vehicle as shown in Figure 2. The top of the rice seed container is a tray partitioned by flat aluminum bars into 50 x 49 cells (50 rows x 49 columns), each of size 1 x 1 cm², for containing seeds before planting. A plastic plate is placed under the

aluminum bars for keeping the seeds in the tray. A stepper motor is used to drive a ball screw which pulls the plastic plate. Each time the plate is pulled, it opens one row (49 cells) of the tray to drop 49 seeds (if one cell contains one seed) to the slot box. The seeds then fall to the ground through 49 small PVC pipes arranged in a 7 x 7 grid as shown in Figure 2(c). The seeding system is designed so that more trays can be added on the top to carry more rice seeds. The ground vehicle carries the rice seed container on the top and drops the seeds when it reaches the seed dropping location. The vehicle has three wheels: two rear wheels for driving the robot and one front wheel for controlling the direction. The front wheel is a standard bicycle wheel and the rear wheels are cartwheels. The advantage of a three-wheel robot over one with four wheels is the ease of steering control. To ensure that the vehicle is strong enough for a rough terrain, the main structure is made from steel bars. The rice seeding system is attached to the support frame which is made from aluminum to minimise the total weight. For each driven wheel, a 500W DC motor is used for robot mobilisation. An incremental encoder (wheel encoder) is attached at the end of each motor to measure the velocity of each wheel. A 36W DC motor is used to drive the front wheel for steering control. An encoder (heading encoder) is also attached to its shaft for measuring the steering angle. Table 1 provides the detailed information of the robot.

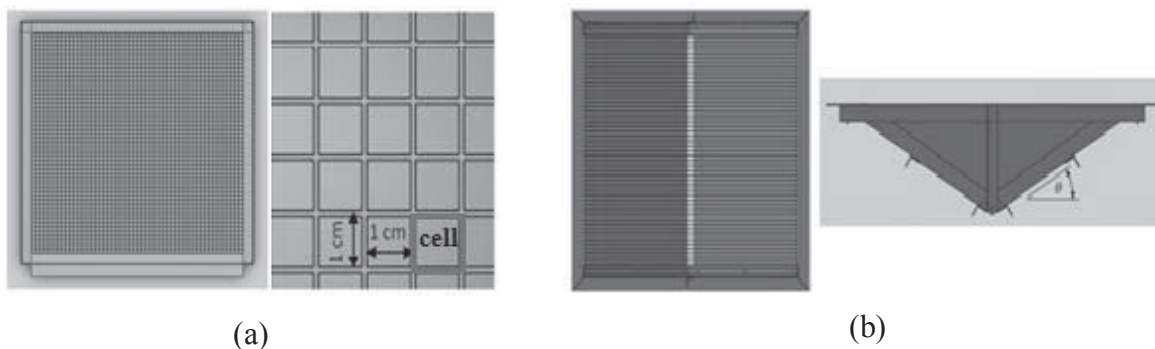


Figure 1. Rice seed container: (a) tray for containing rice seeds; (b) slot box

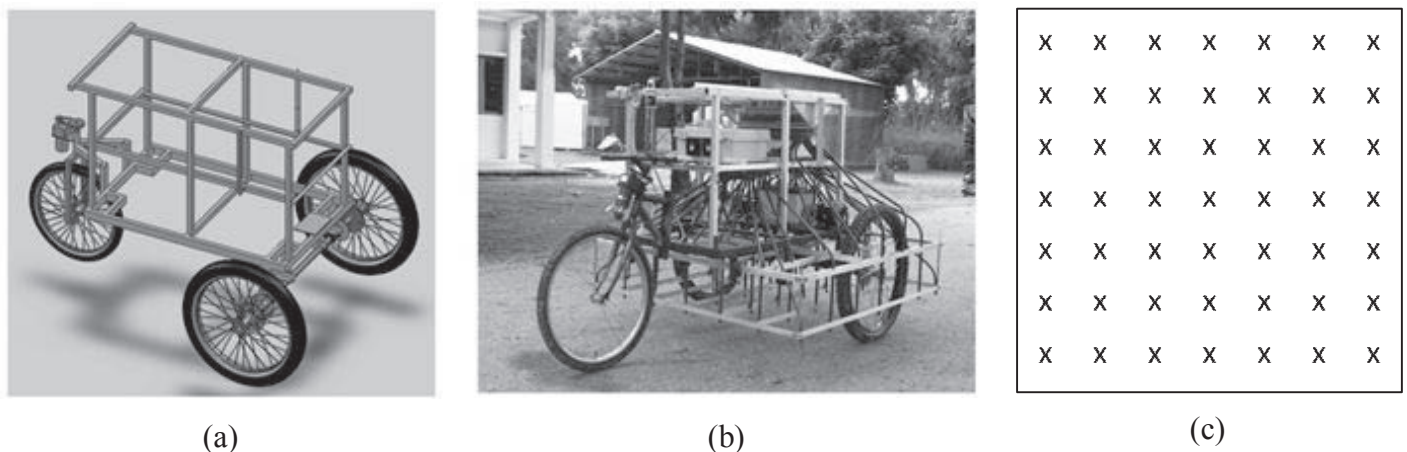


Figure 2. Ground vehicle: (a) frame in solid work; (b) real robot; (c) PVC pipe end arrangement

Table 1. Three-wheel robot information

Item	Detail
Width x length x height	1.4 x 2.25 x 1.2 m
Rear-wheel diameter	66 cm
Front-wheel diameter	58 cm
Motor	500W DC
Weight	90 kg
Power source	battery

Since it is possible that on a rough surface in the field a slip may occur at a rear wheel and cause a measurement error, a small additional wheel with an encoder is added to the vehicle as shown in Figure 3(a) to measure the robot’s travel distance instead of solely relying on the information from the two rear wheels. A compass and a GPS as shown in Figure 3(b) are also used in this robot for localising and path tracking purposes.

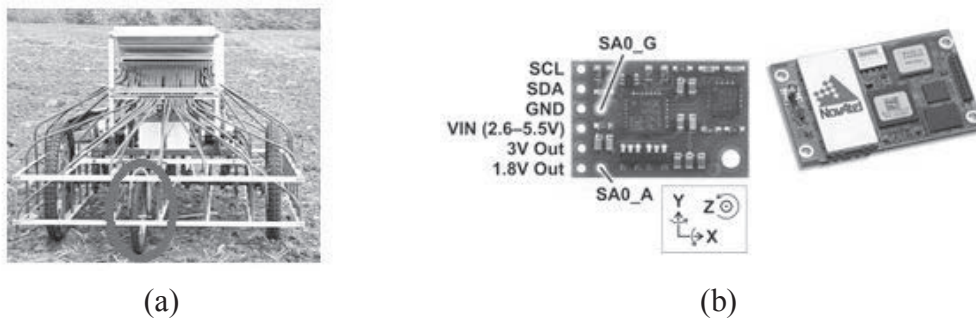


Figure 3. Motion control devices: (a) additional wheel with encoder; (b) IMU and GPS

Automated Control System

The EKF algorithm is adopted to estimate the current position and predict the next position of the robot. The steering control of the front wheel motor is used to track the robot angle along the desired path. The system has three types of sensor: GPS, compass and wheel encoder. The sensor fusion is used for high-accuracy location estimation with respect to the orientation to true north and travel distance of the robot. We did not use a differential GPS such as RTKGPS because it requires setting up a base station which is not practical for Thai farming. The coordinate system of the rice planting robot is shown in Figure 4. A negative value of δ means the front wheel is turned towards the left side of the steered wheel axle and a positive δ , the right side. The system state consists of the robot’s position in the X-axis and Y-axis (x, y) and the orientation (θ) of the robot with respect to the X-axis; $\theta = 0$ represents the inclination along the north direction. At system time, the system state is denoted by

$$X_t = [x_t \ y_t \ \theta_t]^T,$$

where A^T is the transpose of matrix A .

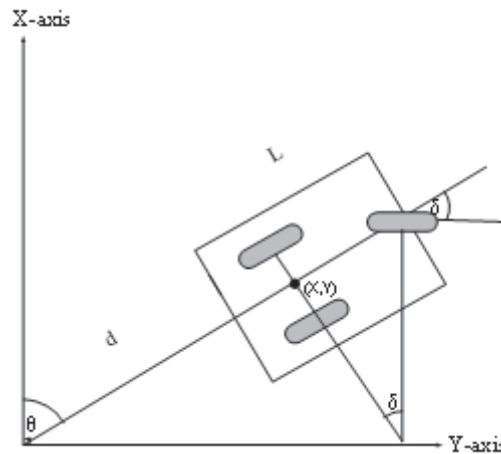


Figure 4. Robot model (x,y = robot position, d = travel distance, L = vehicle length, δ = steering angle, θ = robot orientation)

The motion model in this invention is based on odometry. The input of the motion model at system time t , U_t , is given by

$$U_t = [d_t \quad d_t \tan(\delta_t)]^T$$

where the travel distance of the robot, d_t , is collected from the wheel encoders, and the steering angle δ_t comes from the heading encoder. We use the Ackerman model [8] in discrete time for our motion model. The equation for the model is

$$X_{t+1} = X_t + \begin{bmatrix} \cos(\theta_t) & 0 \\ \sin(\theta_t) & 0 \\ 0 & \frac{1}{L} \end{bmatrix} U_t + V_t$$

where the process noise V_t is a zero-mean white Gaussian noise. In general, the process noise covariance is difficult to estimate because we do not directly observe the process noise. However, it can be obtained by tuning [9]. The measurement output Y_t is the position on the X-axis and Y-axis obtained from the GPS sensor and it is assumed [10] that

$$Y_t = X_t + W_t$$

where the measurement noise W_t is assumed to be a Gaussian noise with zero mean.

There are two subsystems for path tracking in our rice planting robot. The first is the heading control system for controlling the heading of the robot towards the waypoint, and the second is the velocity control system for stopping or moving the robot at a constant speed. The block diagram of the heading control system (Figure 5) is a multi-loop system in which the outer loop is for adjusting the vehicle's direction and the inner loop, the front wheel. For the outer loop, the system obtains the current position (X_c, Y_c) from the localisation method. The input of this system is the desired yaw angle, $\theta_{desired}$, which is obtained from the trigonometric function. The system obtains the current yaw angle, θ_{local} , from the localisation method and calculates the error between the desired and the current yaw angles or $e_1(t)$. The desired steering angle is proportional to $e_1(t)$, with proportional gain K_{P1} . The feed forward gain of the heading control loop for the curve line is K_{P2} , whereas it is zero for straight line. The vehicle speed control diagram is shown in Figure

6. The pulse width modulation (PWM) is used for controlling the speed of the motor of the rear wheels. The PID controller is used for this system and its equation is:

$$PWM = K_p e(t) + K_i \int_0^t e(s) ds + K_d \frac{de(t)}{dt}$$

where K_p , K_i and K_d are gains.

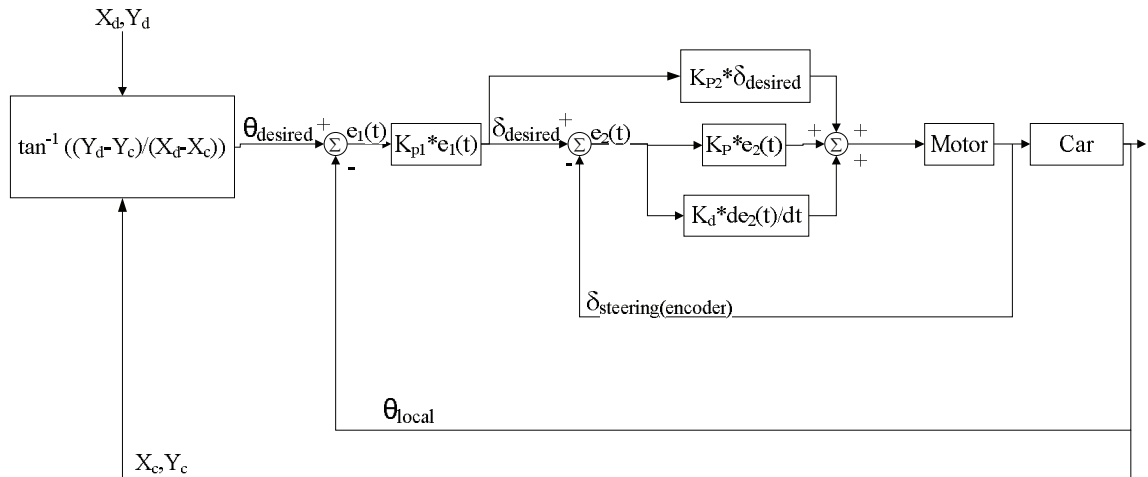


Figure 5. Heading control loop

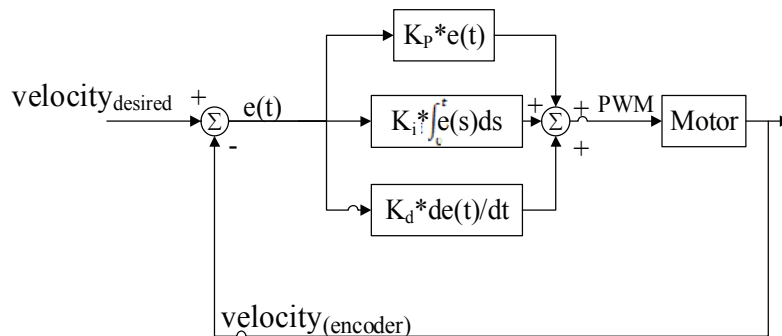


Figure 6. Velocity control system

RESULTS AND DISCUSSION

Simulation Results on Localisation Based on EKF

We tested the performance of the EKF-based localisation using simulation in Matlab. In the simulation we set the length of the vehicle L to 1.4 m., the travel distance d to 2 m and the steering angle δ to 0.07 rad. The covariance matrices of the process noise V_z and measurement noise W_z were assumed to be diagonal. The diagonal entries of V_z were 0.12^2 , 0.14^2 and 0.01^2 , and those of W_z were 1.2^2 , 1.4^2 and 0.037^2 . The position of the vehicle was simulated based on the process equation. The position was updated and plotted as the true path every 0.1 second, which was a circular path. The measured path was obtained from the true path plus the measurement noise W_z . The model path was calculated from the dynamics of the robot assuming the process noise V_z was

zero, and the EKF path was calculated using the EKF algorithm. The results are shown in Figure 7, where the positions of the EKF path are closer to the true path than are those of the measured and model paths. A comparison between the measured, EKF and model path errors in the X-axis and Y-axis shows that the EKF path error is the smallest.

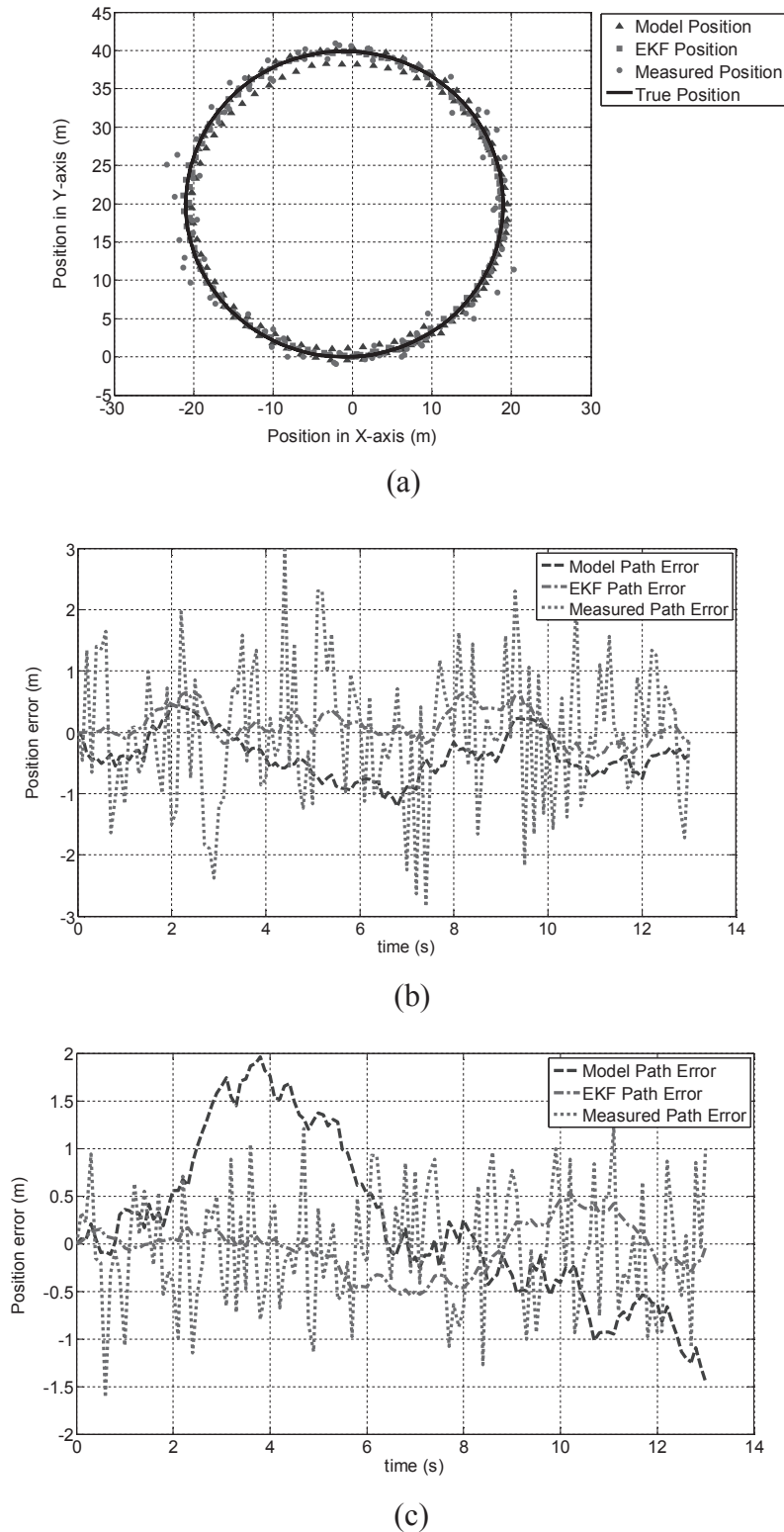


Figure 7. Simulation results: (a) path simulation; (b) position errors in X-axis; (c) position errors in Y-axis

Seeding System's Accuracy and Field Test

We tested the accuracy of the rice seeding system in terms of the number of seeds dropped by dropping 49 seeds per round for ten rounds. The robot was tested without moving. Figure 8 shows the numbers of seeds dropped from the ten rounds, which varied between 41-47 seeds. The average seeding accuracy of the system was 91%.

In the field test the mobile robot was tested on a rough paddy field with an area of about one rai (1,600 m²). The target path for the robot is shown in Figure 9. Position A was the starting position. The robot first moved from position A to position B. Then it made a U-turn and moved to position C and so on, completing a total of four rows along the target path. It stopped every 1.6 metres to drop the rice seeds, making 12 stops along each row. At each stop, the robot dropped 49 seeds (one seed per dropping point). Figure 10 shows the robot moving on the paddy field. In Table 2 the average seed-dropping distances from one side of the field (such as position A-B in Figure 9) are compared with the target distances. The average error is about 5 cm. Table 3 shows the average number of seeds dropped per dropping location (expected number = 49), with an average error of about 4 seeds or 92% accuracy. Note that the results for each location in Tables 2 and 3 are reported using the averages across the four rows along the path.

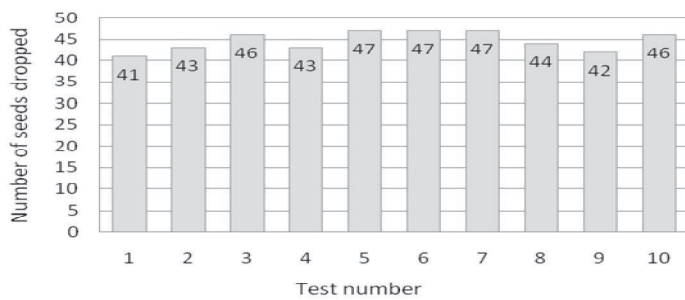


Figure 8. Result of seeding accuracy test

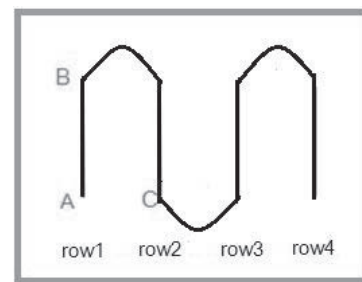


Figure 9. Target path for robot

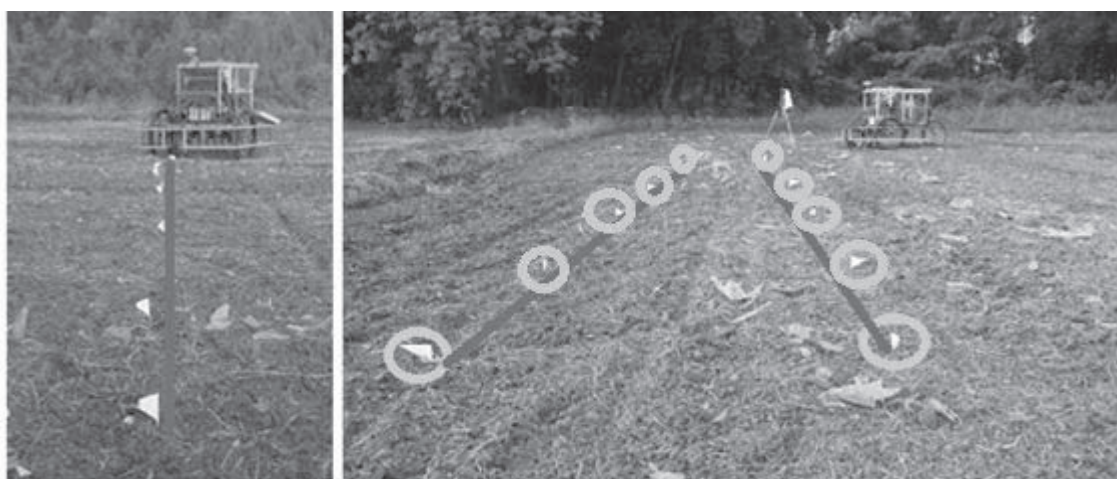


Figure 10. Experiment in paddy field: white flags represent actual seed dropping locations, highlighted with yellow circles to increase visibility.

Table 2. Average seed-dropping distances from field trial

Location	1	2	3	4	5	6	7	8	9	10	11	12
Average (m)	0	1.55	3.14	4.76	6.37	8.01	9.62	11.22	12.84	14.47	16.19	17.68
Target (m)	0	1.60	3.20	4.80	6.40	8.00	9.60	11.20	12.80	14.40	16.00	17.60
Error (m)	0	0.05	0.06	0.04	0.03	0.01	0.02	0.02	0.04	0.07	0.19	0.08

Table 3. Average number of dropped seeds from field trial

Location	1	2	3	4	5	6	7	8	9	10	11	12
Average (seeds)	46	43	47	44	46	46	47	45	44	41	46	46
Error (seeds)	3	6	2	5	3	3	2	4	5	8	3	3

Comparison with Tractor Seeder

A comparison of performance between our three-wheel robot seeder and the traditional tractor seeder [11] is shown in Table 4. The former has a lower (hence better) seeding rate and higher seeding efficiency, but the drawbacks of the three-wheel robot are the high cost and the long working time. Note that the working time is the total time spent to complete one rai. The three-wheel robot runs automatically whereas the traditional tractor seeder is controlled manually.

Table 4. Comparative performance between three-wheel robot and the traditional tractor seeder

Seeder performance	Three-wheel seeding robot	Traditional tractor seeder
Seeding rate	3kg/rai	14 kg/rai
Seeder cost	100,000 Baht (~3,000 USD)	50,000 Baht (~1,500 USD)
Seeding efficiency	92%	76-82 %
Intra-row spacing	25 cm	25-30 cm
Working time	102.6 min./rai	15 min./rai

CONCLUSIONS

The innovation described in this paper has four main contributions: 1) a mechanic design for automated direct rice seeding system; 2) a mathematical model for the dynamic control of a three-wheel robot while most existing agricultural machines are based on a four-wheel system; 3) the applied EKF algorithm for sensor fusion to accurately track the robot system; and 4) the PID- and PD-based control systems provided for driving the control and steering control respectively. In a simulation the position from the EKF estimation was closer to the true path than are the measured and model paths. In a field test a 92% accuracy for the number of dropped seeds and an error of 5 cm in the dropping position was obtained.

ACKNOWLEDGEMENTS

The support by the Agricultural Research Development Agency (Thailand) under contract number PRP5505020380 and by the National Research University Project, Office of Higher

Education Commission (WCU-067-HS-57) was gratefully acknowledged.

REFERENCES

1. Y. Nishimura, K. Hayashi, T. Goto and M. Horio, "Precision-drilling methods for the direct sowing of rice in flooded paddy fields", Proceedings of World Rice Research Conference, **2005**, Tsukuba, Japan, pp.238-240.
2. Y. Nagasaka, K. Taniwaki, R. Otani and K. Shigeta, "An automated rice transplanter with RTKGPS and FOG", *Agric. Eng. Int. CIGR J. Sci. Res. Devel.*, **2002**, 4, 41-46.
3. Y. Nagasaka, Y. Kanetani, N. Umeda and T. Kokuryu, "High-precision autonomous operation using an unmanned rice transplanter", Proceedings of World Rice Research Conference, **2005**, Tsukuba, Japan, pp.235-238.
4. S. Yoshinaga, "Improved lodging resistance in rice (*Oryza Sativa* L.) cultivated by submerged direct seeding using a newly developed hill seeder", *Jpn. Agric. Res. Quart.*, **2005**, 39, 147-152.
5. I. Chaorakam, M. Koike, T. Takigawa, A. Yoda, H. Hasegawa and B. Bahalayodhin, "Field evaluation of slot openers for minimum tillage (part 3) – dried soil cover on the slot", *Maejo Int. J. Sci. Technol.*, **2009**, 1(Sp. Iss.), 95-105.
6. N. Noguchi and O. C. Barawid Jr., "Robot farming system using multiple robot tractors in Japan agriculture", Proceedings of 18th IFAC World Congress, **2011**, Milano, Italy, pp.633-637.
7. T. Watewai, C. Pruetong and M. Ekpanyapong, "A tray-based direct rice seeding machine", *DIP Thailand 1301007037* (**2014**).
8. A. J. Weinstein and K. L. Moore, "Pose estimation of Ackerman steering vehicles for outdoors autonomous navigation", Proceedings of IEEE International Conference on Industrial Technology, **2010**, Vina del Mar, Chile, pp.579-584.
9. J. Aranda, J. M. Diaz, S. D. Canto, R. Munoz and C. H. Cuesta, "An overview about dynamic positioning of ships", in "Automation for the Maritime Industries" (Ed. J. Aranda, M. A. Armada and J. M. De la Cruz), 1st Edn., Produccion Grafica Multimedia, Madrid, **2005**, Ch.4.
10. R. C. Dorf, "The Engineering Handbook", 2nd Edn., CRC Press, Boca Raton, **2004**, pp.105-9–105-10.
11. S. Nakwattanukul, J. Mongkoltanatas, D. Sarathunphithak and C. Chaisattapagon, "Testing and development of rice planters attached to farm tractor", Final Research Report, **2007**, Department of Agricultural, Thailand.

© 2015 by Maejo University, San Sai, Chiang Mai, 50290 Thailand. Reproduction is permitted for noncommercial purposes.

